

MOLECULAR BASIS OF QUANTITATIVE GENETICS REVEALED BY CLONING AND  
ANALYSIS OF 474 GENES CONTROLLING FIBER LENGTH IN COTTON

A Dissertation

by

YUN-HUA LIU

Submitted to the Office of Graduate and Professional Studies of  
Texas A&M University  
in partial fulfillment of the requirements for the degree of

DOCTOR OF PHILOSOPHY

|                        |                     |
|------------------------|---------------------|
| Chair of Committee,    | Hongbin Zhang       |
| Co-Chair of Committee, | C. Wayne Smith      |
| Committee Members,     | Steve Hague         |
|                        | Joshua Yuan         |
| Head of Department,    | David Baltensperger |

August 2014

Major Subject: Plant Breeding

Copyright 2014 Yun-Hua Liu

## ABSTRACT

Cotton (*Gossypium* spp.) is a leading textile crop in the world, generating an annual economic benefit of over hundred billion USD. However, few genes controlling fiber quality and yield traits have been cloned and characterized to date. In this study, a large number of genes controlling the upper half mean length (UHML) of fibers were cloned using a newly-developed high-throughput gene and QTL cloning system and subjected to systems analysis. Furthermore, the molecular basis and regulation mechanisms of UHML were investigated using the cloned fiber length genes.

A total of 474 *GFL* (*Gossypium* Fiber Length) genes were cloned. The effect of each *GFL* gene on UHML varied from 2.64% to 7.92%. Of 474 *GFL* genes, 88.6% decreased UHML when turned on or actively expressed in the developing fibers at the 10 days post-anthesis (10-dpa), whereas only 11.4% increased UHML. The *GFL* genes encode proteins and enzymes that are involved in a variety of biological processes and metabolic pathways. The 474 *GFL* genes interacted to form an interaction network in the 10-dpa fibers, which suggests that UHML is the consequence of interactions among the *GFL* genes. In addition, the evolution of fiber length was examined between diploid and tetraploid cottons using the *GFL* genes. The results showed that the variation of the *GFL* gene networks, including the number of genes and number of gene x gene interactions, also plays an important role in the variation of fiber length during polyploidization.

Therefore, this study has, for the first time worldwide, cloned a large number of genes controlling UHML and deciphered the underlying molecular basis and regulation

mechanisms, thus providing novel resources and knowledge for development of new toolkits for enhanced cotton fiber breeding. The UHML is determined not only by its controlling genes, *GFLs*, but also by their actions, action directions and interactions. Moreover, the results of this study have not only provided a first line of evidence that a quantitative trait is controlled by a large number of genes, but also added new molecular basis, thus forming the molecular mechanisms of quantitative genetics.

## DEDICATION

To my father, mother, brother, and Solomon

## ACKNOWLEDGEMENTS

I would like to thank my committee chairs, Dr. Hongbin Zhang and Dr. C. Wayne Smith, and my committee members, Dr. Steve Hague and Dr. Joshua Yuan, for their guidance and support throughout the course of this research. Especially, I would like to express my best sincere appreciation to my two major professors. Thanks to Dr. Zhang for providing me so many good opportunities and training me to be a quick learner when facing unfamiliar research areas. I was so grateful for his patience for guiding me toward the right directions in the research. Thanks to Dr. Smith for his invaluable suggestions in the field works and breeding issues. Without their helps, this exciting research project may not be on the right track.

Thanks also to my lab colleagues, Dr. Yang Zhang, Mrs. Chantel Scheuring, and Dr. Meiping Zhang for their help and support throughout the entire research and studies at Texas A&M University. Besides, I would like to thank Mrs. Dawn Deno, former graduate students, and all undergraduate assistants in the Cotton Improvement Lab for field trial experiments. I acknowledge for their assistances in the planting, harvesting, de-burring, ginning, and de-lint. I learned a lot from them while working with them as a team in the ginning lab and the field. Thank you!

## TABLE OF CONTENTS

|   | Page |
|---|------|
| ABSTRACT .....  | ii   |
| DEDICATION .....  | iv   |
| ACKNOWLEDGEMENTS .....  | v    |
| TABLE OF CONTENTS .....   | vi   |
| LIST OF FIGURES.....  | vii  |
| LIST OF TABLES .....  | x    |
| 1. INTRODUCTION.....  | 1    |
| 2. MATERIALS AND METHODS .....  | 11   |
| 2.1 Plant materials and fiber phenotyping.....  | 11   |
| 2.2 Transcriptome sequencing and gene digital expression profiling .....  | 13   |
| 2.3 Data analysis .....   | 18   |
| 2.4 Digital expression profiling of genes actively expressed in the 10-dpa<br>fibers of diploid cottons.....                                  | 22   |
| 3. RESULTS.....   | 24   |
| 3.1 UHML genetic variation in the RIL population .....  | 24   |
| 3.2 Transcriptome sequencing and digital expression profiling .....   | 31   |
| 3.3 Isolation and analysis of genes controlling UHML .....  | 44   |
| 3.4 Molecular basis of UHML development.....  | 78   |
| 3.5 <i>GFL</i> genes of diploid cottons and molecular mechanisms of fiber<br>length evolution in the process of cotton polyploidization ..... | 124  |
| 4. DISCUSSION AND CONCLUSION.....   | 143  |
| REFERENCES.....   | 149  |
| APPENDIX A .....  | 156  |

## LIST OF FIGURES

| FIGURE |  | Page |
|--------|--|------|
| 1      | UHML distributions in the TAM 94L-25 x NMSI 1331 RIL population in 2011 .....  | 25   |
| 2      | UHML distributions in the TAM 94L-25 x NMSI 1331 RIL population in 2010.....   | 26   |
| 3      | UHML distributions in the TAM 94L-25 x NMSI 1331 RIL population in 2009.....   | 26   |
| 4      | Average UHML distribution in the TAM 94L-25 x NMSI 1331 RIL population during 2009-11 .....  | 27   |
| 5      | Correlations of UHMLs of the TAM 94L-25 x NMSI 1331 RIL population between replicates in 2010 .....  | 28   |
| 6      | Correlations of UHMLs of the TAM 94L-25 x NMSI 1331 RIL population between replicates in 2011 .....  | 28   |
| 7      | Correlations of UHMLs of the TAM 94L-25 x NMSI 1331 RIL population between 2010 and 2011 .....   | 29   |
| 8      | Correlations of UHML with other HVI traits in the TAM 94L-25 x NMSI 1331 RIL population in 2011 .....  | 31   |
| 9      | Unigene contigs assembled with SOAPdenovo and Trinity .....  | 35   |
| 10     | N50 of unigenes assembled with SOAPdenovo and Trinity.....   | 35   |
| 11     | Correlation of expression levels (TPM) of genes in 10-dpa fibers between plants within a replicate (left) and between replicates (right) of the female parent, TAM 94L-25, in 2011 ..... | 38   |
| 12     | Correlation of expression levels (TPM) of genes in 10-dpa fibers of the female parent, TAM 94L-25, between 2010 and 2011 .....   | 39   |
| 13     | Distribution of numbers of 100-nucleotide (bp) clean reads derived from RNA-Seq among the 198 RILs and 2 parents .....   | 40   |

| FIGURE  | Page |
|---|------|
| 14 Distribution of Q20 of the RNA-Seq reads with a quality of Q20 or higher among the 198 RILs and 2 parents.....                     | 40   |
| 15 Distribution of GC content of the sequence reads derived from RNA-Seq among the 198 RILs and 2 parents.....                        | 41   |
| 16 Unigenes assembled with Trinity for each of the 198 RILs of the TAM 94L-25 x NMSI 1331 population .....                            | 42   |
| 17 N50 of the unigenes assembled with Trinity for each of the 198 RILs of the TAM 94L-25 x NMSI 1331 population .....                 | 42   |
| 18 GO items of the <i>GFL</i> genes assigned to the functional category of biological process (level 2) .....                         | 58   |
| 19 GO items of the <i>GFL</i> genes assigned to the functional category of molecular function (level 2) .....                         | 58   |
| 20 GO items of the <i>GFL</i> genes assigned to genes the functional category of cellular component (level 2) .....                   | 72   |
| 21 Metabolism-related KEGG pathways in which the <i>GFL</i> genes are involved.....   | 76   |
| 22 The co-regulation network of the 474 <i>GFL</i> genes .....  | 77   |
| 23 Association of the variations of <i>GFL</i> gene networks with the UHML of the RILs of the TAM 94L-25 x NMSI 1331 population ..... | 89   |
| 24 Numbers of unique and shared edges among the <i>GFL</i> gene networks of different UHML RIL groups.....                            | 107  |
| 25 The network of the <i>GFL</i> orthologous genes in the A-genome diploids.....  | 126  |
| 26 The network of the <i>GFL</i> orthologous genes in the D-genome diploids.....  | 126  |



| FIGURE |  | Page |
|--------|--|------|
| 27     | Node and edge number variations of the <i>GFL</i> gene network from diploids (AA and DD) to tetraploid cottons (AADD)..... | 128  |
| 28     | Variation of numbers of edges among the <i>GFL</i> networks of A-, D- and AD-genome species.....                           | 129  |

## LIST OF TABLES

| TABLE | Page  |
|-------|---|
| 1     | Fiber UHML (mm) of the RIL population during 2009-2011 ..... 24   |
| 2     | Uniformity index (%) of the RIL population during 2009-2011 ..... 25  |
| 3     | Pearson's correlation of UHMLs between 2009, 2010 and 2011 ..... 27   |
| 4     | Pearson's correlation coefficients of HVI traits ..... 30   |
| 5     | Preliminary examination of computer programs, Trinity and SOAPdenovo, for <i>de novo</i> assembly of 100bp clean reads generated from RNA-seq of the parental lines of the TAM 94L-25 x NMSI 1331 RIL population ..... 34 |
| 6     | Preliminary examination of assembling unigene reference sequences from the parental lines of the RIL population using Trinity ..... 36  |
| 7     | Summary of RNA-Seq in 100-nucleotide paired end reads for 198 RILs and 2 parents..... 39  |
| 8     | <i>GFL</i> genes and their effects and action direction on UHML in cotton ..... 45  |
| 9     | List of published genes controlling fiber length or trichome development ..... 56   |
| 10    | Annotation of <i>GFL</i> genes controlling UHML in 10-dpa tetraploid cotton species ..... 59  |
| 11    | KEGG pathways in which the <i>GFL</i> genes are involved ..... 74   |
| 12    | Number of edges that a single <i>GFL</i> gene has in the 474 <i>GFL</i> network of the entire RIL population ..... 78   |
| 13    | Number of edges and nodes in the gene x gene networks among groups with different UHMLs..... 90   |
| 14    | Pairwise comparison of the nodes of the <i>GFL</i> gene networks between the RIL groups with different UHMLs ..... 91   |

| TABLE  | Page |
|--|------|
| 15 Edge number variation of each gene constituting the <i>GFL</i> gene networks among the five fiber-length RIL groups, and its Pearson's correlation coefficients with that of UHML.....  | 93   |
| 16 Summary of the edges of each gene unique to the <i>GFL</i> gene networks of each fiber-length group derived from 474 <i>GFL</i> genes, and their Pearson correlation coefficients with of UHML and corresponding number of unique edges of <i>GFL</i> genes ..... | 108  |
| 17 Comparison of the networks of the <i>GFL</i> genes among A- and D-genome diploid species and AD-genome tetraploid cottons.....  | 127  |
| 18 Correlation coefficients ( $P \leq 0.05$ ) of edges shared among the <i>GFL</i> networks of tetraploid (AADD), A-genome diploid (AA) and D-genome diploid (DD) species.....   | 130  |
| 19 List of nodes ( <i>GFL</i> genes) that have edges common among the networks of the A-, D- and AD-genome species .....   | 137  |

## 1. INTRODUCTION

Cotton (*Gossypium* spp.) is the most important natural textile crop and one of the most important oilseed crops in the world. Worldwide cotton production was estimated to be 25.4 million MT during 2013-14, and the top cotton producing countries were China (6.96 million MT), India (6.30 million MT), and United States (USA) (2.87 million MT) (USDA 2014). Cotton yarn and related products generate up to one hundred billion USD per year. In the USA, the annual business revenue, including cotton products and farm related activities, generated from cotton production was 27.62 billion USD in 2011 (NCC 2012). The USA has shifted from a primary consumer of domestic production to a primary exporter. In order for the American cotton farmers to remain competitive in this global market, superior fiber quality will be required, including longer, finer, stronger and more uniform fibers.

The cotton genus, *Gossypium* L., contains 50 species, including 45 diploid and five allotetraploid species. Diploid species consists of A, B, C, D, E, F, G and K genome groups, whereas tetraploid species have genomes of (AD)<sub>1</sub> through (AD)<sub>5</sub>. Wendel and Cronn (2003) estimated that the polyploidization event that led to the birth of the tetraploids from the diploids occurred approximately one to two million years ago (MYA), in which two diploid ancestor genomes, AA and DD, merged into a single nucleus (Wendel 1989; Wendel et al. 1989). Two of the resulting tetraploid species were domesticated, including *G. hirsutum* (AD)<sub>1</sub> and *G. barbadense* (AD)<sub>2</sub>, in North America and two of the A-genome diploids, *G. herbaceum* (A)<sub>1</sub> and *G. arboreum* (A)<sub>2</sub>, were

domesticated in Africa-Asia. The two polyploid cultivated cottons, *G. hirsutum* (Upland cotton) and *G. barbadense* (Pima cotton or Egypt cotton), comprise more than 95% of commercial cultivars in the modern textile industry.

Cotton is also a good model for studying the genome evolution and polyploidization. Two tetraploid cultivated cottons used in this study, *G. hirsutum* and *G. barbadense*, are the classic examples of allopolyploidization. Changes in fiber characteristics that became important to civilized mankind were affected by this natural event. Interestingly, a majority of the loci impacting fiber yield and quality traits of tetraploid cottons was found to be derived from the non-spinnable fiber progenitor, the D-genome diploid species (Jiang et al. 1998). However, the morphological characteristics of modern tetraploid cotton fibers showed more similarities with their spinnable fiber progenitor, the A-genome diploid species. Applequist et al. (2001) used Scanning Electron Microscope (SEM) to study the morphological variations on ovules and identify the developmental differences among cultivated and wild diploid and tetraploid species. Based on their observations, fiber growth curves were similar between tetraploid species and A-genome wild types. The comparative findings of this research suggested a speculation that A-genome ancestor was morphogenetically dominant while combining D-genome in wild tetraploid cottons. This “dominance” did not conclude that genes controlling fiber development in the D-genome were silenced at the fiber elongation stage during polyploidization. Hovav et al (2008) reported that genes in tetraploid cottons were significantly biased toward A-genome or D-genome ancestor during fiber development, and the expressions of these genes was shifted strongly

toward the agronomical inferior donor, D-genome. This finding proposed a possibility that genes from the D-genome potentially contribute or provide raw materials of evolutionary innovations toward the superior fiber characteristics in modern tetraploid cultivated cottons.

Fiber quality is paramount to cotton production and textile industries. It is determined by several parameters, such as length, uniformity, micronaire, strength, elongation, color, and trash. The desired premium fiber quality in textile market requires fibers that are longer, stronger and finer, and have higher uniformity. Among the fiber properties, the fiber length is the most important to textile industries. This is because longer fibers can have a higher market price due to their ease in manufacturing. Meredith and Bridge (1972) found that fiber length and uniformity were controlled by both additive and dominant effects. Additive effects had the predominant influence on lint percentage, seed index, fiber strength, fiber elongation and fiber fineness, whereas dominant effect was responsible for boll size.

UHML is the average length of the longer half of the fibers in the sample under measurement. Of the two allopolyploid cultivated species, *G. barbadense*, also known as Extra Long Staple (ELS), produces longer and finer fibers, with an UHML of 35.05 – 36.58 mm (1.38 - 1.44 inch) (Smith and Cothren 1999), that are better suited for premium textile processes. *G. hirsutum*, known as Upland cotton, has higher fiber yield and wider environment adaptability, with an UHML of 22.86 - 29.46 mm (0.9 - 1.16 inch). Although *G. barbadense* has an outstanding fiber length, it only contributes about 8% of the world's cotton because of its lower yield and narrower adaptability. Therefore,

inter-specific crosses are often practiced between *G. hirsutum* and *G. barbadense* in cotton breeding programs to produce varieties combining high fiber quality with high fiber yield. Besides, the crosses between the two species and their derived populations have been widely used to study the molecular and genetic basis of fiber qualities in cotton (Chen et al. 2012).

Cotton fibers are seed trichomes derived from epidermal cells. They are the longest plant cells known to date, thus providing an excellent model to study cell fate, cell differentiation, and cytoskeleton dynamics. Although the highly elongated seed trichomes in cotton (fiber) are distinct from the leaf trichomes in *Arabidopsis* in cell shape and cellular components upon maturity, both of their trichomes are non-glandular hairs and have homologous genes or transcription factors controlling the mechanisms underlying trichome initiation and development (Humphries et al. 2005). Therefore, the leaf trichomes of *Arabidopsis* have served as a model to elucidate the mechanisms of cotton fiber differentiations in the early stage of growth. It has been reported that genes that were found to regulate leaf trichome initiation in *Arabidopsis* were also found to regulate the initiation of trichome development and seed numbers bearing on epidermal trichomes in cotton (Guan et al. 2008).

Fiber development is often separated into four distinct, yet overlapping stages, i.e., initiation, elongation, secondary cell wall biosynthesis and maturation (Basra and Malik 1984). In general, the fiber initiation of tetraploid cottons starts at two days before anthesis, and ends at two days post-anthesis (dpa). After the fiber cell starts to develop from the epidermis of seed coat, the primary cell wall becomes soft and expands. During

the elongation stage, which starts approximately at three dpa and ends at approximately 16-dpa, fiber cells undergo the maximum elongation growth rate. Genes encoding cell extension-related enzymes were found to be highly or moderately highly expressed during the elongation stage, and to be down-regulated afterwards (Michailidis et al. 2009; Wang et al. 2010a; Wang and Ruan 2010; Argiriou et al. 2012; Lacape et al. 2012). Between the elongation and secondary cell wall biosynthesis stages, a short transition stage of cell wall remodeling takes place during 16- to 20-dpa. After that, most celluloses are deposited in the secondary cell wall rather than the primary cell wall during 20- to 45-dpa (Meinert and Delmer 1977), thus leading to a rapid gain of weight per fiber. At the maturation stage, the fiber cell undergoes dehydration, thus losing most of its weight. Although it takes nearly 50 days for a fiber cell to mature, the duration of each stage depends on the environmental (e.g. temperature, irrigation, etc.) and genetic factors.

Approximately 4% of a mature fiber cell is composed of primary cell wall that determines fiber length and diameter, and 96% of it is composed of secondary cell wall that determines strength and maturity. The primary cell wall is biosynthesized largely during the elongation stage that often is coupled with vigorous cell expansion, and the majority of fiber length is developed during this period. Cellulose and hemicellulose (xyloglucan) constitute 50 - 60% of dry weight of primary cell wall in elongating fiber cell, whereas pectin contributes nearly 20-30% of dry weight. Protein and phenolic acid make up the rest of elongating fiber cell. Hemicellulose and pectin that are called matrix polysaccharides are synthesized in Golgi cisternae, while cellulose is synthesized in



plasma membrane in a form of para-crystalline microfibrils (Reiter 2002). The structure network consisting of cellulose and hemicellulose that are the major load-bearing elements in the primary cell wall provides the mechanical strength while fiber cell expansion occurs.

The expansion extent of fiber cells is associated with the duration of the elongation stage, plasmodesmata closure, turgor pressure, and cell wall loosening. Given that the elongation stage is the time of the maximum speed of fiber cell expansion, the duration of this period has been found to play an important role in the determination of final length of a mature fiber. It has been documented that *G. barabense* (Braden and Smith 2004) that often has longer fibers than *G. hirsutum* generally has a prolonged period of the elongation stage compared with short and medium UHML. A prolonged elongation stage had served an important selection factor during cotton domestication in which artificial selections were found to be made toward the prolonged elongation phase in tetraploid and diploid cottons (Applequist et al. 2001). Plasmodesmata that have been recognized to regulate of element transportation/translocation and cell-to-cell communication close at 10-dpa and re-open at 16-dpa. The genes controlling the duration of plasmodesmata closure have been reported to regulate fiber length development (Ruan et al. 2001).

Vacuoles make up 90% of the volume of an elongating fiber cell. Thus, rapid fiber cell expansion is presumed to be driven by the strong turgor pressure that is caused by H<sup>+</sup>-ATPase and major osmoticum, including sugar, K<sup>+</sup>, and malate (Dhindsa et al. 1975). Increased expressions of sucrose and K<sup>+</sup> transporters that transport soluble sugar

and  $K^+$  from phloem in the vascular tissue to fiber cell were found to lead to an elevation of osmotic pressure (Smart et al. 1998; Ruan et al. 2001). PVP carboxylase that synthesizes malate has the highest expression level at 10- to 12-dpa, and decreases at 15-dpa. The expression level of vacuolar invertase was found to be a positive regulator of fiber length during 10-dpa (Wang et al. 2010c). Several genes that were associated with cell wall loosening, such as xyloglucan endotransferase/hydrolase (Lee et al. 2010), pectate lyase (Wang et al. 2010a), fascin-like arabinogalactan protein (Huang et al. 2013), expansin-related protein (Xu et al. 2012) and actin-binding protein (Wang et al. 2009), were found to have significant impacts on fiber length.

In addition to the inner strength of fiber cells, fiber cell extension usually accompanies changes in the orientation, organization and array of the cytoskeleton, including microfilament (actin) and microtubule (tubulin) cytoskeleton. Actin, a major component of microfilament cytoskeleton, plays an important role in fiber elongation, but not in initiation (Li et al. 2005). *GhADF1*, an actin depolymerizing factor (*ADF*) that dissociates actin, was found to suppress fiber length by altering cytoskeleton structure and cellulose contents (Wang et al. 2009). Profilin, an actin-binding protein that plays essential roles in many cellular processes, appeared to play a critical role in constructing microfilament cytoskeleton during fiber elongation. Overexpression of *GhPFN2* caused a pre-terminated elongation and earlier secondary cell wall deposition, thus reducing fiber length (Wang et al. 2010b). Silencing of *KATANIN*, a microtubule protein, resulted in shorter fiber than wild-type cotton, suggesting its essential role in the organization of microtubule cytoskeleton during fiber elongation (Qu et al. 2012).

Fiber length development is regulated by phytohormones and secondary metabolites as well, including ethylene (Shi et al. 2006), gibberellin (Xiao et al. 2010), flavonoid (Tan et al. 2013), and brassinosteroid (Sun et al. 2005; Shi et al. 2006). Exogenous gibberellin (GA) and ethylene have been extensively studied in promoting fiber initiation and elongation in cotton. Recently, a GA 20-oxidase gene (*GhGA20ox1*) was found to improve fiber initiation and elongation by regulating endogenous GA levels in fiber cells (Xiao et al. 2010). The 1-Aminocyclopropane-1-Carboxylic Acid Oxidase (*ACO*) gene responsible for ethylene production was also shown to have regulatory roles in fiber initiation and elongation. Brassinosteroids (BRs), regulators of normal plant growth and development, were reported to be required for fiber initiation and elongation (Sun et al. 2005). Antisense-mediated suppression of *GhDET2* that catalyzes a major rate reduction in BR biosynthesis showed both inhibited fiber initiation and elongation (Luo et al. 2007). Flavonoids, secondary metabolites in the plant kingdom, were found to improve the fiber elongation process (Tan et al. 2013).

Fiber cell expansion during the elongation stage is mediated by several transcription factors. *GaMYB2* encoding a GL1-like MYB protein and expressing in early developing fiber cells rescued the trichome formation when transformed into the *gh1* mutant in *Arabidopsis* and induced seed trichome formation (Wang et al. 2004). Knockdown of *GhMYB109* showed depressed fiber length, providing evidence that this *MYB*-regulated gene is induced before phytohormone biosynthesis and cytoskeleton biosynthesis during fiber initiation and elongation (Pu et al. 2008). *GhMYB25* was found to regulate fiber elongation, trichome development and seed production in cotton

(Machado et al. 2009). TCP transcription factor has the same effect as *GhMYB25* (Hao et al. 2012).

At present, numerous genes differentially expressed among various development stages and between different cultivated species have been studied extensively and reported by using fuzzless-lintless mutants, ESTs (Expressed Sequence Tag), and cDNA microarray hybridizations (Ruan et al. 2001; Ji et al. 2003; Arpat et al. 2004; Shi et al. 2006; Chaudhary et al. 2008; Hovav et al. 2008; Michailidis et al. 2009; Pang et al. 2010; Rapp et al. 2010; Wang and Ruan 2010; Kim et al. 2012; Lacape et al. 2012; Padmalatha et al. 2012; Avci et al. 2013; Li et al. 2013; Liu et al. 2013; Yoo and Wendel 2014). These comparative studies revealed potential key genes and biological pathways involved across different stages in cotton fiber development and cotton genome polyploidization. However, few genes that directly control fiber length during elongation have been cloned and characterized to date. The molecular basis and mechanisms of fiber length development largely remains unknown.

In order to isolate genes controlling fiber length in a more efficient manner, a novel high-throughput gene and quantitative trait locus (QTL) cloning system to clone and characterize genes and QTLs controlling the traits of agronomic importance was developed (patent filed). The objectives of this study were [1] to identify the genes controlling fiber length from cultivated cottons and [2] to use the isolated fiber genes to study the molecular basis and mechanisms of fiber length development. This study has not only cloned 474 genes controlling cotton UHML and allowed systems studies of the molecular basis and mechanisms underlying fiber length development, but also provided

new toolkits enabling development of gene-based breeding system in cotton. This will revolutionize the efficiencies of currently-used plant breeding methods, including marker-assisted breeding.

## 2. MATERIALS AND METHODS

### 2.1 Plant materials and fiber phenotyping

#### 2.1.1 Population selection and preparation

Four recombinant inbred line (RIL) populations at the  $F_{2:8}$  generation were developed by the Cotton Improvement Laboratory, Department of Soil and Crop Sciences, Texas A&M AgriLife Research, College Station, Texas. These populations were all developed from interspecific crosses between *G. hirsutum* and *G. barbadense*, including TAM 94L-25 x SI Barbados, TAM 94L-25 x NMSI 1331, NUSI 1331 x 97M-16, and NUSI 1331 x 97M-17. To find which of the populations was better suited for this study, all of them, including parents, were planted in a completely random design (CRD) in the Texas A&M Agrilife Research Farm near College Station, Texas in 2009. All cultural practices were common for upland cotton production in central and south Texas.

All mature bolls were hand-harvested from four random plants per line. Lint quality, including UHML, micronaire, strength, uniformity index (UI), and fiber elongation (ELONG) before break in the measurement of strength, was measured by High Volume Instrument (HVI) at the Fiber and Biopolymer Research Institute, Texas Tech University, Lubbock, Texas. Since the RIL population derived from TAM 94L-25 x NMSI 1331 was shown to have the most genetic variation in lint fraction, lint yield, micronaire, UHML, UI, strength, and ELONG, it was selected for this study. To

generate sufficient seeds for field trials, the TAM 94L-25/NMSI 1331 RIL population was planted in a greenhouse (day 82 F/night 75 F) located at the Institute for Plant Genomics and Biotechnology, Norman Borlaug Center for Southern Crop Improvement, Texas A&M University in December, 2009. Seeds were harvested from each of the RILs and parents.

### 2.1.2 Field trials for fiber phenomics

One hundred ninety-eight RILs were randomly selected from the TAM 94L-25/NMSI 1331 population for this study. In 2010 and 2011, the 198 RILs and their parents, TAM 94L-25, and NMSI 1331, were grown in randomized complete block designs (RCBD) with three replicates at the Texas A&M Agrilife Research Farm near College Station, Texas. The field practices followed those used in standard upland cotton production in Texas. When completely matured, all cotton bolls were hand-harvested from entire plots and ginned in the Cotton Improvement Laboratory, Texas A&M AgriLife Research, College Station, Texas. Cotton seed yield, lint yield and lint percentage data were collected. Fiber quality, including UHML, micronaire, strength, UI, ELONG, was measured by HVI in the Fiber and Biopolymer Research Institute, Texas Tech University, Lubbock, Texas. Therefore, the field trials were conducted, and the RILs and parents were phenotyped in yield and fiber traits for three years, with no replication for 2009 and three replicates for 2010 and 2011. The seeds of the RIL population harvested in 2010 and 2011 were stored in a cold room (4 °C) of the Cotton Improvement Laboratory, Texas A&M AgriLife Research, College Station, Texas.

## **2.2 Transcriptome sequencing and gene digital expression profiling**

### 2.2.1 RNA isolation and quality check

During cotton growth and development, 10-dpa fibers were collected from all entries of each of the RILs and parents in the 2010 field trial, and 0-dpa ovaries, 10-dpa fibers and 20-dpa fibers were collected from all entries of each of the RILs and parents in the 2011 field trial, utilizing two plants per entry. All tissues were frozen immediately in liquid nitrogen and then stored at -80 °C before use. For this study, only 10-dpa fibers collected from the first replicate of the 2011 field trial and those of the parents from different replicates in both 2010 and 2011 were analyzed. The tissues of 10-dpa fibers were analyzed because this stage of fiber development, as described above, is critical to fiber length development - the focus of this study.

Prior to RNA isolation, the 10-dpa fibers were ground into a fine powder in liquid nitrogen with mortar and pestle. RNA was isolated from each sample, following the manual of Spectrum™ Plant Total RNA Kit (Sigma Aldrich, USA). Briefly, approximately 100 mg of the fine 10-dpa fiber powder was transferred into a 1.5-ml frozen microtube, and 500 µl of the lysis buffer containing 0.1% of β-mercaptoethanol was added and mixed vigorously for 60 seconds. Then, the sample was lysed by incubation in a 56 °C water bath for five minutes. The lysate was filtered by the filtration column (Cat. No C6866, Sigma Aldrich, USA) seated in a 2-ml collection tube and supernatants collected. The filtration column was then discarded, 500 µl of the binding buffer was added to the tube containing the filtered supernatants and mixed thoroughly



by pipetting 6 –10 times. The mixture was transferred into the binding column (Cat. No C6991, Sigma Aldrich, USA) and centrifuged at room temperature and 14,000 rpm for two minutes. After all liquid flowed through the column, the binding column was washed once with 500 µl of the wash solution 1. Any contaminating DNA remaining in the RNA sample in the column was removed by digesting with DNase I (On-column DNase Digest Set, Sigma Aldrich, USA) at room temperature for 15 minutes.

After digestion, the binding column was washed again with 500 µl of wash solution 1 and centrifuged at 14,000 rpm for two minutes. Then, the binding column was washed two times with wash solution 2, 500 µl for each wash, and centrifuged at 14,000 rpm for two minutes. After all liquid flowed through the column, the binding column was transferred into a new 2-ml collection tube, 50 µl of elution buffer was added to the center of the binding column, and incubated at room temperature for two minutes. The total RNA from 10-dpa fiber samples was harvested with the flow-through liquid into the collection tube, and stored at -80°C. The quality and integrity of the isolated RNA was checked by Experion RNA StdSens chips (#700-715, Bio-Rad Laboratories, Inc., USA) and RNA quality indicator (RQI) on the microfluidics-based platforms (Experion Automated Electrophoresis System, Bio-Rad Laboratories, Inc., USA). The RNA with an RQI value of 9.0 or higher was used for further analysis.

### 2.2.2 Construction of RNA-seq cDNA libraries

The RNA-seq cDNA libraries were constructed from the RNAs using the Illumina TruSeq RNA Sample Prep Kit Version 2.0 - Sets A and B (Illumina, Inc., San

Diego, CA). First, 3 – 4  $\mu\text{g}$  of total RNA was purified twice by using poly-T oligo-attached magnetic beads. An equal volume of completely re-suspended RNA purification beads were added to the total RNA and mixed by gentle but thorough pipetting. To denature the RNA and facilitate binding of the poly-A mRNA to the beads, the samples were incubated in a thermal cycler at 65 °C for five minutes. After cooling at room temperature for five minutes, the sample mixtures were placed in a magnetic stand (Magnetic stand-96, Life Technologies, Cat. No. AM10027) for five minutes to collect the poly-A mRNA-bound beads. The supernatant was discarded, and 67  $\mu\text{l}$  of bead washing buffer was added to each sample to remove the unbound RNA by gently pipetting.

Seventeen microliters of the elution buffer was added to the samples and mixed by gentle pipetting. The mRNA and contaminant rRNA that bound non-specifically were eluted from the beads by incubating at 80 °C for two minutes and then holding at 25 °C. An equal volume of the bead binding buffer (17  $\mu\text{l}$ ) was added to the samples to specifically bind mRNA to the beads and reduce the non-specific binding of contaminating rRNA. After the mixture was incubated at room temperature for five minutes, it was placed on the magnetic stand for another five minutes. The supernatant was discarded, and the samples were removed from the magnetic stand and washed with the bead washing buffer again to remove residual rRNA and other contaminants.

The Elute, Prime and Fragment Mix that contains random hexamers for reverse transcription priming and serves as the first strand cDNA synthesis reaction buffer was added to the sample by gentle pipetting. The mRNA was eluted, fragmented and primed

by incubating at 94 °C for eight minutes then holding at 4 °C. After collecting clean primed RNA, the First Strand Master Mix and SuperScript II mix (1:9) was used to reverse-transcribe the mRNA into the first strand of cDNA by the following series of incubations: at 25 °C for 10 minutes, 42 °C for 50 minutes and 70 °C for 15 minutes followed by holding at 4 °C. Then, the Second Strand Master Mix was added and the reaction was incubated at 16 °C for one hour to facilitate the second strand cDNA synthesis.

To capture the double-strand cDNA, AMPure XP beads (Beckman Coulter Genomics, #A63881) were added to the reaction, mixed, and placed on the magnetic stand. After the beads bound with double-strand cDNA were washed twice with fresh 80% ethanol on the magnetic stand, the XP bead-pellets were dried at room temperature for five minutes and then gently mixed in the resuspension buffer. To make the cDNA blunt-ended, End Repair Mix was added to the sample and incubated at 30 °C for 30 minutes. As described above, AMPure XP beads were used again to purify the double-strand cDNA on a magnetic stand. Then, A-Tailing Mix was mixed with the sample and incubated at 37 °C for 30 minutes, 70 °C for five minutes and held at 4 °C to add a single 'A' nucleotide to the 3'-end of the end-blunted cDNA fragments.

Twenty-four specific indexing adapters were supplied with the Illumina's TruSeq RNA Sample Prep Kit. The indexing adapters were ligated to the ends of the double-strand cDNA, with one indexing adaptor per sample, using the ligation mix at 30 °C for 10 minutes. After ligation, ligation stop buffer was added to stop the ligation reaction. AMPure XP beads were used to purify the cDNA with indexing adapters, as described

above. Before sequencing, cDNA fragments were selectively amplified by Polymorphism Chain Reaction (PCR). PCR Primer Cocktail and PCR Master Mix were added to the sample and incubated at 98 °C for 30 seconds, 15 cycles of 98 °C for 10 seconds, 60 °C for 30 seconds and 72 °C for 30 seconds, 72 °C for 5 minutes, and 4 °C for hold. Amplified PCR products were purified with AMPure XP beads twice, as described above.

The quality and concentration of the amplified cDNA library was checked using the Experion 1K DNA Analysis Kit (Bio-Rad, cat #700-7104) on an Experion Automated Electrophoresis System (Bio-Rad, cat #700-7001). cDNA libraries were adjusted to a concentration of 10 nM using the resuspension buffer, and then were sequenced on HiSeq 2000 (Illumina, Inc., San Diego, CA) with a module of 100 PE (100 nucleotide paired ends) by BGI America (formerly Beijing Genomics Institute), Hong Kong. The quality and quantity of each sample were further validated with an Agilent 2100 Bioanalyzer (Agilent Technologies, Austin, TX) by BGI America before sequencing.

### 2.2.3 Multi-indexing strategy

The cDNA libraries were sequenced on HiSeq 2000 with a multi-indexing strategy using 24 indexes, with each library identified with one index. Therefore, 24 samples were multiplexed and sequenced on a flow cell lane of the HiSeq 2000 sequencer. The index sequences of the 24 adaptors supplied with the Illumina's TruSeq RNA Sample Prep Kits are ATCACG, CGATGT, TTAGGC, TGACCA, ACAGTG,

GCCAAT, CAGATC, ACTTGA, GATCAG, TAGCTT, GGCTAC, CTTGTA, AGTCAA, AGTTCC, ATGTCA, CCGTCC, GTCCGC, GTGAAA, GTGGCC, GTTTCG, CGTACG, GAGTGG, ACTGAT, and ATTCCT. Since the HiSeq 2000 sequencer can run two 8-lane flow cells each time, 384 samples can be sequenced per run.

## **2.3 Data analysis**

### 2.3.1 Phenomic data in field performance

Fiber traits, including UHML, micronaire, UI, strength, ELONG, seed weight, lint yield and lint percentage, were analyzed using customized R scripts (R 3.0.1). Statistics results were all validated by JMP, a computer program for statistics developed by the JMP business unit of the SAS Institute.

### 2.3.2 Genotypic data from RNA-seq cDNA library sequencing

#### 2.3.2.1 *de novo* assembly of transcriptome sequences

Library adaptors and nucleotide sequences containing more than 5% unknown nucleotides were removed from the raw sequence data. Low-quality sequencing reads, in which more than 20% of the nucleotides have reading scores of less than Q10 in a read, were also removed from the raw sequence data. Clean reads of each sample were assembled by a RNA-seq data analysis software, Trinity (version of r2013-02-25)

(Grabherr et al. 2011; Haas et al. 2013) on a server with 62 GB of RAM, allocating from eight multicores on a 3168-core IBM (iDataPlex) Linux cluster comprised of Nehalem and Westmere processors, at the Texas A&M Supercomputing Facility (<http://sc.tamu.edu/>), Texas A&M University, College Station, TX.

Due to lack of reference genome information for cultivated tetraploid cotton, the clean sequence reads of HiSeq 10-dpa fiber libraries of six biological replicates of the maternal parent, TAM 94L-25, harvested in 2011 were combined, assembled into a unigene set and used as a reference for gene expression profiling. A total of 85,755,752 100-nucleotide clean reads were used for the assembly. Based on the draft genome of *G. raimondii*, the full-length cDNAs of genes had an average of 2,485 bp (Wang et al. 2012). If tetraploid cottons have about 40,000 genes and approximately 60% of them are expressed in 10-dpa fibers, then, the 85,755,752 100-nucleotide clean reads would represent more than a 140X coverage of all the genes expressed in 10-dpa fibers.

#### 2.3.2.2 Expression level estimation

The expression level of each gene in 10-dpa fibers of each RIL was estimated by the abundance of 100-nucleotide reads among the Trinity transcripts of the TAM 94L-25 reference sequences. The original HiSeq 2000 clean reads of each of the 198 RILs and the parents were aligned to the TAM 94L-25 reference sequences using the modified version of RSEM (Li and Dewey 2011) within Trinity. RSEM is a software package that is widely used to accurately and digitally quantify gene expressions from RNA-Seq data with or without a reference genome.

### 2.3.3 Isolation of genes controlling UHML

The genes controlling UHML was isolated using a genome-wide high-throughput gene and QTL cloning and studying system recently developed in our laboratory. The system has currently been submitted to the Texas A&M AgriLife Innovation Management Office for disclosure and filing for a patent. It is based on the hypothesis that the genetic variation of a phenotypic trait results from gene sequence mutation, variation of gene expression, variation of gene action mode, variation of gene x gene interactions, variation of gene x non-gene element interactions such as related small RNA activities, and/or gene x environment interactions. Using this system, we have successfully cloned 1,253 genes controlling maize grain yield and 606 genes controlling chickpea vernalization and flowering. This system not only determines the function(s) of the genes, as do the current gene/QTL cloning methods, but also constructs the gene networks controlling the trait, determines their molecular basis and regulation mechanisms, and develops toolkits enabling gene-based breeding. Using the system, hundreds of genes controlling different agronomic traits can be cloned within a few scientist-years. The throughput of the new system is >1,000-fold higher than those of the current gene/QTL cloning methods such as map-based cloning, gene mutagenesis and RNA inference (RNAi), thus making it possible to large-scale and rapidly clone and molecularly characterize the genes controlling UHML.

The new gene and QTL cloning system isolates genes controlling a quantitative trait through four critical steps, with a cutoff for each step, although a single such step may be sufficient for isolation of genes controlling a quantitative trait according to the

currently-used gene and QTL cloning methods such as map-based cloning, gene mutagenesis and RNA interference (RNAi). Therefore, the genes isolated using the new gene and QTL cloning system has a confidence of at least 99.999375%, which is four-fold higher than those of the currently-used gene and QTL cloning methods. The genes isolated to control UHML were identified in this study as *Gossypium* fiber length (*GFL*) gene. An Arabic numeral suffix was added to indicate the order of genes isolated, such as *GFL001*, meaning the first UHML gene isolated from *Gossypium*.

#### 2.3.4 Systems analysis of the *GFL* genes controlling UHML

##### 2.3.4.1 Annotation and ontology of the *GFL* genes

The unigenes that were found to control UHML described above were blasted and annotated against the NCBI non-redundant protein database (the version as of September 30, 2013) using a minimal E-value cutoff of 1.0 E-06. The unigenes that were assigned to the same Genbank number and showed overlapping and identical sequences were first merged as a single gene and defined as a *GFL* gene. The *GFL* genes were then subjected to analyses of GO (Gene Ontology, a controlled vocabulary to describe gene product characteristics and gene product annotation data), gene-encoding enzyme functions and involved metabolism pathways against the InterProScan database and KEGG using blast2GO (Conesa et al. 2005; Conesa and Gotz 2008; Gotz et al. 2008; Gotz et al. 2011).



#### 2.3.4.2 Gene network construction

To determine whether there is any relationship in regulation and thus function among the *GFL* genes, the expression profiles of the *GFL* genes in 10-dpa fibers were subjected to correlation analysis by customized R scripts on Spearman's rank correlation using the entire RIL population. The visualization of the gene regulation interaction or network was performed by BioLayout *Expression*<sup>3D</sup> (Theocharidis et al. 2009).

### **2.4 Digital expression profiling of genes actively expressed in the 10-dpa fibers of diploid cottons**

To determine the evolution of the molecular mechanisms underlying UHML during cotton polyploidization, 10-dpa fibers were collected from diploid cotton species, including *G. herbaceum* (A<sub>1</sub>), *G. arboreum* (A<sub>2</sub>), *G. thurberi* (D<sub>1</sub>), *G. davidsonii* (D<sub>3</sub>), *G. aridum* (D<sub>4</sub>), *G. raimondii* (D<sub>5</sub>), and *G. gossypoides* (D<sub>6</sub>), at the Crop Germplasm Unit of USDA/ARS, College Station, TX. The same procedures as those described above were used to isolate RNAs from the tissues and to construct and index the RNA-seq cDNA libraries. The indexed RNA-seq cDNA libraries were sequenced on HiSeq 2000 by BGI America, Hong Kong.

Clean reads of the RNA-seq sequences of diploid cottons were aligned to the *GFL* genes isolated from the tetraploid cottons using the RSEM to quantify the expression levels of the genes in diploid cottons. The diploid orthologues of the *GFL* genes were identified and the network of the orthologues was constructed, as described

above for the network construction of the *GFL* genes in tetraploid cotton using the BioLayout *Expression*<sup>3D</sup>.

### 3. RESULTS

#### 3.1 UHML genetic variation in the RIL population

The UHML of the TAM 94L-25 x NMSI 1331 RIL population was phenotyped by field trials over three years (Table 1). In 2009, the population had an average UHML of 28.5 mm, ranging from 23.62 mm to 33.53 mm with a variation of 41.96%. In 2010, the field trial had three replicates and the population averaged an UHML of 28.61 mm, ranging from 23.11 mm to 35.05 mm with a variation of 51.67%. In 2011, the trial also included three replicates, and the population exhibited an average UHML of 28.83 mm, with a range from 23.03 mm to 34.80 mm and a variation of 51.10%. Moreover, the fiber length of the population was quite uniform, with a UI of greater than 80% over all three years of the field trials (Table 2; Figs 1 – 4).

**Table 1** Fiber UHML (mm) of the RIL population during 2009-2011

|              | 2011  |       |       |              | 2010  |       |       |              | 2009         |
|--------------|-------|-------|-------|--------------|-------|-------|-------|--------------|--------------|
|              | Rep1  | Rep2  | Rep3  | Average      | Rep1  | Rep2  | Rep3  | Average      | Average      |
| Min          | 21.59 | 23.11 | 23.62 | <b>23.03</b> | 23.11 | 23.11 | 23.62 | <b>23.11</b> | <b>23.62</b> |
| 1st Quantile | 27.69 | 27.18 | 27.18 | <b>27.43</b> | 26.92 | 27.43 | 26.92 | <b>27.18</b> | <b>27.18</b> |
| Median       | 29.21 | 28.19 | 28.70 | <b>28.70</b> | 28.45 | 28.70 | 28.19 | <b>28.62</b> | <b>28.45</b> |
| 3rd Quantile | 30.73 | 30.23 | 29.97 | <b>30.14</b> | 30.23 | 29.97 | 29.97 | <b>29.97</b> | <b>29.97</b> |
| Max          | 35.56 | 34.54 | 34.80 | <b>34.80</b> | 35.05 | 32.51 | 34.04 | <b>35.05</b> | <b>33.53</b> |
| Range        | 13.97 | 11.43 | 11.18 | <b>11.77</b> | 11.94 | 9.40  | 10.41 | <b>11.94</b> | <b>9.91</b>  |
| Mean         | 29.22 | 28.56 | 28.66 | <b>28.83</b> | 28.57 | 28.68 | 28.43 | <b>28.61</b> | <b>28.48</b> |
| SD           | 2.30  | 2.24  | 2.13  | <b>2.02</b>  | 2.27  | 1.99  | 2.13  | <b>2.12</b>  | <b>1.95</b>  |
| Skew         | 0.01  | 0.14  | 0.15  | <b>0.12</b>  | 0.18  | -0.33 | 0.18  | <b>0.16</b>  | <b>-0.07</b> |
| Kurtosis     | 0.27  | -0.19 | -0.04 | <b>0.10</b>  | -0.14 | -0.25 | -0.34 | <b>0.03</b>  | <b>-0.40</b> |
| SE           | 0.16  | 0.16  | 0.15  | <b>0.14</b>  | 0.20  | 0.17  | 0.19  | <b>0.16</b>  | <b>0.14</b>  |

**Table 2** Uniformity index (%) of the RIL population during 2009-2011

|              | 2011  |       |       |              | 2010  |       |       |              | 2009         |
|--------------|-------|-------|-------|--------------|-------|-------|-------|--------------|--------------|
|              | Rep1  | Rep2  | Rep3  | Average      | Rep1  | Rep2  | Rep3  | Average      | Average      |
| Min          | 76.20 | 73.00 | 72.90 | <b>75.23</b> | 75.40 | 76.70 | 76.10 | <b>76.75</b> | <b>73.30</b> |
| 1st Quantile | 80.75 | 79.50 | 79.70 | <b>80.20</b> | 80.20 | 80.25 | 79.58 | <b>79.97</b> | <b>79.50</b> |
| Median       | 82.10 | 81.30 | 81.40 | <b>81.57</b> | 81.30 | 81.40 | 80.95 | <b>81.00</b> | <b>81.00</b> |
| 3rd Quantile | 83.40 | 82.50 | 82.80 | <b>82.62</b> | 82.40 | 82.55 | 82.10 | <b>82.20</b> | <b>81.90</b> |
| Max          | 86.70 | 85.50 | 85.60 | <b>85.23</b> | 84.40 | 85.70 | 84.70 | <b>84.80</b> | <b>84.80</b> |
| Range        | 10.50 | 12.50 | 12.70 | <b>10.00</b> | 9.00  | 9.00  | 8.60  | <b>8.05</b>  | <b>11.50</b> |
| Mean         | 81.93 | 80.96 | 81.16 | <b>81.36</b> | 81.05 | 81.24 | 80.76 | <b>80.94</b> | <b>80.63</b> |
| SD           | 2.07  | 2.14  | 2.15  | <b>1.77</b>  | 1.81  | 1.77  | 1.79  | <b>1.63</b>  | <b>1.99</b>  |
| Skew         | -0.51 | -0.51 | -0.64 | <b>-0.54</b> | -0.71 | -0.36 | -0.19 | <b>-0.33</b> | <b>-0.57</b> |
| Kurtosis     | 0.01  | 0.26  | 0.31  | <b>0.28</b>  | 0.20  | -0.16 | -0.45 | <b>-0.30</b> | <b>0.51</b>  |
| SE           | 0.15  | 0.16  | 0.15  | <b>0.12</b>  | 0.16  | 0.15  | 0.16  | <b>0.13</b>  | <b>0.14</b>  |

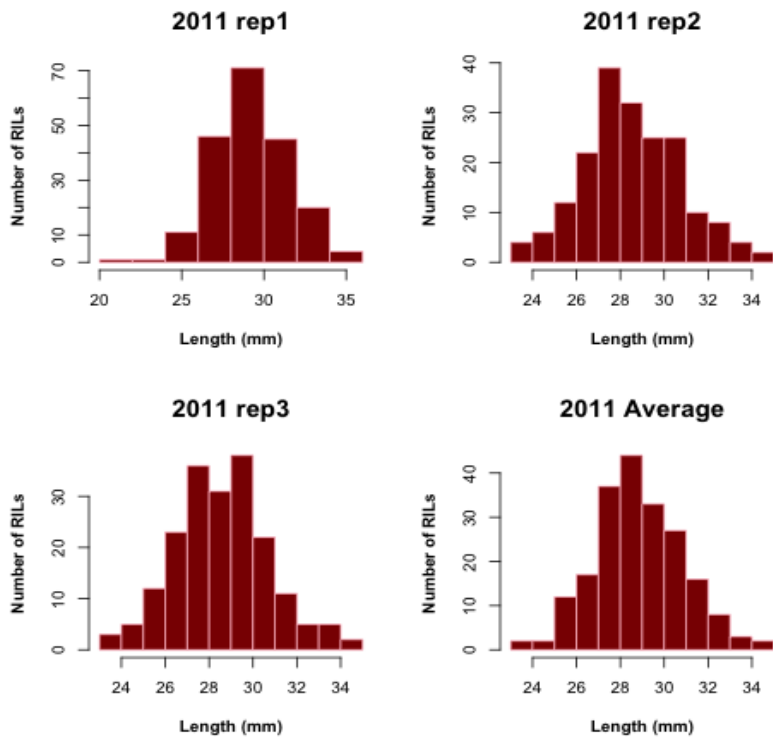


**Figure 1** UHML distributions in the TAM 94L-25 x NMSI 1331 RIL population in 2011

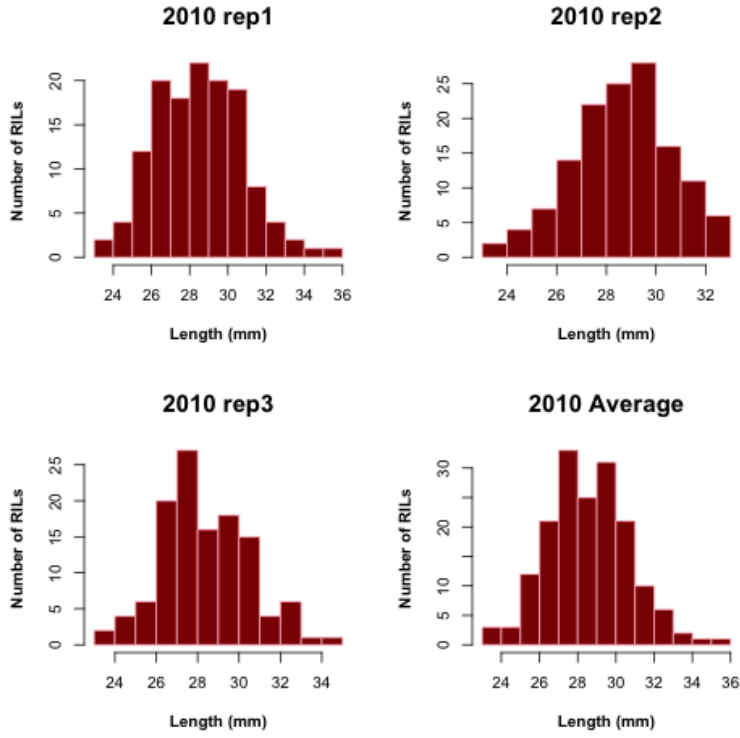


**Figure 2** UHML distributions in the TAM 94L-25 x NMSI 1331 RIL population in 2010

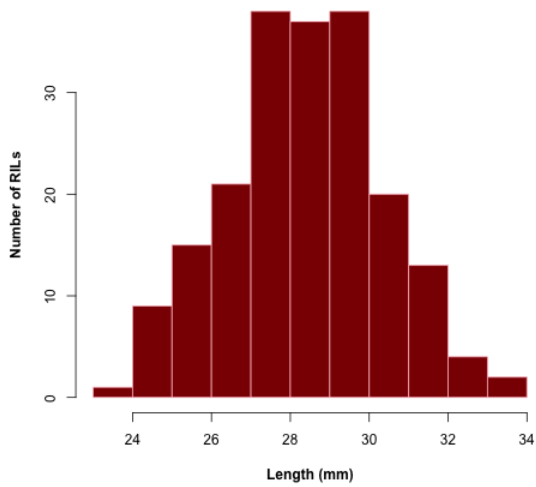


**Figure 3** UHML distributions in the TAM 94L-25 x NMSI 1331 RIL population in 2009

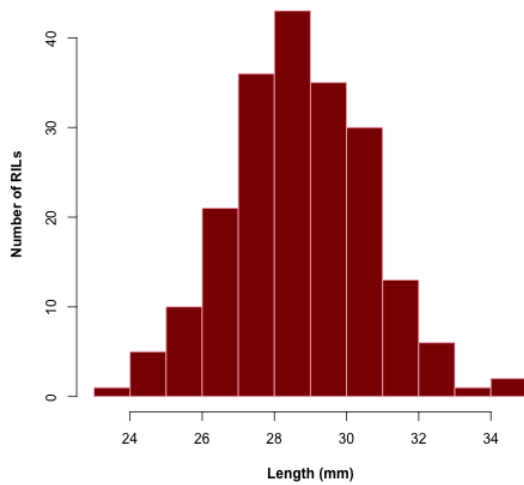


**Figure 4** Average UHML distribution in the TAM 94L-25 x NMSI 1331 RIL population during 2009-11

To check the reproducibility of the fiber phenomic results, we calculated the correlations of the fiber traits, especially UHML, between replicates and between years. Significant correlations of UHMLs were observed between replicates within a year (Figs. 5 – 6) with a correlation coefficient of 0.80 – 0.85 ( $P \leq 0.05$ ) in 2010 and of 0.76 ( $P \leq 0.05$ ) in 2011, and between years, with a correlation coefficient of 0.67 – 0.96 ( $P \leq 0.05$ ) (Table 3 and Fig. 7). These results indicated that the UHML of the RIL population studied in this research was reproducible within and between years.

**Table 3** Pearson's correlation of UHMLs between 2009, 2010 and 2011. "\*" indicates  $P \leq 0.05$ .

| Year     | 2009  | 2010  | 2011  | 3yr-aver |
|----------|-------|-------|-------|----------|
| 2009     | 1     |       |       |          |
| 2010     | 0.72* | 1     |       |          |
| 2011     | 0.67* | 0.91* | 1     |          |
| 3yr-aver | 0.87* | 0.96* | 0.94* | 1        |

The asterisk "\*" indicates  $P \leq 0.05$ .

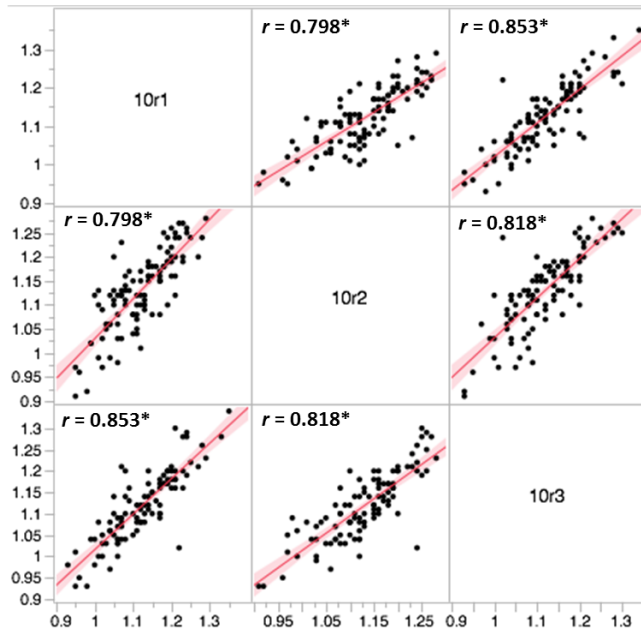


**Figure 5** Correlations of UHMLs of the TAM 94L-25 x NMSI 1331 RIL population between replicates in 2010. “\*” indicates  $P \leq 0.05$ .

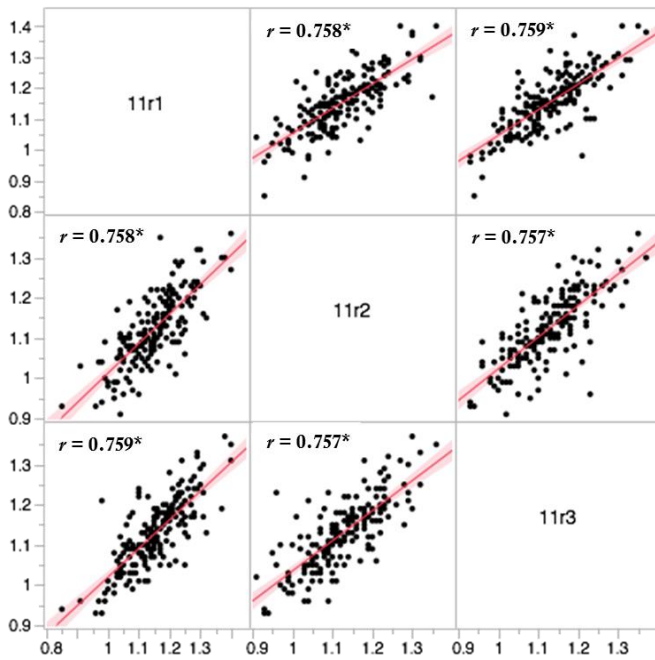


**Figure 6** Correlations of UHMLs of the TAM 94L-25 x NMSI 1331 RIL population between replicates in 2011. “\*” indicates  $P \leq 0.05$ .

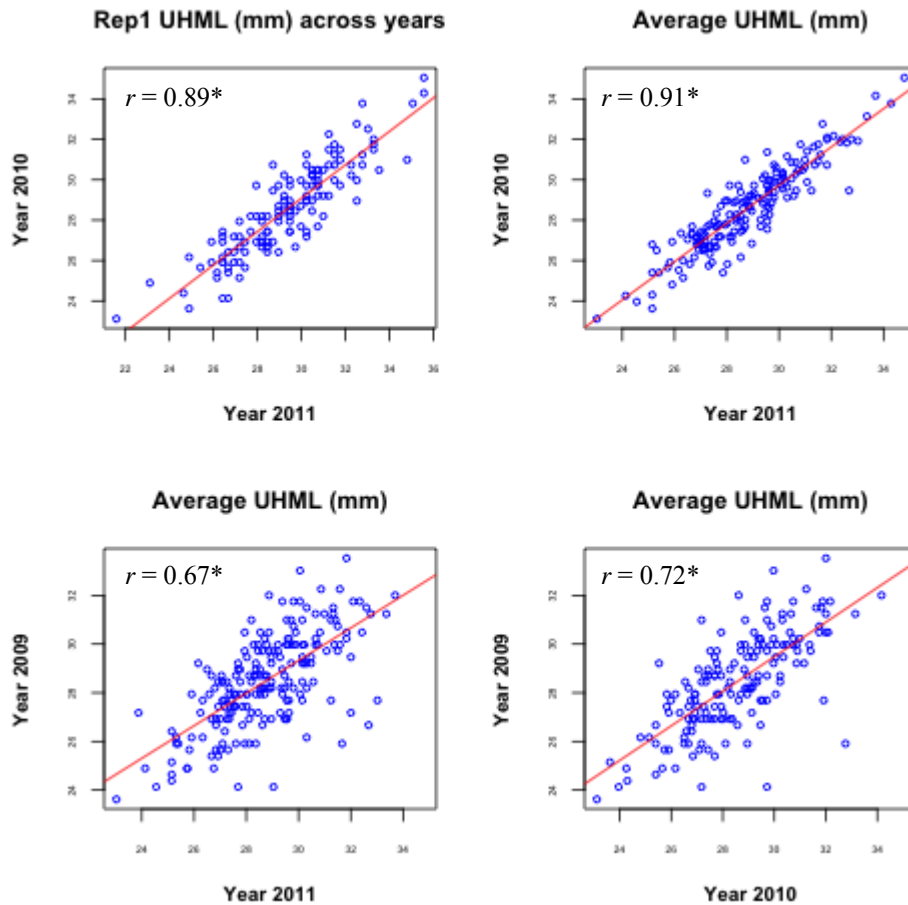


**Figure 7** Correlations of UHMLs of the TAM 94L-25 x NMSI 1331 RIL population between 2010 and 2011. “\*” indicates  $P \leq 0.05$ .

Pearson’s correlation test was also used to test the association relationship between UHML and other quality and yield traits, including micronaire, UI, strength, ELONG, cotton seed yield, cotton lint yield, and lint percentage. The values used in the analyses were the average values of three replicates in 2011 among TAM 94L-25, NMSI 1331 and their RILs (Table 4). In TAM 94L-25, UHML significantly correlated with strength, UI, and ELONG, whereas UHML significantly correlated with UI only in



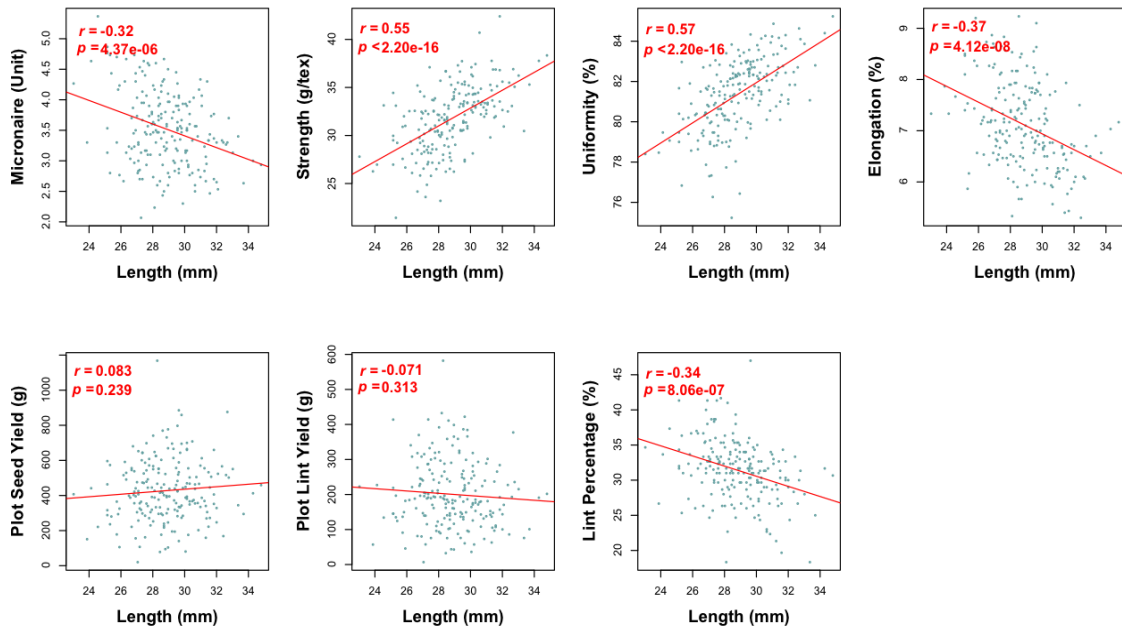
NMSI 1331. In the RIL population, UHML showed similar correlation relationships with fiber strength, UI, and ELONG as their upland cotton parent, TAM 94L-25, while it showed significant and negative correlations with micronaire and lint yield percentage (Fig. 8). These results agreed with the findings of Ulloa and Meredith (2000) and Karademir et al. (2010). Both of them reported strong positive correlations between UHML and strength, and negative correlations between UHML and micronaire. Hence, the results suggest that the UHML of this population could be improved simultaneously with strength and uniformity by UHML selection, while lint percentage and micronaire may be reduced.

**Table 4** Pearson’s correlation coefficients of HVI traits. (a) TAM 94L-25 (n = 6), (b) NMSI 1331 (n = 4), and (c) the RIL population (n = 198) in 2011. LP, Lint Percentage; MIC, Micronaire; UHML, Upper half mean length; STR, Strength; UI, Uniformity index; ELONG, Elongation. (\*) indicates  $P \leq 0.05$ , (\*\*) indicates  $P \leq 0.01$ , and (\*\*\*) indicates  $P \leq 0.001$  at the two-tailed test.

| a. TAM 94L25 |        |        |          |          |        | b. NMSI 1331 |         |          |         |          |       |
|--------------|--------|--------|----------|----------|--------|--------------|---------|----------|---------|----------|-------|
|              | LP     | MIC    | UHML     | STR      | UI     |              | LP      | MIC      | UHML    | STR      | UI    |
| MIC          | 0.367* |        |          |          |        | MIC          | 0.495** |          |         |          |       |
| UHML         | -0.042 | 0.110  |          |          |        | UHML         | 0.127   | -0.015   |         |          |       |
| STR          | -0.024 | 0.066  | 0.694*** |          |        | STR          | 0.403*  | 0.923*** | 0.263   |          |       |
| UI           | 0.200  | 0.385* | 0.546**  | 0.560*** |        | UI           | 0.133   | 0.479**  | 0.517** | 0.596*** |       |
| ELONG        | 0.111  | -0.061 | -0.433*  | -0.342   | -0.097 | ELONG        | -0.059  | 0.263    | -0.266  | 0.286    | 0.133 |

| c. 2011 RILs |           |           |           |          |       |
|--------------|-----------|-----------|-----------|----------|-------|
|              | LP        | MIC       | UHML      | STR      | UI    |
| MIC          | 0.627***  |           |           |          |       |
| UHML         | -0.338*** | -0.316*** |           |          |       |
| STR          | -0.027    | 0.197**   | 0.554***  |          |       |
| UI           | 0.110     | 0.301***  | 0.570***  | 0.804*** |       |
| ELONG        | 0.252***  | 0.356***  | -0.373*** | 0.05     | 0.512 |



**Figure 8** Correlations of UHML with other HVI traits in the TAM 94L-25 x NMSI 1331 RIL population in 2011

## 3.2 Transcriptome sequencing and digital expression profiling

### 3.2.1 Development of strategies for sequencing and expression profiling of the genes expressed in 10-dpa fibers of the RIL population

To isolate the genes controlling the UHML in the RIL population using our newly-developed genome-wide high-throughput gene and QTL cloning system, we need both the nucleotide sequences and expression profiles of all genes expressed in developing fibers of the population. We carried out the field trial for three years, with a total of seven replicates. The question was whether we should sequence the nucleotide sequences and profile the expressions of all the genes expressed in every replicate or just one of them. To answer the questions, we first sequenced and profiled the genes

expressed in 10-dpa fibers collected from eight plants of the maternal parent, TAM 94L-25 and four plants of the paternal parent, NMSI 1331 using a 100 PE (100-nucleotide paired end) sequencing module. Of the eight TAM94L-25 plants, three were collected from Rep 1 and three from Rep 2 in 2011, and two from Rep 1 in 2010. Of the four NMSI 1331 plants, two were from Rep 1 in 2011 and two from Rep 1 in 2010. A number between 11.5 million to 15.3 million 100-bp clean reads was obtained for each biological replicate of the parents. Clean reads were defined as the sequence reads whose adaptor sequences have been removed and that have less than 5% of unknown nucleotides and less than 20% of nucleotides having a sequence quality of Q10, a base calling error rate of one out of 10 times of calling.

Several computer programs specifically designed for RNA-seq assembly using short nucleotide sequence reads have been developed and available to public. To determine which of the programs is better for assembling 100-nucleotide clean reads generated from transcriptome sequencing in this study into unigene contigs, we tested two programs that have been widely used for such research, Trinity and SOAPdenovo (Table 5). The clean reads of RNA-seq from eight biological replicates of the RIL population parental lines were assembled, individually, for this experiment. Although the Trinity program can directly assemble the 100-nucleotide (bp) paired-end clean reads into unigene contigs, the SOAPdenovo program cannot do so; it can only assemble 31-, 63- or 127-nucleotide clean reads. Therefore, the 100-nucleotide paired-end clean reads of each sample were randomly clipped into 63-nucleotide short sequences and then assembled together when using SOAPdenovo. The results showed that in all assemblies,

Trinity assembled many fewer and much larger unigene contigs than SOAPdenovo. Either the mean size or N50 size of the unigene contigs assembled by Trinity was much larger than those assembled by SOAPdenovo (Figs. 9 and 10). N50 is determined as the size of the contigs when the sum of the larger contigs reaches half of the total length of the assembled contigs. Wang et al. (2012) reported that *G. raimondii*, a relative of the D subgenome of the tetraploid cottons, has an average transcript size of 2,485 bp. Therefore, the mean length and N50 size of unigene contigs assembled by SOAPdenovo appeared to be far smaller than the average transcript length of *G. raimondii*. On the other hand, because Trinity could assemble the 100-nucleotide clean reads of our RNA-seq into much larger unigene contigs and provide a well-organized downstream analysis and data visualization, it was selected and used for unigene assembly in this study.

Due to the absence of reference genome information for cultivated tetraploid cotton, unigene contigs were assembled from the clean reads of six biological replicates of the maternal parent, TAM 94L25, and four biological replicates of the paternal parent, NMSI 1331, grown in 2011. The unigenes were assembled from the clean reads that combined the clean reads from 1, 3, 4, and 6 biological replicates of the parents (Table 6). The result showed that more clean reads were combined and used, more unigene contigs were assembled, giving longer unigene contigs, larger N50 and N90 sizes.

**Table 5** Preliminary examination of computer programs, Trinity and SOAPdenovo, for *de novo* assembly of 100bp clean reads generated from RNA-seq of the parental lines of the TAM 94L-25 x NMSI 1331 RIL population

| Parent line              | TAM 94L-25 | TAM 94L-25 | NMSI 1331 | NMSI 1331 | TAM 94L-25 | TAM 94L-25 | NMSI 1331 | NMSI 1331 |
|--------------------------|------------|------------|-----------|-----------|------------|------------|-----------|-----------|
| Year                     | 2011       | 2011       | 2011      | 2011      | 2010       | 2010       | 2010      | 2010      |
| Replicate                | 1          | 1          | 1         | 1         | 1          | 1          | 2         | 2         |
| Entry ID                 | 1080       | 1220       | 1150      | 1210      | 1060       | 1120       | 2030      | 2050      |
| Clean reads (100 PE)     | 13772920   | 13390508   | 15291936  | 13264046  | 12157416   | 12482222   | 11473044  | 13731484  |
| <b>SOAPdenovo</b>        |            |            |           |           |            |            |           |           |
| No. of contigs           | 120526     | 118520     | 110109    | 102507    | 118606     | 101141     | 99209     | 98018     |
| Mean length (nuclotides) | 229        | 301        | 297       | 304       | 303        | 301        | 302       | 301       |
| Max length (nuclotides)  | 3156       | 3453       | 6178      | 4825      | 3623       | 10141      | 3476      | 4793      |
| N50 (nuclotides)         | 322        | 325        | 321       | 325       | 325        | 324        | 323       | 326       |
| N90 (nuclotides)         | 190        | 191        | 189       | 192       | 192        | 191        | 192       | 190       |
| Min length (nuclotides)  | 100        | 100        | 100       | 100       | 100        | 100        | 100       | 100       |
| <b>Trinity</b>           |            |            |           |           |            |            |           |           |
| No. of contigs           | 78338      | 76282      | 70897     | 68401     | 79293      | 67557      | 67463     | 61916     |
| Mean length (nuclotides) | 785.75     | 803.97     | 806.25    | 774.72    | 791.26     | 740.08     | 757.63    | 759.67    |
| Max length (nuclotides)  | 9261       | 10898      | 24022     | 17387     | 10509      | 11847      | 8558      | 8183      |
| N50 (nuclotides)         | 1223       | 1283       | 1263      | 1224      | 1249       | 1143       | 1183      | 1190      |
| N90 (nuclotides)         | 326        | 325        | 326       | 312       | 323        | 307        | 312       | 313       |
| Min length (nuclotides)  | 201        | 201        | 201       | 201       | 201        | 201        | 201       | 201       |

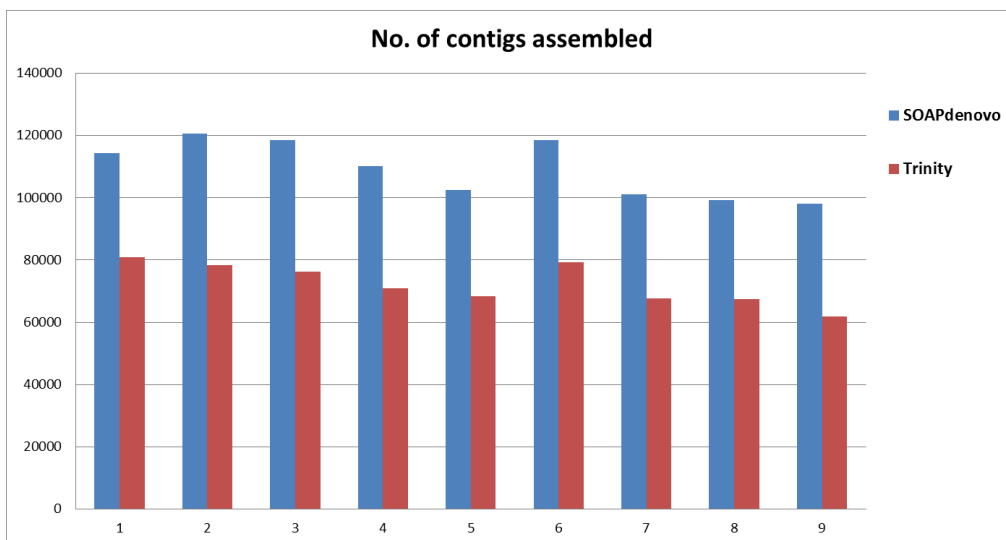


**Figure 9** Unigene contigs assembled with SOAPdenovo and Trinity. The x-axis shows the biological replicates of the TAM 94L-25 x NMSI 1331 RIL population parental lines in 2011 and 2010: 1, RIL-1146; 2, 1080; 3, 1220; 4, 1150; 5, 1210; 6, 1060 (2010); 7, 1120 (2010); 8, 2030 (2010); 9, 2050 (2010).

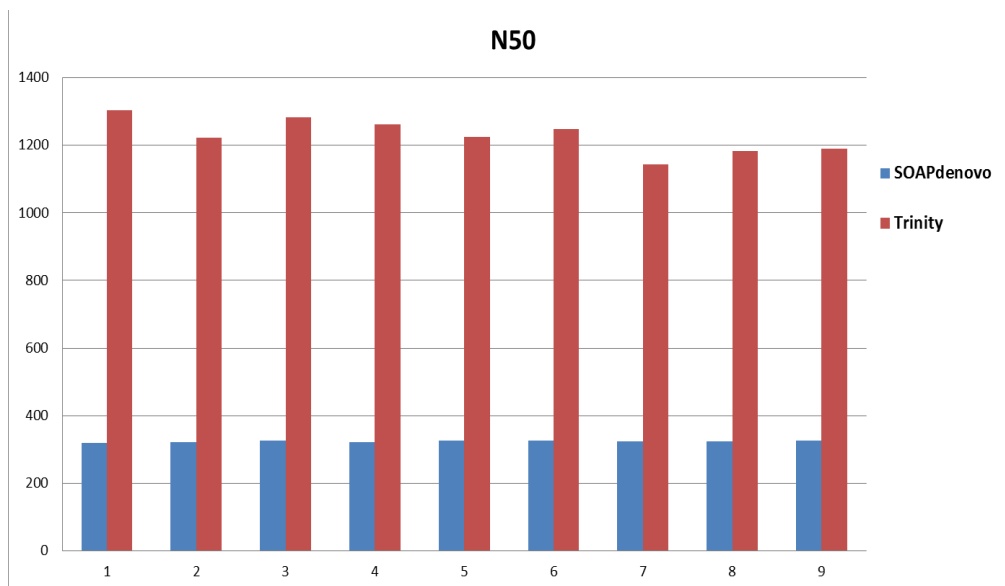


**Figure 10** N50 of unigenes assembled with SOAPdenovo and Trinity. The x-axis shows the biological replicates of the TAM 94L-25 x NMSI 1331 RIL population parental lines in 2011 and 2010: 1, RIL-1146; 2, 1080; 3, 1220; 4, 1150; 5, 1210; 6, 1060 (2010); 7, 1120 (2010); 8, 2030 (2010); 9, 2050 (2010).

Therefore, the unigenes assembled from six replicates of the maternal parent, TAM 94L-25, were selected and used to be the unigene reference sequences in this study. A total of 85,755,752 100-nucleotide clean reads were generated from the six biological replicates of the maternal parent, TAM 94L-25. Assembly of these reads by Trinity resulted in a total of 159,936 unigenes, with a N50 of 1,746 bp and an average length of 1,071.6 bp, ranging from 201 bp to 19,507 bp.

**Table 6** Preliminary examination of assembling unigene reference sequences from the parental lines of the RIL population using Trinity

|            | No. of sample assembled | No. of clean reads at each end | No. of unigenes | Average length | Max length | Min length | N50   | N90 |
|------------|-------------------------|--------------------------------|-----------------|----------------|------------|------------|-------|-----|
| TAM 94L-25 | x1                      | 6,886,460                      | 78,338          | 786            | 9,261      | 201        | 1,223 | 326 |
|            | x3                      | 19,668,055                     | 117,999         | 751            | 9,917      | 201        | 1,116 | 319 |
|            | x6                      | 42,877,876                     | 159,936         | 1,072          | 19,507     | 201        | 1,746 | 451 |
| NMSI 1331  | x1                      | 7,618,243                      | 77,624          | 787            | 9,261      | 201        | 1,265 | 316 |
|            | x4                      | 28,882,178                     | 132,986         | 1,018          | 29,210     | 201        | 1,685 | 416 |

To answer the question of how many biological replicates of each RIL or parent should be used to profile the expression abundances of the genes expressed in 10-dpa fibers, the clean reads of each biological replicate was aligned to the reference unigene sequences assembled from the six biological replicates of the maternal parent, TAM 94L-25 and the expression level of each gene presented in transcript per million reads (TPM) were calculated using Trinity. The expression levels of each biological replicate were compared between different plants within a replicate, between replicates within the same year, and between years (2010 and 2011) using those of the maternal parent, TAM 94L-25. The result showed that there were significant and strong association between

plants within a field trial replicate ( $r = 0.9713$ ,  $P < 0.0001$ ), between field trial replicates within the same year ( $r = 0.9813$ ,  $P < 0.0001$ ) and between years ( $r = 0.9636$ ,  $P < 0.0001$ ) (Figs. 11 and 12). This result indicated that it was acceptable to profile the expression of the genes expressed in 10-dpa fibers just for one biological replicate for a parent or an RIL.

Therefore, the first replicate (Rep 1) in the 2011 field trial was selected for sequencing and profiling the expression abundances of the genes expressed in 10-dpa fibers of the entire RIL population. This replicate had the widest genetic variation among all seven replicates in UHML (Table 1). It had an average UHML of 29.22 mm, with a range from 21.59 mm to 35.56 mm and a standard deviation of 2.30 mm ( $CV = 7.87\%$ ). The average fiber uniformity of the population was 81.93% in 2011, with a range from 76.2% to 86.7%. These results indicated that it had sufficient fiber length variations for the study.

### 3.2.2 Transcriptome sequencing and expression profiling of the genes expressed in 10-dpa fibers of the entire RIL population

The genes expressed in 10-dpa fibers of all 198 RILs were sequenced and profiled in expression using the same 100 PE sequencing module and the same multiplex method as those used above for their parents. A total of 2.686 billion of 100-nucleotide paired-end RNA-Seq clean reads were obtained for the entire TAM 94L-25 x NMSI 1331 RIL population (Table 7). An average of 13.23 million 100-nucleotide paired-end



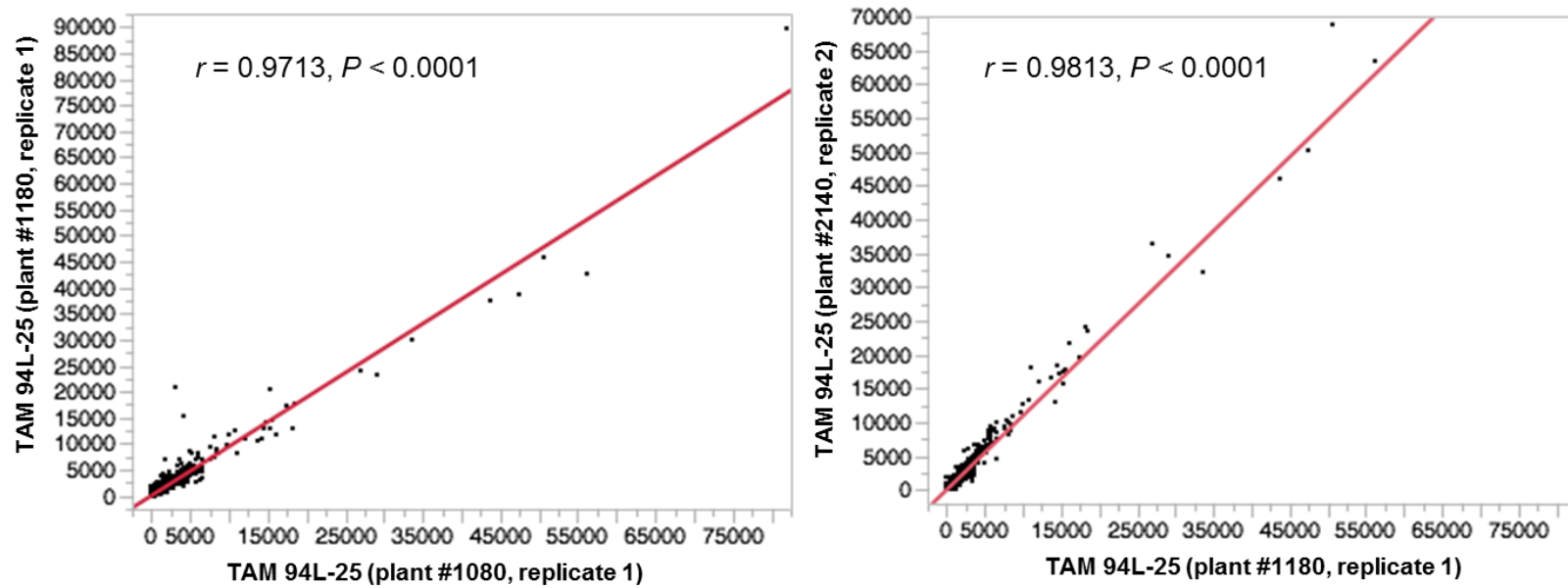


**Figure 11** Correlation of expression levels (TPM) of genes in 10-dpa fibers between plants within a replicate (left) and between replicates (right) of the female parent, TAM 94L-25, in 2011

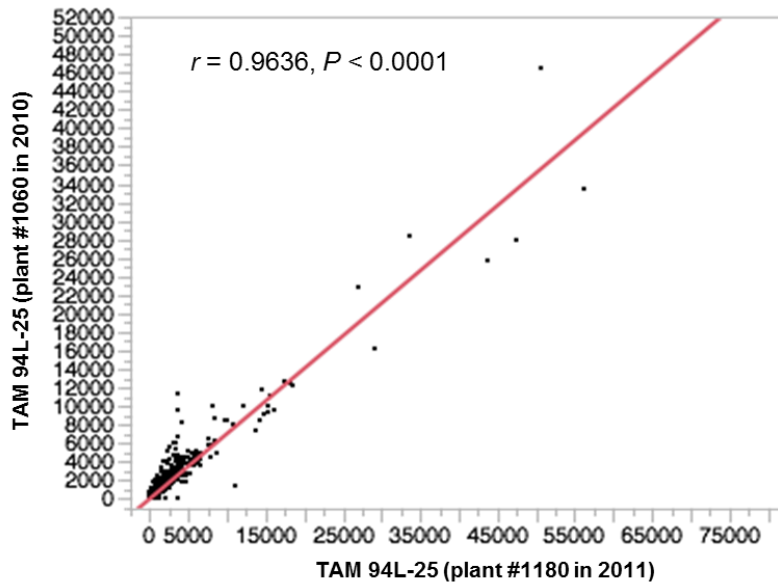


**Figure 12** Correlation of expression levels (TPM) of genes in 10-dpa fibers of the female parent, TAM 94L-25, between 2010 and 2011

clean reads were sequenced for each RIL, with a range from 7 million to 19 million of clean reads (Fig. 13 and Table 7). The Q20, which represents a base calling error rate of one out of 100 times of calling, averaged 98.74%, with a range from 96.43% to 99.07% (Table 7 and Fig. 14). The clean reads of the RNA-seq had an average GC content of 44.21%, ranging from 43.13% to 50.61% among the 198 RILs and two parents (Table 7 and Fig. 15).

**Table 7** Summary of RNA-Seq in 100-nucleotide paired end reads for 198 RILs and 2 parents. TAM 94L-25 had three biological replicates and NMSI 1331 had two biological replicates

|                       | Total      | Mean        | Maximum  | Minimum |
|-----------------------|------------|-------------|----------|---------|
| Number of Clean Reads | 2686403478 | 13233514.67 | 19044152 | 6608566 |
| Q20                   |            | 98.74       | 99.07    | 96.43   |
| QC (%)                |            | 44.21       | 50.61    | 43.13   |

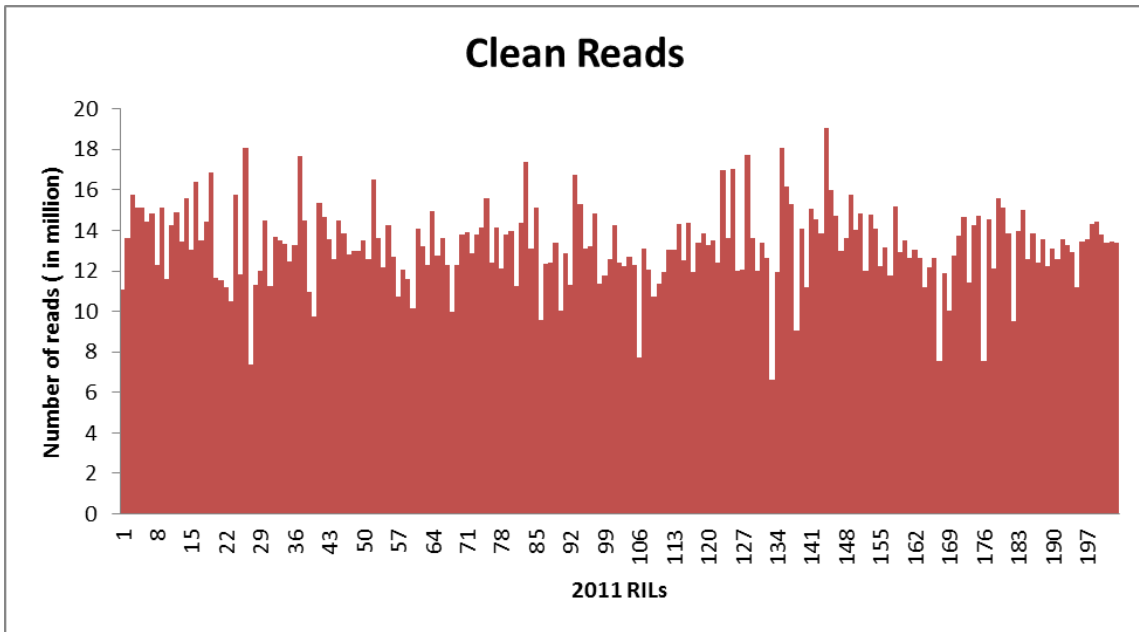


**Figure 13** Distribution of numbers of 100-nucleotide (bp) clean reads derived from RNA-Seq among the 198 RILs and 2 parents

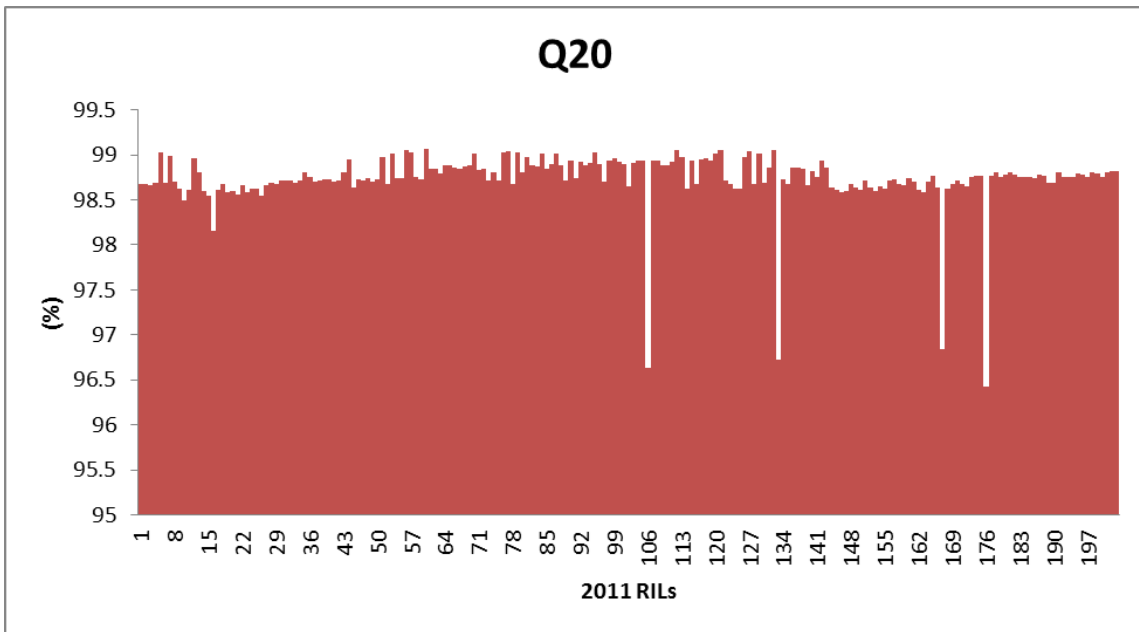


**Figure 14** Distribution of Q20 of the RNA-Seq reads with a quality of Q20 or higher among the 198 RILs and 2 parents

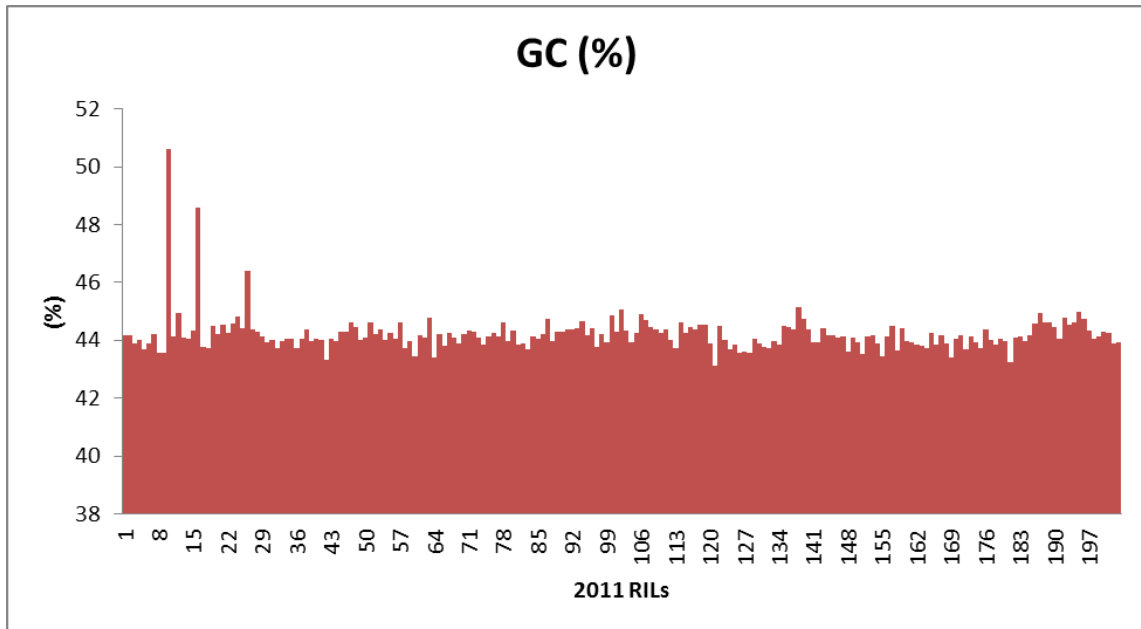


**Figure 15** Distribution of GC content of the sequence reads derived from RNA-Seq among the 198 RILs and 2 parents

### 3.2.3 *de novo* assembly of 100-nucleotide clean reads for RILs

Unigene contigs were assembled from 100-nucleotide clean reads of the RNA-seq with the program Trinity for the 198 RILs derived from an interspecific cross between TAM 94L-25 and NMSI 1331. A total of 14.86 million unigene contigs were assembled for the RILs, with an average of 73,185 unigene contigs for each RIL. The average length of assembled unigenes for each RIL was 778.17 bp, with an average N50 size of 1,215 bp, ranging from 201 bp to 14,378 bp (Figs 16 and 17).

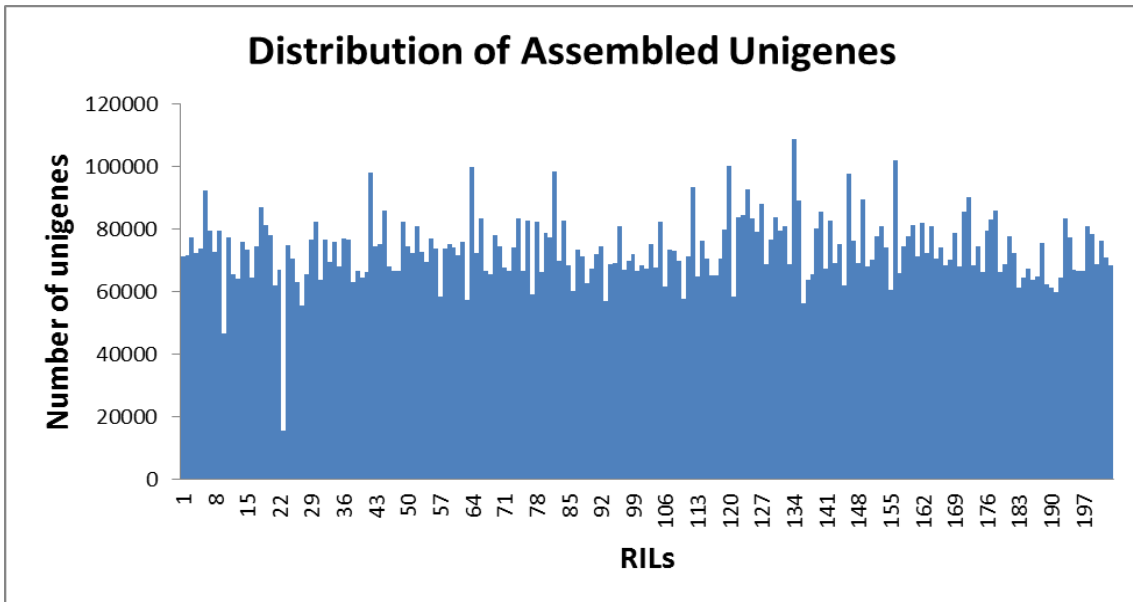


**Figure 16** Unigenes assembled with Trinity for each of the 198 RILs of the TAM 94L-25 x NMSI 1331 population

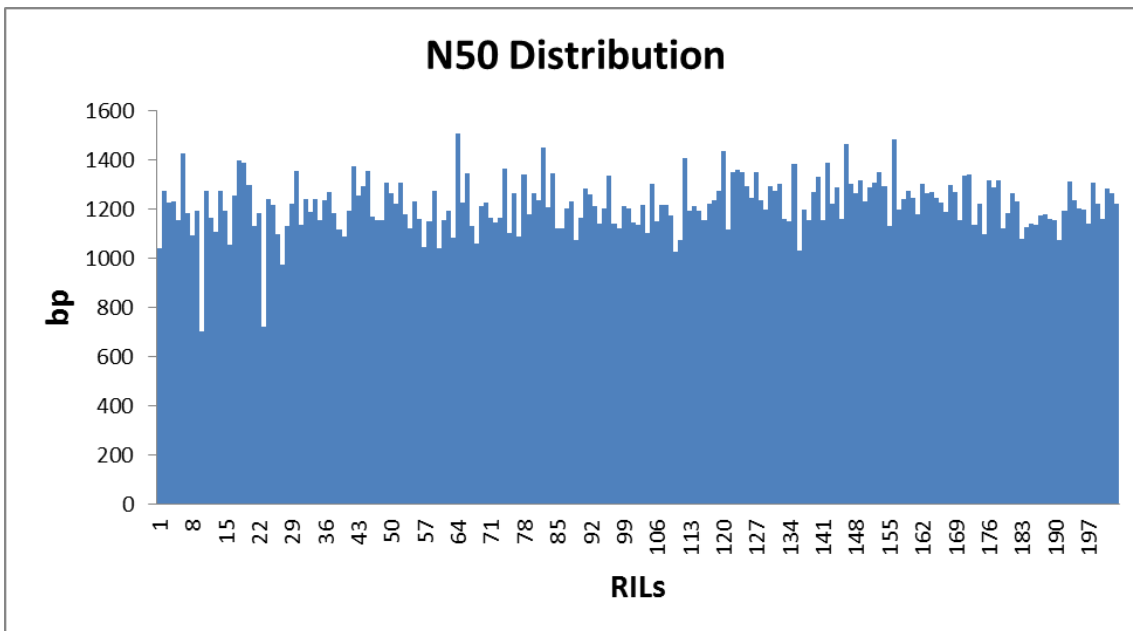


**Figure 17** N50 of the unigenes assembled with Trinity for each of the 198 RILs of the TAM 94L-25 x NMSI 1331 population

### 3.2.4 Expression of each gene in 10-dpa fibers of the RILs and parents

To estimate the expression level of each gene expressed in 10 dpa fibers and their expression variations among the 198 RILs, the clean reads of each RIL or parent was aligned to the reference unigene sequences assembled from the six biological replicates of the maternal parent, TAM 94L-25, using Trinity. The expression profile of each gene, presented in number of transcripts per million clean reads (TPM), was obtained. The result showed that the expression of a large number of the genes expressed in 10-dpa fibers varied dramatically among different RILs. The largest expression variations were found at the unigene “comp30157\_c0\_seq1”, with a maximum TPM of 360,800, a minimum TPM of 410, and a standard deviation of 27,936.34 across different RILs. It was also observed that 2,576 unigenes, accounting for 1.6% of the reference unigenes, had no expression levels detected across RILs. The reasons of this are probably that [1] expression levels of these unigenes might be too few, so that they were automatically excluded from TPM calculation formula in Trinity, and/or [2] most of short reads of different RILs were aligned into the gaps between these unigenes and others, thus giving no TPM values in these unigenes. Of the 159,936 reference unigenes assembled from the six TAM 94L-25 biological replicates, 18,919 expressed in the 10-dpa fibers of all the 198 RILs and 79,708 expressed in the 10-dpa fibers of more than 100 of the RILs. In order to maximize the results of this study, the unigenes expressed in the 10-dpa fibers of more than 100 RILs were used for further analysis of this study.

### 3.3 Isolation and analysis of genes controlling UHML

A total of 482 unigenes controlling UHML were isolated, with a confidence of 99.9994% ( $P \leq 6E-5$ ), using our new genome-wide high-throughput gene and QTL cloning system. After those that shared identical sequences with an overlap of more than 20 nucleotides were merged, 474 independent genes resulted (Table 8). These genes were named as the *GFL* genes with Arabic number suffixes 001 through 474 such as *GFL001* for the first gene in the list. To further verify the *GFL* genes, an extensive literature search was performed to find the genes previously cloned that have been shown to control UHML or trichomes. As a result of the search, a total of 21 genes were reported in the literature as controlling UHML or trichomes (Table 9). When these genes were searched against the list of the 474 *GFL* genes isolated in this study, 9 (42.86%) also were found in our 474 *GFL* genes. However, when the confidence of gene isolation was reduced to 99.75% ( $P \leq 0.0025$ ), 15 (71.43%) of the 21 genes were in the list of the UHML genes isolated in this study. When the confidence of gene isolation was reduced to 95.00% ( $P \leq 0.05$ ), all (100%) of the 21 genes were in the list of the UHML genes isolated in the process of fiber gene isolation in this study. This result has further confirmed the reliability of the *GFL* genes isolated in this study.

**Table 8** *GFL* genes and their effects and action direction on UHML in cotton

| Gene ID       | TPM <sup>a</sup> | Length (mm) <sup>a</sup> | TPM <sup>b</sup> | Length (mm) <sup>b</sup> | Δ TPM   | Length (mm) | Δ ratio (%) |
|---------------|------------------|--------------------------|------------------|--------------------------|---------|-------------|-------------|
| <i>GFL001</i> | 0.00             | 29.11                    | 3.00             | 26.81                    | 3.00    | -2.31       | -7.92       |
| <i>GFL002</i> | 0.00             | 29.86                    | 6.05             | 27.87                    | 6.05    | -1.99       | -6.67       |
| <i>GFL003</i> | 0.00             | 29.18                    | 3.58             | 27.24                    | 3.58    | -1.94       | -6.64       |
| <i>GFL004</i> | 0.00             | 28.87                    | 4.25             | 27.00                    | 4.25    | -1.87       | -6.47       |
| <i>GFL005</i> | 0.00             | 29.30                    | 4.60             | 27.43                    | 4.60    | -1.87       | -6.37       |
| <i>GFL006</i> | 0.00             | 29.23                    | 4.75             | 27.37                    | 4.75    | -1.86       | -6.35       |
| <i>GFL007</i> | 0.04             | 29.73                    | 56.57            | 27.87                    | 56.53   | -1.86       | -6.26       |
| <i>GFL008</i> | 202.45           | 29.54                    | 535.78           | 27.70                    | 333.33  | -1.84       | -6.22       |
| <i>GFL009</i> | 3.63             | 30.18                    | 45.37            | 28.31                    | 41.74   | -1.86       | -6.17       |
| <i>GFL010</i> | 65.89            | 29.67                    | 252.71           | 27.84                    | 186.82  | -1.83       | -6.16       |
| <i>GFL011</i> | 5.80             | 29.79                    | 38.38            | 27.97                    | 32.58   | -1.83       | -6.13       |
| <i>GFL012</i> | 0.65             | 29.17                    | 7.76             | 27.39                    | 7.11    | -1.79       | -6.12       |
| <i>GFL013</i> | 2.35             | 29.69                    | 11.54            | 27.88                    | 9.19    | -1.81       | -6.10       |
| <i>GFL014</i> | 1.00             | 29.73                    | 41.76            | 27.92                    | 40.77   | -1.81       | -6.09       |
| <i>GFL015</i> | 0.00             | 28.80                    | 3.91             | 27.06                    | 3.91    | -1.74       | -6.04       |
| <i>GFL016</i> | 11.03            | 29.33                    | 99.33            | 27.56                    | 88.30   | -1.76       | -6.00       |
| <i>GFL017</i> | 0.83             | 29.92                    | 8.96             | 28.15                    | 8.13    | -1.77       | -5.93       |
| <i>GFL018</i> | 34.32            | 30.02                    | 137.10           | 28.25                    | 102.78  | -1.77       | -5.88       |
| <i>GFL019</i> | 1279.37          | 29.87                    | 2365.35          | 28.11                    | 1085.98 | -1.76       | -5.88       |
| <i>GFL020</i> | 42.88            | 29.79                    | 101.65           | 28.05                    | 58.77   | -1.74       | -5.83       |
| <i>GFL021</i> | 1.75             | 29.80                    | 10.52            | 28.07                    | 8.77    | -1.73       | -5.82       |
| <i>GFL022</i> | 2.46             | 29.43                    | 18.09            | 27.73                    | 15.64   | -1.70       | -5.77       |
| <i>GFL023</i> | 4.38             | 29.89                    | 20.15            | 28.18                    | 15.77   | -1.71       | -5.72       |
| <i>GFL024</i> | 0.00             | 29.42                    | 68.84            | 27.74                    | 68.84   | -1.68       | -5.70       |
| <i>GFL025</i> | 18.56            | 29.16                    | 44.11            | 27.52                    | 25.55   | -1.65       | -5.65       |
| <i>GFL026</i> | 76.73            | 29.09                    | 166.91           | 27.46                    | 90.18   | -1.64       | -5.62       |
| <i>GFL027</i> | 4.34             | 29.93                    | 127.18           | 28.25                    | 122.85  | -1.68       | -5.60       |
| <i>GFL028</i> | 0.62             | 29.43                    | 7.88             | 27.79                    | 7.26    | -1.65       | -5.60       |
| <i>GFL029</i> | 387.85           | 29.50                    | 958.77           | 27.87                    | 570.92  | -1.63       | -5.52       |
| <i>GFL030</i> | 73.21            | 29.59                    | 174.55           | 27.96                    | 101.34  | -1.63       | -5.50       |
| <i>GFL031</i> | 2.25             | 29.32                    | 10.25            | 27.72                    | 8.01    | -1.60       | -5.45       |
| <i>GFL032</i> | 16.78            | 29.70                    | 108.31           | 28.08                    | 91.54   | -1.62       | -5.45       |
| <i>GFL033</i> | 0.51             | 29.02                    | 8.26             | 27.45                    | 7.75    | -1.57       | -5.42       |
| <i>GFL034</i> | 4.95             | 29.33                    | 20.22            | 27.74                    | 15.27   | -1.59       | -5.42       |
| <i>GFL035</i> | 0.67             | 29.37                    | 7.08             | 27.78                    | 6.41    | -1.59       | -5.41       |
| <i>GFL036</i> | 0.50             | 29.34                    | 17.58            | 27.76                    | 17.08   | -1.58       | -5.39       |
| <i>GFL037</i> | 17.04            | 29.62                    | 56.56            | 28.04                    | 39.52   | -1.59       | -5.35       |
| <i>GFL038</i> | 8.82             | 28.97                    | 33.52            | 27.42                    | 24.70   | -1.55       | -5.34       |
| <i>GFL039</i> | 30.25            | 29.57                    | 133.95           | 27.99                    | 103.70  | -1.58       | -5.33       |
| <i>GFL040</i> | 16.53            | 29.91                    | 59.61            | 28.31                    | 43.08   | -1.60       | -5.33       |
| <i>GFL041</i> | 140.44           | 29.43                    | 310.19           | 27.87                    | 169.75  | -1.56       | -5.30       |
| <i>GFL042</i> | 1.47             | 29.43                    | 14.57            | 27.87                    | 13.11   | -1.56       | -5.29       |
| <i>GFL043</i> | 7.56             | 29.78                    | 44.72            | 28.21                    | 37.16   | -1.57       | -5.29       |
| <i>GFL044</i> | 0.00             | 29.01                    | 3.61             | 27.47                    | 3.61    | -1.53       | -5.29       |
| <i>GFL045</i> | 15.53            | 29.68                    | 163.86           | 28.11                    | 148.33  | -1.57       | -5.28       |
| <i>GFL046</i> | 42.97            | 29.67                    | 129.71           | 28.11                    | 86.74   | -1.56       | -5.25       |
| <i>GFL047</i> | 450.78           | 29.63                    | 996.19           | 28.08                    | 545.41  | -1.55       | -5.24       |
| <i>GFL048</i> | 24.69            | 29.40                    | 78.39            | 27.86                    | 53.70   | -1.54       | -5.23       |
| <i>GFL049</i> | 250.94           | 29.26                    | 597.10           | 27.73                    | 346.16  | -1.53       | -5.22       |
| <i>GFL050</i> | 17.51            | 29.30                    | 43.33            | 27.78                    | 25.83   | -1.53       | -5.21       |



**Table 8** Continued

| Gene ID       | TPM <sup>a</sup> Length (mm) <sup>a</sup> |       | TPM <sup>b</sup> Length (mm) <sup>b</sup> |       | Δ TPM  | Length (mm) | Δ ratio (%) |
|---------------|---|-------|---|-------|--------|-------------|-------------|
| <i>GFL051</i> | 59.73                                     | 29.74 | 165.37                                    | 28.20 | 105.64 | -1.54       | -5.18       |
| <i>GFL052</i> | 18.84                                     | 29.56 | 54.22                                     | 28.04 | 35.38  | -1.52       | -5.14       |
| <i>GFL053</i> | 42.44                                     | 29.27 | 105.85                                    | 27.77 | 63.41  | -1.50       | -5.14       |
| <i>GFL054</i> | 0.62                                      | 29.24 | 10.32                                     | 27.74 | 9.70   | -1.50       | -5.13       |
| <i>GFL055</i> | 7.37                                      | 29.56 | 20.95                                     | 28.07 | 13.58  | -1.49       | -5.04       |
| <i>GFL056</i> | 0.71                                      | 29.31 | 9.64                                      | 27.83 | 8.93   | -1.47       | -5.03       |
| <i>GFL057</i> | 25.91                                     | 29.90 | 142.14                                    | 28.40 | 116.23 | -1.50       | -5.02       |
| <i>GFL058</i> | 2.14                                      | 29.44 | 18.38                                     | 27.97 | 16.24  | -1.48       | -5.02       |
| <i>GFL059</i> | 0.00                                      | 29.23 | 3.50                                      | 27.76 | 3.50   | -1.46       | -5.01       |
| <i>GFL060</i> | 4.28                                      | 29.54 | 45.63                                     | 28.06 | 41.35  | -1.48       | -5.00       |
| <i>GFL061</i> | 14.42                                     | 29.56 | 45.71                                     | 28.09 | 31.29  | -1.48       | -4.99       |
| <i>GFL062</i> | 1.02                                      | 29.36 | 11.03                                     | 27.90 | 10.01  | -1.47       | -4.99       |
| <i>GFL063</i> | 9.98                                      | 29.08 | 65.48                                     | 27.63 | 55.49  | -1.45       | -4.99       |
| <i>GFL064</i> | 11.32                                     | 29.69 | 42.43                                     | 28.21 | 31.11  | -1.48       | -4.99       |
| <i>GFL065</i> | 16.31                                     | 29.50 | 46.11                                     | 28.03 | 29.79  | -1.47       | -4.98       |
| <i>GFL066</i> | 0.64                                      | 29.13 | 6.57                                      | 27.68 | 5.93   | -1.45       | -4.98       |
| <i>GFL067</i> | 15.29                                     | 29.55 | 85.86                                     | 28.08 | 70.57  | -1.47       | -4.96       |
| <i>GFL068</i> | 54.31                                     | 29.47 | 107.66                                    | 28.01 | 53.36  | -1.46       | -4.96       |
| <i>GFL069</i> | 12.88                                     | 29.02 | 46.95                                     | 27.59 | 34.07  | -1.43       | -4.94       |
| <i>GFL070</i> | 0.00                                      | 29.10 | 33.28                                     | 27.66 | 33.28  | -1.44       | -4.94       |
| <i>GFL071</i> | 0.67                                      | 29.19 | 6.02                                      | 27.76 | 5.35   | -1.44       | -4.92       |
| <i>GFL072</i> | 0.00                                      | 29.20 | 4.58                                      | 27.77 | 4.58   | -1.44       | -4.92       |
| <i>GFL073</i> | 28.83                                     | 29.45 | 196.14                                    | 28.01 | 167.31 | -1.44       | -4.90       |
| <i>GFL074</i> | 0.00                                      | 29.24 | 7.41                                      | 27.81 | 7.41   | -1.43       | -4.90       |
| <i>GFL075</i> | 25.99                                     | 29.57 | 63.97                                     | 28.12 | 37.98  | -1.45       | -4.90       |
| <i>GFL076</i> | 0.37                                      | 28.99 | 23.90                                     | 27.57 | 23.53  | -1.42       | -4.89       |
| <i>GFL077</i> | 1.31                                      | 29.67 | 14.42                                     | 28.22 | 13.11  | -1.45       | -4.89       |
| <i>GFL078</i> | 40.68                                     | 29.24 | 106.90                                    | 27.81 | 66.22  | -1.43       | -4.88       |
| <i>GFL079</i> | 234.19                                    | 29.61 | 485.82                                    | 28.16 | 251.64 | -1.45       | -4.88       |
| <i>GFL080</i> | 105.54                                    | 29.47 | 216.75                                    | 28.03 | 111.22 | -1.44       | -4.88       |
| <i>GFL081</i> | 0.37                                      | 29.64 | 8.59                                      | 28.19 | 8.22   | -1.44       | -4.87       |
| <i>GFL082</i> | 46.21                                     | 29.52 | 149.58                                    | 28.08 | 103.37 | -1.44       | -4.87       |
| <i>GFL083</i> | 1.52                                      | 29.26 | 8.92                                      | 27.84 | 7.40   | -1.42       | -4.86       |
| <i>GFL084</i> | 18.87                                     | 29.42 | 68.58                                     | 28.00 | 49.70  | -1.42       | -4.83       |
| <i>GFL085</i> | 131.36                                    | 29.92 | 250.14                                    | 28.47 | 118.78 | -1.44       | -4.83       |
| <i>GFL086</i> | 0.14                                      | 29.53 | 27.32                                     | 28.11 | 27.18  | -1.42       | -4.82       |
| <i>GFL087</i> | 4.01                                      | 29.29 | 22.43                                     | 27.88 | 18.43  | -1.41       | -4.81       |
| <i>GFL088</i> | 0.00                                      | 29.25 | 32.58                                     | 27.85 | 32.58  | -1.40       | -4.80       |
| <i>GFL089</i> | 3.47                                      | 29.56 | 28.98                                     | 28.15 | 25.50  | -1.42       | -4.80       |
| <i>GFL090</i> | 7.96                                      | 29.37 | 38.39                                     | 27.96 | 30.43  | -1.41       | -4.79       |
| <i>GFL091</i> | 22.37                                     | 29.47 | 118.51                                    | 28.06 | 96.14  | -1.41       | -4.78       |
| <i>GFL092</i> | 2.27                                      | 29.53 | 12.43                                     | 28.12 | 10.16  | -1.41       | -4.77       |
| <i>GFL093</i> | 0.00                                      | 29.19 | 3.50                                      | 27.80 | 3.50   | -1.39       | -4.76       |
| <i>GFL094</i> | 32.45                                     | 29.61 | 84.04                                     | 28.21 | 51.59  | -1.41       | -4.75       |
| <i>GFL095</i> | 1.46                                      | 29.61 | 9.61                                      | 28.21 | 8.15   | -1.41       | -4.75       |
| <i>GFL096</i> | 15.81                                     | 29.61 | 72.67                                     | 28.20 | 56.86  | -1.40       | -4.74       |
| <i>GFL097</i> | 10.33                                     | 29.63 | 63.53                                     | 28.23 | 53.20  | -1.40       | -4.72       |
| <i>GFL098</i> | 11.38                                     | 29.12 | 87.85                                     | 27.74 | 76.47  | -1.37       | -4.72       |
| <i>GFL099</i> | 48.53                                     | 29.03 | 133.69                                    | 27.67 | 85.16  | -1.37       | -4.71       |
| <i>GFL100</i> | 24.83                                     | 29.43 | 58.10                                     | 28.05 | 33.27  | -1.38       | -4.71       |

**Table 8** Continued

| Gene ID       | TPM <sup>a</sup> | Length (mm) <sup>a</sup> | TPM <sup>b</sup> | Length (mm) <sup>b</sup> | Δ TPM  | Length (mm) | Δ ratio (%) |
|---------------|------------------|--------------------------|------------------|--------------------------|--------|-------------|-------------|
| <i>GFL101</i> | 0.00             | 29.10                    | 47.97            | 27.73                    | 47.97  | -1.37       | -4.70       |
| <i>GFL102</i> | 42.76            | 29.58                    | 536.37           | 28.19                    | 493.61 | -1.39       | -4.70       |
| <i>GFL103</i> | 80.38            | 29.35                    | 197.32           | 27.97                    | 116.94 | -1.38       | -4.70       |
| <i>GFL104</i> | 0.00             | 29.02                    | 4.34             | 27.66                    | 4.34   | -1.36       | -4.70       |
| <i>GFL105</i> | 0.59             | 29.19                    | 10.85            | 27.82                    | 10.26  | -1.37       | -4.69       |
| <i>GFL106</i> | 47.71            | 29.40                    | 253.18           | 28.02                    | 205.47 | -1.38       | -4.69       |
| <i>GFL107</i> | 0.00             | 28.98                    | 3.56             | 27.62                    | 3.56   | -1.36       | -4.68       |
| <i>GFL108</i> | 15.82            | 29.56                    | 59.18            | 28.18                    | 43.37  | -1.38       | -4.67       |
| <i>GFL109</i> | 5.43             | 29.43                    | 31.33            | 28.05                    | 25.90  | -1.37       | -4.67       |
| <i>GFL110</i> | 33.41            | 29.41                    | 80.49            | 28.04                    | 47.08  | -1.37       | -4.66       |
| <i>GFL111</i> | 0.00             | 29.09                    | 5.93             | 27.74                    | 5.93   | -1.35       | -4.66       |
| <i>GFL112</i> | 0.00             | 28.99                    | 4.83             | 27.65                    | 4.83   | -1.35       | -4.65       |
| <i>GFL113</i> | 0.00             | 29.29                    | 25.76            | 27.93                    | 25.76  | -1.36       | -4.65       |
| <i>GFL114</i> | 3.86             | 29.16                    | 18.31            | 27.80                    | 14.45  | -1.35       | -4.64       |
| <i>GFL115</i> | 70.03            | 29.17                    | 153.91           | 27.81                    | 83.88  | -1.35       | -4.64       |
| <i>GFL116</i> | 0.00             | 29.03                    | 15.07            | 27.69                    | 15.07  | -1.34       | -4.62       |
| <i>GFL117</i> | 167.48           | 29.35                    | 463.65           | 27.99                    | 296.16 | -1.36       | -4.62       |
| <i>GFL118</i> | 0.07             | 29.61                    | 21.68            | 28.25                    | 21.61  | -1.37       | -4.62       |
| <i>GFL119</i> | 0.00             | 29.34                    | 77.42            | 27.99                    | 77.42  | -1.35       | -4.60       |
| <i>GFL120</i> | 410.29           | 29.43                    | 751.09           | 28.08                    | 340.80 | -1.35       | -4.58       |
| <i>GFL121</i> | 84.81            | 29.51                    | 247.61           | 28.16                    | 162.80 | -1.35       | -4.58       |
| <i>GFL122</i> | 0.67             | 29.20                    | 6.61             | 27.87                    | 5.94   | -1.33       | -4.57       |
| <i>GFL123</i> | 75.11            | 29.05                    | 163.11           | 27.73                    | 88.00  | -1.32       | -4.56       |
| <i>GFL124</i> | 58.80            | 29.53                    | 120.20           | 28.19                    | 61.40  | -1.35       | -4.55       |
| <i>GFL125</i> | 0.45             | 29.61                    | 58.65            | 28.27                    | 58.20  | -1.35       | -4.55       |
| <i>GFL126</i> | 51.71            | 29.31                    | 132.98           | 27.98                    | 81.28  | -1.33       | -4.55       |
| <i>GFL127</i> | 18.36            | 29.30                    | 54.86            | 27.97                    | 36.50  | -1.33       | -4.54       |
| <i>GFL128</i> | 4.73             | 29.55                    | 23.52            | 28.21                    | 18.79  | -1.33       | -4.51       |
| <i>GFL129</i> | 25.43            | 29.43                    | 90.07            | 28.10                    | 64.64  | -1.33       | -4.51       |
| <i>GFL130</i> | 252.46           | 29.44                    | 550.00           | 28.12                    | 297.54 | -1.33       | -4.50       |
| <i>GFL131</i> | 0.07             | 29.49                    | 53.32            | 28.16                    | 53.25  | -1.33       | -4.50       |
| <i>GFL132</i> | 0.00             | 29.23                    | 12.25            | 27.92                    | 12.25  | -1.31       | -4.49       |
| <i>GFL133</i> | 35.55            | 29.70                    | 162.78           | 28.37                    | 127.22 | -1.33       | -4.49       |
| <i>GFL134</i> | 0.00             | 29.03                    | 4.48             | 27.73                    | 4.48   | -1.30       | -4.48       |
| <i>GFL135</i> | 12.87            | 29.67                    | 48.48            | 28.34                    | 35.60  | -1.33       | -4.48       |
| <i>GFL136</i> | 0.00             | 29.33                    | 12.03            | 28.02                    | 12.03  | -1.31       | -4.47       |
| <i>GFL137</i> | 0.00             | 29.03                    | 3.95             | 27.73                    | 3.95   | -1.30       | -4.47       |
| <i>GFL138</i> | 18.81            | 29.27                    | 46.82            | 27.97                    | 28.01  | -1.31       | -4.46       |
| <i>GFL139</i> | 291.00           | 29.56                    | 590.31           | 28.24                    | 299.31 | -1.32       | -4.46       |
| <i>GFL140</i> | 1.58             | 29.55                    | 10.74            | 28.23                    | 9.16   | -1.32       | -4.46       |
| <i>GFL141</i> | 0.00             | 28.97                    | 6.33             | 27.68                    | 6.33   | -1.29       | -4.46       |
| <i>GFL142</i> | 1.55             | 29.39                    | 9.53             | 28.08                    | 7.98   | -1.31       | -4.45       |
| <i>GFL143</i> | 4.70             | 29.18                    | 17.92            | 27.88                    | 13.23  | -1.30       | -4.45       |
| <i>GFL144</i> | 0.29             | 29.24                    | 49.35            | 27.94                    | 49.06  | -1.30       | -4.45       |
| <i>GFL145</i> | 24.70            | 29.34                    | 71.70            | 28.04                    | 47.00  | -1.30       | -4.44       |
| <i>GFL146</i> | 0.73             | 29.20                    | 6.88             | 27.91                    | 6.14   | -1.30       | -4.44       |
| <i>GFL147</i> | 426.90           | 29.19                    | 1019.35          | 27.89                    | 592.45 | -1.30       | -4.44       |
| <i>GFL148</i> | 11.51            | 29.30                    | 93.73            | 28.00                    | 82.22  | -1.30       | -4.43       |
| <i>GFL149</i> | 0.00             | 29.06                    | 3.40             | 27.77                    | 3.40   | -1.29       | -4.42       |
| <i>GFL150</i> | 108.35           | 29.92                    | 231.87           | 28.59                    | 123.52 | -1.32       | -4.42       |

**Table 8** Continued

| Gene ID       | TPM <sup>a</sup> | Length (mm) <sup>a</sup> | TPM <sup>b</sup> | Length (mm) <sup>b</sup> | $\Delta$ TPM | Length (mm) | $\Delta$ ratio (%) |
|---------------|------------------|--------------------------|------------------|--------------------------|--------------|-------------|--------------------|
| <i>GFL151</i> | 2.31             | 29.36                    | 17.38            | 28.07                    | 15.07        | -1.29       | -4.41              |
| <i>GFL152</i> | 6.99             | 29.73                    | 27.24            | 28.43                    | 20.25        | -1.31       | -4.40              |
| <i>GFL153</i> | 276.41           | 29.37                    | 511.83           | 28.08                    | 235.42       | -1.29       | -4.40              |
| <i>GFL154</i> | 0.00             | 29.36                    | 10.49            | 28.07                    | 10.49        | -1.29       | -4.40              |
| <i>GFL155</i> | 42.56            | 29.56                    | 107.70           | 28.26                    | 65.15        | -1.30       | -4.39              |
| <i>GFL156</i> | 5.22             | 29.84                    | 29.32            | 28.53                    | 24.10        | -1.31       | -4.38              |
| <i>GFL157</i> | 48.97            | 29.38                    | 117.05           | 28.09                    | 68.08        | -1.29       | -4.38              |
| <i>GFL158</i> | 77.31            | 29.19                    | 173.16           | 27.91                    | 95.86        | -1.28       | -4.38              |
| <i>GFL159</i> | 43.10            | 29.60                    | 85.28            | 28.31                    | 42.18        | -1.29       | -4.37              |
| <i>GFL160</i> | 0.00             | 29.38                    | 8.79             | 28.09                    | 8.79         | -1.28       | -4.37              |
| <i>GFL161</i> | 0.00             | 29.19                    | 32.40            | 27.91                    | 32.40        | -1.27       | -4.37              |
| <i>GFL162</i> | 0.81             | 29.16                    | 34.94            | 27.88                    | 34.13        | -1.27       | -4.37              |
| <i>GFL163</i> | 125.24           | 29.41                    | 232.18           | 28.12                    | 106.93       | -1.28       | -4.36              |
| <i>GFL164</i> | 5.75             | 29.32                    | 31.53            | 28.05                    | 25.77        | -1.28       | -4.35              |
| <i>GFL165</i> | 124.57           | 29.57                    | 238.78           | 28.28                    | 114.21       | -1.29       | -4.35              |
| <i>GFL166</i> | 37.28            | 29.60                    | 78.40            | 28.32                    | 41.13        | -1.29       | -4.34              |
| <i>GFL167</i> | 3.92             | 29.39                    | 34.59            | 28.12                    | 30.68        | -1.28       | -4.34              |
| <i>GFL168</i> | 19.07            | 29.63                    | 64.77            | 28.34                    | 45.70        | -1.29       | -4.34              |
| <i>GFL169</i> | 103.52           | 29.63                    | 282.65           | 28.34                    | 179.13       | -1.29       | -4.34              |
| <i>GFL170</i> | 88.80            | 29.85                    | 175.32           | 28.56                    | 86.52        | -1.29       | -4.32              |
| <i>GFL171</i> | 78.32            | 29.71                    | 156.53           | 28.43                    | 78.20        | -1.28       | -4.32              |
| <i>GFL172</i> | 0.00             | 29.11                    | 4.95             | 27.85                    | 4.95         | -1.26       | -4.32              |
| <i>GFL173</i> | 71.75            | 29.58                    | 187.66           | 28.31                    | 115.91       | -1.28       | -4.32              |
| <i>GFL174</i> | 7.73             | 29.95                    | 27.04            | 28.66                    | 19.31        | -1.29       | -4.30              |
| <i>GFL175</i> | 0.00             | 29.80                    | 59.35            | 28.52                    | 59.35        | -1.28       | -4.29              |
| <i>GFL176</i> | 0.19             | 29.34                    | 47.64            | 28.09                    | 47.46        | -1.25       | -4.28              |
| <i>GFL177</i> | 5.64             | 29.51                    | 36.06            | 28.25                    | 30.41        | -1.26       | -4.27              |
| <i>GFL178</i> | 10.42            | 29.13                    | 58.30            | 27.89                    | 47.88        | -1.24       | -4.27              |
| <i>GFL179</i> | 6.76             | 29.25                    | 26.97            | 28.00                    | 20.20        | -1.25       | -4.26              |
| <i>GFL180</i> | 33.83            | 29.19                    | 108.60           | 27.95                    | 74.77        | -1.24       | -4.26              |
| <i>GFL181</i> | 119.85           | 29.46                    | 373.13           | 28.20                    | 253.27       | -1.25       | -4.26              |
| <i>GFL182</i> | 155.26           | 29.41                    | 375.98           | 28.16                    | 220.72       | -1.25       | -4.26              |
| <i>GFL183</i> | 1.93             | 29.36                    | 17.31            | 28.11                    | 15.38        | -1.25       | -4.26              |
| <i>GFL184</i> | 0.00             | 29.31                    | 27.10            | 28.06                    | 27.10        | -1.24       | -4.24              |
| <i>GFL185</i> | 22.30            | 28.92                    | 68.63            | 27.70                    | 46.34        | -1.22       | -4.24              |
| <i>GFL186</i> | 0.04             | 29.38                    | 28.42            | 28.14                    | 28.38        | -1.24       | -4.23              |
| <i>GFL187</i> | 87.17            | 29.44                    | 196.20           | 28.20                    | 109.02       | -1.24       | -4.23              |
| <i>GFL188</i> | 11.39            | 29.65                    | 95.53            | 28.39                    | 84.14        | -1.25       | -4.22              |
| <i>GFL189</i> | 20.25            | 29.51                    | 148.92           | 28.27                    | 128.67       | -1.24       | -4.21              |
| <i>GFL190</i> | 3.28             | 29.33                    | 13.74            | 28.10                    | 10.46        | -1.23       | -4.21              |
| <i>GFL191</i> | 0.00             | 29.06                    | 4.58             | 27.83                    | 4.58         | -1.22       | -4.21              |
| <i>GFL192</i> | 13.65            | 29.22                    | 33.61            | 27.99                    | 19.97        | -1.23       | -4.20              |
| <i>GFL193</i> | 36.46            | 29.05                    | 109.99           | 27.83                    | 73.53        | -1.22       | -4.20              |
| <i>GFL194</i> | 60.38            | 28.99                    | 262.31           | 27.77                    | 201.93       | -1.22       | -4.20              |
| <i>GFL195</i> | 2.95             | 29.55                    | 24.71            | 28.31                    | 21.76        | -1.24       | -4.20              |
| <i>GFL196</i> | 18.04            | 29.96                    | 209.02           | 28.70                    | 190.98       | -1.26       | -4.20              |
| <i>GFL197</i> | 1.48             | 29.38                    | 8.18             | 28.15                    | 6.70         | -1.23       | -4.20              |
| <i>GFL198</i> | 6.43             | 28.96                    | 23.52            | 27.74                    | 17.10        | -1.22       | -4.20              |
| <i>GFL199</i> | 32.08            | 29.51                    | 82.13            | 28.27                    | 50.04        | -1.24       | -4.19              |
| <i>GFL200</i> | 8.69             | 29.84                    | 67.68            | 28.59                    | 58.99        | -1.25       | -4.19              |

**Table 8** Continued

| Gene ID       | TPM <sup>a</sup> | Length (mm) <sup>a</sup> | TPM <sup>b</sup> | Length (mm) <sup>b</sup> | $\Delta$ TPM | Length (mm) | $\Delta$ ratio (%) |
|---------------|------------------|--------------------------|------------------|--------------------------|--------------|-------------|--------------------|
| <i>GFL201</i> | 126.55           | 29.59                    | 340.56           | 28.36                    | 214.02       | -1.24       | -4.19              |
| <i>GFL202</i> | 3.19             | 29.39                    | 15.73            | 28.16                    | 12.55        | -1.23       | -4.18              |
| <i>GFL203</i> | 8.12             | 29.20                    | 26.93            | 27.98                    | 18.82        | -1.22       | -4.18              |
| <i>GFL204</i> | 5.45             | 29.55                    | 23.60            | 28.31                    | 18.15        | -1.23       | -4.18              |
| <i>GFL205</i> | 44.97            | 29.45                    | 133.31           | 28.22                    | 88.34        | -1.23       | -4.17              |
| <i>GFL206</i> | 53.09            | 29.59                    | 192.17           | 28.36                    | 139.08       | -1.23       | -4.16              |
| <i>GFL207</i> | 9.11             | 29.37                    | 102.61           | 28.15                    | 93.51        | -1.22       | -4.16              |
| <i>GFL208</i> | 0.00             | 28.98                    | 5.80             | 27.78                    | 5.80         | -1.21       | -4.16              |
| <i>GFL209</i> | 6.30             | 29.34                    | 30.53            | 28.12                    | 24.23        | -1.22       | -4.16              |
| <i>GFL210</i> | 98.08            | 29.23                    | 227.47           | 28.02                    | 129.39       | -1.22       | -4.16              |
| <i>GFL211</i> | 61.03            | 29.34                    | 371.95           | 28.12                    | 310.93       | -1.22       | -4.15              |
| <i>GFL212</i> | 0.62             | 29.00                    | 9.69             | 27.80                    | 9.07         | -1.20       | -4.15              |
| <i>GFL213</i> | 0.60             | 29.22                    | 8.21             | 28.01                    | 7.61         | -1.21       | -4.14              |
| <i>GFL214</i> | 2.93             | 29.03                    | 12.20            | 27.83                    | 9.27         | -1.20       | -4.13              |
| <i>GFL215</i> | 18.48            | 29.63                    | 58.75            | 28.41                    | 40.27        | -1.22       | -4.13              |
| <i>GFL216</i> | 1.17             | 28.99                    | 28.14            | 27.80                    | 26.97        | -1.20       | -4.13              |
| <i>GFL217</i> | 179.24           | 29.73                    | 401.61           | 28.51                    | 222.37       | -1.23       | -4.12              |
| <i>GFL218</i> | 1.47             | 29.29                    | 14.81            | 28.08                    | 13.34        | -1.21       | -4.12              |
| <i>GFL219</i> | 1.94             | 29.78                    | 40.26            | 28.55                    | 38.31        | -1.23       | -4.12              |
| <i>GFL220</i> | 42.31            | 29.36                    | 138.36           | 28.16                    | 96.05        | -1.21       | -4.12              |
| <i>GFL221</i> | 9.69             | 29.46                    | 35.73            | 28.25                    | 26.04        | -1.21       | -4.11              |
| <i>GFL222</i> | 243.41           | 29.34                    | 842.44           | 28.14                    | 599.04       | -1.21       | -4.11              |
| <i>GFL223</i> | 9.28             | 29.38                    | 38.79            | 28.17                    | 29.51        | -1.21       | -4.11              |
| <i>GFL224</i> | 5.16             | 29.25                    | 23.28            | 28.05                    | 18.12        | -1.20       | -4.10              |
| <i>GFL225</i> | 171.66           | 29.74                    | 536.91           | 28.52                    | 365.25       | -1.22       | -4.10              |
| <i>GFL226</i> | 7.86             | 29.62                    | 34.00            | 28.41                    | 26.14        | -1.21       | -4.10              |
| <i>GFL227</i> | 0.71             | 29.40                    | 61.51            | 28.20                    | 60.79        | -1.20       | -4.10              |
| <i>GFL228</i> | 7.08             | 29.43                    | 30.84            | 28.23                    | 23.76        | -1.21       | -4.10              |
| <i>GFL229</i> | 17.83            | 29.28                    | 75.68            | 28.08                    | 57.85        | -1.20       | -4.10              |
| <i>GFL230</i> | 15.84            | 29.29                    | 87.92            | 28.10                    | 72.08        | -1.20       | -4.09              |
| <i>GFL231</i> | 1.61             | 29.40                    | 60.32            | 28.20                    | 58.71        | -1.20       | -4.09              |
| <i>GFL232</i> | 10.70            | 29.00                    | 39.24            | 27.81                    | 28.54        | -1.18       | -4.08              |
| <i>GFL233</i> | 242.86           | 29.65                    | 518.02           | 28.44                    | 275.16       | -1.21       | -4.08              |
| <i>GFL234</i> | 0.50             | 29.22                    | 6.29             | 28.03                    | 5.79         | -1.19       | -4.07              |
| <i>GFL235</i> | 0.00             | 29.43                    | 11.58            | 28.23                    | 11.58        | -1.20       | -4.07              |
| <i>GFL236</i> | 124.35           | 29.67                    | 263.29           | 28.46                    | 138.94       | -1.21       | -4.07              |
| <i>GFL237</i> | 123.03           | 29.48                    | 223.75           | 28.29                    | 100.71       | -1.20       | -4.06              |
| <i>GFL238</i> | 34.49            | 29.57                    | 189.38           | 28.36                    | 154.89       | -1.20       | -4.06              |
| <i>GFL239</i> | 529.39           | 29.18                    | 1294.70          | 27.99                    | 765.31       | -1.18       | -4.05              |
| <i>GFL240</i> | 254.93           | 29.16                    | 518.15           | 27.98                    | 263.23       | -1.18       | -4.05              |
| <i>GFL241</i> | 0.00             | 29.26                    | 137.88           | 28.08                    | 137.88       | -1.18       | -4.04              |
| <i>GFL242</i> | 115.46           | 28.97                    | 291.52           | 27.80                    | 176.05       | -1.17       | -4.03              |
| <i>GFL243</i> | 0.00             | 29.02                    | 40.00            | 27.86                    | 40.00        | -1.16       | -4.01              |
| <i>GFL244</i> | 0.00             | 28.87                    | 3.30             | 27.71                    | 3.30         | -1.16       | -4.01              |
| <i>GFL245</i> | 1.97             | 29.44                    | 53.29            | 28.26                    | 51.33        | -1.18       | -4.01              |
| <i>GFL246</i> | 7.47             | 29.34                    | 32.72            | 28.17                    | 25.25        | -1.17       | -4.00              |
| <i>GFL247</i> | 33.67            | 29.65                    | 137.70           | 28.47                    | 104.03       | -1.18       | -3.99              |
| <i>GFL248</i> | 2.93             | 28.76                    | 15.99            | 27.62                    | 13.06        | -1.15       | -3.99              |
| <i>GFL249</i> | 22.20            | 29.09                    | 79.99            | 27.93                    | 57.78        | -1.16       | -3.99              |
| <i>GFL250</i> | 24.78            | 29.15                    | 70.17            | 27.99                    | 45.39        | -1.16       | -3.98              |

**Table 8** Continued

| Gene ID       | TPM <sup>a</sup> | Length (mm) <sup>a</sup> | TPM <sup>b</sup> | Length (mm) <sup>b</sup> | $\Delta$ TPM | Length (mm) | $\Delta$ ratio (%) |
|---------------|------------------|--------------------------|------------------|--------------------------|--------------|-------------|--------------------|
| <i>GFL251</i> | 60.64            | 29.74                    | 146.73           | 28.56                    | 86.09        | -1.18       | -3.98              |
| <i>GFL252</i> | 33.08            | 29.51                    | 138.19           | 28.34                    | 105.10       | -1.17       | -3.97              |
| <i>GFL253</i> | 259.05           | 29.26                    | 660.96           | 28.10                    | 401.91       | -1.16       | -3.97              |
| <i>GFL254</i> | 0.00             | 28.98                    | 23.63            | 27.83                    | 23.63        | -1.15       | -3.97              |
| <i>GFL255</i> | 0.00             | 29.24                    | 3.50             | 28.08                    | 3.50         | -1.16       | -3.97              |
| <i>GFL256</i> | 0.81             | 29.26                    | 6.83             | 28.11                    | 6.02         | -1.16       | -3.96              |
| <i>GFL257</i> | 1.43             | 29.01                    | 9.06             | 27.87                    | 7.64         | -1.15       | -3.95              |
| <i>GFL258</i> | 6.81             | 29.04                    | 142.77           | 27.90                    | 135.97       | -1.15       | -3.95              |
| <i>GFL259</i> | 28.56            | 29.19                    | 169.26           | 28.04                    | 140.69       | -1.15       | -3.94              |
| <i>GFL260</i> | 6.90             | 29.34                    | 101.33           | 28.18                    | 94.43        | -1.16       | -3.94              |
| <i>GFL261</i> | 8.00             | 29.35                    | 37.54            | 28.20                    | 29.54        | -1.16       | -3.94              |
| <i>GFL262</i> | 0.00             | 29.31                    | 47.15            | 28.16                    | 47.15        | -1.15       | -3.94              |
| <i>GFL263</i> | 8.41             | 29.84                    | 49.42            | 28.67                    | 41.01        | -1.17       | -3.94              |
| <i>GFL264</i> | 0.00             | 29.13                    | 8.80             | 27.98                    | 8.80         | -1.14       | -3.93              |
| <i>GFL265</i> | 7.03             | 29.20                    | 49.19            | 28.06                    | 42.16        | -1.15       | -3.93              |
| <i>GFL266</i> | 1.13             | 29.35                    | 12.49            | 28.20                    | 11.36        | -1.15       | -3.92              |
| <i>GFL267</i> | 24.65            | 29.39                    | 93.17            | 28.24                    | 68.52        | -1.15       | -3.92              |
| <i>GFL268</i> | 320.30           | 29.24                    | 630.07           | 28.10                    | 309.77       | -1.15       | -3.92              |
| <i>GFL269</i> | 0.99             | 29.28                    | 47.72            | 28.13                    | 46.74        | -1.15       | -3.92              |
| <i>GFL270</i> | 10.10            | 29.26                    | 132.38           | 28.11                    | 122.28       | -1.15       | -3.92              |
| <i>GFL271</i> | 0.00             | 29.17                    | 29.94            | 28.03                    | 29.94        | -1.14       | -3.91              |
| <i>GFL272</i> | 28.67            | 29.16                    | 211.20           | 28.02                    | 182.53       | -1.14       | -3.91              |
| <i>GFL273</i> | 20.28            | 29.93                    | 75.91            | 28.76                    | 55.63        | -1.17       | -3.90              |
| <i>GFL274</i> | 153.84           | 29.25                    | 272.67           | 28.11                    | 118.82       | -1.14       | -3.89              |
| <i>GFL275</i> | 457.12           | 29.36                    | 1119.68          | 28.22                    | 662.56       | -1.14       | -3.89              |
| <i>GFL276</i> | 0.00             | 29.06                    | 7.30             | 27.93                    | 7.30         | -1.13       | -3.89              |
| <i>GFL277</i> | 2.17             | 29.34                    | 15.08            | 28.20                    | 12.92        | -1.14       | -3.89              |
| <i>GFL278</i> | 51.87            | 29.44                    | 124.27           | 28.30                    | 72.40        | -1.14       | -3.89              |
| <i>GFL279</i> | 5.39             | 29.15                    | 30.69            | 28.02                    | 25.30        | -1.13       | -3.88              |
| <i>GFL280</i> | 17.47            | 29.05                    | 44.24            | 27.92                    | 26.77        | -1.13       | -3.88              |
| <i>GFL281</i> | 9.88             | 29.68                    | 65.22            | 28.53                    | 55.34        | -1.15       | -3.88              |
| <i>GFL282</i> | 738.77           | 28.95                    | 1473.32          | 27.83                    | 734.55       | -1.12       | -3.87              |
| <i>GFL283</i> | 9.11             | 29.43                    | 65.18            | 28.29                    | 56.07        | -1.14       | -3.87              |
| <i>GFL284</i> | 2.84             | 29.23                    | 26.60            | 28.10                    | 23.77        | -1.13       | -3.87              |
| <i>GFL285</i> | 75.81            | 29.46                    | 266.62           | 28.33                    | 190.81       | -1.14       | -3.86              |
| <i>GFL286</i> | 2.18             | 29.20                    | 18.58            | 28.08                    | 16.40        | -1.12       | -3.84              |
| <i>GFL287</i> | 22.07            | 29.30                    | 91.44            | 28.18                    | 69.36        | -1.12       | -3.83              |
| <i>GFL288</i> | 0.00             | 28.99                    | 15.65            | 27.88                    | 15.65        | -1.11       | -3.82              |
| <i>GFL289</i> | 20.00            | 29.46                    | 48.36            | 28.34                    | 28.36        | -1.12       | -3.82              |
| <i>GFL290</i> | 1.51             | 29.03                    | 14.29            | 27.92                    | 12.77        | -1.11       | -3.81              |
| <i>GFL291</i> | 21.09            | 29.15                    | 111.93           | 28.04                    | 90.84        | -1.11       | -3.81              |
| <i>GFL292</i> | 102.64           | 29.33                    | 242.87           | 28.21                    | 140.23       | -1.12       | -3.80              |
| <i>GFL293</i> | 32.35            | 29.60                    | 96.62            | 28.48                    | 64.27        | -1.13       | -3.80              |
| <i>GFL294</i> | 5.02             | 29.04                    | 42.05            | 27.94                    | 37.03        | -1.10       | -3.79              |
| <i>GFL295</i> | 174.99           | 29.43                    | 426.21           | 28.31                    | 251.22       | -1.12       | -3.79              |
| <i>GFL296</i> | 92.56            | 29.58                    | 263.69           | 28.46                    | 171.13       | -1.12       | -3.79              |
| <i>GFL297</i> | 2.10             | 29.33                    | 26.90            | 28.22                    | 24.80        | -1.11       | -3.79              |
| <i>GFL298</i> | 23.09            | 29.53                    | 69.79            | 28.41                    | 46.70        | -1.12       | -3.79              |
| <i>GFL299</i> | 0.00             | 29.12                    | 18.63            | 28.02                    | 18.63        | -1.10       | -3.77              |
| <i>GFL300</i> | 0.00             | 28.83                    | 3.35             | 27.74                    | 3.35         | -1.09       | -3.77              |

**Table 8** Continued

| Gene ID       | TPM <sup>a</sup> | Length (mm) <sup>a</sup> | TPM <sup>b</sup> | Length (mm) <sup>b</sup> | $\Delta$ TPM | Length (mm) | $\Delta$ ratio (%) |
|---------------|------------------|--------------------------|------------------|--------------------------|--------------|-------------|--------------------|
| <i>GFL301</i> | 130.59           | 29.30                    | 283.37           | 28.19                    | 152.77       | -1.10       | -3.76              |
| <i>GFL302</i> | 4.18             | 29.27                    | 38.12            | 28.17                    | 33.94        | -1.10       | -3.75              |
| <i>GFL303</i> | 71.07            | 28.99                    | 188.74           | 27.90                    | 117.67       | -1.09       | -3.75              |
| <i>GFL304</i> | 4.61             | 29.33                    | 26.80            | 28.23                    | 22.19        | -1.10       | -3.74              |
| <i>GFL305</i> | 17.02            | 29.23                    | 58.04            | 28.13                    | 41.02        | -1.09       | -3.74              |
| <i>GFL306</i> | 2.64             | 29.42                    | 53.41            | 28.33                    | 50.77        | -1.10       | -3.74              |
| <i>GFL307</i> | 2.32             | 29.46                    | 11.00            | 28.36                    | 8.68         | -1.10       | -3.73              |
| <i>GFL308</i> | 85.23            | 29.46                    | 243.05           | 28.36                    | 157.82       | -1.10       | -3.73              |
| <i>GFL309</i> | 15.41            | 29.32                    | 59.63            | 28.23                    | 44.22        | -1.09       | -3.71              |
| <i>GFL310</i> | 0.79             | 29.16                    | 6.63             | 28.08                    | 5.84         | -1.08       | -3.70              |
| <i>GFL311</i> | 4.47             | 29.32                    | 76.02            | 28.23                    | 71.55        | -1.08       | -3.69              |
| <i>GFL312</i> | 0.64             | 28.90                    | 10.09            | 27.83                    | 9.45         | -1.07       | -3.69              |
| <i>GFL313</i> | 5.93             | 29.24                    | 19.33            | 28.16                    | 13.40        | -1.08       | -3.69              |
| <i>GFL314</i> | 17.86            | 29.02                    | 113.99           | 27.95                    | 96.12        | -1.07       | -3.68              |
| <i>GFL315</i> | 1.37             | 29.31                    | 11.60            | 28.24                    | 10.23        | -1.08       | -3.68              |
| <i>GFL316</i> | 6.92             | 29.23                    | 18.85            | 28.15                    | 11.92        | -1.07       | -3.67              |
| <i>GFL317</i> | 305.35           | 29.40                    | 543.75           | 28.32                    | 238.40       | -1.08       | -3.67              |
| <i>GFL318</i> | 147.79           | 29.29                    | 485.06           | 28.21                    | 337.27       | -1.07       | -3.66              |
| <i>GFL319</i> | 2.27             | 29.44                    | 16.74            | 28.37                    | 14.47        | -1.08       | -3.66              |
| <i>GFL320</i> | 0.00             | 29.09                    | 42.12            | 28.03                    | 42.12        | -1.06       | -3.65              |
| <i>GFL321</i> | 0.00             | 28.87                    | 3.75             | 27.82                    | 3.75         | -1.05       | -3.64              |
| <i>GFL322</i> | 15.04            | 29.20                    | 466.97           | 28.14                    | 451.93       | -1.06       | -3.64              |
| <i>GFL323</i> | 1.52             | 29.22                    | 15.14            | 28.16                    | 13.62        | -1.06       | -3.64              |
| <i>GFL324</i> | 118.96           | 29.75                    | 235.09           | 28.67                    | 116.13       | -1.08       | -3.64              |
| <i>GFL325</i> | 94.37            | 29.11                    | 190.93           | 28.05                    | 96.56        | -1.06       | -3.64              |
| <i>GFL326</i> | 19.77            | 29.22                    | 538.85           | 28.16                    | 519.07       | -1.06       | -3.64              |
| <i>GFL327</i> | 43.32            | 29.25                    | 91.78            | 28.19                    | 48.47        | -1.06       | -3.63              |
| <i>GFL328</i> | 70.37            | 29.54                    | 182.16           | 28.47                    | 111.80       | -1.07       | -3.63              |
| <i>GFL329</i> | 64.86            | 29.47                    | 137.13           | 28.39                    | 72.27        | -1.07       | -3.63              |
| <i>GFL330</i> | 103.64           | 28.92                    | 245.59           | 27.87                    | 141.94       | -1.05       | -3.63              |
| <i>GFL331</i> | 93.90            | 29.16                    | 289.27           | 28.11                    | 195.37       | -1.06       | -3.63              |
| <i>GFL332</i> | 33.20            | 29.20                    | 95.08            | 28.15                    | 61.88        | -1.06       | -3.62              |
| <i>GFL333</i> | 0.00             | 28.96                    | 32.78            | 27.92                    | 32.78        | -1.05       | -3.62              |
| <i>GFL334</i> | 0.00             | 29.05                    | 5.71             | 28.00                    | 5.71         | -1.05       | -3.61              |
| <i>GFL335</i> | 226.44           | 28.94                    | 491.33           | 27.90                    | 264.89       | -1.04       | -3.61              |
| <i>GFL336</i> | 112.41           | 29.30                    | 330.14           | 28.24                    | 217.73       | -1.06       | -3.60              |
| <i>GFL337</i> | 13.00            | 29.20                    | 300.59           | 28.15                    | 287.59       | -1.05       | -3.60              |
| <i>GFL338</i> | 50.41            | 29.24                    | 122.32           | 28.19                    | 71.91        | -1.05       | -3.60              |
| <i>GFL339</i> | 141.91           | 29.40                    | 378.40           | 28.34                    | 236.49       | -1.06       | -3.60              |
| <i>GFL340</i> | 0.00             | 28.87                    | 11.83            | 27.83                    | 11.83        | -1.04       | -3.59              |
| <i>GFL341</i> | 26.04            | 29.51                    | 81.76            | 28.45                    | 55.72        | -1.06       | -3.59              |
| <i>GFL342</i> | 2.43             | 29.18                    | 24.22            | 28.14                    | 21.78        | -1.05       | -3.59              |
| <i>GFL343</i> | 77.76            | 29.47                    | 259.63           | 28.41                    | 181.87       | -1.06       | -3.59              |
| <i>GFL344</i> | 0.00             | 28.64                    | 3.57             | 27.61                    | 3.57         | -1.03       | -3.58              |
| <i>GFL345</i> | 0.57             | 29.07                    | 8.47             | 28.03                    | 7.90         | -1.04       | -3.58              |
| <i>GFL346</i> | 0.00             | 28.90                    | 35.92            | 27.86                    | 35.92        | -1.03       | -3.58              |
| <i>GFL347</i> | 1.21             | 29.21                    | 12.13            | 28.17                    | 10.92        | -1.04       | -3.58              |
| <i>GFL348</i> | 0.00             | 28.86                    | 3.58             | 27.83                    | 3.58         | -1.03       | -3.57              |
| <i>GFL349</i> | 0.02             | 28.70                    | 30.48            | 27.68                    | 30.46        | -1.02       | -3.56              |
| <i>GFL350</i> | 464.82           | 29.47                    | 939.01           | 28.42                    | 474.20       | -1.05       | -3.56              |

**Table 8** Continued

| Gene ID       | TPM <sup>a</sup> | Length (mm) <sup>a</sup> | TPM <sup>b</sup> | Length (mm) <sup>b</sup> | Δ TPM   | Length (mm) | Δ ratio (%) |
|---------------|------------------|--------------------------|------------------|--------------------------|---------|-------------|-------------|
| <i>GFL351</i> | 3.99             | 29.40                    | 20.27            | 28.35                    | 16.28   | -1.05       | -3.56       |
| <i>GFL352</i> | 23.84            | 28.98                    | 106.31           | 27.95                    | 82.47   | -1.03       | -3.56       |
| <i>GFL353</i> | 0.85             | 29.50                    | 32.69            | 28.45                    | 31.84   | -1.05       | -3.56       |
| <i>GFL354</i> | 713.39           | 29.50                    | 1722.58          | 28.46                    | 1009.18 | -1.05       | -3.55       |
| <i>GFL355</i> | 142.13           | 29.35                    | 273.83           | 28.31                    | 131.70  | -1.04       | -3.55       |
| <i>GFL356</i> | 5.74             | 29.47                    | 46.66            | 28.43                    | 40.91   | -1.05       | -3.55       |
| <i>GFL357</i> | 0.00             | 29.26                    | 49.80            | 28.22                    | 49.80   | -1.04       | -3.55       |
| <i>GFL358</i> | 0.00             | 29.25                    | 33.94            | 28.21                    | 33.94   | -1.04       | -3.54       |
| <i>GFL359</i> | 0.00             | 28.99                    | 32.56            | 27.96                    | 32.56   | -1.02       | -3.54       |
| <i>GFL360</i> | 0.00             | 29.17                    | 13.84            | 28.13                    | 13.84   | -1.03       | -3.53       |
| <i>GFL361</i> | 0.00             | 29.16                    | 13.42            | 28.13                    | 13.42   | -1.03       | -3.52       |
| <i>GFL362</i> | 0.47             | 29.18                    | 55.29            | 28.15                    | 54.81   | -1.03       | -3.51       |
| <i>GFL363</i> | 0.00             | 29.09                    | 19.77            | 28.07                    | 19.77   | -1.02       | -3.51       |
| <i>GFL364</i> | 0.00             | 29.01                    | 16.63            | 28.00                    | 16.63   | -1.01       | -3.50       |
| <i>GFL365</i> | 0.97             | 29.36                    | 52.42            | 28.34                    | 51.45   | -1.02       | -3.49       |
| <i>GFL366</i> | 47.76            | 29.46                    | 101.35           | 28.44                    | 53.59   | -1.02       | -3.47       |
| <i>GFL367</i> | 350.09           | 29.37                    | 633.23           | 28.35                    | 283.13  | -1.02       | -3.47       |
| <i>GFL368</i> | 0.00             | 28.97                    | 21.83            | 27.96                    | 21.83   | -1.00       | -3.46       |
| <i>GFL369</i> | 11.43            | 29.11                    | 35.96            | 28.11                    | 24.53   | -1.01       | -3.46       |
| <i>GFL370</i> | 42.35            | 29.43                    | 104.25           | 28.41                    | 61.90   | -1.02       | -3.46       |
| <i>GFL371</i> | 8.71             | 29.45                    | 72.28            | 28.43                    | 63.56   | -1.02       | -3.45       |
| <i>GFL372</i> | 0.03             | 29.22                    | 27.76            | 28.21                    | 27.73   | -1.01       | -3.44       |
| <i>GFL373</i> | 0.00             | 29.04                    | 75.21            | 28.04                    | 75.21   | -1.00       | -3.44       |
| <i>GFL374</i> | 0.00             | 29.09                    | 12.49            | 28.09                    | 12.49   | -1.00       | -3.43       |
| <i>GFL375</i> | 79.07            | 29.27                    | 159.60           | 28.26                    | 80.53   | -1.01       | -3.43       |
| <i>GFL376</i> | 0.00             | 29.11                    | 24.82            | 28.12                    | 24.82   | -1.00       | -3.42       |
| <i>GFL377</i> | 24.60            | 29.54                    | 212.37           | 28.53                    | 187.77  | -1.01       | -3.41       |
| <i>GFL378</i> | 2.93             | 28.73                    | 61.51            | 27.75                    | 58.58   | -0.98       | -3.41       |
| <i>GFL379</i> | 0.00             | 28.80                    | 55.03            | 27.82                    | 55.03   | -0.98       | -3.40       |
| <i>GFL380</i> | 1.05             | 29.22                    | 94.33            | 28.23                    | 93.28   | -0.99       | -3.40       |
| <i>GFL381</i> | 101.14           | 29.21                    | 204.97           | 28.23                    | 103.83  | -0.98       | -3.37       |
| <i>GFL382</i> | 0.36             | 29.29                    | 19.93            | 28.31                    | 19.56   | -0.99       | -3.37       |
| <i>GFL383</i> | 0.00             | 28.99                    | 14.51            | 28.02                    | 14.51   | -0.98       | -3.37       |
| <i>GFL384</i> | 0.00             | 28.78                    | 3.38             | 27.81                    | 3.38    | -0.97       | -3.36       |
| <i>GFL385</i> | 198.79           | 29.30                    | 499.05           | 28.33                    | 300.25  | -0.98       | -3.34       |
| <i>GFL386</i> | 0.00             | 28.84                    | 25.23            | 27.88                    | 25.23   | -0.96       | -3.33       |
| <i>GFL387</i> | 19.24            | 29.19                    | 55.46            | 28.22                    | 36.22   | -0.97       | -3.32       |
| <i>GFL388</i> | 46.29            | 29.53                    | 125.29           | 28.55                    | 79.00   | -0.98       | -3.32       |
| <i>GFL389</i> | 5.16             | 29.37                    | 27.61            | 28.39                    | 22.45   | -0.98       | -3.32       |
| <i>GFL390</i> | 0.05             | 29.08                    | 14.60            | 28.12                    | 14.54   | -0.96       | -3.31       |
| <i>GFL391</i> | 0.00             | 28.76                    | 3.30             | 27.81                    | 3.30    | -0.95       | -3.31       |
| <i>GFL392</i> | 7.24             | 29.02                    | 44.77            | 28.07                    | 37.53   | -0.95       | -3.29       |
| <i>GFL393</i> | 1.17             | 28.89                    | 27.65            | 27.95                    | 26.47   | -0.95       | -3.28       |
| <i>GFL394</i> | 14.09            | 28.99                    | 65.35            | 28.04                    | 51.26   | -0.95       | -3.27       |
| <i>GFL395</i> | 1.22             | 28.98                    | 9.52             | 28.04                    | 8.30    | -0.94       | -3.25       |
| <i>GFL396</i> | 29.79            | 29.45                    | 72.78            | 28.49                    | 42.99   | -0.95       | -3.24       |
| <i>GFL397</i> | 0.00             | 28.95                    | 44.46            | 28.02                    | 44.46   | -0.94       | -3.23       |
| <i>GFL398</i> | 13.49            | 29.08                    | 34.27            | 28.14                    | 20.78   | -0.94       | -3.23       |
| <i>GFL399</i> | 8.49             | 29.45                    | 38.29            | 28.51                    | 29.80   | -0.94       | -3.21       |
| <i>GFL400</i> | 0.00             | 28.92                    | 5.11             | 27.99                    | 5.11    | -0.93       | -3.20       |

**Table 8** Continued

| Gene ID       | TPM <sup>a</sup> Length (mm) <sup>a</sup> |       | TPM <sup>b</sup> Length (mm) <sup>b</sup> |       | Δ TPM Length (mm) |       | Δ ratio (%) |
|---------------|---|-------|---|-------|-------------------|-------|-------------|
| <i>GFL401</i> | 28.27                                     | 29.09 | 76.37                                     | 28.16 | 48.10             | -0.93 | -3.19       |
| <i>GFL402</i> | 0.00                                      | 28.95 | 13.51                                     | 28.03 | 13.51             | -0.92 | -3.17       |
| <i>GFL403</i> | 0.00                                      | 29.03 | 10.36                                     | 28.12 | 10.36             | -0.91 | -3.15       |
| <i>GFL404</i> | 0.00                                      | 28.93 | 12.26                                     | 28.02 | 12.26             | -0.91 | -3.14       |
| <i>GFL405</i> | 0.49                                      | 29.05 | 10.45                                     | 28.14 | 9.96              | -0.91 | -3.13       |
| <i>GFL406</i> | 0.00                                      | 28.88 | 18.89                                     | 27.98 | 18.89             | -0.90 | -3.12       |
| <i>GFL407</i> | 9.25                                      | 29.22 | 34.04                                     | 28.31 | 24.79             | -0.91 | -3.12       |
| <i>GFL408</i> | 0.00                                      | 29.02 | 33.65                                     | 28.12 | 33.65             | -0.90 | -3.10       |
| <i>GFL409</i> | 290.07                                    | 29.52 | 668.39                                    | 28.61 | 378.32            | -0.91 | -3.08       |
| <i>GFL410</i> | 14.22                                     | 29.48 | 66.44                                     | 28.58 | 52.22             | -0.91 | -3.08       |
| <i>GFL411</i> | 0.00                                      | 29.01 | 4.34                                      | 28.12 | 4.34              | -0.89 | -3.06       |
| <i>GFL412</i> | 0.00                                      | 28.88 | 24.43                                     | 28.00 | 24.43             | -0.88 | -3.05       |
| <i>GFL413</i> | 0.00                                      | 29.09 | 38.53                                     | 28.21 | 38.53             | -0.88 | -3.02       |
| <i>GFL414</i> | 0.00                                      | 28.75 | 4.79                                      | 27.89 | 4.79              | -0.86 | -2.98       |
| <i>GFL415</i> | 0.00                                      | 29.04 | 9.30                                      | 28.18 | 9.30              | -0.86 | -2.98       |
| <i>GFL416</i> | 0.00                                      | 28.89 | 15.95                                     | 28.04 | 15.95             | -0.85 | -2.96       |
| <i>GFL417</i> | 7.47                                      | 29.18 | 43.18                                     | 28.32 | 35.71             | -0.86 | -2.93       |
| <i>GFL418</i> | 0.00                                      | 29.09 | 10.20                                     | 28.27 | 10.20             | -0.81 | -2.79       |
| <i>GFL419</i> | 0.00                                      | 29.11 | 4.82                                      | 28.31 | 4.82              | -0.80 | -2.74       |
| <i>GFL420</i> | 0.69                                      | 28.86 | 7.21                                      | 28.10 | 6.52              | -0.76 | -2.64       |
| <i>GFL421</i> | 0.00                                      | 28.55 | 15.30                                     | 29.43 | 15.30             | 0.88  | 3.08        |
| <i>GFL422</i> | 0.00                                      | 28.81 | 8.85                                      | 29.70 | 8.85              | 0.89  | 3.09        |
| <i>GFL423</i> | 0.00                                      | 28.64 | 17.44                                     | 29.57 | 17.44             | 0.92  | 3.23        |
| <i>GFL424</i> | 2.15                                      | 28.39 | 10.32                                     | 29.33 | 8.17              | 0.94  | 3.33        |
| <i>GFL425</i> | 0.00                                      | 28.56 | 38.43                                     | 29.51 | 38.43             | 0.95  | 3.33        |
| <i>GFL426</i> | 0.00                                      | 28.65 | 26.66                                     | 29.61 | 26.66             | 0.97  | 3.38        |
| <i>GFL427</i> | 0.49                                      | 28.45 | 16.21                                     | 29.42 | 15.72             | 0.97  | 3.40        |
| <i>GFL428</i> | 0.00                                      | 28.63 | 10.93                                     | 29.62 | 10.93             | 0.98  | 3.43        |
| <i>GFL429</i> | 0.00                                      | 28.61 | 23.12                                     | 29.61 | 23.12             | 0.99  | 3.47        |
| <i>GFL430</i> | 34.06                                     | 28.30 | 57008.56                                  | 29.31 | 56974.50          | 1.01  | 3.57        |
| <i>GFL431</i> | 68.98                                     | 28.20 | 272.05                                    | 29.22 | 203.07            | 1.02  | 3.63        |
| <i>GFL432</i> | 95.71                                     | 28.33 | 228.11                                    | 29.38 | 132.40            | 1.04  | 3.68        |
| <i>GFL433</i> | 1.29                                      | 28.56 | 11.43                                     | 29.63 | 10.14             | 1.06  | 3.72        |
| <i>GFL434</i> | 0.00                                      | 28.64 | 21.62                                     | 29.72 | 21.62             | 1.08  | 3.75        |
| <i>GFL435</i> | 0.00                                      | 28.94 | 7.83                                      | 30.03 | 7.83              | 1.09  | 3.76        |
| <i>GFL436</i> | 0.00                                      | 28.71 | 12.28                                     | 29.79 | 12.28             | 1.08  | 3.77        |
| <i>GFL437</i> | 0.00                                      | 28.55 | 12.20                                     | 29.63 | 12.20             | 1.08  | 3.78        |
| <i>GFL438</i> | 3.25                                      | 28.29 | 12.51                                     | 29.36 | 9.26              | 1.07  | 3.79        |
| <i>GFL439</i> | 8.58                                      | 28.15 | 70.99                                     | 29.23 | 62.41             | 1.08  | 3.82        |
| <i>GFL440</i> | 0.00                                      | 28.52 | 14.24                                     | 29.61 | 14.24             | 1.09  | 3.82        |
| <i>GFL441</i> | 0.00                                      | 28.75 | 70.79                                     | 29.86 | 70.79             | 1.10  | 3.83        |
| <i>GFL442</i> | 0.83                                      | 28.13 | 11.56                                     | 29.21 | 10.72             | 1.08  | 3.85        |
| <i>GFL443</i> | 0.59                                      | 28.45 | 7.26                                      | 29.56 | 6.66              | 1.11  | 3.89        |
| <i>GFL444</i> | 0.00                                      | 28.71 | 3.45                                      | 29.84 | 3.45              | 1.13  | 3.94        |
| <i>GFL445</i> | 0.00                                      | 28.20 | 25.56                                     | 29.32 | 25.56             | 1.12  | 3.97        |
| <i>GFL446</i> | 5.06                                      | 28.40 | 80.68                                     | 29.55 | 75.62             | 1.15  | 4.04        |
| <i>GFL447</i> | 0.00                                      | 28.66 | 10.72                                     | 29.81 | 10.72             | 1.16  | 4.04        |
| <i>GFL448</i> | 0.00                                      | 28.46 | 31.34                                     | 29.64 | 31.34             | 1.18  | 4.15        |
| <i>GFL449</i> | 0.28                                      | 28.51 | 32.40                                     | 29.70 | 32.12             | 1.19  | 4.17        |
| <i>GFL450</i> | 1.06                                      | 28.22 | 33.82                                     | 29.43 | 32.76             | 1.21  | 4.29        |



**Table 8** Continued

| Gene ID       | TPM <sup>a</sup> | Length (mm) <sup>a</sup> | TPM <sup>b</sup> | Length (mm) <sup>b</sup> | $\Delta$ TPM | Length (mm) | $\Delta$ ratio (%) |
|---------------|------------------|--------------------------|------------------|--------------------------|--------------|-------------|--------------------|
| <i>GFL451</i> | 2.00             | 28.29                    | 16.64            | 29.51                    | 14.64        | 1.22        | 4.31               |
| <i>GFL452</i> | 36.98            | 28.33                    | 127.91           | 29.57                    | 90.93        | 1.24        | 4.38               |
| <i>GFL453</i> | 1.34             | 28.08                    | 28.52            | 29.32                    | 27.18        | 1.24        | 4.42               |
| <i>GFL454</i> | 0.60             | 27.95                    | 13.76            | 29.19                    | 13.16        | 1.24        | 4.44               |
| <i>GFL455</i> | 1.36             | 28.12                    | 18.66            | 29.38                    | 17.29        | 1.26        | 4.48               |
| <i>GFL456</i> | 1.13             | 28.08                    | 30.91            | 29.36                    | 29.78        | 1.28        | 4.54               |
| <i>GFL457</i> | 0.89             | 28.39                    | 46.57            | 29.68                    | 45.68        | 1.30        | 4.58               |
| <i>GFL458</i> | 0.13             | 28.30                    | 11.75            | 29.60                    | 11.63        | 1.30        | 4.61               |
| <i>GFL459</i> | 73.85            | 28.01                    | 372.19           | 29.30                    | 298.34       | 1.29        | 4.61               |
| <i>GFL460</i> | 0.00             | 27.93                    | 40.01            | 29.21                    | 40.01        | 1.29        | 4.61               |
| <i>GFL461</i> | 0.00             | 28.44                    | 4.83             | 29.76                    | 4.83         | 1.32        | 4.66               |
| <i>GFL462</i> | 0.76             | 28.39                    | 50.70            | 29.73                    | 49.94        | 1.34        | 4.70               |
| <i>GFL463</i> | 0.00             | 28.54                    | 9.31             | 29.89                    | 9.31         | 1.35        | 4.72               |
| <i>GFL464</i> | 0.00             | 28.41                    | 4.58             | 29.76                    | 4.58         | 1.35        | 4.77               |
| <i>GFL465</i> | 0.00             | 28.49                    | 10.34            | 29.85                    | 10.34        | 1.36        | 4.77               |
| <i>GFL466</i> | 0.02             | 28.33                    | 57.91            | 29.78                    | 57.89        | 1.44        | 5.10               |
| <i>GFL467</i> | 39.42            | 28.71                    | 208.15           | 30.20                    | 168.73       | 1.49        | 5.19               |
| <i>GFL468</i> | 1.23             | 28.44                    | 10.87            | 29.93                    | 9.64         | 1.48        | 5.21               |
| <i>GFL469</i> | 0.63             | 28.35                    | 14.55            | 29.84                    | 13.91        | 1.49        | 5.26               |
| <i>GFL470</i> | 0.00             | 28.49                    | 8.44             | 30.00                    | 8.44         | 1.50        | 5.27               |
| <i>GFL471</i> | 1.49             | 27.95                    | 47.92            | 29.44                    | 46.43        | 1.50        | 5.36               |
| <i>GFL472</i> | 0.00             | 28.46                    | 14.57            | 30.02                    | 14.57        | 1.56        | 5.48               |
| <i>GFL473</i> | 3.23             | 28.45                    | 151.10           | 30.22                    | 147.87       | 1.77        | 6.23               |
| <i>GFL474</i> | 268.78           | 28.33                    | 1136.29          | 30.25                    | 867.52       | 1.93        | 6.80               |

a: The mean of 30 RILs that showed the least active expression for the *GFL* gene.

b: The mean of 30 RILs that showed the most active expression for the *GFL* gene.

To determine the action directions and effects of the *GFL* genes on UHML, the expression data of the genes in the 198 RILs of the TAM 94L-25 x NMSI 1331 population were extracted from the gene expression profiles of 10-dpa fibers of the population generated by RNA-seq in this study and subjected to statistical analysis against the genetic variation of the UHML of the population. The results showed that 429 (88.6%) of the *GFL* genes were shown to contribute to UHML negatively, whereas 54 (11.4%) contributed to UHML positively (Table 8). The *GFL* genes that negatively contributed UHML, including *GFL001* through *GFL420*, were found to have shorter UHML when their expression levels increased or expression modes were turned on. For *GFL* genes that positively contributed UHML, their higher expression levels were found to result in longer UHML. Furthermore, to determine the effect of each *GFL* gene, 30 RILs that showed the most active expression and 30 RILs that showed the least active expression for each gene among the 198 RILs of the population were compiled into two differently expressed groups of RILs for each *GFL* gene. The UHML of the two RIL groups with different expression levels for the *GFL* gene were subjected to statistical analysis (t-test). The result showed that the *GFL* genes had a positive or negative effect of 2.64 – 7.92% on UHML. In other words, when the gene is turned on or more actively expressed in 10-dpa fibers, the UHML of the RIL will be increased or decreased by 2.64 – 7.92%. Of the *GFL* genes that had negative effects on UHML, *GFL001* showed the largest negative effect on UHML (-7.92%) when it was actively expressed in 10-dpa fibers. Of the *GFL* genes with positive effects on UHML, *GFL474* increased UHML by 6.80% when its expression level increased from 268.78 TPM to 1,136.29 TPM.

**Table 9** List of published genes controlling fiber length or trichome development

| Gene        | Gene description                          | GenBank no. | Reference                        | <i>P</i> value |          |        |
|-------------|---|-------------|----------------------------------|----------------|----------|--------|
|             |   |             |                                  | ≤ 6.25e-05     | ≤ 0.0025 | ≤ 0.05 |
| XET/XTH     | Xyloglucan endotransglycosylase/hydrolase | HM749062.1  | Lee <i>et al.</i> 2010           | ✓              | ✓        | ✓      |
| PHYA        | Phytochrome                               | HM143740.1  | Abdurakhmonov <i>et al.</i> 2014 | ✓              | ✓        | ✓      |
| GhACT1      | Actin                                     | AY305723.1  | Li <i>et al.</i> 2005            |                | ✓        | ✓      |
| GhADF1      | Actin-depolymerizing factor               | AI731080    | Wang <i>et al.</i> 2008          | ✓              | ✓        | ✓      |
| GhPEL       | Pectate lyase                             | DQ073046.1  | Wang <i>et al.</i> 2010          |                | ✓        | ✓      |
| F3H         | Flavanone 3-hydroxylase                   | GU434116.1  | Tan <i>et al.</i> 2013           | ✓              | ✓        | ✓      |
| GhPFN2      | Profilin                                  | GU237487.1  | Wang <i>et al.</i> 2010          |                |          | ✓      |
| GhFLA1      | Fasciclin-like arabinogalactan protein    | EF672627.1  | Huang <i>et al.</i> 2013         | ✓              | ✓        | ✓      |
| GhAGP4      | Arabinogalactan                           | EF470295.1  | Li <i>et al.</i> 2010            |                | ✓        | ✓      |
| GbTCP       | TCP transcription factor                  | DQ359121.1  | Hao <i>et al.</i> 2012           |                |          | ✓      |
| GhMYB109    | R2R3 MYB transcription factor             | AJ549758.1  | Pu <i>et al.</i> 2008            |                | ✓        | ✓      |
| GhMYB25     | R2R3 MYB transcription factor             | AF336283.1  | Machado <i>et al.</i> 2009       |                | ✓        | ✓      |
| GhRDL1      | <i>AtRD22-Like 1</i> gene                 | AY072821.1  | Xu <i>et al.</i> 2013            |                |          | ✓      |
| WLIM1a      | LIN-11, Isl1 and MEC-3 domain protein     | JX648310.1  | Han <i>et al.</i> 2013           | ✓              | ✓        | ✓      |
| GhVIN1      | Vacuolar Invertase                        | FJ915120.1  | Wang <i>et al.</i> 2010          |                | ✓        | ✓      |
| GhSusA1     | Sucrose synthase                          | HQ702185    | Jiang <i>et al.</i> 2012         | ✓              | ✓        | ✓      |
| GhGA20ox1-3 | Gibberellin 20-oxidase                    | AY603789.1  | Xiao <i>et al.</i> 2010          |                |          | ✓      |
| GhDET2      | Steroid 5a-reductase                      | DQ116446.1  | Luo <i>et al.</i> 2007           |                | ✓        | ✓      |
| GhTTG1      | TRANSPARENT TESTA GLABRA1                 | AF336281.1  | Humphries <i>et al.</i> 2005     | ✓              | ✓        | ✓      |
| GhTTG3      | TRANSPARENT TESTA GLABRA1                 | AF530911.1  | Humphries <i>et al.</i> 2005     | ✓              |          | ✓      |

✓ : published fiber genes that were isolated by the new high-throughput gene/QTL cloning systems at different significant levels.

To determine what the *GFL* genes are and what they do in the 10-dpa developing fibers, the biochemical functions of the *GFL* genes were inferred by BLASTX to the NCBI's non-redundant protein database. Three hundred ninety-nine of the 474 *GFL* genes (84.18%) were annotated (Table 10). Of the 399 annotated *GFL* genes, 353 (88.47%) genes were annotated with gene descriptions under an E-value cutoff of 1.0E-06 and 116 were assigned to at least one enzyme code, with a total of 164 assigned enzyme codes. These results totally agreed with the 21 genes previously cloned by different scientists that encoded diverged proteins or enzymes (Table 9). The *GFL* genes isolated in this study encode a diversity of proteins or enzymes, such as cytochromes, alcohol dehydrogenase transcription factor Myb/SANT-like family protein, 2-oxoglutarate and Fe(II)-dependent oxygenase superfamily protein, AMP-dependent synthetase and ligase family protein, cellulose synthase, Galactosyltransferase family protein, etc. (Table 10).

GO analysis assigned the *GFL* genes to 3,117 GO items, with an average of 3.775 GO terms per gene and a standard deviation of 1.498. Two hundred ninety *GFL* genes were assigned to the category of biological process, 298 *GFL* genes were assigned to the category of molecular function and 316 *GFL* genes were assigned to the category of cellular component (Figs. 18 – 20). Of the 290 *GFL* genes assigned to the category of biological process, 32% participate in cellular and metabolic processes (Fig. 18). Of the 298 *GFL* genes assigned to the category of molecular function, 85% are involved in binding and catalytic activities (Fig. 19). Of the 316 *GFL* genes assigned to the category of cellular component, 75% take part in cell and organelle components (Fig. 20).

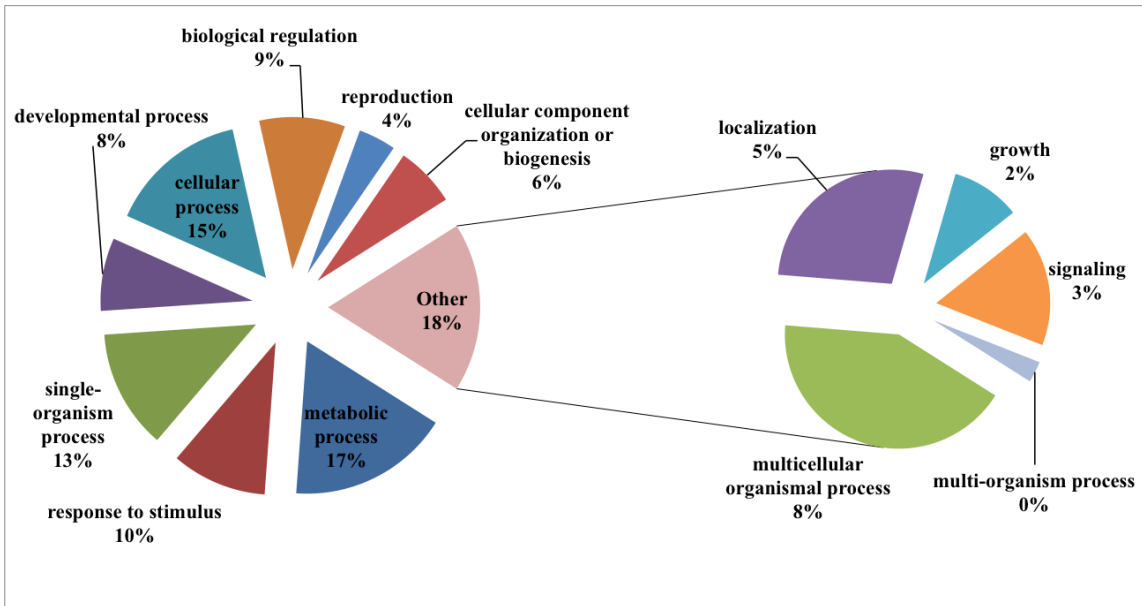


**Figure 18** GO items of the *GFL* genes assigned to the functional category of biological process (level 2)

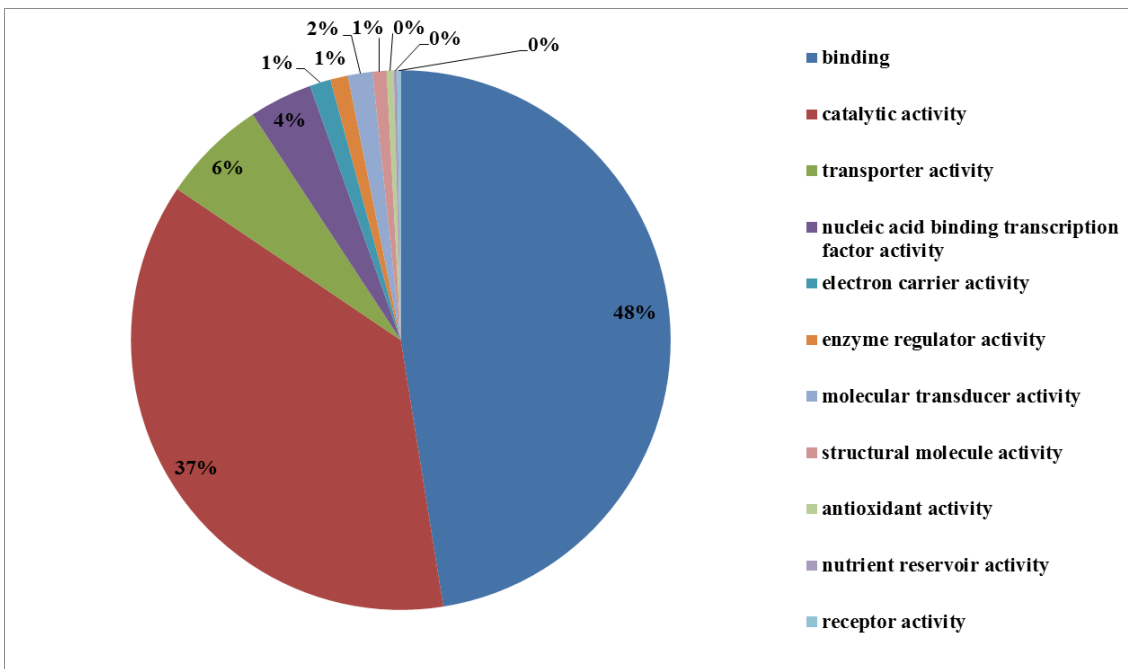


**Figure 19** GO items of the *GFL* genes assigned to the functional category of molecular function (level 2)

**Table 10** Annotation of *GFL* genes controlling UHML in 10-dpa tetraploid cotton species

| Gene ID       | Seq. Description | Seq. Length | #GOs | Enzyme Codes |
|---------------|------------------|-------------|------|--------------|
| <i>GFL015</i> | -                | 448         | 0    |              |
| <i>GFL001</i> | -                | 309         | 1    | -            |
| <i>GFL420</i> | -                | 334         | 0    |              |
| <i>GFL111</i> | -                | 300         | 0    |              |
| <i>GFL234</i> | -                | 595         | 0    |              |
| <i>GFL451</i> | -                | 932         | 0    |              |
| <i>GFL122</i> | -                | 202         | 0    |              |
| <i>GFL056</i> | -                | 225         | 0    |              |
| <i>GFL464</i> | -                | 627         | 0    |              |
| <i>GFL212</i> | -                | 533         | 0    |              |
| <i>GFL348</i> | -                | 232         | 0    |              |
| <i>GFL151</i> | -                | 381         | 0    |              |
| <i>GFL172</i> | -                | 332         | 0    |              |
| <i>GFL140</i> | -                | 481         | 0    |              |
| <i>GFL384</i> | -                | 300         | 0    |              |
| <i>GFL149</i> | -                | 232         | 0    |              |
| <i>GFL323</i> | -                | 283         | 0    |              |
| <i>GFL012</i> | -                | 464         | 0    |              |
| <i>GFL059</i> | -                | 414         | 0    |              |
| <i>GFL442</i> | -                | 636         | 0    |              |
| <i>GFL042</i> | -                | 960         | 0    |              |
| <i>GFL002</i> | -                | 413         | 0    |              |
| <i>GFL107</i> | -                | 372         | 0    |              |
| <i>GFL132</i> | -                | 789         | 0    |              |
| <i>GFL345</i> | -                | 376         | 0    |              |
| <i>GFL112</i> | -                | 358         | 0    |              |
| <i>GFL034</i> | -                | 457         | 0    |              |
| <i>GFL141</i> | -                | 449         | 0    |              |
| <i>GFL005</i> | -                | 727         | 0    |              |
| <i>GFL443</i> | -                | 615         | 0    |              |
| <i>GFL197</i> | -                | 344         | 0    |              |
| <i>GFL047</i> | -                | 475         | 0    |              |
| <i>GFL344</i> | -                | 431         | 0    |              |
| <i>GFL224</i> | -                | 343         | 0    |              |
| <i>GFL297</i> | -                | 387         | 0    |              |
| <i>GFL028</i> | -                | 789         | 0    |              |
| <i>GFL022</i> | -                | 452         | 0    |              |
| <i>GFL315</i> | -                | 242         | 0    |              |
| <i>GFL254</i> | -                | 540         | 0    |              |

**Table 10** Continued

| Gene ID | Seq. Description  | Seq. Length | #GOs | Enzyme Codes |
|---------|---|-------------|------|--------------|
| GFL351  | -   | 381         | 0    |              |
| GFL411  | -   | 403         | 0    |              |
| GFL036  | -   | 428         | 0    |              |
| GFL074  | -   | 474         | 0    |              |
| GFL093  | -   | 288         | 0    |              |
| GFL386  | -   | 1249        | 0    |              |
| GFL221  | -   | 367         | 0    |              |
| GFL369  | -   | 613         | 0    |              |
| GFL003  | -   | 249         | 0    |              |
| GFL073  | -   | 1199        | 0    |              |
| GFL334  | -   | 434         | 0    |              |
| GFL087  | -   | 431         | 0    |              |
| GFL300  | -   | 410         | 0    |              |
| GFL305  | -   | 377         | 0    |              |
| GFL261  | -   | 396         | 0    |              |
| GFL441  | -   | 542         | 0    |              |
| GFL382  | -   | 240         | 0    |              |
| GFL359  | -   | 2300        | 0    |              |
| GFL067  | -   | 507         | 0    |              |
| GFL368  | -   | 715         | 0    |              |
| GFL370  | -   | 699         | 0    |              |
| GFL391  | -   | 350         | 0    |              |
| GFL248  | -   | 256         | 0    |              |
| GFL414  | -   | 348         | 0    |              |
| GFL167  | -   | 1148        | 0    |              |
| GFL428  | -   | 812         | 0    |              |
| GFL309  | -   | 685         | 0    |              |
| GFL255  | -   | 235         | 0    |              |
| GFL072  | -   | 229         | 0    |              |
| GFL389  | -   | 360         | 0    |              |
| GFL179  | -   | 312         | 0    |              |
| GFL033  | -   | 349         | 4    | EC:2.7.1.23  |
| GFL244  | -   | 230         | 0    |              |
| GFL444  | -   | 323         | 0    |              |
| GFL066  | -   | 296         | 0    |              |
| GFL312  | -   | 806         | 0    |              |
| GFL263  | 14-3-3f protein   | 766         | 21   | -            |
| GFL459  | 14-3-3h protein   | 1335        | 1    | -            |
| GFL102  | 2-oxoglutarate and Fe(II)-dependent oxygenase superfamily protein, putative | 1277        | 1    | EC:1.14.11.0 |

**Table 10** Continued

| Gene ID | Seq. Description  | Seq. Length | #GOs | Enzyme Codes                           |
|---------|---|-------------|------|--|
| GFL380  | 20S proteasome subunit alpha-1  | 1274        | 15   | EC:3.4.25.0                            |
| GFL426  | 3-ketoacyl-acyl carrier protein synthase III, III isoform 1             | 3682        | 16   | EC:2.3.1.41                            |
| GFL242  | 51 kDa subunit of complex I   | 1962        | 17   | EC:1.6.5.3                             |
| GFL456  | 6-phosphogluconolactonase 1 isoform 1                                   | 769         | 7    | EC:3.1.1.31                            |
| GFL241  | AAA-type ATPase family protein  | 1769        | 16   | EC:3.6.4.3                             |
| GFL214  | AarF domain-containing kinase isoform 2                                 | 310         | 4    | -                                      |
| GFL032  | ABI-1-like 1 isoform 1  | 1205        | 8    | -                                      |
| GFL397  | AC002423_8T23E23.16   | 4555        | 4    | EC:2.7.7.49                            |
| GFL004  | AC007323_16T25K16.5   | 357         | 10   | EC:3.6.1.1                             |
| GFL205  | Acetyl-CoA synthetase isoform 1   | 1805        | 12   | EC:6.2.1.1                             |
| GFL336  | Actin depolymerizing factor 5   | 797         | 5    | -                                      |
| GFL121  | actin-97  | 301         | 3    | -                                      |
| GFL454  | Acyl-CoA binding protein 4 isoform 3                                    | 337         | 15   | -                                      |
| GFL376  | Adenosine-5'-phosphosulfate (APS) kinase 3 isoform 1                    | 1124        | 11   | EC:2.7.1.25; EC:2.7.2.4; EC:1.3.1.74   |
| GFL181  | ADP-glucose pyrophosphorylase family protein isoform 1                  | 2365        | 6    | EC:2.7.7.13                            |
| GFL430  | AF218378_1protein kinase  | 1212        | 4    | -                                      |
| GFL190  | Alba DNA/RNA-binding protein  | 262         | 6    | -                                      |
| GFL398  | Alcohol dehydrogenase transcription factor Myb/SANT-like family protein | 801         | 1    | -                                      |
| GFL039  | Alkaline-phosphatase-like family protein isoform 1                      | 1983        | 7    | EC:3.6.1.9; EC:3.1.4.1                 |
| GFL372  | Alpha-1,6-mannosyl-glycoprotein 2-beta-N-acetylglucosaminyltransferase  | 2446        | 3    | -                                      |
| GFL409  | Alpha/beta-Hydrolases superfamily protein isoform 1                     | 2606        | 5    | -                                      |
| GFL302  | Alpha/beta-Hydrolases superfamily protein isoform 2                     | 1284        | 13   | -                                      |
| GFL153  | Alpha/beta-Hydrolases superfamily protein, putative isoform 1           | 1048        | 1    | -                                      |
| GFL400  | AMP-dependent synthetase and ligase family protein                      | 559         | 10   | EC:2.3.1.86; EC:1.13.12.7; EC:6.2.1.12 |
| GFL466  | AMP-dependent synthetase and ligase family protein isoform 1            | 3083        | 9    | EC:6.2.1.3                             |
| GFL355  | angustifolia  | 2839        | 26   | EC:1.1.1.29                            |
| GFL168  | Ankyrin repeat domain-containing protein 50 isoform 3                   | 864         | 1    | -                                      |
| GFL063  | Ankyrin repeat family protein   | 1665        | 17   | -                                      |
| GFL223  | Arabinanase/levansucrase/invertase, putative                            | 1894        | 3    | -                                      |
| GFL326  | Arginine decarboxylase  | 2697        | 17   | EC:4.1.1.19                            |
| GFL159  | Arginine methyltransferase 11   | 635         | 9    | EC:2.1.1.125                           |
| GFL403  | Asparagine synthase family protein, putative                            | 1607        | 4    | -                                      |
| GFL058  | ASYMMETRIC LEAVES 2-like 1  | 1263        | 6    | -                                      |
| GFL269  | Auxin efflux carrier family protein isoform 1                           | 1140        | 2    | -                                      |
| GFL128  | Basic helix-loop-helix DNA-binding superfamily protein                  | 1341        | 12   | -                                      |
| GFL225  | Basic leucine-zipper 44   | 1357        | 12   | -                                      |
| GFL250  | Basic-leucine zipper transcription factor family protein isoform 3      | 1419        | 12   | -                                      |
| GFL282  | Beige-related and WD-40 repeat-containing protein isoform 2             | 390         | 2    | -                                      |
| GFL152  | Beige/BEACH domain,WD domain, G-beta repeat protein                     | 9339        | 10   | -                                      |
| GFL185  | beta-mannosidase  | 1891        | 4    | EC:3.2.1.152                           |



**Table 10** Continued

| Gene ID       | Seq. Description  | Seq. Length | #GOs | Enzyme Codes                                       |
|---------------|---|-------------|------|--|
| <i>GFL272</i> | Bifunctional methylthioribulose-1-phosphate dehydratase/enolase-phosphatase E1, putative                            | 1592        | 8    | EC:4.2.1.109; EC:3.1.3.18; EC:3.1.3.77             |
| <i>GFL327</i> | Binding to TOMV RNA 1L (long form) isoform 1  | 1072        | 10   | EC:3.1.2.15  |
| <i>GFL360</i> | Biotin carboxyl carrier protein subunit of of Het-ACCCase (BCCP1), putative isoform 3                               | 478         | 20   | EC:6.4.1.2   |
| <i>GFL105</i> | BR-signaling kinase 2 isoform 1   | 1705        | 19   | EC:2.7.11.0; EC:2.7.10.0; EC:2.7.1.40; EC:3.2.1.15 |
| <i>GFL069</i> | Bromodomain 4, putative   | 800         | 2    | -  |
| <i>GFL299</i> | BSD domain (BTF2-like transcription factors, Synapse-associated proteins and DOS2-like proteins) isoform 4, partial | 1161        | 5    | -  |
| <i>GFL280</i> | BSD domain-containing protein, putative   | 834         | 3    | -  |
| <i>GFL048</i> | BTB-POZ and MATH domain 2   | 3930        | 8    | -  |
| <i>GFL158</i> | BTB/POZ domain with WD40/YVTN repeat-like protein   | 1347        | 7    | -  |
| <i>GFL288</i> | BTB/POZ domain-containing protein   | 2314        | 1    | -  |
| <i>GFL045</i> | BTB/POZ domain-containing protein isoform 1   | 876         | 1    | -  |
| <i>GFL247</i> | C2H2 zinc-finger protein SERRATE isoform 2, partial   | 2660        | 17   | -  |
| <i>GFL377</i> | Calcium-binding EF-hand family protein  | 588         | 10   | -  |
| <i>GFL096</i> | Calcium-binding EF-hand family protein, putative isoform 1  | 1027        | 4    | -  |
| <i>GFL050</i> | Calcium-dependent lipid-binding (CaLB domain) family protein isoform 1  | 442         | 11   | -  |
| <i>GFL278</i> | Calcium-dependent lipid-binding family protein isoform 2, partial   | 731         | 6    | -  |
| <i>GFL182</i> | Calcium-dependent protein kinase 13 isoform 2   | 2758        | 6    | EC:2.7.11.17                                       |
| <i>GFL440</i> | Calcium-dependent protein kinase 6 isoform 2  | 2317        | 17   | EC:2.7.11.17                                       |
| <i>GFL014</i> | CDK inhibitor P21 binding protein, putative   | 1635        | 2    | -  |
| <i>GFL086</i> | Cellulose-synthase-like C12   | 2781        | 7    | EC:2.4.1.12  |
| <i>GFL251</i> | Chloride channel F isoform 2  | 1256        | 7    | -  |
| <i>GFL071</i> | Chloride channel protein CLC-d isoform 6  | 247         | 14   | -  |
| <i>GFL407</i> | Chloroplast isoform 2, partial  | 879         | 4    | -  |
| <i>GFL343</i> | Chloroplast-targeted copper chaperone-like protein  | 749         | 0    | -  |
| <i>GFL267</i> | Chloroplast-targeted copper chaperone-like protein  | 642         | 9    | EC:3.1.3.0   |
| <i>GFL268</i> | Chromatin remodeling complex subunit isoform 1  | 3709        | 17   | -  |
| <i>GFL230</i> | Cleavage stimulation factor 64 kDa subunit, putative  | 2348        | 7    | -  |
| <i>GFL354</i> | CLIP-associated protein isoform 1   | 4930        | 21   | -  |
| <i>GFL201</i> | Cobalt ion binding  | 1482        | 5    | -  |
| <i>GFL029</i> | COBRA-like extracellular glycosyl-phosphatidyl inositol-anchored protein family isoform 2                           | 2075        | 27   | EC:1.10.2.2  |
| <i>GFL245</i> | Concanavalin A-like lectin protein kinase family protein  | 907         | 2    | -  |
| <i>GFL266</i> | conserved hypothetical protein  | 833         | 4    | EC:1.6.5.3   |
| <i>GFL054</i> | Core-2/I-branching beta-1,6-N-acetylglucosaminyltransferase family protein  | 333         | 7    | EC:2.4.2.26  |
| <i>GFL052</i> | CRT-like transporter 3 isoform 1  | 1801        | 7    | -  |
| <i>GFL298</i> | Cullin 1  | 431         | 27   | -  |
| <i>GFL264</i> | Cyclin b2,4 isoform 2   | 1343        | 16   | -  |
| <i>GFL329</i> | Cyclin family protein isoform 2   | 1887        | 10   | -  |
| <i>GFL169</i> | Cyclin p1,1 isoform 1   | 1049        | 5    | -  |

**Table 10** Continued

| Gene ID       | Seq. Description   | Seq. Length | #GOs | Enzyme Codes              |
|---------------|--|-------------|------|---------------------------|
| <i>GFL450</i> | Cyclin p4,1  | 893         | 10   | EC:2.7.11.22              |
| <i>GFL319</i> | Cysteine-rich RLK 42   | 1143        | 7    | EC:2.7.10.0               |
| <i>GFL196</i> | Cytochrome P450  | 2101        | 3    | -                         |
| <i>GFL455</i> | Cytochrome P450, putative                                    | 914         | 9    | EC:1.14.13.0              |
| <i>GFL038</i> | D6 protein kinase like 2                                     | 323         | 13   | EC:2.7.11.0               |
| <i>GFL025</i> | DEA(D/H)-box RNA helicase family protein isoform 3           | 596         | 0    |                           |
| <i>GFL240</i> | Developmental regulator, ULTRAPETALA                         | 1340        | 7    | -                         |
| <i>GFL145</i> | DHHC-type zinc finger family protein                         | 1036        | 2    | -                         |
| <i>GFL171</i> | DNA binding/zinc ion binding protein                         | 734         | 3    | -                         |
| <i>GFL082</i> | DNA glycosylase superfamily protein                          | 1627        | 10   | EC:3.2.2.21; EC:3.2.2.20  |
| <i>GFL412</i> | DNA glycosylase superfamily protein isoform 2                | 1376        | 9    | -                         |
| <i>GFL422</i> | DNAse I-like superfamily protein isoform 1                   | 1288        | 6    | -                         |
| <i>GFL421</i> | DNAse I-like superfamily protein, putative isoform 2         | 1439        | 5    | -                         |
| <i>GFL425</i> | Domain of Uncharacterized protein function isoform 1         | 1545        | 4    | -                         |
| <i>GFL139</i> | Drought-responsive family protein                            | 1178        | 6    | -                         |
| <i>GFL166</i> | Dynamin-related protein 3A isoform 2                         | 702         | 14   | -                         |
| <i>GFL306</i> | E3 ubiquitin-protein ligase UPL5                             | 4323        | 12   | EC:2.7.7.49; EC:6.3.2.19  |
| <i>GFL293</i> | EIN2-like protein, nramp transporter isoform 1               | 747         | 25   | -                         |
| <i>GFL203</i> | Electron transport complex protein rnfC, putative isoform 3  | 783         | 0    |                           |
| <i>GFL194</i> | Emb:CAB89363.1   | 2931        | 1    | -                         |
| <i>GFL387</i> | Embryo defective 1703, putative isoform 2                    | 2326        | 5    | -                         |
| <i>GFL262</i> | Embryo defective 2423, putative                              | 3267        | 5    | -                         |
| <i>GFL410</i> | Endonuclease or glycosyl hydrolase                           | 2036        | 2    | -                         |
| <i>GFL419</i> | Endonuclease/exonuclease/phosphatase family protein          | 374         | 2    | -                         |
| <i>GFL084</i> | Enhanced disease resistance 2 isoform 1                      | 772         | 14   | -                         |
| <i>GFL103</i> | ENTH/VHS   | 2417        | 2    | -                         |
| <i>GFL416</i> | Ethylene-insensitive 3f isoform 1                            | 1287        | 3    | -                         |
| <i>GFL364</i> | Exostosin family protein                                     | 1813        | 3    | -                         |
| <i>GFL173</i> | Extra-large G-protein 1                                      | 3645        | 14   | -                         |
| <i>GFL142</i> | F-box/RNI-like superfamily protein isoform 1                 | 1090        | 16   | EC:6.3.2.19               |
| <i>GFL010</i> | Far1-related sequence 3 isoform 1                            | 373         | 1    | -                         |
| <i>GFL447</i> | Fatty acyl-ACP thioesterases B isoform 2                     | 1415        | 9    | EC:3.1.2.14               |
| <i>GFL274</i> | FKBP-type peptidyl-prolyl cis-trans isomerase family protein | 1249        | 10   | EC:5.2.1.8                |
| <i>GFL026</i> | Flavin-binding monooxygenase family protein isoform 1        | 1815        | 13   | EC:4.6.1.2; EC:1.14.13.8  |
| <i>GFL011</i> | Floral homeotic protein DEFICIENS isoform 1                  | 970         | 14   | -                         |
| <i>GFL362</i> | FMN-linked oxidoreductases superfamily protein isoform 1     | 1638        | 9    | -                         |
| <i>GFL328</i> | Formin-like protein 5 isoform 1                              | 3499        | 10   | -                         |
| <i>GFL431</i> | Fructose-2,6-bisphosphatase isoform 1                        | 4773        | 9    | EC:2.7.1.105; EC:3.1.3.46 |
| <i>GFL257</i> | Galactose oxidase/kelch repeat superfamily protein           | 223         | 21   | EC:6.3.2.19               |

**Table 10** Continued

| Gene ID       | Seq. Description  | Seq. Length | #GOs | Enzyme Codes                         |
|---------------|---|-------------|------|--------------------------------------|
| <i>GFL385</i> | Galactosyltransferase family protein  | 2022        | 6    | EC:2.4.1.134                         |
| <i>GFL191</i> | GATA transcription factor 2, putative   | 693         | 9    | -                                    |
| <i>GFL217</i> | GCIIP-interacting family protein isoform 1  | 1352        | 1    | -                                    |
| <i>GFL134</i> | GDP-fucose protein O-fucosyltransferase 1 isoform 1   | 437         | 1    | EC:2.4.1.221                         |
| <i>GFL342</i> | Geminivirus rep interacting kinase 2  | 2260        | 9    | EC:2.7.10.0; EC:2.7.11.17            |
| <i>GFL258</i> | Global transcription factor group E4, putative isoform 1  | 2300        | 8    | -                                    |
| <i>GFL178</i> | GLU-ADT subunit B isoform 1   | 2137        | 11   | EC:6.3.5.7                           |
| <i>GFL404</i> | glucosamine-fructose-6-phosphate aminotransferase, putative   | 631         | 9    | EC:2.6.1.16                          |
| <i>GFL070</i> | Glucose-inhibited division family A protein isoform 1   | 2399        | 9    | EC:2.1.1.74                          |
| <i>GFL357</i> | Glutamate-ammonia ligases, catalytic, glutamate-ammonia ligases isoform 3                               | 2240        | 17   | EC:6.3.1.2                           |
| <i>GFL363</i> | Glutamyl-tRNA(Gln) amidotransferase subunit A isoform 1   | 2115        | 14   | EC:6.3.5.0; EC:3.5.1.4               |
| <i>GFL130</i> | Glutathione-disulfide reductase isoform 1   | 1879        | 26   | EC:1.8.1.7; EC:1.1.1.44; EC:1.1.1.30 |
| <i>GFL055</i> | Glycosyl transferase family 1 protein isoform 1   | 443         | 7    | -                                    |
| <i>GFL108</i> | Glycosyltransferase isoform 2   | 773         | 7    | EC:2.4.1.43                          |
| <i>GFL160</i> | GRAM domain family protein, putative isoform 1  | 418         | 0    | -                                    |
| <i>GFL206</i> | GRIP and coiled-coil domain-containing protein 2, putative isoform 1                                    | 2632        | 14   | -                                    |
| <i>GFL155</i> | Haloacid dehalogenase-like hydrolase (HAD) superfamily protein isoform 1                                | 1396        | 8    | EC:3.1.3.0                           |
| <i>GFL291</i> | HAT dimerization domain-containing protein isoform 2  | 3182        | 3    | -                                    |
| <i>GFL365</i> | HD domain class transcription factor isoform 2  | 3321        | 16   | -                                    |
| <i>GFL040</i> | Heat shock factor protein HSF8, putative  | 2609        | 9    | -                                    |
| <i>GFL249</i> | Heat shock protein DnaJ, N-terminal with domain of Uncharacterized protein function (DUF1977) isoform 1 | 2021        | 4    | -                                    |
| <i>GFL136</i> | Helicase/SANT-associated, putative isoform 5  | 450         | 4    | -                                    |
| <i>GFL120</i> | Hexokinase 1 isoform 2  | 2081        | 18   | EC:2.7.1.2; EC:2.7.1.4               |
| <i>GFL043</i> | Histidine acid phosphatase family protein isoform 1   | 2327        | 7    | EC:3.1.3.2; EC:3.1.3.62              |
| <i>GFL424</i> | histone deacetylase   | 254         | 15   | EC:3.5.1.98                          |
| <i>GFL175</i> | Histone deacetylase 6 isoform 1   | 1415        | 21   | EC:3.5.1.98                          |
| <i>GFL390</i> | Homeodomain-like superfamily protein  | 563         | 9    | -                                    |
| <i>GFL448</i> | Hydroxyproline-rich glycoprotein family protein, putative   | 2322        | 3    | -                                    |
| <i>GFL237</i> | Hydroxyproline-rich glycoprotein family protein, putative isoform 1                                     | 1122        | 10   | -                                    |
| <i>GFL110</i> | Hydroxyproline-rich glycoprotein family protein, putative isoform 2                                     | 1178        | 2    | -                                    |
| <i>GFL177</i> | hypothetical protein  | 481         | 16   | EC:2.7.11.22                         |
| <i>GFL284</i> | hypothetical protein M569_00896, partial  | 994         | 2    | -                                    |
| <i>GFL406</i> | hypothetical protein PRUPE_ppa008947mg  | 1010        | 8    | -                                    |
| <i>GFL228</i> | hypothetical protein PRUPE_ppa008972mg  | 574         | 17   | -                                    |
| <i>GFL075</i> | hypothetical protein PRUPE_ppa014254mg  | 294         | 5    | -                                    |
| <i>GFL281</i> | hypothetical protein PRUPE_ppa022115mg  | 2165        | 7    | -                                    |
| <i>GFL154</i> | hypothetical protein TAANSRALLha_1144N5.t00004  | 723         | 10   | -                                    |
| <i>GFL077</i> | hypothetical protein VITISV_002159  | 1014        | 5    | -                                    |

**Table 10** Continued

| Gene ID | Seq. Description  | Seq. Length | #GOs | Enzyme Codes                          |
|---------|---|-------------|------|---------------------------------------|
| GFL035  | hypothetical protein VITISV_032906  | 555         | 3    | -                                     |
| GFL174  | Inhibitor-3   | 450         | 7    | -                                     |
| GFL304  | Inositol monophosphatase family protein isoform 2                                     | 739         | 11   | EC:3.1.3.25; EC:3.1.3.7               |
| GFL060  | Insulinase (Peptidase family M16) family protein isoform 1                            | 1051        | 9    | EC:3.4.24.0                           |
| GFL433  | Integral membrane single C2 domain protein, putative isoform 1                        | 715         | 5    | -                                     |
| GFL378  | Integrase-type DNA-binding superfamily protein  | 1195        | 13   | -                                     |
| GFL394  | Integrase-type DNA-binding superfamily protein isoform 1                              | 1464        | 7    | -                                     |
| GFL318  | IQ calmodulin-binding motif family protein  | 1834        | 2    | -                                     |
| GFL413  | IQ-domain 17 isoform 2  | 1466        | 2    | -                                     |
| GFL127  | Iron-sulfur cluster biosynthesis family protein isoform 1                             | 886         | 5    | -                                     |
| GFL163  | Isopropyl malate isomerase large subunit 1  | 1809        | 14   | EC:4.2.1.33; EC:5.4.4.0               |
| GFL308  | K <sup>+</sup> uptake permease 7 isoform 1  | 3403        | 8    | -                                     |
| GFL210  | Kinase domain-containing protein isoform 1  | 4374        | 7    | EC:2.7.12.1; EC:2.7.11.0              |
| GFL215  | Kinase superfamily protein with octicosapeptide/Phox/Bem1p domain, putative isoform 1 | 660         | 7    | EC:2.7.10.2; EC:2.7.12.1; EC:2.7.11.0 |
| GFL310  | Leucine-rich repeat containing-like protein isoform 1                                 | 991         | 2    | -                                     |
| GFL276  | Leucine-rich repeat containing-like protein isoform 1                                 | 1016        | 7    | -                                     |
| GFL461  | Leucine-rich repeat-containing protein, putative                                      | 576         | 2    | -                                     |
| GFL437  | Lipases,hydrolases, acting on ester bonds isoform 1                                   | 1818        | 5    | -                                     |
| GFL156  | lipoxygenase, putative  | 1773        | 11   | EC:1.13.11.12                         |
| GFL202  | LRR and NB-ARC domains-containing disease resistance protein, putative                | 345         | 4    | -                                     |
| GFL465  | LRR receptor-like serine/threonine-protein kinase, putative                           | 541         | 15   | -                                     |
| GFL289  | Lupus la ribonucleoprotein, putative isoform 3  | 496         | 6    | -                                     |
| GFL239  | Major facilitator superfamily protein isoform 1                                       | 2404        | 4    | -                                     |
| GFL375  | Mannose-P-dolichol utilization defect 1 protein isoform 1                             | 1312        | 1    | -                                     |
| GFL271  | MATE efflux family protein isoform 2  | 2482        | 5    | -                                     |
| GFL150  | Metacaspase 1 isoform 1   | 1379        | 11   | EC:3.4.22.0                           |
| GFL295  | Metal-dependent phosphohydrolase isoform 1  | 1295        | 4    | EC:3.1.4.0                            |
| GFL439  | Methyltransferase family protein, putative  | 1073        | 6    | -                                     |
| GFL246  | Microtubule-associated protein 6, putative  | 1030        | 2    | -                                     |
| GFL366  | MIF4G domain-containing protein / MA3 domain-containing protein                       | 742         | 13   | -                                     |
| GFL023  | Mitochondrial editing factor 22   | 1919        | 3    | -                                     |
| GFL064  | Mitochondrial substrate carrier family protein  | 1679        | 5    | -                                     |
| GFL358  | Mitochondrial transcription termination factor family protein                         | 1758        | 6    | -                                     |
| GFL332  | Mitochondrial-processing peptidase subunit beta, mitochondrial, putative              | 3545        | 6    | EC:3.4.24.0                           |
| GFL401  | Monogalactosyl diacylglycerol synthase 1  | 1914        | 13   | EC:2.4.1.46                           |
| GFL399  | MRNA splicing factor, thioredoxin-like U5 snRNP                                       | 842         | 5    | -                                     |
| GFL232  | MSCS-like 3 isoform 1   | 1187        | 10   | -                                     |
| GFL216  | Myb-like transcription factor family protein, putative                                | 958         | 6    | -                                     |
| GFL235  | Na <sup>+</sup> /H <sup>+</sup> antiporter 6 isoform 3                                | 536         | 12   | -                                     |

**Table 10** Continued

| Gene ID | Seq. Description  | Seq. Length | #GOs | Enzyme Codes                          |
|---------|---|-------------|------|---------------------------------------|
| GFL432  | NAD kinase 1 isoform 1  | 2282        | 8    | EC:2.7.1.86; EC:2.7.1.23              |
| GFL458  | NAD(P)-binding Rossmann-fold superfamily protein  | 1127        | 3    | -                                     |
| GFL018  | NADH-ubiquinone oxidoreductase 21 kDa subunit   | 778         | 8    | -                                     |
| GFL463  | NB-ARC domain-containing disease resistance protein, putative   | 915         | 7    | -                                     |
| GFL097  | NB-ARC domain-containing disease resistance-like protein isoform 2  | 3483        | 2    | -                                     |
| GFL226  | Neutral invertase isoform 1   | 2791        | 10   | EC:3.2.1.26; EC:3.2.1.48; EC:3.2.1.97 |
| GFL285  | Nicotinamidase 2  | 911         | 5    | EC:3.5.1.19; EC:3.3.2.1               |
| GFL231  | No lysine kinase 3 isoform 1  | 2426        | 11   | EC:2.7.11.25                          |
| GFL330  | Non-intrinsic ABC protein 6 isoform 1   | 1531        | 17   | -                                     |
| GFL192  | NPL4-like protein 1   | 631         | 9    | EC:1.11.1.7                           |
| GFL030  | Nuclear transcription factor Y subunit B-10 isoform 2   | 704         | 9    | -                                     |
| GFL109  | nuclease, putative  | 1554        | 2    | -                                     |
| GFL275  | Nucleotide-sugar transporter family protein   | 1674        | 10   | -                                     |
| GFL273  | Nucleotide-sugar transporter family protein   | 1350        | 5    | -                                     |
| GFL200  | Nucleotidyltransferase family protein isoform 5   | 2249        | 2    | EC:2.7.7.0                            |
| GFL335  | O-acetylserine lyase B isoform 1  | 1665        | 29   | EC:2.5.1.47                           |
| GFL147  | O-fucosyltransferase family protein   | 810         | 3    | -                                     |
| GFL256  | O-fucosyltransferase family protein isoform 1   | 2190        | 5    | -                                     |
| GFL021  | Oberon 2 isoform 1  | 2176        | 14   | -                                     |
| GFL322  | OEP37_PEARName: Full=Outer envelope pore protein 37, chloroplastic;<br>AltName: Full=Chloroplastic outer envelope pore protein of 37 kDa; Short=PsOEP37; Flags: Precursor | 446         | 10   | -                                     |
| GFL393  | P-loop containing nucleoside triphosphate hydrolases superfamily protein  | 601         | 11   | -                                     |
| GFL188  | P-loop containing nucleoside triphosphate hydrolases superfamily protein  | 1754        | 7    | EC:3.6.1.3                            |
| GFL016  | P-loop containing nucleoside triphosphate hydrolases superfamily protein isoform 1  | 2153        | 15   | -                                     |
| GFL083  | P4H isoform 1   | 1626        | 10   | EC:1.14.11.2                          |
| GFL089  | PAP10   | 1654        | 14   | EC:3.1.3.2                            |
| GFL164  | PATATIN-like protein 9, IIIB isoform 1  | 1559        | 7    | -                                     |
| GFL341  | Pentatricopeptide repeat (PPR) superfamily protein, putative  | 1236        | 2    | -                                     |
| GFL311  | Pentatricopeptide repeat (PPR) superfamily protein, putative isoform 1  | 1242        | 2    | -                                     |
| GFL395  | Pentatricopeptide repeat-containing protein, putative   | 2231        | 2    | -                                     |
| GFL170  | Peptidase M20/M25/M40 family protein isoform 5  | 999         | 13   | -                                     |
| GFL438  | Peptide n-glycanase, putative isoform 2   | 1910        | 10   | EC:3.5.1.52                           |
| GFL388  | PfkB-like carbohydrate kinase family protein  | 230         | 9    | EC:2.7.7.49; EC:2.7.1.4               |
| GFL402  | Phenylalanyl-tRNA synthetase / phenylalanine--tRNA ligase, putative isoform 1   | 881         | 10   | EC:6.1.1.20                           |
| GFL017  | Phloem protein 2-A15  | 426         | 3    | -                                     |
| GFL468  | Phloem protein 2-like a10, putative   | 1647        | 1    | -                                     |
| GFL471  | Phosphatase 2A, regulatory subunit PR55, BETA isoform 1   | 1271        | 7    | -                                     |
| GFL113  | Phosphatidylinositol-4-phosphate 5-kinase family protein, putative isoform 3, partial   | 441         | 11   | EC:2.7.1.150; EC:2.7.1.68             |
| GFL162  | Phosphoprotein phosphatase  | 294         | 1    | -                                     |

**Table 10** Continued

| Gene ID       | Seq. Description  | Seq. Length | #GOs | Enzyme Codes                                    |
|---------------|---|-------------|------|---|
| <i>GFL453</i> | Photosystem II subunit Q-2  | 1063        | 18   | -   |
| <i>GFL472</i> | Phototropic-responsive NPH3 family protein isoform 1                                      | 1439        | 11   | -   |
| <i>GFL374</i> | Plant calmodulin-binding protein-related, putative isoform 1                              | 809         | 2    | -   |
| <i>GFL148</i> | Pleiotropic drug resistance 12 isoform 2  | 1351        | 8    | EC:3.6.3.41; EC:3.6.3.28; EC:3.6.3.31           |
| <i>GFL313</i> | Poly(A) binding protein 8 isoform 2   | 213         | 5    | -   |
| <i>GFL092</i> | Polyketide cyclase / dehydrase and lipid transport protein                                | 438         | 9    | -   |
| <i>GFL144</i> | Polymerase gamma 2 isoform 4  | 3667        | 14   | EC:2.7.7.7                                      |
| <i>GFL009</i> | Polynucleotide adenylyltransferase family protein isoform 1                               | 2493        | 7    | EC:2.7.7.25; EC:2.7.7.56                        |
| <i>GFL208</i> | predicted protein   | 217         | 13   | EC:5.1.3.5; EC:5.1.3.2                          |
| <i>GFL321</i> | predicted protein   | 250         | 4    | -   |
| <i>GFL317</i> | predicted protein   | 2265        | 7    | -   |
| <i>GFL220</i> | predicted protein   | 2116        | 7    | EC:2.7.11.0; EC:2.7.12.1                        |
| <i>GFL469</i> | predicted protein   | 594         | 2    | -   |
| <i>GFL041</i> | PREDICTED: DEAD-box ATP-dependent RNA helicase 35 isoform 1                               | 2281        | 10   | -   |
| <i>GFL044</i> | PREDICTED: GMP synthase   | 295         | 16   | EC:3.4.21.0; EC:3.2.1.0; EC:6.3.5.2; EC:6.3.5.4 |
| <i>GFL462</i> | PREDICTED: GTP-binding protein SAR1A-like   | 1320        | 26   | -   |
| <i>GFL435</i> | PREDICTED: monosaccharide-sensing protein 2-like  | 509         | 7    | -   |
| <i>GFL307</i> | PREDICTED: probable sugar phosphate/phosphate translocator At3g11320-like                 | 398         | 14   | -   |
| <i>GFL347</i> | PREDICTED: putative ribonuclease H protein At1g65750-like                                 | 982         | 14   | -   |
| <i>GFL183</i> | PREDICTED: ruBisCO large subunit-binding protein subunit beta, chloroplastic              | 308         | 20   | -   |
| <i>GFL124</i> | PREDICTED: serine/threonine-protein phosphatase PP2A catalytic subunit-like               | 1437        | 11   | -   |
| <i>GFL353</i> | PREDICTED: TATA-binding protein-associated factor 2N-like isoform X1                      | 1290        | 2    | -   |
| <i>GFL467</i> | PREDICTED: uncharacterized amino-acid permease C15C4.04c-like                             | 1814        | 19   | -   |
| <i>GFL333</i> | PREDICTED: uncharacterized protein LOC100815379   | 715         | 6    | -   |
| <i>GFL460</i> | PREDICTED: uncharacterized protein LOC101205308, partial                                  | 2432        | 2    | -   |
| <i>GFL213</i> | proline-rich protein  | 302         | 2    | -   |
| <i>GFL445</i> | Protochlorophyllide oxidoreductase C, C,PORC  | 1546        | 22   | EC:1.6.99.1; EC:1.3.1.33                        |
| <i>GFL024</i> | PRP38 family protein isoform 1  | 1690        | 5    | -   |
| <i>GFL331</i> | putative p-coumarate 3-hydroxylase  | 1746        | 15   | EC:1.14.13.21                                   |
| <i>GFL279</i> | putative PDF1-interacting protein 2, partial  | 384         | 0    | -   |
| <i>GFL436</i> | RAC-like 9 isoform 1  | 1808        | 28   | EC:3.1.4.12                                     |
| <i>GFL131</i> | Radiation sensitive 17, putative  | 2688        | 8    | -   |
| <i>GFL270</i> | RAN GTPase activating protein 1 isoform 1   | 2547        | 20   | -   |
| <i>GFL405</i> | Receptor protein kinase, putative   | 630         | 4    | -   |
| <i>GFL294</i> | Receptor-like protein kinase 1, putative  | 699         | 7    | EC:2.7.11.0                                     |
| <i>GFL418</i> | REF4-related 1  | 4599        | 8    | -   |
| <i>GFL316</i> | Regulator of chromosome condensation (RCC1) family with FYVE zinc finger domain isoform 1 | 334         | 19   | -   |
| <i>GFL367</i> | Regulatory particle AAA-ATPase 2A   | 1688        | 31   | EC:3.6.4.3                                      |
| <i>GFL195</i> | retrotransposon protein, putative, unclassified   | 514         | 5    | -   |

**Table 10** Continued

| Gene ID | Seq. Description   | Seq. Length | #GOs | Enzyme Codes               |
|---------|--|-------------|------|----------------------------|
| GFL079  | Reversibly glycosylated polypeptide 3  | 703         | 10   | EC:5.4.99.30; EC:2.4.1.186 |
| GFL106  | Ribonucleoside-diphosphate reductase small chain A isoform 1                                     | 1313        | 14   | EC:1.17.4.1                |
| GFL119  | Ribosomal protein L30/L7 family protein isoform 1  | 848         | 4    | -                          |
| GFL198  | Ribosomal protein L7Ae/L30e/S12e/Gadd45 family protein   | 321         | 10   | -                          |
| GFL252  | Ribosomal protein S24e family protein isoform 1  | 683         | 12   | -                          |
| GFL027  | RING/FYVE/PHD zinc finger superfamily protein, putative isoform 1                                | 3936        | 7    | -                          |
| GFL099  | RING/FYVE/PHD-type zinc finger family protein isoform 1  | 2085        | 4    | -                          |
| GFL187  | RING/U-box superfamily protein   | 1667        | 2    | -                          |
| GFL076  | RING/U-box superfamily protein isoform 1   | 1459        | 15   | EC:6.3.2.19                |
| GFL068  | RING/U-box superfamily protein isoform 1   | 1051        | 4    | EC:6.3.2.19                |
| GFL260  | RING/U-box superfamily protein isoform 1   | 2126        | 4    | -                          |
| GFL157  | RING/U-box superfamily protein, putative   | 1858        | 2    | -                          |
| GFL114  | RNA binding protein, putative  | 1523        | 1    | -                          |
| GFL470  | RNA helicase-like protein  | 551         | 11   | -                          |
| GFL046  | RNA-binding KH domain-containing protein   | 1590        | 3    | -                          |
| GFL051  | RNA-binding KH domain-containing protein isoform 1   | 2264        | 1    | -                          |
| GFL233  | Root hair defective 3 GTP-binding protein (RHD3) isoform 2                                       | 2360        | 27   | -                          |
| GFL116  | Root hair defective 6-like 2, putative   | 848         | 0    | -                          |
| GFL379  | Root phototropism protein, putative isoform 2  | 1757        | 4    | -                          |
| GFL013  | RP non-ATPase subunit 8A   | 363         | 20   | -                          |
| GFL429  | Rubisco methyltransferase family protein   | 2287        | 1    | -                          |
| GFL053  | S-adenosyl-L-methionine-dependent methyltransferases superfamily protein                         | 278         | 3    | -                          |
| GFL081  | S-adenosyl-L-methionine-dependent methyltransferases superfamily protein                         | 2448        | 5    | EC:2.1.1.0                 |
| GFL184  | S-adenosyl-L-methionine-dependent methyltransferases superfamily protein isoform 1               | 1666        | 4    | EC:2.1.1.0                 |
| GFL085  | S-adenosyl-L-methionine-dependent methyltransferases superfamily protein isoform 1               | 2722        | 8    | EC:2.1.1.0                 |
| GFL125  | S-adenosyl-L-methionine-dependent methyltransferases superfamily protein isoform 1               | 2973        | 8    | EC:2.1.1.0                 |
| GFL473  | SAD1/UNC-84 domain protein 2, putative   | 1831        | 5    | -                          |
| GFL090  | Sec14p-like phosphatidylinositol transfer family protein   | 673         | 8    | -                          |
| GFL361  | Serine/threonine-protein kinase 24 isoform 1   | 479         | 12   | EC:2.7.11.25               |
| GFL356  | Serine/threonine-protein kinase-like protein, putative   | 436         | 0    | -                          |
| GFL339  | Seryl-tRNA synthetase isoform 1  | 3268        | 20   | EC:6.1.1.11                |
| GFL324  | SH3 domain-containing protein  | 1596        | 7    | -                          |
| GFL265  | SIN3-like 2, putative isoform 1  | 910         | 16   | -                          |
| GFL057  | Splicing factor PWI domain-containing protein / RNA recognition motif-containing protein isoform | 4443        | 8    | -                          |
| GFL352  | Squamosa promoter-binding protein, putative isoform 1  | 2753        | 4    | -                          |
| GFL019  | Steroid binding protein, putative  | 1356        | 17   | EC:1.3.1.74                |
| GFL381  | Stress responsive alpha-beta barrel domain protein, putative isoform 2                           | 1297        | 12   | -                          |
| GFL301  | Sugar transporter, putative isoform 2, partial   | 1715        | 11   | EC:1.3.1.74                |
| GFL189  | Sulfate transporter 4.1 isoform 1  | 2382        | 5    | -                          |

**Table 10** Continued

| Gene ID | Seq. Description   | Seq. Length | #GOs | Enzyme Codes                                      |
|---------|--|-------------|------|---|
| GFL292  | TATA-box binding protein, putative                                       | 1677        | 7    | EC:1.3.1.74                                       |
| GFL061  | Teosinte branched 1, putative isoform 4, partial                         | 418         | 0    |   |
| GFL031  | Terpenoid synthases superfamily protein                                  | 594         | 9    | -   |
| GFL138  | Tetratricopeptide repeat (TPR)-like superfamily protein                  | 1591        | 4    | -   |
| GFL126  | Tetratricopeptide repeat (TPR)-like superfamily protein                  | 1752        | 1    | -   |
| GFL176  | Tetratricopeptide repeat (TPR)-like superfamily protein isoform 3        | 1315        | 6    | -   |
| GFL277  | Tetratricopeptide repeat (TPR)-like superfamily protein, putative        | 1007        | 2    | -   |
| GFL290  | Tetratricopeptide repeat-like superfamily protein                        | 720         | 2    | -   |
| GFL165  | Tetratricopeptide repeat-like superfamily protein                        | 1807        | 11   | -   |
| GFL062  | Tetratricopeptide repeat-like superfamily protein isoform 2              | 1117        | 3    | -   |
| GFL474  | Thiamine pyrophosphate dependent pyruvate decarboxylase family protein   | 2362        | 17   | EC:4.1.1.1  |
| GFL006  | Tir-nbs resistance protein   | 1012        | 6    | EC:3.6.1.15                                       |
| GFL238  | Topoisomerase II-associated protein PAT1, putative isoform 2             | 1585        | 0    |   |
| GFL283  | Toxicos en levadura 4, putative  | 1280        | 4    | EC:6.3.2.19                                       |
| GFL180  | Transcription factor   | 1250        | 14   | EC:2.4.2.30                                       |
| GFL078  | Transcription factor jumonji family protein / zinc finger family protein | 2150        | 14   | -   |
| GFL091  | Transcription regulator NOT2/NOT3/NOT5 family protein                    | 2129        | 3    | -   |
| GFL427  | Transducin/WD40 repeat-like superfamily protein                          | 1158        | 2    | -   |
| GFL243  | Transducin/WD40 repeat-like superfamily protein isoform 1                | 2437        | 20   | EC:1.3.1.74; EC:6.3.2.19                          |
| GFL204  | Transducin/WD40 repeat-like superfamily protein isoform 2                | 724         | 0    |   |
| GFL320  | Transducin/WD40 repeat-like superfamily protein, putative isoform 1      | 2336        | 1    | -   |
| GFL117  | translation factor sui1, putative  | 477         | 11   | -   |
| GFL007  | Translation initiation factor 3B1 isoform 2                              | 1897        | 11   | -   |
| GFL452  | Translation initiation factor IF2/IF5 isoform 1                          | 698         | 7    | -   |
| GFL100  | Translocase of outer membrane 22-l                                       | 658         | 14   | -   |
| GFL186  | Transmembrane amino acid transporter family protein isoform 1            | 1715        | 4    | -   |
| GFL417  | Transmembrane amino acid transporter family protein isoform 4            | 994         | 6    | -   |
| GFL236  | Trichome birefringence-like 13   | 2563        | 3    | -   |
| GFL383  | Trigger factor, putative   | 2126        | 13   | EC:5.2.1.8  |
| GFL207  | Tryptophan aminotransferase related 2, putative                          | 2016        | 16   | EC:2.6.1.28; EC:2.6.1.27; EC:4.4.1.4              |
| GFL350  | TUDOR-SN protein 1 isoform 1   | 3617        | 23   | -   |
| GFL101  | Type one serine/threonine protein phosphatase 2                          | 1498        | 8    | -   |
| GFL115  | Type one serine/threonine protein phosphatase 4 isoform 1                | 1035        | 6    | -   |
| GFL218  | Type-b response regulator, putative                                      | 832         | 1    | -   |
| GFL227  | Ubiquitin carboxyl-terminal hydrolase 19, putative isoform 1             | 2462        | 8    | EC:3.1.2.15; EC:3.4.22.0                          |
| GFL373  | Ubiquitin ligase protein cop1, putative isoform 6                        | 2413        | 18   | EC:1.3.1.74                                       |
| GFL209  | Ubiquitin-specific protease family C19-related protein                   | 340         | 1    | -   |
| GFL211  | UDP-glucuronic acid decarboxylase 3                                      | 1287        | 8    | EC:4.1.1.35                                       |
| GFL080  | UDP-sugar pyrophosphorylase  | 2056        | 8    | EC:2.7.7.9; EC:2.7.7.11; EC:2.7.7.10; EC:2.7.7.44 |



**Table 10** Continued

| Gene ID       | Seq. Description                                 | Seq. Length | #GOs | Enzyme Codes |
|---------------|--|-------------|------|--------------|
| <i>GFL133</i> | Uncharacterized protein isoform 1                | 1727        | 3    |              |
| <i>GFL396</i> | Uncharacterized protein isoform 1                | 1579        | 6    | -            |
| <i>GFL098</i> | Uncharacterized protein isoform 1                | 1516        | 2    |              |
| <i>GFL037</i> | Uncharacterized protein isoform 1                | 1161        | 1    |              |
| <i>GFL008</i> | Uncharacterized protein isoform 1                | 1993        | 1    | -            |
| <i>GFL219</i> | Uncharacterized protein isoform 1                | 1889        | 2    | -            |
| <i>GFL296</i> | Uncharacterized protein isoform 1                | 2936        | 1    | -            |
| <i>GFL259</i> | Uncharacterized protein isoform 1                | 3595        | 4    |              |
| <i>GFL340</i> | Uncharacterized protein isoform 1                | 1269        | 2    | -            |
| <i>GFL199</i> | Uncharacterized protein isoform 1                | 1096        | 2    | -            |
| <i>GFL088</i> | Uncharacterized protein isoform 2                | 1787        | 4    | -            |
| <i>GFL457</i> | Uncharacterized protein isoform 2                | 2383        | 6    |              |
| <i>GFL286</i> | Uncharacterized protein isoform 2, partial       | 702         | 6    | -            |
| <i>GFL146</i> | Uncharacterized protein isoform 3                | 516         | 13   | -            |
| <i>GFL104</i> | Uncharacterized protein isoform 4                | 496         | 0    |              |
| <i>GFL338</i> | Uncharacterized protein isoform 6                | 926         | 1    | -            |
| <i>GFL408</i> | Uncharacterized protein TCM_000519               | 1754        | 1    | -            |
| <i>GFL065</i> | Uncharacterized protein TCM_001288               | 754         | 3    |              |
| <i>GFL434</i> | Uncharacterized protein TCM_002116               | 494         | 7    | -            |
| <i>GFL135</i> | Uncharacterized protein TCM_004747               | 839         | 2    | -            |
| <i>GFL423</i> | Uncharacterized protein TCM_006792               | 1272        | 7    | -            |
| <i>GFL287</i> | Uncharacterized protein TCM_007249               | 936         | 3    |              |
| <i>GFL129</i> | Uncharacterized protein TCM_014639               | 1245        | 2    | -            |
| <i>GFL137</i> | Uncharacterized protein TCM_015620               | 551         | 2    |              |
| <i>GFL049</i> | Uncharacterized protein TCM_016081               | 2142        | 2    | -            |
| <i>GFL325</i> | Uncharacterized protein TCM_017339               | 1301        | 1    | -            |
| <i>GFL123</i> | Uncharacterized protein TCM_025519               | 995         | 1    | -            |
| <i>GFL095</i> | Uncharacterized protein TCM_025926               | 316         | 3    |              |
| <i>GFL446</i> | Uncharacterized protein TCM_025992               | 779         | 0    |              |
| <i>GFL449</i> | Uncharacterized protein TCM_027411               | 1940        | 1    | -            |
| <i>GFL349</i> | Uncharacterized protein TCM_029945               | 816         | 3    |              |
| <i>GFL118</i> | Uncharacterized protein TCM_029952               | 1549        | 3    | -            |
| <i>GFL253</i> | Uncharacterized protein TCM_031178               | 1316        | 3    |              |
| <i>GFL193</i> | Uncharacterized protein TCM_037753               | 701         | 2    | -            |
| <i>GFL337</i> | Uncharacterized protein TCM_041352               | 626         | 0    |              |
| <i>GFL346</i> | unnamed protein product                          | 1425        | 7    | -            |
| <i>GFL314</i> | Uridyltransferase-related                        | 2483        | 11   | -            |
| <i>GFL161</i> | Vacuolar sorting protein 9 domain isoform 1      | 1502        | 10   | -            |
| <i>GFL303</i> | Vascular plant one zinc finger protein isoform 1 | 2112        | 10   | -            |

**Table 10** Continued

| Gene ID       | Seq. Description  | Seq. Length | #GOs | Enzyme Codes             |
|---------------|---|-------------|------|--------------------------|
| <i>GFL371</i> | VIRE2-interacting protein 1, putative                                     | 700         | 10   | -                        |
| <i>GFL020</i> | Vps51/Vps67 family (components of vesicular transport) protein isoform 1  | 843         | 6    | -                        |
| <i>GFL143</i> | Winged-helix DNA-binding transcription factor family protein, putative    | 443         | 1    | -                        |
| <i>GFL229</i> | WW domain-containing protein, putative isoform 1                          | 1945        | 4    | -                        |
| <i>GFL222</i> | WWE protein-protein interaction domain protein family, putative isoform 1 | 2786        | 17   | EC:2.4.2.30              |
| <i>GFL415</i> | XB3 in isoform 1  | 1904        | 10   | EC:6.3.2.19; EC:3.4.21.0 |
| <i>GFL094</i> | Zinc finger (C2H2 type, AN1-like) family protein                          | 1175        | 4    | -                        |
| <i>GFL392</i> | zinc finger protein   | 1384        | 21   | -                        |

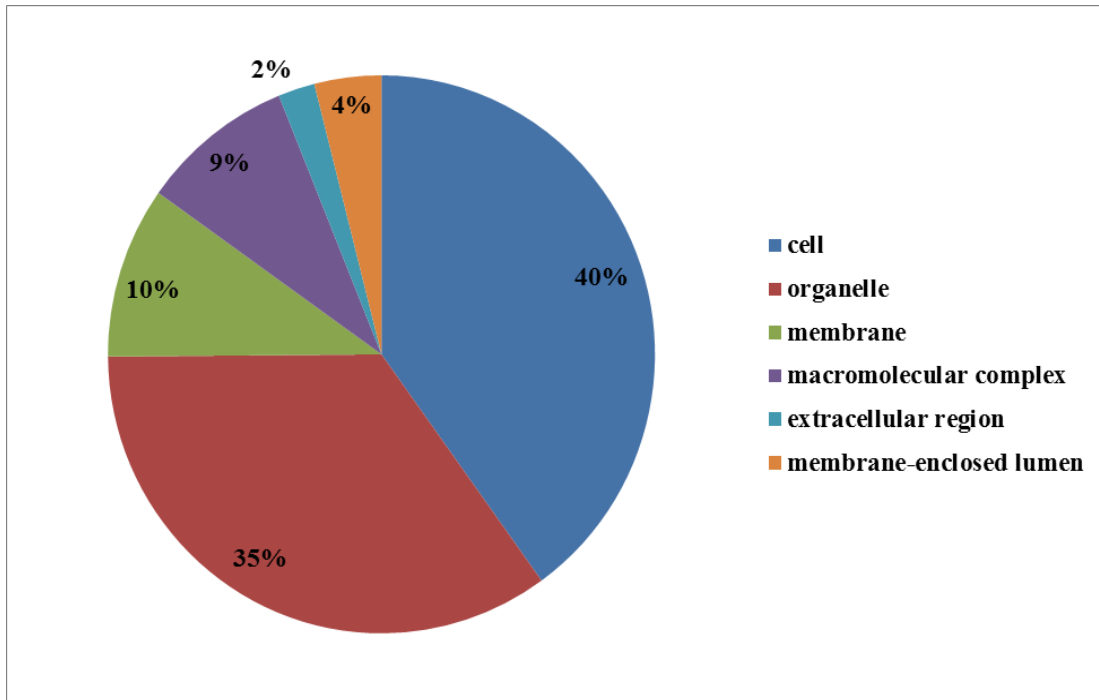


**Figure 20** GO items of the *GFL* genes assigned to genes the functional category of cellular component (level 2)

Furthermore, a search was made using the KEGG database to determine the biological pathways that are associated with the *GFL* genes. The 474 *GFL* genes were mapped to 60 KEGG pathways that are categorized into 13 different biological processes, including carbohydrate metabolism, nucleotide metabolism and lipid metabolism (Table 11). The two biological pathways that included the largest numbers of the *GFL* genes were found to be the “Starch and Sucrose Metabolism” (KEGG map00500) of the carbohydrate metabolism category and the “Purine Metabolism” (KEGG map00230) of the nucleotide metabolism category (Kanehisa and Goto 2000;

Kanehisa et al. 2014). Nine of the *GFL* genes were found to encode key enzymes in starch and sucrose metabolism, including *GFL108*, *GFL226*, *GFL080*, *GFL039*, *GFL086*, *GFL395*, *GFL120*, *GFL211* and *GFL069*. Nine *GFL* genes encode enzymes in purine metabolism, including *GFL106*, *GFL006*, *GFL144*, *GFL026*, *GFL044*, *GFL069*, *GFL039*, *GFL374* and *GFL376*.

Of the 60 pathways to which the *GFL* genes were mapped, 95% were metabolism-related, including carbohydrate metabolism, nucleotide metabolism, lipid metabolism, cofactors and vitamins metabolism, energy metabolism, etc. (Table 11). Among these metabolism-related pathways, the carbohydrate and nucleotide metabolisms represented the two major biological processes in which the largest numbers of pathways are included (Fig. 21). Only six of the *GFL* genes were mapped to three KEGG non-metabolism pathways that belong to genetic information processing, environmental information processing, and organismal systems.

**Table 11** KEGG pathways in which the *GFL* genes are involved

| Function   | No. of pathways | KEGG category                        | No. of pathways | KEGG pathway                                | Seq. in the pathway |   |   |
|------------|-----------------|--------------------------------------|-----------------|---|---------------------|---|---|
| Metabolism | 57              | Carbohydrate metabolism              | 12              | Amino sugar and nucleotide sugar metabolism | 8                   |   |   |
|            |                 |                                      |                 | Ascorbate and aldarate metabolism           | 1                   |   |   |
|            |                 |                                      |                 | Butanoate metabolism                        | 1                   |   |   |
|            |                 |                                      |                 | Fructose and mannose metabolism             | 4                   |   |   |
|            |                 |                                      |                 | Galactose metabolism                        | 4                   |   |   |
|            |                 |                                      |                 | Glycolysis / Gluconeogenesis                | 4                   |   |   |
|            |                 |                                      |                 | Glyoxylate and dicarboxylate metabolism     | 3                   |   |   |
|            |                 |                                      |                 | Inositol phosphate metabolism               | 3                   |   |   |
|            |                 |                                      |                 | Pentose and glucuronate interconversions    | 2                   |   |   |
|            |                 |                                      |                 | Pentose phosphate pathway                   | 2                   |   |   |
|            |                 |                                      |                 | Pyruvate metabolism                         | 3                   |   |   |
|            |                 |                                      |                 | Starch and sucrose metabolism               | 9                   |   |   |
|            |                 | Nucleotide metabolism                | 10              | Nucleotide metabolism                       | 10                  | Alanine, aspartate and glutamate metabolism         | 3 |
|            |                 |                                      |                 |   |                     | Arginine and proline metabolism                     | 4 |
|            |                 |                                      |                 |   |                     | Cysteine and methionine metabolism                  | 3 |
|            |                 |                                      |                 |   |                     | Glycine, serine and threonine metabolism            | 2 |
|            |                 |                                      |                 |   |                     | Lysine biosynthesis                                 | 1 |
|            |                 |                                      |                 |   |                     | Phenylalanine metabolism                            | 3 |
|            |                 |                                      |                 |   |                     | Purine metabolism                                   | 9 |
|            |                 |                                      |                 |   |                     | Pyrimidine metabolism                               | 2 |
|            |                 |                                      |                 |   |                     | Tryptophan metabolism                               | 2 |
|            |                 |                                      |                 |   |                     | Valine, leucine and isoleucine biosynthesis         | 1 |
|            |                 | Lipid metabolism                     | 7               | Lipid metabolism                            | 7                   | alpha-Linolenic acid metabolism                     | 1 |
|            |                 |                                      |                 |   |                     | Fatty acid biosynthesis                             | 4 |
|            |                 |                                      |                 |   |                     | Fatty acid degradation                              | 1 |
|            |                 |                                      |                 |   |                     | Glycerolipid metabolism                             | 1 |
|            |                 |                                      |                 |   |                     | Linoleic acid metabolism                            | 1 |
|            |                 |                                      |                 |   |                     | Sphingolipid metabolism                             | 1 |
|            |                 |                                      |                 |   |                     | Synthesis and degradation of ketone bodies          | 1 |
|            |                 | Metabolism of cofactors and vitamins | 7               | Metabolism of cofactors and vitamins        | 7                   | Biotin metabolism                                   | 1 |
|            |                 |                                      |                 |   |                     | Nicotinate and nicotinamide metabolism              | 4 |
|            |                 |                                      |                 |   |                     | Pantothenate and CoA biosynthesis                   | 1 |
|            |                 |                                      |                 |   |                     | Porphyrin and chlorophyll metabolism                | 1 |
|            |                 |                                      |                 |   |                     | Riboflavin metabolism                               | 3 |
|            |                 |                                      |                 |   |                     | Thiamine metabolism                                 | 1 |
|            |                 |                                      |                 |   |                     | Ubiquinone and other terpenoid-quinone biosynthesis | 1 |

**Table 11** Continued

| Function                             | No. of pathways | KEGG category                               | No. of pathways | KEGG pathway   | Seq. in the pathway |
|--------------------------------------|-----------------|---|-----------------|--|---------------------|
|                                      |                 | Biosynthesis of other secondary metabolites | 6               | Aflatoxin biosynthesis                                 | 1                   |
|                                      |                 |   |                 | Butirosin and neomycin biosynthesis                    | 1                   |
|                                      |                 |   |                 | Flavone and flavonol biosynthesis                      | 1                   |
|                                      |                 |   |                 | Flavonoid biosynthesis                                 | 1                   |
|                                      |                 |   |                 | Phenylpropanoid biosynthesis                           | 2                   |
|                                      |                 |   |                 | Streptomycin biosynthesis                              | 2                   |
|                                      |                 | Energy metabolism                           | 5               | Carbon fixation pathways in prokaryotes                | 2                   |
|                                      |                 |   |                 | Methane metabolism                                     | 3                   |
|                                      |                 |   |                 | Nitrogen metabolism                                    | 1                   |
|                                      |                 |   |                 | Oxidative phosphorylation                              | 4                   |
|                                      |                 |   |                 | Sulfur metabolism                                      | 3                   |
|                                      |                 | Xenobiotics biodegradation and metabolism   | 4               | Aminobenzoate degradation                              | 3                   |
|                                      |                 |   |                 | Drug metabolism - cytochrome P450                      | 1                   |
|                                      |                 |   |                 | Drug metabolism - other enzymes                        | 1                   |
|                                      |                 |   |                 | Styrene degradation                                    | 1                   |
|                                      |                 | Glycan biosynthesis and metabolism          | 3               | Glycosaminoglycan biosynthesis - chondroitin sulfate / | 2                   |
|                                      |                 |   |                 | Glycosaminoglycan biosynthesis - heparan sulfate / hep | 2                   |
|                                      |                 |   |                 | Other types of O-glycan biosynthesis                   | 1                   |
|                                      |                 | Metabolism of terpenoids and polyketides    | 2               | Biosynthesis of siderophore group nonribosomal peptid  | 1                   |
|                                      |                 |   |                 | Tetracycline biosynthesis                              | 1                   |
|                                      |                 | Metabolism of other amino acids             | 1               | Glutathione metabolism                                 | 2                   |
| Genetic Information Processing       | 1               | Translation                                 | 1               | Aminoacyl-tRNA biosynthesis                            | 3                   |
| Environmental Information Processing | 1               | Signal transduction                         | 1               | Phosphatidylinositol signaling system                  | 2                   |
| Organismal Systems                   | 1               | Immune system                               | 1               | T cell receptor signaling pathway                      | 1                   |

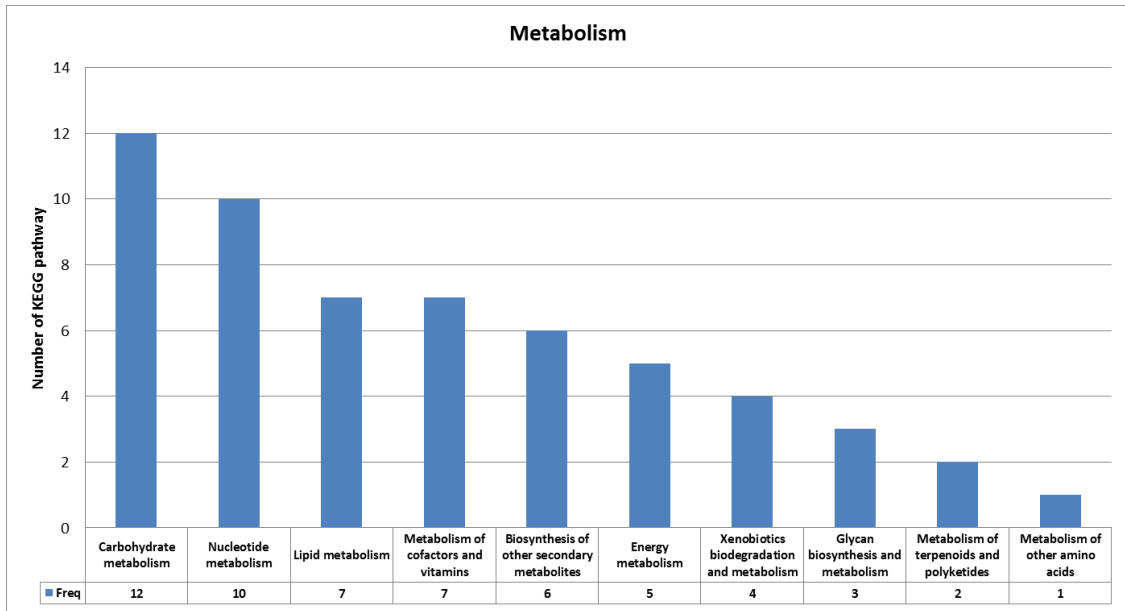


**Figure 21** Metabolism-related KEGG pathways in which the *GFL* genes are involved

### 3.4 Molecular basis of UHML development

#### 3.4.1 Interactions of the 474 *GFL* genes

Is there any biological relationship among the 474 *GFL* genes? In other words, do they work independent or as a team to contribute to the UFML? We hypothesized that they should be independent of each other in expression if they contribute to the UFML independently or that they should be correlated in expression or action if they work as a team to contribute to the UHML. To this hypothesis, the *GFL* genes were subjected to co-regulation network analysis using the expression data of *GFL* genes in 10-dpa fibers of the 198 RILs of the TAM 94L-25 x MNSI 1331 population. Consequently, all of the 474 *GFL* genes were found in a single regulation network ( $P \leq 0.05$ ) (Fig. 22). The formation of a single interaction network from all 474 *GFL* genes further confirmed the

*GFL* genes. The *GFL* gene network consisted of 474 genes (nodes) and 51,993 interactions (edges), accounting for 46.38% of all 112,101 possible interactions of the 474 *GFL* genes. In the gene network, each of the 474 *GFL* genes interacted with an average of 220 other *GFL* genes, varying from 20 (*GFL412*) to 383 (*GFL165*) (Table 12). The number of edges connected from a node had significant correlations ( $r = 0.1037$ ,  $P \leq 0.05$ ) with the absolute gene effects on UHML. More gene-gene interactions derived from a *GFL* gene and other *GFL* genes contributed more gene effects on UHML. A gene involved in a large number of gene-gene interactions contributed more gene effects on UHML than a gene involved in fewer gene-gene interactions.

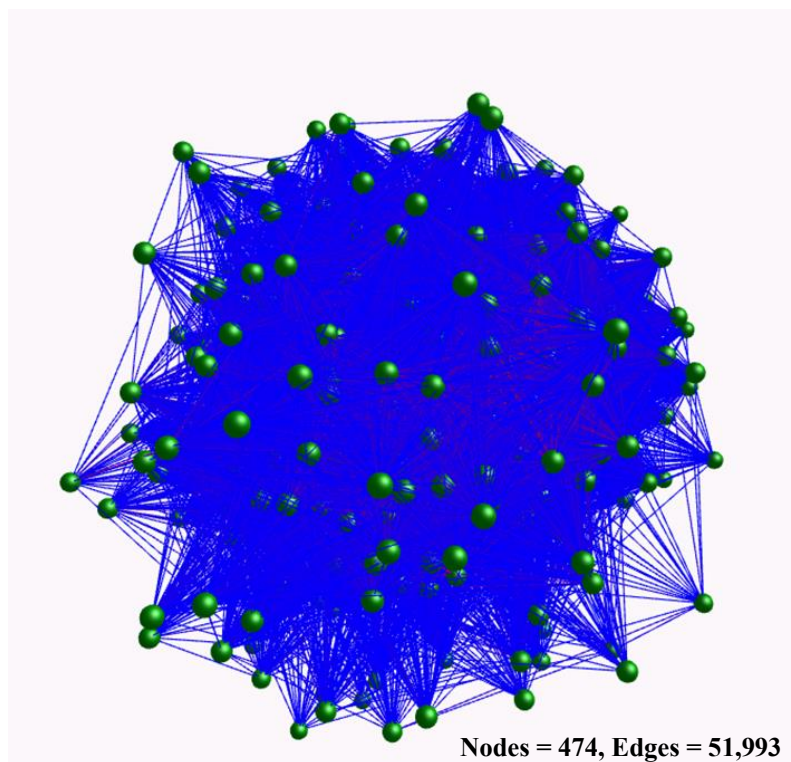


**Figure 22** The co-regulation network of the 474 *GFL* genes



**Table 12** Number of edges that a single *GFL* gene has in the 474 *GFL* network of the entire RIL population

| Gene ID       | Number of edges | LEN ratio (%) | Abs(LEN ratio) | Aver TPM |
|---------------|-----------------|---------------|----------------|----------|
| <i>GFL412</i> | 20              | -3.05         | 3.05           | 7.27     |
| <i>GFL364</i> | 23              | -3.50         | 3.50           | 3.90     |
| <i>GFL425</i> | 23              | 3.33          | 3.33           | 7.72     |
| <i>GFL429</i> | 24              | 3.47          | 3.47           | 6.08     |
| <i>GFL434</i> | 24              | 3.75          | 3.75           | 6.70     |
| <i>GFL104</i> | 25              | -4.70         | 4.70           | 1.20     |
| <i>GFL437</i> | 27              | 3.78          | 3.78           | 2.77     |
| <i>GFL447</i> | 28              | 4.04          | 4.04           | 3.34     |
| <i>GFL470</i> | 28              | 5.27          | 5.27           | 2.15     |
| <i>GFL421</i> | 29              | 3.08          | 3.08           | 4.26     |
| <i>GFL423</i> | 33              | 3.23          | 3.23           | 4.83     |
| <i>GFL472</i> | 36              | 5.48          | 5.48           | 4.24     |
| <i>GFL093</i> | 40              | -4.76         | 4.76           | 0.86     |
| <i>GFL004</i> | 42              | -6.47         | 6.47           | 1.15     |
| <i>GFL426</i> | 42              | 3.38          | 3.38           | 7.69     |
| <i>GFL340</i> | 43              | -3.59         | 3.59           | 3.07     |
| <i>GFL299</i> | 44              | -3.77         | 3.77           | 5.46     |
| <i>GFL461</i> | 44              | 4.66          | 4.66           | 1.13     |
| <i>GFL428</i> | 46              | 3.43          | 3.43           | 3.77     |
| <i>GFL264</i> | 47              | -3.93         | 3.93           | 2.33     |
| <i>GFL457</i> | 49              | 4.58          | 4.58           | 18.91    |
| <i>GFL460</i> | 49              | 4.61          | 4.61           | 15.24    |
| <i>GFL344</i> | 50              | -3.58         | 3.58           | 0.90     |
| <i>GFL448</i> | 50              | 4.15          | 4.15           | 11.18    |
| <i>GFL471</i> | 51              | 5.36          | 5.36           | 21.04    |
| <i>GFL415</i> | 59              | -2.98         | 2.98           | 2.57     |
| <i>GFL191</i> | 61              | -4.21         | 4.21           | 1.16     |
| <i>GFL436</i> | 61              | 3.77          | 3.77           | 3.55     |
| <i>GFL465</i> | 61              | 4.77          | 4.77           | 2.78     |
| <i>GFL320</i> | 62              | -3.65         | 3.65           | 11.19    |
| <i>GFL397</i> | 63              | -3.23         | 3.23           | 10.80    |
| <i>GFL440</i> | 64              | 3.82          | 3.82           | 3.89     |
| <i>GFL464</i> | 69              | 4.77          | 4.77           | 1.89     |
| <i>GFL276</i> | 70              | -3.89         | 3.89           | 2.14     |
| <i>GFL439</i> | 71              | 3.82          | 3.82           | 31.40    |
| <i>GFL402</i> | 72              | -3.17         | 3.17           | 4.45     |
| <i>GFL184</i> | 73              | -4.24         | 4.24           | 7.51     |
| <i>GFL384</i> | 74              | -3.36         | 3.36           | 0.88     |
| <i>GFL416</i> | 75              | -2.96         | 2.96           | 5.29     |
| <i>GFL449</i> | 75              | 4.17          | 4.17           | 15.76    |
| <i>GFL072</i> | 78              | -4.92         | 4.92           | 1.19     |
| <i>GFL458</i> | 78              | 4.61          | 4.61           | 4.72     |
| <i>GFL374</i> | 80              | -3.43         | 3.43           | 4.30     |
| <i>GFL422</i> | 81              | 3.09          | 3.09           | 2.06     |
| <i>GFL441</i> | 82              | 3.83          | 3.83           | 16.43    |
| <i>GFL442</i> | 82              | 3.85          | 3.85           | 5.73     |
| <i>GFL116</i> | 84              | -4.62         | 4.62           | 4.01     |
| <i>GFL243</i> | 84              | -4.01         | 4.01           | 12.49    |

**Table 12** Continued

| Gene ID       | Number of edges | LEN ratio (%) | Abs(LEN ratio) | Aver TPM |
|---------------|-----------------|---------------|----------------|----------|
| <i>GFL300</i> | 84              | -3.77         | 3.77           | 0.79     |
| <i>GFL361</i> | 84              | -3.52         | 3.52           | 5.29     |
| <i>GFL444</i> | 87              | 3.94          | 3.94           | 1.03     |
| <i>GFL254</i> | 90              | -3.97         | 3.97           | 9.05     |
| <i>GFL386</i> | 90              | -3.33         | 3.33           | 7.34     |
| <i>GFL459</i> | 91              | 4.61          | 4.61           | 221.72   |
| <i>GFL349</i> | 93              | -3.56         | 3.56           | 12.44    |
| <i>GFL433</i> | 93              | 3.72          | 3.72           | 5.35     |
| <i>GFL469</i> | 93              | 5.26          | 5.26           | 5.21     |
| <i>GFL466</i> | 94              | 5.10          | 5.10           | 16.41    |
| <i>GFL101</i> | 98              | -4.70         | 4.70           | 23.33    |
| <i>GFL446</i> | 99              | 4.04          | 4.04           | 29.73    |
| <i>GFL122</i> | 100             | -4.57         | 4.57           | 2.63     |
| <i>GFL373</i> | 103             | -3.44         | 3.44           | 24.84    |
| <i>GFL413</i> | 103             | -3.02         | 3.02           | 14.18    |
| <i>GFL001</i> | 104             | -7.92         | 7.92           | 0.75     |
| <i>GFL007</i> | 104             | -6.26         | 6.26           | 23.88    |
| <i>GFL021</i> | 104             | -5.82         | 5.82           | 5.25     |
| <i>GFL358</i> | 104             | -3.54         | 3.54           | 13.80    |
| <i>GFL379</i> | 104             | -3.40         | 3.40           | 21.39    |
| <i>GFL112</i> | 105             | -4.65         | 4.65           | 1.54     |
| <i>GFL244</i> | 107             | -4.01         | 4.01           | 1.03     |
| <i>GFL266</i> | 108             | -3.92         | 3.92           | 5.39     |
| <i>GFL337</i> | 109             | -3.60         | 3.60           | 110.58   |
| <i>GFL453</i> | 109             | 4.42          | 4.42           | 10.78    |
| <i>GFL113</i> | 111             | -4.65         | 4.65           | 8.26     |
| <i>GFL263</i> | 113             | -3.94         | 3.94           | 27.04    |
| <i>GFL411</i> | 114             | -3.06         | 3.06           | 1.51     |
| <i>GFL435</i> | 114             | 3.76          | 3.76           | 2.97     |
| <i>GFL363</i> | 115             | -3.51         | 3.51           | 4.99     |
| <i>GFL090</i> | 118             | -4.79         | 4.79           | 23.16    |
| <i>GFL149</i> | 118             | -4.42         | 4.42           | 1.05     |
| <i>GFL451</i> | 118             | 4.31          | 4.31           | 7.93     |
| <i>GFL279</i> | 121             | -3.88         | 3.88           | 16.94    |
| <i>GFL146</i> | 122             | -4.44         | 4.44           | 2.97     |
| <i>GFL058</i> | 123             | -5.02         | 5.02           | 8.18     |
| <i>GFL152</i> | 123             | -4.40         | 4.40           | 15.87    |
| <i>GFL408</i> | 124             | -3.10         | 3.10           | 9.83     |
| <i>GFL070</i> | 127             | -4.94         | 4.94           | 10.54    |
| <i>GFL467</i> | 127             | 5.19          | 5.19           | 100.01   |
| <i>GFL102</i> | 128             | -4.70         | 4.70           | 303.56   |
| <i>GFL290</i> | 128             | -3.81         | 3.81           | 6.33     |
| <i>GFL125</i> | 129             | -4.55         | 4.55           | 22.74    |
| <i>GFL430</i> | 130             | 3.57          | 3.57           | 23676.20 |
| <i>GFL368</i> | 131             | -3.46         | 3.46           | 7.03     |
| <i>GFL406</i> | 131             | -3.12         | 3.12           | 6.94     |
| <i>GFL420</i> | 131             | -2.64         | 2.64           | 3.03     |
| <i>GFL455</i> | 131             | 4.48          | 4.48           | 7.32     |

**Table 12** Continued

| Gene ID       | Number of edges | LEN ratio (%) | Abs(LEN ratio) | Aver TPM |
|---------------|-----------------|---------------|----------------|----------|
| <i>GFL005</i> | 132             | -6.37         | 6.37           | 1.29     |
| <i>GFL006</i> | 132             | -6.35         | 6.35           | 1.38     |
| <i>GFL351</i> | 133             | -3.56         | 3.56           | 10.44    |
| <i>GFL132</i> | 134             | -4.49         | 4.49           | 4.21     |
| <i>GFL131</i> | 137             | -4.50         | 4.50           | 22.00    |
| <i>GFL208</i> | 137             | -4.16         | 4.16           | 2.28     |
| <i>GFL427</i> | 137             | 3.40          | 3.40           | 5.69     |
| <i>GFL462</i> | 137             | 4.70          | 4.70           | 23.65    |
| <i>GFL443</i> | 140             | 3.89          | 3.89           | 2.73     |
| <i>GFL456</i> | 140             | 4.54          | 4.54           | 14.82    |
| <i>GFL017</i> | 142             | -5.93         | 5.93           | 4.07     |
| <i>GFL118</i> | 142             | -4.62         | 4.62           | 8.53     |
| <i>GFL241</i> | 142             | -4.04         | 4.04           | 63.19    |
| <i>GFL310</i> | 142             | -3.70         | 3.70           | 3.26     |
| <i>GFL360</i> | 143             | -3.53         | 3.53           | 4.43     |
| <i>GFL378</i> | 143             | -3.41         | 3.41           | 24.06    |
| <i>GFL463</i> | 144             | 4.72          | 4.72           | 2.15     |
| <i>GFL074</i> | 147             | -4.90         | 4.90           | 2.29     |
| <i>GFL390</i> | 147             | -3.31         | 3.31           | 6.64     |
| <i>GFL273</i> | 148             | -3.90         | 3.90           | 46.92    |
| <i>GFL391</i> | 148             | -3.31         | 3.31           | 0.85     |
| <i>GFL044</i> | 150             | -5.29         | 5.29           | 0.90     |
| <i>GFL172</i> | 150             | -4.32         | 4.32           | 1.55     |
| <i>GFL200</i> | 151             | -4.19         | 4.19           | 36.90    |
| <i>GFL468</i> | 152             | 5.21          | 5.21           | 4.63     |
| <i>GFL033</i> | 153             | -5.42         | 5.42           | 3.73     |
| <i>GFL315</i> | 153             | -3.68         | 3.68           | 5.83     |
| <i>GFL346</i> | 153             | -3.58         | 3.58           | 10.60    |
| <i>GFL015</i> | 154             | -6.04         | 6.04           | 0.81     |
| <i>GFL234</i> | 155             | -4.07         | 4.07           | 2.70     |
| <i>GFL380</i> | 156             | -3.40         | 3.40           | 39.29    |
| <i>GFL424</i> | 156             | 3.33          | 3.33           | 5.60     |
| <i>GFL059</i> | 157             | -5.01         | 5.01           | 0.97     |
| <i>GFL419</i> | 157             | -2.74         | 2.74           | 1.94     |
| <i>GFL474</i> | 157             | 6.80          | 6.80           | 635.38   |
| <i>GFL088</i> | 158             | -4.80         | 4.80           | 13.97    |
| <i>GFL297</i> | 158             | -3.79         | 3.79           | 9.22     |
| <i>GFL345</i> | 159             | -3.58         | 3.58           | 3.91     |
| <i>GFL096</i> | 160             | -4.74         | 4.74           | 35.58    |
| <i>GFL322</i> | 160             | -3.64         | 3.64           | 283.10   |
| <i>GFL359</i> | 160             | -3.54         | 3.54           | 11.45    |
| <i>GFL211</i> | 162             | -4.15         | 4.15           | 170.65   |
| <i>GFL333</i> | 162             | -3.62         | 3.62           | 10.12    |
| <i>GFL394</i> | 162             | -3.27         | 3.27           | 36.64    |
| <i>GFL286</i> | 163             | -3.84         | 3.84           | 8.95     |
| <i>GFL031</i> | 164             | -5.45         | 5.45           | 5.30     |
| <i>GFL209</i> | 164             | -4.16         | 4.16           | 13.80    |
| <i>GFL395</i> | 164             | -3.25         | 3.25           | 4.82     |
| <i>GFL438</i> | 164             | 3.79          | 3.79           | 7.09     |
| <i>GFL119</i> | 165             | -4.60         | 4.60           | 26.88    |

**Table 12** Continued

| Gene ID       | Number of edges | LEN ratio (%) | Abs(LEN ratio) | Aver TPM |
|---------------|-----------------|---------------|----------------|----------|
| <i>GFL262</i> | 166             | -3.94         | 3.94           | 16.65    |
| <i>GFL137</i> | 169             | -4.47         | 4.47           | 0.94     |
| <i>GFL259</i> | 169             | -3.94         | 3.94           | 93.27    |
| <i>GFL221</i> | 170             | -4.11         | 4.11           | 22.28    |
| <i>GFL260</i> | 170             | -3.94         | 3.94           | 49.06    |
| <i>GFL107</i> | 171             | -4.68         | 4.68           | 1.18     |
| <i>GFL111</i> | 171             | -4.66         | 4.66           | 1.51     |
| <i>GFL308</i> | 171             | -3.73         | 3.73           | 164.44   |
| <i>GFL353</i> | 172             | -3.56         | 3.56           | 13.76    |
| <i>GFL133</i> | 173             | -4.49         | 4.49           | 90.41    |
| <i>GFL403</i> | 174             | -3.15         | 3.15           | 3.19     |
| <i>GFL075</i> | 176             | -4.90         | 4.90           | 42.41    |
| <i>GFL272</i> | 176             | -3.91         | 3.91           | 103.67   |
| <i>GFL032</i> | 177             | -5.45         | 5.45           | 56.10    |
| <i>GFL089</i> | 177             | -4.80         | 4.80           | 13.39    |
| <i>GFL372</i> | 179             | -3.44         | 3.44           | 9.05     |
| <i>GFL454</i> | 179             | 4.44          | 4.44           | 6.60     |
| <i>GFL376</i> | 180             | -3.42         | 3.42           | 8.50     |
| <i>GFL404</i> | 181             | -3.14         | 3.14           | 4.74     |
| <i>GFL473</i> | 181             | 6.23          | 6.23           | 56.23    |
| <i>GFL086</i> | 183             | -4.82         | 4.82           | 11.09    |
| <i>GFL024</i> | 184             | -5.70         | 5.70           | 22.23    |
| <i>GFL348</i> | 184             | -3.57         | 3.57           | 1.01     |
| <i>GFL418</i> | 184             | -2.79         | 2.79           | 2.74     |
| <i>GFL235</i> | 185             | -4.07         | 4.07           | 5.16     |
| <i>GFL336</i> | 187             | -3.60         | 3.60           | 211.49   |
| <i>GFL383</i> | 188             | -3.37         | 3.37           | 4.39     |
| <i>GFL003</i> | 189             | -6.64         | 6.64           | 0.79     |
| <i>GFL431</i> | 189             | 3.63          | 3.63           | 155.80   |
| <i>GFL010</i> | 191             | -6.16         | 6.16           | 151.67   |
| <i>GFL342</i> | 191             | -3.59         | 3.59           | 12.06    |
| <i>GFL181</i> | 193             | -4.26         | 4.26           | 228.73   |
| <i>GFL307</i> | 193             | -3.73         | 3.73           | 5.50     |
| <i>GFL287</i> | 194             | -3.83         | 3.83           | 54.36    |
| <i>GFL305</i> | 194             | -3.74         | 3.74           | 34.30    |
| <i>GFL094</i> | 195             | -4.75         | 4.75           | 57.64    |
| <i>GFL255</i> | 195             | -3.97         | 3.97           | 1.31     |
| <i>GFL405</i> | 197             | -3.13         | 3.13           | 4.21     |
| <i>GFL347</i> | 198             | -3.58         | 3.58           | 5.94     |
| <i>GFL140</i> | 199             | -4.46         | 4.46           | 4.95     |
| <i>GFL352</i> | 199             | -3.56         | 3.56           | 66.02    |
| <i>GFL445</i> | 199             | 3.97          | 3.97           | 9.27     |
| <i>GFL452</i> | 199             | 4.38          | 4.38           | 78.55    |
| <i>GFL154</i> | 200             | -4.40         | 4.40           | 4.19     |
| <i>GFL288</i> | 200             | -3.82         | 3.82           | 5.78     |
| <i>GFL042</i> | 201             | -5.29         | 5.29           | 6.48     |
| <i>GFL174</i> | 201             | -4.30         | 4.30           | 16.26    |
| <i>GFL314</i> | 202             | -3.68         | 3.68           | 66.98    |
| <i>GFL393</i> | 202             | -3.28         | 3.28           | 13.66    |

**Table 12** Continued

| Gene ID       | Number of edges | LEN ratio (%) | Abs(LEN ratio) | Aver TPM |
|---------------|-----------------|---------------|----------------|----------|
| <i>GFL054</i> | 205             | -5.13         | 5.13           | 4.17     |
| <i>GFL304</i> | 205             | -3.74         | 3.74           | 14.39    |
| <i>GFL321</i> | 205             | -3.64         | 3.64           | 1.19     |
| <i>GFL023</i> | 206             | -5.72         | 5.72           | 10.70    |
| <i>GFL106</i> | 207             | -4.69         | 4.69           | 145.10   |
| <i>GFL450</i> | 208             | 4.29          | 4.29           | 15.40    |
| <i>GFL334</i> | 211             | -3.61         | 3.61           | 2.08     |
| <i>GFL407</i> | 211             | -3.12         | 3.12           | 20.81    |
| <i>GFL048</i> | 212             | -5.23         | 5.23           | 46.22    |
| <i>GFL067</i> | 212             | -4.96         | 4.96           | 47.88    |
| <i>GFL377</i> | 212             | -3.41         | 3.41           | 86.70    |
| <i>GFL036</i> | 213             | -5.39         | 5.39           | 8.76     |
| <i>GFL156</i> | 213             | -4.38         | 4.38           | 14.35    |
| <i>GFL256</i> | 213             | -3.96         | 3.96           | 3.24     |
| <i>GFL014</i> | 214             | -6.09         | 6.09           | 18.98    |
| <i>GFL362</i> | 214             | -3.51         | 3.51           | 22.24    |
| <i>GFL141</i> | 215             | -4.46         | 4.46           | 2.29     |
| <i>GFL302</i> | 215             | -3.75         | 3.75           | 21.53    |
| <i>GFL369</i> | 216             | -3.46         | 3.46           | 22.65    |
| <i>GFL091</i> | 217             | -4.78         | 4.78           | 73.38    |
| <i>GFL177</i> | 218             | -4.27         | 4.27           | 17.40    |
| <i>GFL388</i> | 219             | -3.32         | 3.32           | 82.55    |
| <i>GFL207</i> | 220             | -4.16         | 4.16           | 38.98    |
| <i>GFL219</i> | 221             | -4.12         | 4.12           | 16.89    |
| <i>GFL231</i> | 221             | -4.09         | 4.09           | 28.36    |
| <i>GFL354</i> | 221             | -3.55         | 3.55           | 1134.56  |
| <i>GFL039</i> | 222             | -5.33         | 5.33           | 83.28    |
| <i>GFL382</i> | 224             | -3.37         | 3.37           | 6.94     |
| <i>GFL081</i> | 225             | -4.87         | 4.87           | 3.69     |
| <i>GFL239</i> | 225             | -4.05         | 4.05           | 909.74   |
| <i>GFL270</i> | 225             | -3.92         | 3.92           | 56.50    |
| <i>GFL365</i> | 226             | -3.49         | 3.49           | 19.28    |
| <i>GFL357</i> | 228             | -3.55         | 3.55           | 22.11    |
| <i>GFL134</i> | 230             | -4.48         | 4.48           | 1.58     |
| <i>GFL245</i> | 230             | -4.01         | 4.01           | 19.38    |
| <i>GFL410</i> | 230             | -3.08         | 3.08           | 38.95    |
| <i>GFL121</i> | 231             | -4.58         | 4.58           | 160.67   |
| <i>GFL198</i> | 231             | -4.20         | 4.20           | 12.95    |
| <i>GFL013</i> | 232             | -6.10         | 6.10           | 5.92     |
| <i>GFL012</i> | 233             | -6.12         | 6.12           | 3.29     |
| <i>GFL283</i> | 233             | -3.87         | 3.87           | 29.33    |
| <i>GFL311</i> | 234             | -3.69         | 3.69           | 39.29    |
| <i>GFL341</i> | 234             | -3.59         | 3.59           | 53.53    |
| <i>GFL381</i> | 234             | -3.37         | 3.37           | 153.14   |
| <i>GFL022</i> | 235             | -5.77         | 5.77           | 9.63     |
| <i>GFL043</i> | 236             | -5.29         | 5.29           | 25.09    |
| <i>GFL180</i> | 236             | -4.26         | 4.26           | 68.70    |
| <i>GFL225</i> | 236             | -4.10         | 4.10           | 318.42   |
| <i>GFL316</i> | 236             | -3.67         | 3.67           | 11.65    |

**Table 12** Continued

| Gene ID       | Number of edges | LEN ratio (%) | Abs(LEN ratio) | Aver TPM |
|---------------|-----------------|---------------|----------------|----------|
| <i>GFL186</i> | 237             | -4.23         | 4.23           | 11.37    |
| <i>GFL389</i> | 237             | -3.32         | 3.32           | 14.83    |
| <i>GFL144</i> | 238             | -4.45         | 4.45           | 20.29    |
| <i>GFL009</i> | 240             | -6.17         | 6.17           | 21.79    |
| <i>GFL066</i> | 240             | -4.98         | 4.98           | 2.60     |
| <i>GFL228</i> | 241             | -4.10         | 4.10           | 18.14    |
| <i>GFL250</i> | 241             | -3.98         | 3.98           | 46.95    |
| <i>GFL020</i> | 243             | -5.83         | 5.83           | 69.10    |
| <i>GFL178</i> | 243             | -4.27         | 4.27           | 32.98    |
| <i>GFL248</i> | 246             | -3.99         | 3.99           | 8.49     |
| <i>GFL319</i> | 247             | -3.66         | 3.66           | 7.58     |
| <i>GFL018</i> | 248             | -5.88         | 5.88           | 87.13    |
| <i>GFL176</i> | 249             | -4.28         | 4.28           | 20.47    |
| <i>GFL002</i> | 250             | -6.67         | 6.67           | 2.56     |
| <i>GFL056</i> | 250             | -5.03         | 5.03           | 4.13     |
| <i>GFL076</i> | 251             | -4.89         | 4.89           | 9.71     |
| <i>GFL196</i> | 251             | -4.20         | 4.20           | 132.80   |
| <i>GFL335</i> | 251             | -3.61         | 3.61           | 362.13   |
| <i>GFL385</i> | 251             | -3.34         | 3.34           | 309.12   |
| <i>GFL392</i> | 251             | -3.29         | 3.29           | 24.38    |
| <i>GFL055</i> | 252             | -5.04         | 5.04           | 13.87    |
| <i>GFL109</i> | 252             | -4.67         | 4.67           | 15.50    |
| <i>GFL202</i> | 253             | -4.18         | 4.18           | 8.67     |
| <i>GFL226</i> | 253             | -4.10         | 4.10           | 19.76    |
| <i>GFL162</i> | 254             | -4.37         | 4.37           | 13.30    |
| <i>GFL160</i> | 255             | -4.37         | 4.37           | 3.55     |
| <i>GFL301</i> | 255             | -3.76         | 3.76           | 203.29   |
| <i>GFL356</i> | 255             | -3.55         | 3.55           | 23.86    |
| <i>GFL169</i> | 256             | -4.34         | 4.34           | 178.52   |
| <i>GFL204</i> | 256             | -4.18         | 4.18           | 13.02    |
| <i>GFL212</i> | 256             | -4.15         | 4.15           | 3.91     |
| <i>GFL040</i> | 257             | -5.33         | 5.33           | 35.93    |
| <i>GFL095</i> | 257             | -4.75         | 4.75           | 4.78     |
| <i>GFL213</i> | 257             | -4.14         | 4.14           | 2.67     |
| <i>GFL281</i> | 257             | -3.88         | 3.88           | 37.56    |
| <i>GFL285</i> | 257             | -3.86         | 3.86           | 185.44   |
| <i>GFL214</i> | 258             | -4.13         | 4.13           | 6.88     |
| <i>GFL224</i> | 258             | -4.10         | 4.10           | 12.52    |
| <i>GFL011</i> | 259             | -6.13         | 6.13           | 17.14    |
| <i>GFL193</i> | 259             | -4.20         | 4.20           | 69.99    |
| <i>GFL246</i> | 259             | -4.00         | 4.00           | 16.88    |
| <i>GFL414</i> | 259             | -2.98         | 2.98           | 1.52     |
| <i>GFL432</i> | 259             | 3.68          | 3.68           | 163.63   |
| <i>GFL077</i> | 260             | -4.89         | 4.89           | 6.40     |
| <i>GFL136</i> | 260             | -4.47         | 4.47           | 5.06     |
| <i>GFL175</i> | 260             | -4.29         | 4.29           | 26.98    |
| <i>GFL271</i> | 260             | -3.91         | 3.91           | 12.50    |
| <i>GFL167</i> | 261             | -4.34         | 4.34           | 15.35    |
| <i>GFL179</i> | 261             | -4.26         | 4.26           | 15.05    |

**Table 12** Continued

| Gene ID       | Number of edges | LEN ratio (%) | Abs(LEN ratio) | Aver TPM |
|---------------|-----------------|---------------|----------------|----------|
| <i>GFL323</i> | 261             | -3.64         | 3.64           | 7.55     |
| <i>GFL142</i> | 262             | -4.45         | 4.45           | 4.41     |
| <i>GFL400</i> | 262             | -3.20         | 3.20           | 1.70     |
| <i>GFL035</i> | 263             | -5.41         | 5.41           | 3.16     |
| <i>GFL063</i> | 263             | -4.99         | 4.99           | 35.51    |
| <i>GFL161</i> | 263             | -4.37         | 4.37           | 12.73    |
| <i>GFL326</i> | 263             | -3.64         | 3.64           | 165.88   |
| <i>GFL227</i> | 264             | -4.10         | 4.10           | 30.14    |
| <i>GFL105</i> | 265             | -4.69         | 4.69           | 3.95     |
| <i>GFL150</i> | 265             | -4.42         | 4.42           | 162.00   |
| <i>GFL232</i> | 265             | -4.08         | 4.08           | 24.41    |
| <i>GFL257</i> | 265             | -3.95         | 3.95           | 4.50     |
| <i>GFL399</i> | 265             | -3.21         | 3.21           | 22.46    |
| <i>GFL197</i> | 266             | -4.20         | 4.20           | 3.91     |
| <i>GFL324</i> | 266             | -3.64         | 3.64           | 174.98   |
| <i>GFL371</i> | 267             | -3.45         | 3.45           | 31.16    |
| <i>GFL019</i> | 268             | -5.88         | 5.88           | 1801.61  |
| <i>GFL188</i> | 268             | -4.22         | 4.22           | 40.51    |
| <i>GFL183</i> | 269             | -4.26         | 4.26           | 8.24     |
| <i>GFL318</i> | 269             | -3.66         | 3.66           | 300.14   |
| <i>GFL062</i> | 270             | -4.99         | 4.99           | 5.59     |
| <i>GFL218</i> | 270             | -4.12         | 4.12           | 5.79     |
| <i>GFL296</i> | 270             | -3.79         | 3.79           | 171.60   |
| <i>GFL108</i> | 271             | -4.67         | 4.67           | 30.97    |
| <i>GFL083</i> | 272             | -4.86         | 4.86           | 4.02     |
| <i>GFL045</i> | 274             | -5.28         | 5.28           | 73.60    |
| <i>GFL073</i> | 274             | -4.90         | 4.90           | 96.62    |
| <i>GFL028</i> | 275             | -5.60         | 5.60           | 3.25     |
| <i>GFL057</i> | 275             | -5.02         | 5.02           | 71.15    |
| <i>GFL182</i> | 275             | -4.26         | 4.26           | 259.33   |
| <i>GFL230</i> | 275             | -4.09         | 4.09           | 46.89    |
| <i>GFL195</i> | 276             | -4.20         | 4.20           | 12.61    |
| <i>GFL253</i> | 276             | -3.97         | 3.97           | 470.65   |
| <i>GFL110</i> | 277             | -4.66         | 4.66           | 55.77    |
| <i>GFL275</i> | 277             | -3.89         | 3.89           | 737.16   |
| <i>GFL367</i> | 277             | -3.47         | 3.47           | 487.68   |
| <i>GFL016</i> | 278             | -6.00         | 6.00           | 43.27    |
| <i>GFL060</i> | 279             | -5.00         | 5.00           | 21.39    |
| <i>GFL092</i> | 279             | -4.77         | 4.77           | 6.55     |
| <i>GFL274</i> | 279             | -3.89         | 3.89           | 209.27   |
| <i>GFL252</i> | 280             | -3.97         | 3.97           | 82.34    |
| <i>GFL306</i> | 280             | -3.74         | 3.74           | 23.32    |
| <i>GFL229</i> | 281             | -4.10         | 4.10           | 43.50    |
| <i>GFL223</i> | 282             | -4.11         | 4.11           | 21.02    |
| <i>GFL417</i> | 282             | -2.93         | 2.93           | 23.60    |
| <i>GFL409</i> | 283             | -3.08         | 3.08           | 480.68   |
| <i>GFL205</i> | 284             | -4.17         | 4.17           | 84.51    |
| <i>GFL265</i> | 285             | -3.93         | 3.93           | 26.70    |
| <i>GFL355</i> | 285             | -3.55         | 3.55           | 208.29   |

**Table 12** Continued

| Gene ID       | Number of edges | LEN ratio (%) | Abs(LEN ratio) | Aver TPM |
|---------------|-----------------|---------------|----------------|----------|
| <i>GFL128</i> | 286             | -4.51         | 4.51           | 12.08    |
| <i>GFL164</i> | 287             | -4.35         | 4.35           | 17.28    |
| <i>GFL216</i> | 287             | -4.13         | 4.13           | 11.57    |
| <i>GFL071</i> | 288             | -4.92         | 4.92           | 2.49     |
| <i>GFL098</i> | 289             | -4.72         | 4.72           | 47.02    |
| <i>GFL069</i> | 290             | -4.94         | 4.94           | 26.95    |
| <i>GFL151</i> | 290             | -4.41         | 4.41           | 8.37     |
| <i>GFL190</i> | 291             | -4.21         | 4.21           | 7.69     |
| <i>GFL249</i> | 292             | -3.99         | 3.99           | 47.49    |
| <i>GFL258</i> | 292             | -3.95         | 3.95           | 66.18    |
| <i>GFL050</i> | 293             | -5.21         | 5.21           | 28.99    |
| <i>GFL087</i> | 293             | -4.81         | 4.81           | 11.75    |
| <i>GFL240</i> | 293             | -4.05         | 4.05           | 383.81   |
| <i>GFL251</i> | 293             | -3.98         | 3.98           | 97.39    |
| <i>GFL284</i> | 293             | -3.87         | 3.87           | 12.73    |
| <i>GFL267</i> | 294             | -3.92         | 3.92           | 53.50    |
| <i>GFL312</i> | 294             | -3.69         | 3.69           | 3.82     |
| <i>GFL157</i> | 295             | -4.38         | 4.38           | 79.72    |
| <i>GFL215</i> | 295             | -4.13         | 4.13           | 36.53    |
| <i>GFL034</i> | 297             | -5.42         | 5.42           | 10.54    |
| <i>GFL206</i> | 297             | -4.16         | 4.16           | 114.14   |
| <i>GFL280</i> | 297             | -3.88         | 3.88           | 31.04    |
| <i>GFL261</i> | 298             | -3.94         | 3.94           | 21.25    |
| <i>GFL084</i> | 299             | -4.83         | 4.83           | 41.39    |
| <i>GFL277</i> | 300             | -3.89         | 3.89           | 7.28     |
| <i>GFL027</i> | 302             | -5.60         | 5.60           | 59.64    |
| <i>GFL120</i> | 302             | -4.58         | 4.58           | 571.22   |
| <i>GFL143</i> | 302             | -4.45         | 4.45           | 10.80    |
| <i>GFL398</i> | 302             | -3.23         | 3.23           | 22.10    |
| <i>GFL171</i> | 303             | -4.32         | 4.32           | 116.06   |
| <i>GFL238</i> | 304             | -4.06         | 4.06           | 106.30   |
| <i>GFL126</i> | 305             | -4.55         | 4.55           | 87.27    |
| <i>GFL331</i> | 305             | -3.63         | 3.63           | 163.49   |
| <i>GFL387</i> | 305             | -3.32         | 3.32           | 34.85    |
| <i>GFL135</i> | 307             | -4.48         | 4.48           | 27.42    |
| <i>GFL138</i> | 307             | -4.46         | 4.46           | 31.46    |
| <i>GFL201</i> | 307             | -4.19         | 4.19           | 233.72   |
| <i>GFL291</i> | 307             | -3.81         | 3.81           | 64.36    |
| <i>GFL046</i> | 308             | -5.25         | 5.25           | 77.96    |
| <i>GFL189</i> | 308             | -4.21         | 4.21           | 68.62    |
| <i>GFL192</i> | 309             | -4.20         | 4.20           | 21.92    |
| <i>GFL194</i> | 309             | -4.20         | 4.20           | 149.05   |
| <i>GFL269</i> | 309             | -3.92         | 3.92           | 13.72    |
| <i>GFL203</i> | 310             | -4.18         | 4.18           | 16.20    |
| <i>GFL293</i> | 310             | -3.80         | 3.80           | 57.99    |
| <i>GFL375</i> | 310             | -3.43         | 3.43           | 117.48   |
| <i>GFL401</i> | 310             | -3.19         | 3.19           | 51.76    |
| <i>GFL061</i> | 311             | -4.99         | 4.99           | 27.04    |
| <i>GFL097</i> | 312             | -4.72         | 4.72           | 31.79    |



**Table 12** Continued

| Gene ID       | Number of edges | LEN ratio (%) | Abs(LEN ratio) | Aver TPM |
|---------------|-----------------|---------------|----------------|----------|
| <i>GFL139</i> | 312             | -4.46         | 4.46           | 419.40   |
| <i>GFL170</i> | 312             | -4.32         | 4.32           | 129.10   |
| <i>GFL173</i> | 312             | -4.32         | 4.32           | 123.70   |
| <i>GFL233</i> | 312             | -4.08         | 4.08           | 362.30   |
| <i>GFL153</i> | 313             | -4.40         | 4.40           | 387.83   |
| <i>GFL294</i> | 313             | -3.79         | 3.79           | 17.95    |
| <i>GFL100</i> | 314             | -4.71         | 4.71           | 39.73    |
| <i>GFL309</i> | 314             | -3.71         | 3.71           | 33.79    |
| <i>GFL038</i> | 316             | -5.34         | 5.34           | 19.69    |
| <i>GFL047</i> | 316             | -5.24         | 5.24           | 699.51   |
| <i>GFL313</i> | 316             | -3.69         | 3.69           | 11.50    |
| <i>GFL082</i> | 317             | -4.87         | 4.87           | 96.49    |
| <i>GFL114</i> | 317             | -4.64         | 4.64           | 10.23    |
| <i>GFL242</i> | 317             | -4.03         | 4.03           | 199.04   |
| <i>GFL068</i> | 318             | -4.96         | 4.96           | 79.35    |
| <i>GFL343</i> | 318             | -3.59         | 3.59           | 149.66   |
| <i>GFL117</i> | 319             | -4.62         | 4.62           | 283.58   |
| <i>GFL026</i> | 320             | -5.62         | 5.62           | 121.52   |
| <i>GFL168</i> | 320             | -4.34         | 4.34           | 38.97    |
| <i>GFL185</i> | 321             | -4.24         | 4.24           | 41.89    |
| <i>GFL289</i> | 321             | -3.82         | 3.82           | 32.05    |
| <i>GFL295</i> | 323             | -3.79         | 3.79           | 313.96   |
| <i>GFL317</i> | 323             | -3.67         | 3.67           | 422.43   |
| <i>GFL052</i> | 324             | -5.14         | 5.14           | 33.68    |
| <i>GFL220</i> | 327             | -4.12         | 4.12           | 78.81    |
| <i>GFL303</i> | 328             | -3.75         | 3.75           | 129.99   |
| <i>GFL129</i> | 329             | -4.51         | 4.51           | 51.12    |
| <i>GFL222</i> | 331             | -4.11         | 4.11           | 516.41   |
| <i>GFL085</i> | 332             | -4.83         | 4.83           | 187.35   |
| <i>GFL158</i> | 334             | -4.38         | 4.38           | 122.63   |
| <i>GFL236</i> | 334             | -4.07         | 4.07           | 193.65   |
| <i>GFL366</i> | 335             | -3.47         | 3.47           | 74.05    |
| <i>GFL247</i> | 336             | -3.99         | 3.99           | 76.76    |
| <i>GFL217</i> | 337             | -4.12         | 4.12           | 273.81   |
| <i>GFL298</i> | 337             | -3.79         | 3.79           | 43.21    |
| <i>GFL148</i> | 338             | -4.43         | 4.43           | 50.30    |
| <i>GFL350</i> | 338             | -3.56         | 3.56           | 689.50   |
| <i>GFL037</i> | 340             | -5.35         | 5.35           | 33.28    |
| <i>GFL064</i> | 341             | -4.99         | 4.99           | 25.65    |
| <i>GFL338</i> | 342             | -3.60         | 3.60           | 82.23    |
| <i>GFL155</i> | 343             | -4.39         | 4.39           | 71.14    |
| <i>GFL328</i> | 343             | -3.63         | 3.63           | 121.77   |
| <i>GFL339</i> | 343             | -3.60         | 3.60           | 224.23   |
| <i>GFL065</i> | 344             | -4.98         | 4.98           | 29.06    |
| <i>GFL079</i> | 344             | -4.88         | 4.88           | 341.33   |
| <i>GFL187</i> | 345             | -4.23         | 4.23           | 134.42   |
| <i>GFL199</i> | 345             | -4.19         | 4.19           | 52.34    |
| <i>GFL396</i> | 345             | -3.24         | 3.24           | 49.35    |
| <i>GFL051</i> | 346             | -5.18         | 5.18           | 104.06   |

**Table 12** Continued

| Gene ID       | Number of edges | LEN ratio (%) | Abs(LEN ratio) | Aver TPM |
|---------------|-----------------|---------------|----------------|----------|
| <i>GFL147</i> | 347             | -4.44         | 4.44           | 670.11   |
| <i>GFL278</i> | 347             | -3.89         | 3.89           | 85.34    |
| <i>GFL053</i> | 348             | -5.14         | 5.14           | 69.38    |
| <i>GFL145</i> | 348             | -4.44         | 4.44           | 43.26    |
| <i>GFL030</i> | 349             | -5.50         | 5.50           | 115.26   |
| <i>GFL127</i> | 351             | -4.54         | 4.54           | 36.11    |
| <i>GFL159</i> | 351             | -4.37         | 4.37           | 63.05    |
| <i>GFL237</i> | 351             | -4.06         | 4.06           | 172.01   |
| <i>GFL078</i> | 352             | -4.88         | 4.88           | 69.40    |
| <i>GFL025</i> | 353             | -5.65         | 5.65           | 29.98    |
| <i>GFL282</i> | 353             | -3.87         | 3.87           | 1106.15  |
| <i>GFL370</i> | 354             | -3.46         | 3.46           | 67.70    |
| <i>GFL124</i> | 355             | -4.55         | 4.55           | 87.88    |
| <i>GFL029</i> | 357             | -5.52         | 5.52           | 644.92   |
| <i>GFL080</i> | 357             | -4.88         | 4.88           | 159.40   |
| <i>GFL123</i> | 357             | -4.56         | 4.56           | 119.43   |
| <i>GFL330</i> | 357             | -3.63         | 3.63           | 172.65   |
| <i>GFL049</i> | 358             | -5.22         | 5.22           | 417.68   |
| <i>GFL099</i> | 358             | -4.71         | 4.71           | 88.91    |
| <i>GFL103</i> | 358             | -4.70         | 4.70           | 130.65   |
| <i>GFL329</i> | 358             | -3.63         | 3.63           | 97.91    |
| <i>GFL210</i> | 359             | -4.16         | 4.16           | 159.98   |
| <i>GFL292</i> | 360             | -3.80         | 3.80           | 167.16   |
| <i>GFL332</i> | 361             | -3.62         | 3.62           | 59.87    |
| <i>GFL008</i> | 362             | -6.22         | 6.22           | 345.32   |
| <i>GFL166</i> | 363             | -4.34         | 4.34           | 57.59    |
| <i>GFL041</i> | 365             | -5.30         | 5.30           | 211.70   |
| <i>GFL130</i> | 365             | -4.50         | 4.50           | 397.25   |
| <i>GFL327</i> | 365             | -3.63         | 3.63           | 65.35    |
| <i>GFL163</i> | 369             | -4.36         | 4.36           | 177.25   |
| <i>GFL268</i> | 370             | -3.92         | 3.92           | 464.80   |
| <i>GFL115</i> | 374             | -4.64         | 4.64           | 109.54   |
| <i>GFL325</i> | 382             | -3.64         | 3.64           | 138.46   |
| <i>GFL165</i> | 383             | -4.35         | 4.35           | 177.36   |

### 3.4.2 Variations of *GFL* gene networks and UHMLs

#### 3.4.2.1 Variation of the 474 *GFL* gene network among RILs with different UHMLs

The next question was whether or not the *GFL* gene network is stable across RILs with different UHML phenotypes and if not, what would happen to the UHML. To answer this question, the 198 RILs and the parents of the TAM 94L-25 x NMSI 1331 population were grouped in a quantile of 20% into five groups based on their UHMLs, with each group having 40 lines. The group having the shortest fibers was defined as G1 while the group having the longest fibers was defined as G5. The co-regulation networks of the 474 *GFL* genes were constructed for each group (Fig. 23) and examined in terms of number of nodes, number of edges and the node components of the network. Under a significance level of  $P \leq 0.05$ , 465 (98.10%) of the 474 *GFL* genes were included in the gene network for G1, G2 and G3, but the numbers of edges varied from 19,443 for G1, 19,327 for G2 and 27,580 for G3. From G3 to G4, the number of nodes in the network was increased by one, whereas the number of nodes in the network was reduced by four from G4 to G5. The numbers of edges varied dramatically - 27,580, 16,835 and 16,195 from G3, G4, and G5 (Table 13). Consequently, UHML was increased by 2.64 mm for G3, when 8,137 edges were added to the G1 network. The loss of three nodes from the G3 network led to the loss of 11,385 edges for the G5 network, which resulted in a UHML increase of 2.92 mm for G5. These results indicated that UHML was determined not only by the variation of number of nodes, but also by the variation of numbers of

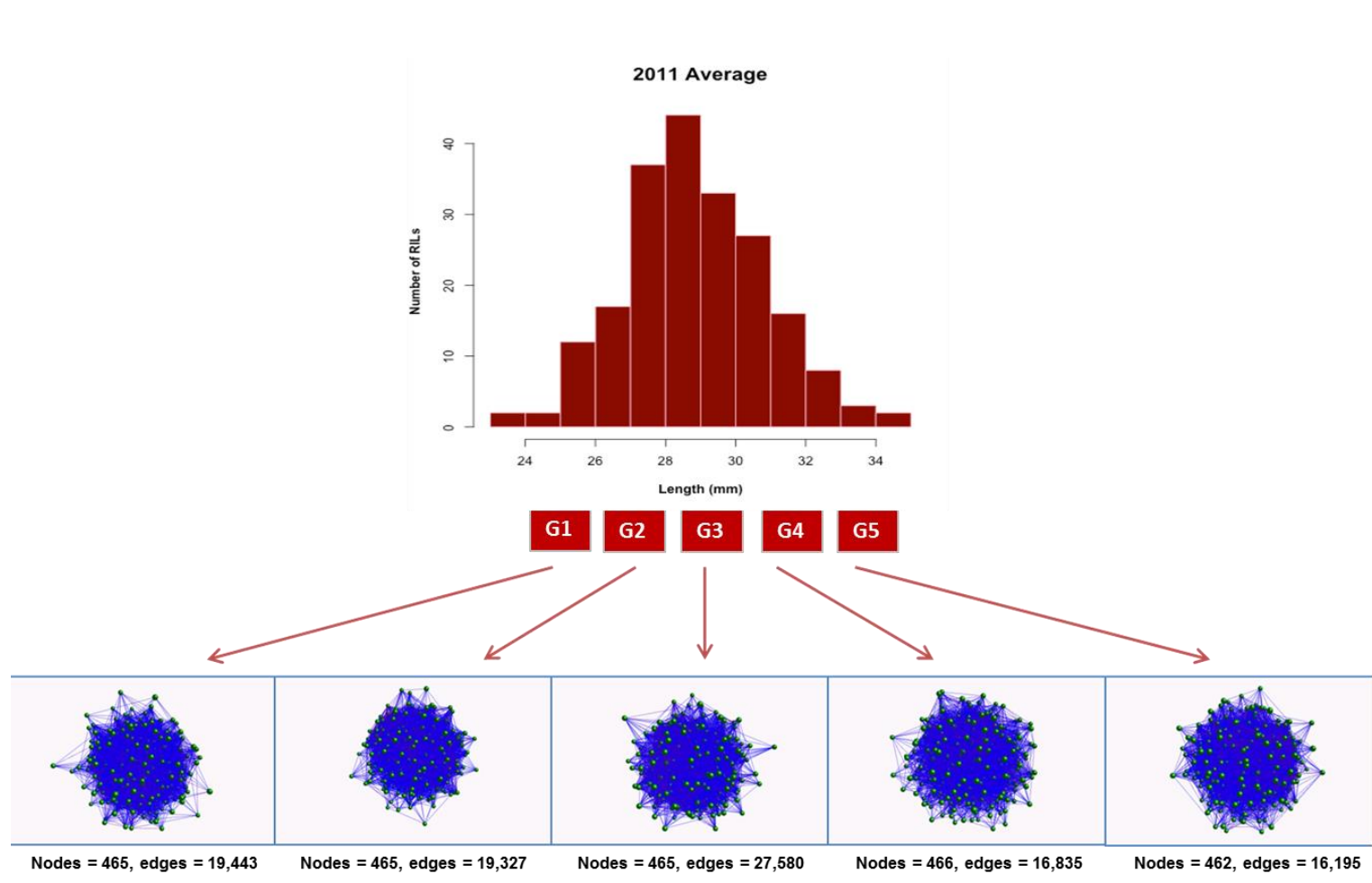


**Figure 23** Association of the variations of *GFL* gene networks with the UHML of the RILs of the TAM 94L-25 x NMSI 1331 population

**Table 13** Number of edges and nodes in the gene x gene networks among groups with different UHMLs

|                                      | G1    | G2    | G3    | G4    | G5    |
|--------------------------------------|-------|-------|-------|-------|-------|
| Average length within the group (mm) | 26.16 | 27.76 | 28.80 | 29.85 | 31.72 |
| Total node                           | 474   | 474   | 474   | 474   | 474   |
| No. of significant edges             | 19443 | 19327 | 27580 | 16835 | 16195 |
| No. of node in edges*                | 465   | 465   | 465   | 466   | 462   |
| No. of unique edges*                 | 6043  | 5564  | 9841  | 4763  | 5033  |
| Ratio of unique edges (%)            | 31.08 | 28.79 | 35.68 | 28.29 | 31.08 |
| Markov clusters                      | 6     | 7     | 5     | 10    | 8     |

(\*) significant at the 0.05 probability level

edges. Therefore, the dynamic of *GFL* genes and their interactions led to UHML variations between groups.

Moreover, the composition of nodes in the *GFL* gene networks may also vary with network variation, thus influencing UHML. It was noted that although the numbers of nodes of the G1, G2 and G3 networks were the same, the node compositions of the networks varied among the three groups of RILs (Table 14). For example, both the gene networks of G1 and G2 consisted of 465 *GFL* genes (nodes), but three of the nodes, *GFL115*, *GFL351* and *GFL457*, were found to be specific for the G1 network and three of them, *GFL093*, *GFL088* and *GFL434*, were specific for the G2 network. Therefore, there were a total of six nodes different between the G1 and G2 networks, accounting for 0.65% [ $6/(465 + 465)$ ] of the nodes constituting the networks. Similar changes in the node compositions of the *GFL* gene networks were observed between other pairs of UHML RIL groups. Among all 10 possible pairs of the RIL groups with different UHMLs, the node compositions of the networks changed by three nodes between G3 and G4, and by 11 nodes between G3 and G5. These findings suggested that the node

**Table 14** Pairwise comparison of the nodes of the *GFL* gene networks between the RIL groups with different UHMLs

| Subject                                     | G1  | G2  | G3  | G4  | G5   |
|---|---|---|---|---|--|
| Mean of UHMLd of RIL group (in)             | 1.03  | 1.093   | 1.134   | 1.175   | 1.249  |
| No. of edges in the <i>GFL</i> gene network | 19443   | 19327   | 27580   | 16835   | 16195  |
| No. of nodes in the <i>GFL</i> gene network | 465   | 465   | 465   | 466   | 462  |
| Nodes specific for RIL group network pair   | <i>GFL115</i><br><i>GFL351</i><br><i>GFL457</i>                                   | <i>GFL093</i><br><i>GFL088</i><br><i>GFL434</i>                                   |   |   |  |
|   | <i>GFL234</i><br><i>GFL428</i>  |   | <i>GFL088</i><br><i>GFL470</i>  |   |  |
|   | <i>GFL383</i><br><i>GFL428</i>  |   |   | <i>GFL088</i><br><i>GFL434</i><br><i>GFL470</i>   |  |
|   | <i>GFL286</i><br><i>GFL036</i><br><i>GFL272</i><br><i>GFL115</i><br><i>GFL457</i> |   |   |   | <i>GFL450</i><br><i>GFL434</i>                                   |
|   |   | <i>GFL234</i><br><i>GFL093</i><br><i>GFL428</i><br><i>GFL434</i>                  | <i>GFL457</i><br><i>GFL351</i><br><i>GFL115</i><br><i>GFL470</i>  |   |  |
|   |   | <i>GFL093</i><br><i>GFL383</i><br><i>GFL428</i>                                   |   | <i>GFL457</i><br><i>GFL470</i><br><i>GFL351</i><br><i>GFL115</i>  |  |
|   |   | <i>GFL272</i><br><i>GFL093</i><br><i>GFL088</i><br><i>GFL036</i><br><i>GFL286</i> |   |   | <i>GFL351</i><br><i>GFL450</i>                                   |
|   |   |   | <i>GFL383</i>   | <i>GFL234</i><br><i>GFL434</i>  |  |
|   |   |   | <i>GFL286</i><br><i>GFL088</i><br><i>GFL036</i><br><i>GFL272</i><br><i>GFL457</i><br><i>GFL115</i><br><i>GFL470</i> |   | <i>GFL234</i><br><i>GFL450</i><br><i>GFL434</i><br><i>GFL428</i> |
|   |   |   |   | <i>GFL286</i><br><i>GFL036</i><br><i>GFL088</i><br><i>GFL272</i><br><i>GFL457</i><br><i>GFL470</i><br><i>GFL115</i> | <i>GFL450</i><br><i>GFL383</i><br><i>GFL428</i>                  |

variation caused the variations of number of edges between RIL groups with the same number of nodes and that the variations of gene networks could be attributed to the node component changes of the networks. Such changes of node composition of the networks may also play a role in UHML.

\*\*\*\*\*Although the numbers of edges varied dramatically among the *GFL* gene networks of different fiber-length groups of RILs (G1 through G5), the largest number of edges was observed for the group with a median UHML (G3). For the two RIL groups with the shortest and longest fibers (G1 and G5), the numbers of edges of their networks were fewer than those of the G3 network by 8,137 and 11,385 edges, respectively (Table 13). This difference may be attributed to both the node constitution of edges, as observed above, and the number of edges connecting each gene in the networks of different fiber-length groups. To determine the variations in number of edges for each gene (node) constituting the *GFL* gene networks across the RIL groups with different UHMLs (G1 through G5), the network of each group was scrutinized (Table 15). The results showed that the number of edges of each *GFL* gene varied across the gene networks of the RIL groups with different UHMLs. For example, gene *GFL325* had the largest numbers of edges in the gene networks of G1, G2, and G3 that had shorter fibers, whereas it had fewer edges in the gene networks of G4 and G5 that had longer fibers. Similarly, variations in number of edges for individual genes were observed across the gene networks of different fiber-length RIL groups. Some of the genes did not have any edges in some fiber-length RIL groups, e.g., *GFL115* did not have any edges in G2 and G5, whereas it had 2, 1, and 1 edges in G1, G3, and G4, respectively.

**Table 15** Edge number variation of each gene constituting the *GFL* gene networks among the five fiber-length RIL groups, and its Pearson's correlation coefficients with that of UHML

|                 | G1              | G2    | G3    | G4    | G5    |          |
|-----------------|-----------------|-------|-------|-------|-------|----------|
| Number of edges | 19443           | 19327 | 27580 | 16835 | 16195 |          |
| UHM (mm)        | 26.16           | 27.76 | 28.80 | 29.85 | 31.72 |          |
|                 | Number of edges |       |       |       |       | <i>r</i> |
| <i>GFL001</i>   | 10              | 13    | 15    | 2     | 11    | -0.206   |
| <i>GFL002</i>   | 22              | 9     | 81    | 14    | 39    | 0.211    |
| <i>GFL003</i>   | 3               | 3     | 1     | 1     | 1     | -0.824   |
| <i>GFL004</i>   | 22              | 7     | 20    | 7     | 11    | -0.494   |
| <i>GFL005</i>   | 59              | 11    | 12    | 53    | 10    | -0.437   |
| <i>GFL006</i>   | 16              | 26    | 50    | 34    | 21    | 0.172    |
| <i>GFL007</i>   | 0               | 0     | 0     | 0     | 0     | NA       |
| <i>GFL008</i>   | 50              | 27    | 66    | 39    | 33    | -0.272   |
| <i>GFL009</i>   | 15              | 25    | 57    | 27    | 43    | 0.565    |
| <i>GFL010</i>   | 36              | 69    | 22    | 37    | 54    | 0.112    |
| <i>GFL011</i>   | 59              | 23    | 44    | 48    | 53    | 0.107    |
| <i>GFL012</i>   | 95              | 36    | 109   | 14    | 16    | -0.641   |
| <i>GFL013</i>   | 74              | 45    | 38    | 42    | 24    | -0.916*  |
| <i>GFL014</i>   | 28              | 21    | 36    | 9     | 43    | 0.284    |
| <i>GFL015</i>   | 68              | 32    | 46    | 29    | 19    | -0.866   |
| <i>GFL016</i>   | 76              | 86    | 52    | 63    | 67    | -0.444   |
| <i>GFL017</i>   | 29              | 72    | 22    | 47    | 34    | -0.089   |
| <i>GFL018</i>   | 29              | 41    | 45    | 19    | 17    | -0.550   |
| <i>GFL019</i>   | 83              | 95    | 115   | 73    | 77    | -0.295   |
| <i>GFL020</i>   | 44              | 79    | 71    | 70    | 46    | -0.064   |
| <i>GFL021</i>   | 2               | 4     | 3     | 2     | 1     | -0.534   |
| <i>GFL022</i>   | 10              | 38    | 48    | 12    | 11    | -0.186   |
| <i>GFL023</i>   | 4               | 10    | 18    | 10    | 2     | -0.136   |
| <i>GFL024</i>   | 28              | 23    | 46    | 7     | 19    | -0.350   |
| <i>GFL025</i>   | 83              | 73    | 125   | 66    | 74    | -0.171   |
| <i>GFL026</i>   | 83              | 118   | 122   | 106   | 68    | -0.312   |
| <i>GFL027</i>   | 114             | 106   | 93    | 105   | 68    | -0.866   |
| <i>GFL028</i>   | 16              | 22    | 27    | 16    | 19    | 0.036    |
| <i>GFL029</i>   | 122             | 135   | 158   | 111   | 95    | -0.519   |
| <i>GFL030</i>   | 87              | 94    | 151   | 77    | 104   | 0.114    |
| <i>GFL031</i>   | 38              | 24    | 17    | 25    | 36    | -0.027   |
| <i>GFL032</i>   | 5               | 9     | 14    | 8     | 5     | -0.062   |
| <i>GFL033</i>   | 13              | 19    | 17    | 1     | 28    | 0.294    |
| <i>GFL034</i>   | 0               | 0     | 0     | 0     | 0     | NA       |
| <i>GFL035</i>   | 4               | 12    | 33    | 16    | 13    | 0.303    |
| <i>GFL036</i>   | 3               | 2     | 3     | 2     | 0     | NA       |
| <i>GFL037</i>   | 123             | 102   | 144   | 97    | 101   | -0.400   |
| <i>GFL038</i>   | 32              | 30    | 48    | 27    | 11    | -0.575   |
| <i>GFL039</i>   | 33              | 103   | 131   | 17    | 38    | -0.201   |
| <i>GFL040</i>   | 19              | 21    | 13    | 26    | 40    | 0.762    |



**Table 15** Continued

|                 | G1              | G2    | G3    | G4    | G5    |          |
|-----------------|-----------------|-------|-------|-------|-------|----------|
| Number of edges | 19443           | 19327 | 27580 | 16835 | 16195 |          |
| UHM (mm)        | 26.16           | 27.76 | 28.80 | 29.85 | 31.72 |          |
|                 | Number of edges |       |       |       |       | <i>r</i> |
| <i>GFL041</i>   | 125             | 137   | 209   | 134   | 97    | -0.256   |
| <i>GFL042</i>   | 0               | 0     | 0     | 0     | 0     | NA       |
| <i>GFL043</i>   | 29              | 33    | 85    | 25    | 18    | -0.190   |
| <i>GFL044</i>   | 25              | 30    | 7     | 27    | 17    | -0.326   |
| <i>GFL045</i>   | 14              | 15    | 36    | 21    | 12    | -0.014   |
| <i>GFL046</i>   | 64              | 75    | 141   | 105   | 109   | 0.598    |
| <i>GFL047</i>   | 26              | 59    | 103   | 38    | 32    | -0.044   |
| <i>GFL048</i>   | 59              | 70    | 86    | 92    | 55    | 0.055    |
| <i>GFL049</i>   | 142             | 126   | 237   | 149   | 119   | -0.117   |
| <i>GFL050</i>   | 79              | 83    | 67    | 73    | 90    | 0.293    |
| <i>GFL051</i>   | 126             | 122   | 162   | 65    | 96    | -0.472   |
| <i>GFL052</i>   | 9               | 11    | 27    | 10    | 15    | 0.241    |
| <i>GFL053</i>   | 90              | 79    | 111   | 63    | 42    | -0.695   |
| <i>GFL054</i>   | 23              | 22    | 23    | 30    | 13    | -0.406   |
| <i>GFL055</i>   | 25              | 15    | 22    | 17    | 6     | -0.832   |
| <i>GFL056</i>   | 25              | 11    | 38    | 9     | 18    | -0.214   |
| <i>GFL057</i>   | 43              | 45    | 68    | 52    | 25    | -0.354   |
| <i>GFL058</i>   | 36              | 51    | 37    | 27    | 16    | -0.758   |
| <i>GFL059</i>   | 27              | 11    | 15    | 11    | 39    | 0.359    |
| <i>GFL060</i>   | 86              | 81    | 122   | 77    | 79    | -0.161   |
| <i>GFL061</i>   | 140             | 160   | 140   | 68    | 79    | -0.775   |
| <i>GFL062</i>   | 78              | 58    | 39    | 60    | 53    | -0.553   |
| <i>GFL063</i>   | 3               | 2     | 1     | 5     | 1     | -0.181   |
| <i>GFL064</i>   | 15              | 6     | 16    | 5     | 12    | -0.203   |
| <i>GFL065</i>   | 28              | 22    | 35    | 19    | 21    | -0.415   |
| <i>GFL066</i>   | 35              | 27    | 46    | 14    | 24    | -0.436   |
| <i>GFL067</i>   | 20              | 26    | 65    | 44    | 22    | 0.127    |
| <i>GFL068</i>   | 44              | 39    | 58    | 34    | 34    | -0.404   |
| <i>GFL069</i>   | 129             | 119   | 100   | 24    | 40    | -0.866   |
| <i>GFL070</i>   | 16              | 19    | 22    | 16    | 20    | 0.357    |
| <i>GFL071</i>   | 106             | 79    | 82    | 31    | 37    | -0.896*  |
| <i>GFL072</i>   | 15              | 6     | 41    | 9     | 7     | -0.166   |
| <i>GFL073</i>   | 40              | 45    | 91    | 49    | 66    | 0.430    |
| <i>GFL074</i>   | 16              | 6     | 9     | 3     | 14    | -0.158   |
| <i>GFL075</i>   | 29              | 111   | 48    | 71    | 30    | -0.162   |
| <i>GFL076</i>   | 62              | 72    | 106   | 62    | 41    | -0.368   |
| <i>GFL077</i>   | 3               | 5     | 2     | 3     | 2     | -0.486   |
| <i>GFL078</i>   | 111             | 125   | 186   | 101   | 76    | -0.375   |
| <i>GFL079</i>   | 124             | 150   | 172   | 141   | 118   | -0.175   |
| <i>GFL080</i>   | 104             | 98    | 147   | 71    | 52    | -0.584   |

**Table 15** Continued

|                 | G1              | G2    | G3    | G4    | G5    |          |
|-----------------|-----------------|-------|-------|-------|-------|----------|
| Number of edges | 19443           | 19327 | 27580 | 16835 | 16195 |          |
| UHM (mm)        | 26.16           | 27.76 | 28.80 | 29.85 | 31.72 |          |
|                 | Number of edges |       |       |       |       | <i>r</i> |
| <i>GFL081</i>   | 23              | 20    | 16    | 22    | 28    | 0.462    |
| <i>GFL082</i>   | 60              | 53    | 77    | 46    | 38    | -0.561   |
| <i>GFL083</i>   | 67              | 59    | 108   | 14    | 36    | -0.453   |
| <i>GFL084</i>   | 3               | 3     | 2     | 4     | 2     | -0.259   |
| <i>GFL085</i>   | 140             | 118   | 171   | 112   | 119   | -0.321   |
| <i>GFL086</i>   | 27              | 27    | 45    | 63    | 23    | 0.162    |
| <i>GFL087</i>   | 68              | 66    | 165   | 78    | 104   | 0.316    |
| <i>GFL088</i>   | 0               | 3     | 8     | 2     | 0     | NA       |
| <i>GFL089</i>   | 62              | 91    | 47    | 68    | 38    | -0.546   |
| <i>GFL090</i>   | 11              | 15    | 5     | 6     | 13    | -0.089   |
| <i>GFL091</i>   | 40              | 11    | 36    | 32    | 34    | 0.073    |
| <i>GFL092</i>   | 46              | 70    | 85    | 77    | 33    | -0.191   |
| <i>GFL093</i>   | 0               | 3     | 0     | 0     | 0     | NA       |
| <i>GFL094</i>   | 33              | 31    | 86    | 62    | 51    | 0.416    |
| <i>GFL095</i>   | 11              | 52    | 22    | 24    | 22    | -0.010   |
| <i>GFL096</i>   | 39              | 30    | 40    | 51    | 25    | -0.219   |
| <i>GFL097</i>   | 44              | 37    | 50    | 27    | 45    | -0.087   |
| <i>GFL098</i>   | 51              | 34    | 45    | 31    | 9     | -0.891*  |
| <i>GFL099</i>   | 143             | 136   | 222   | 132   | 142   | -0.033   |
| <i>GFL100</i>   | 36              | 62    | 72    | 34    | 22    | -0.413   |
| <i>GFL101</i>   | 4               | 5     | 3     | 2     | 6     | 0.204    |
| <i>GFL102</i>   | 20              | 32    | 8     | 12    | 9     | -0.617   |
| <i>GFL103</i>   | 132             | 134   | 203   | 111   | 145   | 0.036    |
| <i>GFL104</i>   | 16              | 18    | 18    | 14    | 17    | -0.100   |
| <i>GFL105</i>   | 19              | 18    | 28    | 9     | 14    | -0.400   |
| <i>GFL106</i>   | 54              | 63    | 52    | 36    | 46    | -0.599   |
| <i>GFL107</i>   | 60              | 21    | 69    | 23    | 39    | -0.300   |
| <i>GFL108</i>   | 18              | 25    | 38    | 20    | 35    | 0.558    |
| <i>GFL109</i>   | 27              | 82    | 63    | 36    | 54    | 0.130    |
| <i>GFL110</i>   | 10              | 16    | 12    | 9     | 7     | -0.566   |
| <i>GFL111</i>   | 22              | 64    | 23    | 11    | 52    | 0.153    |
| <i>GFL112</i>   | 17              | 9     | 30    | 4     | 10    | -0.293   |
| <i>GFL113</i>   | 3               | 7     | 14    | 6     | 11    | 0.574    |
| <i>GFL114</i>   | 101             | 57    | 134   | 72    | 25    | -0.570   |
| <i>GFL115</i>   | 2               | 0     | 1     | 1     | 0     | NA       |
| <i>GFL116</i>   | 30              | 50    | 39    | 12    | 29    | -0.365   |
| <i>GFL117</i>   | 97              | 73    | 153   | 70    | 73    | -0.244   |
| <i>GFL118</i>   | 8               | 10    | 4     | 4     | 6     | -0.531   |
| <i>GFL119</i>   | 31              | 13    | 58    | 52    | 12    | -0.086   |
| <i>GFL120</i>   | 14              | 16    | 14    | 13    | 10    | -0.795   |

**Table 15** Continued

|                 | G1              | G2    | G3    | G4    | G5    |          |
|-----------------|-----------------|-------|-------|-------|-------|----------|
| Number of edges | 19443           | 19327 | 27580 | 16835 | 16195 |          |
| UHM (mm)        | 26.16           | 27.76 | 28.80 | 29.85 | 31.72 |          |
|                 | Number of edges |       |       |       |       | <i>r</i> |
| <i>GFL121</i>   | 57              | 54    | 98    | 65    | 37    | -0.256   |
| <i>GFL122</i>   | 18              | 32    | 26    | 14    | 16    | -0.401   |
| <i>GFL123</i>   | 68              | 64    | 80    | 52    | 24    | -0.772   |
| <i>GFL124</i>   | 22              | 19    | 24    | 19    | 19    | -0.433   |
| <i>GFL125</i>   | 23              | 33    | 23    | 22    | 8     | -0.732   |
| <i>GFL126</i>   | 21              | 34    | 29    | 23    | 18    | -0.394   |
| <i>GFL127</i>   | 85              | 74    | 143   | 96    | 47    | -0.301   |
| <i>GFL128</i>   | 3               | 8     | 6     | 3     | 5     | 0.004    |
| <i>GFL129</i>   | 76              | 74    | 99    | 67    | 87    | 0.223    |
| <i>GFL130</i>   | 100             | 94    | 125   | 68    | 51    | -0.689   |
| <i>GFL131</i>   | 9               | 1     | 1     | 4     | 2     | -0.558   |
| <i>GFL132</i>   | 6               | 4     | 2     | 2     | 1     | -0.943*  |
| <i>GFL133</i>   | 20              | 29    | 41    | 21    | 26    | 0.100    |
| <i>GFL134</i>   | 12              | 5     | 18    | 11    | 3     | -0.387   |
| <i>GFL135</i>   | 93              | 81    | 121   | 79    | 81    | -0.246   |
| <i>GFL136</i>   | 115             | 32    | 165   | 64    | 36    | -0.394   |
| <i>GFL137</i>   | 64              | 20    | 41    | 12    | 19    | -0.730   |
| <i>GFL138</i>   | 36              | 35    | 32    | 37    | 15    | -0.753   |
| <i>GFL139</i>   | 35              | 54    | 57    | 62    | 33    | -0.011   |
| <i>GFL140</i>   | 19              | 62    | 11    | 81    | 51    | 0.429    |
| <i>GFL141</i>   | 57              | 33    | 124   | 52    | 101   | 0.454    |
| <i>GFL142</i>   | 23              | 37    | 74    | 18    | 30    | -0.017   |
| <i>GFL143</i>   | 96              | 54    | 168   | 122   | 35    | -0.239   |
| <i>GFL144</i>   | 132             | 22    | 100   | 45    | 50    | -0.525   |
| <i>GFL145</i>   | 141             | 171   | 214   | 115   | 140   | -0.205   |
| <i>GFL146</i>   | 45              | 24    | 26    | 34    | 7     | -0.813   |
| <i>GFL147</i>   | 53              | 51    | 75    | 37    | 37    | -0.463   |
| <i>GFL148</i>   | 30              | 33    | 55    | 21    | 28    | -0.178   |
| <i>GFL149</i>   | 26              | 14    | 25    | 5     | 3     | -0.809   |
| <i>GFL150</i>   | 25              | 51    | 54    | 56    | 45    | 0.547    |
| <i>GFL151</i>   | 20              | 24    | 32    | 12    | 22    | -0.119   |
| <i>GFL152</i>   | 16              | 12    | 21    | 10    | 15    | -0.132   |
| <i>GFL153</i>   | 155             | 134   | 197   | 121   | 106   | -0.516   |
| <i>GFL154</i>   | 40              | 14    | 34    | 17    | 10    | -0.719   |
| <i>GFL155</i>   | 25              | 20    | 29    | 19    | 17    | -0.572   |
| <i>GFL156</i>   | 63              | 66    | 40    | 43    | 58    | -0.363   |
| <i>GFL157</i>   | 13              | 17    | 15    | 15    | 12    | -0.329   |
| <i>GFL158</i>   | 145             | 175   | 203   | 148   | 96    | -0.520   |
| <i>GFL159</i>   | 56              | 93    | 111   | 80    | 90    | 0.457    |
| <i>GFL160</i>   | 37              | 31    | 71    | 9     | 33    | -0.183   |

**Table 15** Continued

|                 | G1              | G2    | G3    | G4    | G5    |          |
|-----------------|-----------------|-------|-------|-------|-------|----------|
| Number of edges | 19443           | 19327 | 27580 | 16835 | 16195 |          |
| UHM (mm)        | 26.16           | 27.76 | 28.80 | 29.85 | 31.72 |          |
|                 | Number of edges |       |       |       |       | <i>r</i> |
| <i>GFL161</i>   | 58              | 52    | 105   | 38    | 63    | -0.007   |
| <i>GFL162</i>   | 69              | 51    | 89    | 30    | 24    | -0.654   |
| <i>GFL163</i>   | 168             | 152   | 168   | 123   | 75    | -0.887*  |
| <i>GFL164</i>   | 35              | 16    | 33    | 2     | 21    | -0.457   |
| <i>GFL165</i>   | 85              | 85    | 123   | 85    | 82    | -0.073   |
| <i>GFL166</i>   | 162             | 100   | 219   | 151   | 141   | -0.017   |
| <i>GFL167</i>   | 37              | 41    | 58    | 18    | 14    | -0.598   |
| <i>GFL168</i>   | 67              | 68    | 137   | 45    | 80    | 0.036    |
| <i>GFL169</i>   | 20              | 29    | 53    | 28    | 29    | 0.210    |
| <i>GFL170</i>   | 95              | 92    | 137   | 90    | 73    | -0.336   |
| <i>GFL171</i>   | 64              | 95    | 117   | 80    | 66    | -0.083   |
| <i>GFL172</i>   | 67              | 12    | 33    | 38    | 34    | -0.368   |
| <i>GFL173</i>   | 89              | 104   | 152   | 93    | 90    | -0.059   |
| <i>GFL174</i>   | 9               | 32    | 51    | 27    | 21    | 0.189    |
| <i>GFL175</i>   | 3               | 4     | 13    | 3     | 2     | -0.119   |
| <i>GFL176</i>   | 67              | 67    | 33    | 25    | 19    | -0.909*  |
| <i>GFL177</i>   | 82              | 25    | 37    | 19    | 30    | -0.691   |
| <i>GFL178</i>   | 14              | 20    | 9     | 1     | 14    | -0.321   |
| <i>GFL179</i>   | 10              | 18    | 27    | 17    | 25    | 0.702    |
| <i>GFL180</i>   | 3               | 1     | 3     | 2     | 2     | -0.235   |
| <i>GFL181</i>   | 0               | 0     | 0     | 0     | 0     | NA       |
| <i>GFL182</i>   | 41              | 47    | 71    | 31    | 52    | 0.107    |
| <i>GFL183</i>   | 76              | 53    | 34    | 68    | 73    | 0.076    |
| <i>GFL184</i>   | 7               | 30    | 17    | 9     | 12    | -0.123   |
| <i>GFL185</i>   | 8               | 1     | 11    | 6     | 4     | -0.185   |
| <i>GFL186</i>   | 14              | 11    | 27    | 23    | 4     | -0.221   |
| <i>GFL187</i>   | 130             | 142   | 173   | 177   | 94    | -0.253   |
| <i>GFL188</i>   | 104             | 35    | 82    | 109   | 117   | 0.429    |
| <i>GFL189</i>   | 16              | 13    | 27    | 17    | 11    | -0.205   |
| <i>GFL190</i>   | 95              | 24    | 133   | 62    | 66    | -0.117   |
| <i>GFL191</i>   | 9               | 16    | 14    | 23    | 13    | 0.400    |
| <i>GFL192</i>   | 53              | 42    | 44    | 37    | 25    | -0.965** |
| <i>GFL193</i>   | 5               | 13    | 10    | 12    | 4     | -0.146   |
| <i>GFL194</i>   | 13              | 27    | 45    | 20    | 22    | 0.153    |
| <i>GFL195</i>   | 41              | 60    | 97    | 40    | 64    | 0.210    |
| <i>GFL196</i>   | 51              | 60    | 73    | 37    | 50    | -0.248   |
| <i>GFL197</i>   | 68              | 95    | 89    | 33    | 26    | -0.699   |
| <i>GFL198</i>   | 27              | 24    | 24    | 5     | 12    | -0.770   |
| <i>GFL199</i>   | 93              | 136   | 190   | 125   | 134   | 0.328    |
| <i>GFL200</i>   | 7               | 9     | 17    | 7     | 5     | -0.215   |

**Table 15** Continued

|                 | G1              | G2    | G3    | G4    | G5    |          |
|-----------------|-----------------|-------|-------|-------|-------|----------|
| Number of edges | 19443           | 19327 | 27580 | 16835 | 16195 |          |
| UHM (mm)        | 26.16           | 27.76 | 28.80 | 29.85 | 31.72 |          |
|                 | Number of edges |       |       |       |       | <i>r</i> |
| <i>GFL201</i>   | 20              | 54    | 76    | 56    | 20    | -0.024   |
| <i>GFL202</i>   | 6               | 3     | 11    | 3     | 12    | 0.477    |
| <i>GFL203</i>   | 36              | 62    | 81    | 39    | 37    | -0.151   |
| <i>GFL204</i>   | 13              | 38    | 56    | 22    | 29    | 0.180    |
| <i>GFL205</i>   | 39              | 62    | 102   | 89    | 69    | 0.519    |
| <i>GFL206</i>   | 5               | 2     | 6     | 2     | 5     | 0.018    |
| <i>GFL207</i>   | 6               | 18    | 7     | 13    | 14    | 0.393    |
| <i>GFL208</i>   | 75              | 51    | 22    | 26    | 19    | -0.891*  |
| <i>GFL209</i>   | 11              | 13    | 16    | 12    | 12    | 0.085    |
| <i>GFL210</i>   | 78              | 84    | 135   | 68    | 80    | -0.063   |
| <i>GFL211</i>   | 15              | 8     | 9     | 14    | 11    | -0.173   |
| <i>GFL212</i>   | 80              | 45    | 141   | 40    | 56    | -0.211   |
| <i>GFL213</i>   | 13              | 4     | 7     | 10    | 5     | -0.504   |
| <i>GFL214</i>   | 11              | 13    | 30    | 4     | 11    | -0.125   |
| <i>GFL215</i>   | 63              | 81    | 151   | 47    | 81    | 0.033    |
| <i>GFL216</i>   | 36              | 51    | 70    | 29    | 41    | -0.082   |
| <i>GFL217</i>   | 23              | 29    | 53    | 38    | 25    | 0.119    |
| <i>GFL218</i>   | 39              | 16    | 55    | 1     | 16    | -0.439   |
| <i>GFL219</i>   | 48              | 38    | 109   | 65    | 58    | 0.230    |
| <i>GFL220</i>   | 81              | 62    | 135   | 49    | 71    | -0.152   |
| <i>GFL221</i>   | 27              | 60    | 47    | 43    | 56    | 0.568    |
| <i>GFL222</i>   | 81              | 75    | 114   | 56    | 77    | -0.178   |
| <i>GFL223</i>   | 14              | 19    | 21    | 23    | 13    | 0.003    |
| <i>GFL224</i>   | 68              | 118   | 165   | 43    | 60    | -0.257   |
| <i>GFL225</i>   | 42              | 40    | 87    | 31    | 49    | 0.049    |
| <i>GFL226</i>   | 16              | 33    | 61    | 69    | 87    | 0.979**  |
| <i>GFL227</i>   | 13              | 12    | 23    | 4     | 3     | -0.544   |
| <i>GFL228</i>   | 34              | 62    | 21    | 84    | 27    | -0.003   |
| <i>GFL229</i>   | 88              | 88    | 81    | 58    | 37    | -0.932*  |
| <i>GFL230</i>   | 112             | 31    | 131   | 73    | 56    | -0.324   |
| <i>GFL231</i>   | 16              | 13    | 38    | 18    | 7     | -0.221   |
| <i>GFL232</i>   | 49              | 82    | 130   | 38    | 50    | -0.155   |
| <i>GFL233</i>   | 107             | 140   | 122   | 138   | 135   | 0.632    |
| <i>GFL234</i>   | 1               | 4     | 0     | 2     | 2     | NA       |
| <i>GFL235</i>   | 11              | 9     | 15    | 16    | 16    | 0.787    |
| <i>GFL236</i>   | 6               | 3     | 2     | 3     | 2     | -0.789   |
| <i>GFL237</i>   | 70              | 71    | 72    | 54    | 56    | -0.770   |
| <i>GFL238</i>   | 61              | 55    | 113   | 16    | 31    | -0.406   |
| <i>GFL239</i>   | 88              | 95    | 111   | 104   | 45    | -0.535   |
| <i>GFL240</i>   | 14              | 19    | 18    | 9     | 12    | -0.468   |

**Table 15** Continued

|                 | G1              | G2    | G3    | G4    | G5    |          |
|-----------------|-----------------|-------|-------|-------|-------|----------|
| Number of edges | 19443           | 19327 | 27580 | 16835 | 16195 |          |
| UHM (mm)        | 26.16           | 27.76 | 28.80 | 29.85 | 31.72 |          |
|                 | Number of edges |       |       |       |       | <i>r</i> |
| <i>GFL241</i>   | 32              | 24    | 34    | 12    | 12    | -0.771   |
| <i>GFL242</i>   | 167             | 97    | 165   | 125   | 55    | -0.716   |
| <i>GFL243</i>   | 8               | 11    | 23    | 8     | 5     | -0.215   |
| <i>GFL244</i>   | 16              | 20    | 32    | 22    | 84    | 0.827    |
| <i>GFL245</i>   | 5               | 11    | 19    | 8     | 9     | 0.159    |
| <i>GFL246</i>   | 107             | 101   | 51    | 79    | 36    | -0.853   |
| <i>GFL247</i>   | 137             | 114   | 172   | 89    | 108   | -0.400   |
| <i>GFL248</i>   | 9               | 10    | 21    | 12    | 12    | 0.244    |
| <i>GFL249</i>   | 23              | 33    | 69    | 60    | 24    | 0.144    |
| <i>GFL250</i>   | 7               | 5     | 3     | 2     | 1     | -0.973** |
| <i>GFL251</i>   | 15              | 34    | 18    | 25    | 20    | 0.051    |
| <i>GFL252</i>   | 76              | 73    | 114   | 129   | 87    | 0.410    |
| <i>GFL253</i>   | 36              | 31    | 71    | 27    | 26    | -0.216   |
| <i>GFL254</i>   | 7               | 7     | 23    | 1     | 7     | -0.098   |
| <i>GFL255</i>   | 59              | 46    | 45    | 25    | 12    | -0.975** |
| <i>GFL256</i>   | 27              | 20    | 18    | 53    | 25    | 0.237    |
| <i>GFL257</i>   | 4               | 15    | 20    | 17    | 8     | 0.204    |
| <i>GFL258</i>   | 111             | 73    | 147   | 61    | 76    | -0.372   |
| <i>GFL259</i>   | 28              | 46    | 8     | 19    | 12    | -0.577   |
| <i>GFL260</i>   | 9               | 24    | 9     | 5     | 17    | 0.039    |
| <i>GFL261</i>   | 46              | 55    | 77    | 50    | 61    | 0.347    |
| <i>GFL262</i>   | 30              | 7     | 41    | 18    | 37    | 0.279    |
| <i>GFL263</i>   | 32              | 20    | 15    | 17    | 11    | -0.908*  |
| <i>GFL264</i>   | 16              | 5     | 1     | 4     | 6     | -0.577   |
| <i>GFL265</i>   | 70              | 58    | 117   | 16    | 62    | -0.217   |
| <i>GFL266</i>   | 15              | 4     | 10    | 12    | 16    | 0.305    |
| <i>GFL267</i>   | 74              | 73    | 170   | 53    | 43    | -0.267   |
| <i>GFL268</i>   | 146             | 151   | 223   | 143   | 116   | -0.294   |
| <i>GFL269</i>   | 128             | 108   | 193   | 73    | 116   | -0.191   |
| <i>GFL270</i>   | 36              | 25    | 27    | 11    | 17    | -0.824   |
| <i>GFL271</i>   | 38              | 49    | 48    | 40    | 18    | -0.648   |
| <i>GFL272</i>   | 3               | 4     | 3     | 2     | 0     | NA       |
| <i>GFL273</i>   | 15              | 30    | 90    | 20    | 33    | 0.141    |
| <i>GFL274</i>   | 86              | 130   | 99    | 84    | 56    | -0.607   |
| <i>GFL275</i>   | 5               | 11    | 5     | 6     | 6     | -0.130   |
| <i>GFL276</i>   | 3               | 1     | 3     | 4     | 7     | 0.795    |
| <i>GFL277</i>   | 72              | 81    | 86    | 91    | 72    | 0.114    |
| <i>GFL278</i>   | 134             | 127   | 176   | 113   | 96    | -0.494   |
| <i>GFL279</i>   | 15              | 11    | 12    | 12    | 6     | -0.880*  |
| <i>GFL280</i>   | 1               | 5     | 7     | 2     | 5     | 0.375    |

**Table 15** Continued

|                 | G1              | G2    | G3    | G4    | G5    |          |
|-----------------|-----------------|-------|-------|-------|-------|----------|
| Number of edges | 19443           | 19327 | 27580 | 16835 | 16195 |          |
| UHM (mm)        | 26.16           | 27.76 | 28.80 | 29.85 | 31.72 |          |
|                 | Number of edges |       |       |       |       | <i>r</i> |
| <i>GFL281</i>   | 5               | 6     | 9     | 3     | 2     | -0.516   |
| <i>GFL282</i>   | 93              | 94    | 167   | 75    | 63    | -0.320   |
| <i>GFL283</i>   | 22              | 44    | 30    | 39    | 39    | 0.555    |
| <i>GFL284</i>   | 38              | 31    | 65    | 52    | 44    | 0.337    |
| <i>GFL285</i>   | 113             | 104   | 170   | 107   | 39    | -0.541   |
| <i>GFL286</i>   | 11              | 2     | 12    | 3     | 0     | NA       |
| <i>GFL287</i>   | 73              | 103   | 122   | 56    | 94    | 0.036    |
| <i>GFL288</i>   | 8               | 7     | 26    | 20    | 25    | 0.788    |
| <i>GFL289</i>   | 45              | 58    | 120   | 56    | 62    | 0.165    |
| <i>GFL290</i>   | 33              | 26    | 11    | 17    | 27    | -0.328   |
| <i>GFL291</i>   | 48              | 12    | 58    | 26    | 25    | -0.309   |
| <i>GFL292</i>   | 58              | 39    | 74    | 35    | 50    | -0.195   |
| <i>GFL293</i>   | 32              | 56    | 123   | 66    | 67    | 0.364    |
| <i>GFL294</i>   | 141             | 111   | 150   | 99    | 139   | -0.080   |
| <i>GFL295</i>   | 38              | 31    | 32    | 26    | 19    | -0.973** |
| <i>GFL296</i>   | 66              | 63    | 43    | 74    | 42    | -0.466   |
| <i>GFL297</i>   | 74              | 76    | 67    | 62    | 59    | -0.914*  |
| <i>GFL298</i>   | 112             | 123   | 209   | 89    | 130   | 0.030    |
| <i>GFL299</i>   | 34              | 27    | 22    | 20    | 16    | -0.977** |
| <i>GFL300</i>   | 33              | 27    | 39    | 19    | 19    | -0.647   |
| <i>GFL301</i>   | 17              | 48    | 28    | 18    | 19    | -0.254   |
| <i>GFL302</i>   | 23              | 28    | 44    | 13    | 26    | -0.084   |
| <i>GFL303</i>   | 23              | 13    | 17    | 4     | 13    | -0.619   |
| <i>GFL304</i>   | 84              | 15    | 72    | 24    | 53    | -0.286   |
| <i>GFL305</i>   | 23              | 36    | 73    | 42    | 38    | 0.287    |
| <i>GFL306</i>   | 1               | 1     | 2     | 2     | 1     | 0.202    |
| <i>GFL307</i>   | 22              | 14    | 17    | 18    | 17    | -0.380   |
| <i>GFL308</i>   | 56              | 76    | 59    | 51    | 24    | -0.750   |
| <i>GFL309</i>   | 32              | 23    | 39    | 19    | 23    | -0.426   |
| <i>GFL310</i>   | 3               | 4     | 1     | 2     | 3     | -0.206   |
| <i>GFL311</i>   | 31              | 45    | 87    | 39    | 26    | -0.122   |
| <i>GFL312</i>   | 61              | 33    | 75    | 30    | 37    | -0.417   |
| <i>GFL313</i>   | 19              | 13    | 30    | 12    | 10    | -0.392   |
| <i>GFL314</i>   | 74              | 54    | 62    | 53    | 29    | -0.916*  |
| <i>GFL315</i>   | 26              | 18    | 83    | 41    | 51    | 0.431    |
| <i>GFL316</i>   | 40              | 75    | 78    | 29    | 28    | -0.414   |
| <i>GFL317</i>   | 9               | 8     | 8     | 9     | 3     | -0.760   |
| <i>GFL318</i>   | 60              | 63    | 59    | 37    | 31    | -0.874   |
| <i>GFL319</i>   | 60              | 85    | 64    | 103   | 74    | 0.376    |
| <i>GFL320</i>   | 6               | 2     | 15    | 3     | 5     | -0.045   |

**Table 15** Continued

|                 | G1              | G2    | G3    | G4    | G5    |          |
|-----------------|-----------------|-------|-------|-------|-------|----------|
| Number of edges | 19443           | 19327 | 27580 | 16835 | 16195 |          |
| UHM (mm)        | 26.16           | 27.76 | 28.80 | 29.85 | 31.72 |          |
|                 | Number of edges |       |       |       |       | <i>r</i> |
| <i>GFL321</i>   | 6               | 7     | 12    | 6     | 4     | -0.284   |
| <i>GFL322</i>   | 72              | 75    | 65    | 25    | 37    | -0.793   |
| <i>GFL323</i>   | 59              | 45    | 169   | 34    | 48    | -0.101   |
| <i>GFL324</i>   | 55              | 60    | 61    | 70    | 52    | 0.006    |
| <i>GFL325</i>   | 179             | 183   | 241   | 152   | 135   | -0.473   |
| <i>GFL326</i>   | 13              | 26    | 32    | 12    | 19    | 0.012    |
| <i>GFL327</i>   | 44              | 40    | 50    | 33    | 32    | -0.648   |
| <i>GFL328</i>   | 17              | 31    | 36    | 22    | 30    | 0.403    |
| <i>GFL329</i>   | 114             | 131   | 195   | 127   | 95    | -0.204   |
| <i>GFL330</i>   | 23              | 28    | 28    | 20    | 17    | -0.633   |
| <i>GFL331</i>   | 12              | 9     | 19    | 12    | 13    | 0.187    |
| <i>GFL332</i>   | 138             | 106   | 190   | 95    | 121   | -0.188   |
| <i>GFL333</i>   | 21              | 5     | 30    | 6     | 3     | -0.493   |
| <i>GFL334</i>   | 64              | 26    | 85    | 52    | 34    | -0.288   |
| <i>GFL335</i>   | 85              | 104   | 90    | 129   | 66    | -0.163   |
| <i>GFL336</i>   | 51              | 59    | 56    | 73    | 59    | 0.517    |
| <i>GFL337</i>   | 20              | 35    | 29    | 14    | 37    | 0.313    |
| <i>GFL338</i>   | 91              | 77    | 147   | 90    | 75    | -0.140   |
| <i>GFL339</i>   | 167             | 172   | 226   | 168   | 151   | -0.223   |
| <i>GFL340</i>   | 35              | 34    | 5     | 22    | 27    | -0.322   |
| <i>GFL341</i>   | 32              | 17    | 46    | 17    | 24    | -0.215   |
| <i>GFL342</i>   | 2               | 10    | 23    | 8     | 3     | -0.017   |
| <i>GFL343</i>   | 38              | 21    | 55    | 19    | 21    | -0.380   |
| <i>GFL344</i>   | 18              | 36    | 21    | 15    | 27    | 0.042    |
| <i>GFL345</i>   | 11              | 33    | 52    | 13    | 26    | 0.132    |
| <i>GFL346</i>   | 3               | 7     | 30    | 22    | 8     | 0.282    |
| <i>GFL347</i>   | 30              | 29    | 50    | 41    | 51    | 0.803    |
| <i>GFL348</i>   | 43              | 22    | 21    | 72    | 12    | -0.178   |
| <i>GFL349</i>   | 8               | 4     | 8     | 6     | 7     | -0.032   |
| <i>GFL350</i>   | 91              | 96    | 123   | 79    | 68    | -0.487   |
| <i>GFL351</i>   | 1               | 0     | 2     | 1     | 2     | NA       |
| <i>GFL352</i>   | 43              | 21    | 37    | 32    | 17    | -0.667   |
| <i>GFL353</i>   | 31              | 33    | 9     | 13    | 16    | -0.673   |
| <i>GFL354</i>   | 45              | 60    | 64    | 67    | 77    | 0.977**  |
| <i>GFL355</i>   | 50              | 53    | 87    | 61    | 46    | -0.043   |
| <i>GFL356</i>   | 19              | 41    | 82    | 12    | 28    | -0.038   |
| <i>GFL357</i>   | 90              | 23    | 76    | 28    | 33    | -0.581   |
| <i>GFL358</i>   | 27              | 17    | 111   | 24    | 21    | -0.041   |
| <i>GFL359</i>   | 5               | 2     | 2     | 2     | 5     | 0.036    |
| <i>GFL360</i>   | 17              | 3     | 43    | 6     | 6     | -0.205   |



**Table 15** Continued

|                 | G1              | G2    | G3    | G4    | G5    |          |
|-----------------|-----------------|-------|-------|-------|-------|----------|
| Number of edges | 19443           | 19327 | 27580 | 16835 | 16195 |          |
| UHM (mm)        | 26.16           | 27.76 | 28.80 | 29.85 | 31.72 |          |
|                 | Number of edges |       |       |       |       | <i>r</i> |
| <i>GFL361</i>   | 31              | 12    | 38    | 15    | 7     | -0.576   |
| <i>GFL362</i>   | 9               | 10    | 41    | 11    | 10    | 0.017    |
| <i>GFL363</i>   | 10              | 13    | 56    | 17    | 38    | 0.492    |
| <i>GFL364</i>   | 5               | 34    | 13    | 7     | 9     | -0.190   |
| <i>GFL365</i>   | 10              | 1     | 7     | 2     | 3     | -0.563   |
| <i>GFL366</i>   | 113             | 128   | 212   | 151   | 147   | 0.356    |
| <i>GFL367</i>   | 55              | 77    | 82    | 56    | 65    | 0.039    |
| <i>GFL368</i>   | 29              | 20    | 8     | 11    | 11    | -0.802   |
| <i>GFL369</i>   | 17              | 20    | 48    | 17    | 11    | -0.181   |
| <i>GFL370</i>   | 34              | 28    | 38    | 28    | 29    | -0.371   |
| <i>GFL371</i>   | 48              | 71    | 97    | 55    | 96    | 0.611    |
| <i>GFL372</i>   | 23              | 27    | 50    | 22    | 8     | -0.390   |
| <i>GFL373</i>   | 30              | 24    | 87    | 8     | 17    | -0.212   |
| <i>GFL374</i>   | 10              | 19    | 15    | 17    | 19    | 0.716    |
| <i>GFL375</i>   | 68              | 107   | 110   | 77    | 90    | 0.174    |
| <i>GFL376</i>   | 19              | 18    | 29    | 8     | 19    | -0.165   |
| <i>GFL377</i>   | 15              | 28    | 19    | 26    | 22    | 0.372    |
| <i>GFL378</i>   | 21              | 37    | 9     | 12    | 9     | -0.601   |
| <i>GFL379</i>   | 15              | 42    | 29    | 45    | 23    | 0.208    |
| <i>GFL380</i>   | 68              | 79    | 48    | 31    | 31    | -0.842   |
| <i>GFL381</i>   | 13              | 17    | 26    | 19    | 13    | 0.018    |
| <i>GFL382</i>   | 29              | 31    | 33    | 40    | 35    | 0.722    |
| <i>GFL383</i>   | 4               | 2     | 1     | 0     | 1     | NA       |
| <i>GFL384</i>   | 9               | 4     | 61    | 23    | 11    | 0.114    |
| <i>GFL385</i>   | 13              | 22    | 31    | 18    | 17    | 0.096    |
| <i>GFL386</i>   | 1               | 3     | 3     | 2     | 2     | 0.220    |
| <i>GFL387</i>   | 12              | 10    | 14    | 9     | 6     | -0.709   |
| <i>GFL388</i>   | 71              | 85    | 91    | 60    | 67    | -0.359   |
| <i>GFL389</i>   | 27              | 22    | 60    | 18    | 17    | -0.225   |
| <i>GFL390</i>   | 1               | 5     | 10    | 6     | 5     | 0.426    |
| <i>GFL391</i>   | 13              | 24    | 18    | 10    | 26    | 0.380    |
| <i>GFL392</i>   | 66              | 103   | 124   | 52    | 61    | -0.278   |
| <i>GFL393</i>   | 22              | 21    | 34    | 47    | 12    | -0.031   |
| <i>GFL394</i>   | 14              | 18    | 8     | 12    | 8     | -0.651   |
| <i>GFL395</i>   | 5               | 10    | 11    | 1     | 2     | -0.480   |
| <i>GFL396</i>   | 35              | 48    | 53    | 17    | 21    | -0.547   |
| <i>GFL397</i>   | 17              | 10    | 17    | 15    | 12    | -0.329   |
| <i>GFL398</i>   | 50              | 25    | 66    | 28    | 7     | -0.612   |
| <i>GFL399</i>   | 14              | 33    | 53    | 55    | 18    | 0.180    |
| <i>GFL400</i>   | 16              | 10    | 15    | 4     | 6     | -0.758   |

**Table 15** Continued

|                 | G1              | G2    | G3    | G4    | G5    |          |
|-----------------|-----------------|-------|-------|-------|-------|----------|
| Number of edges | 19443           | 19327 | 27580 | 16835 | 16195 |          |
| UHM (mm)        | 26.16           | 27.76 | 28.80 | 29.85 | 31.72 |          |
|                 | Number of edges |       |       |       |       | <i>r</i> |
| <i>GFL401</i>   | 73              | 62    | 120   | 53    | 37    | -0.430   |
| <i>GFL402</i>   | 21              | 60    | 23    | 6     | 10    | -0.497   |
| <i>GFL403</i>   | 10              | 4     | 7     | 6     | 6     | -0.470   |
| <i>GFL404</i>   | 40              | 23    | 32    | 20    | 21    | -0.763   |
| <i>GFL405</i>   | 27              | 23    | 59    | 11    | 6     | -0.421   |
| <i>GFL406</i>   | 22              | 45    | 58    | 15    | 59    | 0.420    |
| <i>GFL407</i>   | 25              | 50    | 48    | 28    | 29    | -0.142   |
| <i>GFL408</i>   | 17              | 28    | 8     | 25    | 13    | -0.217   |
| <i>GFL409</i>   | 95              | 135   | 126   | 82    | 90    | -0.370   |
| <i>GFL410</i>   | 25              | 16    | 70    | 26    | 20    | -0.032   |
| <i>GFL411</i>   | 33              | 25    | 11    | 14    | 11    | -0.870   |
| <i>GFL412</i>   | 6               | 5     | 14    | 14    | 7     | 0.306    |
| <i>GFL413</i>   | 3               | 3     | 4     | 5     | 4     | 0.680    |
| <i>GFL414</i>   | 48              | 66    | 75    | 52    | 47    | -0.195   |
| <i>GFL415</i>   | 11              | 12    | 10    | 33    | 9     | 0.175    |
| <i>GFL416</i>   | 10              | 11    | 63    | 19    | 26    | 0.277    |
| <i>GFL417</i>   | 36              | 48    | 95    | 51    | 50    | 0.202    |
| <i>GFL418</i>   | 33              | 67    | 36    | 8     | 66    | 0.155    |
| <i>GFL419</i>   | 39              | 16    | 66    | 19    | 23    | -0.241   |
| <i>GFL420</i>   | 16              | 3     | 11    | 4     | 3     | -0.701   |
| <i>GFL421</i>   | 1               | 4     | 5     | 8     | 12    | 0.992*** |
| <i>GFL422</i>   | 5               | 16    | 24    | 6     | 24    | 0.543    |
| <i>GFL423</i>   | 4               | 11    | 6     | 11    | 22    | 0.864    |
| <i>GFL424</i>   | 5               | 7     | 7     | 6     | 2     | -0.569   |
| <i>GFL425</i>   | 9               | 17    | 50    | 8     | 19    | 0.115    |
| <i>GFL426</i>   | 24              | 12    | 22    | 11    | 23    | -0.045   |
| <i>GFL427</i>   | 6               | 4     | 8     | 3     | 6     | -0.053   |
| <i>GFL428</i>   | 1               | 1     | 0     | 0     | 1     | NA       |
| <i>GFL429</i>   | 12              | 17    | 12    | 13    | 24    | 0.693    |
| <i>GFL430</i>   | 5               | 10    | 4     | 7     | 29    | 0.753    |
| <i>GFL431</i>   | 13              | 28    | 35    | 27    | 14    | -0.013   |
| <i>GFL432</i>   | 38              | 46    | 90    | 33    | 31    | -0.179   |
| <i>GFL433</i>   | 30              | 12    | 26    | 32    | 23    | 0.029    |
| <i>GFL434</i>   | 0               | 1     | 0     | 2     | 2     | NA       |
| <i>GFL435</i>   | 24              | 24    | 36    | 19    | 48    | 0.639    |
| <i>GFL436</i>   | 43              | 69    | 30    | 14    | 36    | -0.451   |
| <i>GFL437</i>   | 6               | 3     | 7     | 4     | 3     | -0.480   |
| <i>GFL438</i>   | 14              | 4     | 13    | 8     | 9     | -0.271   |
| <i>GFL439</i>   | 39              | 18    | 23    | 12    | 11    | -0.867   |
| <i>GFL440</i>   | 18              | 10    | 14    | 8     | 27    | 0.394    |

**Table 15** Continued

|                 | G1              | G2    | G3    | G4    | G5    |          |
|-----------------|-----------------|-------|-------|-------|-------|----------|
| Number of edges | 19443           | 19327 | 27580 | 16835 | 16195 |          |
| UHM (mm)        | 26.16           | 27.76 | 28.80 | 29.85 | 31.72 |          |
|                 | Number of edges |       |       |       |       | <i>r</i> |
| <i>GFL441</i>   | 8               | 2     | 33    | 6     | 10    | 0.087    |
| <i>GFL442</i>   | 48              | 14    | 34    | 13    | 11    | -0.746   |
| <i>GFL443</i>   | 13              | 31    | 81    | 19    | 12    | -0.085   |
| <i>GFL444</i>   | 12              | 7     | 12    | 5     | 11    | -0.159   |
| <i>GFL445</i>   | 66              | 77    | 136   | 82    | 86    | 0.251    |
| <i>GFL446</i>   | 34              | 10    | 21    | 6     | 26    | -0.243   |
| <i>GFL447</i>   | 29              | 29    | 14    | 24    | 17    | -0.665   |
| <i>GFL448</i>   | 27              | 15    | 57    | 19    | 22    | -0.076   |
| <i>GFL449</i>   | 13              | 6     | 41    | 6     | 10    | -0.076   |
| <i>GFL450</i>   | 0               | 0     | 0     | 0     | 2     | NA       |
| <i>GFL451</i>   | 8               | 13    | 11    | 5     | 7     | -0.427   |
| <i>GFL452</i>   | 83              | 110   | 128   | 94    | 38    | -0.526   |
| <i>GFL453</i>   | 20              | 20    | 33    | 22    | 21    | 0.088    |
| <i>GFL454</i>   | 37              | 14    | 21    | 19    | 54    | 0.414    |
| <i>GFL455</i>   | 5               | 7     | 3     | 7     | 3     | -0.348   |
| <i>GFL456</i>   | 3               | 5     | 46    | 48    | 27    | 0.600    |
| <i>GFL457</i>   | 1               | 0     | 3     | 2     | 0     | NA       |
| <i>GFL458</i>   | 22              | 37    | 25    | 16    | 30    | 0.006    |
| <i>GFL459</i>   | 29              | 8     | 16    | 14    | 20    | -0.256   |
| <i>GFL460</i>   | 2               | 4     | 2     | 2     | 4     | 0.384    |
| <i>GFL461</i>   | 8               | 15    | 52    | 23    | 8     | 0.030    |
| <i>GFL462</i>   | 31              | 12    | 10    | 15    | 31    | 0.072    |
| <i>GFL463</i>   | 29              | 17    | 24    | 16    | 62    | 0.600    |
| <i>GFL464</i>   | 20              | 36    | 16    | 38    | 51    | 0.745    |
| <i>GFL465</i>   | 15              | 17    | 78    | 12    | 20    | 0.024    |
| <i>GFL466</i>   | 47              | 14    | 79    | 16    | 26    | -0.246   |
| <i>GFL467</i>   | 60              | 50    | 104   | 26    | 30    | -0.422   |
| <i>GFL468</i>   | 39              | 7     | 19    | 18    | 26    | -0.219   |
| <i>GFL469</i>   | 98              | 22    | 68    | 33    | 21    | -0.706   |
| <i>GFL470</i>   | 0               | 0     | 1     | 2     | 0     | NA       |
| <i>GFL471</i>   | 3               | 23    | 5     | 11    | 8     | 0.002    |
| <i>GFL472</i>   | 11              | 6     | 11    | 8     | 9     | -0.179   |
| <i>GFL473</i>   | 7               | 14    | 7     | 7     | 17    | 0.522    |
| <i>GFL474</i>   | 46              | 46    | 31    | 21    | 33    | -0.679   |

(\*) significant at  $P \leq 0.05$ ; (\*\*) significant at  $P \leq 0.01$ ; (\*\*\*) significant at  $P \leq 0.001$

To determine whether number of edges from a node is associated with UHML, Pearson's correlation analysis was used to test the relationship between number of edges from a single node across different fiber-length groups and its corresponding average UHML in each group. In consideration of the lack of edges from a single gene in some fiber-length groups and the sufficient number of samples in statistical analyses, *GFL* genes that did not have edges in any one of the fiber-length groups were excluded from the test. Significant correlations between number of edges from 20 *GFL* genes and UHML were observed. These *GFL* genes included *GFL013*, *GFL071*, *GFL098*, *GFL132*, *GFL163*, *GFL176*, *GFL192*, *GFL208*, *GFL226*, *GFL229*, *GFL250*, *GFL255*, *GFL263*, *GFL279*, *GFL295*, *GFL297*, *GFL299*, *GFL314*, *GFL354*, and *GFL421*. The gain or loss of edges for these genes has significant influence on UHML, thus the interaction of genes may be an important determinant of UHML. For example, *GFL354* was observed as having an increasing number of edges from shorter to longer fiber groups, whereas *GFL255* had reduced number of edges from shorter to longer fiber groups. Of the *GFL* genes that did not have significant correlations between the number of edges and UHML, 72 tended to have an increasing number of edges from the short fiber groups (G1 and G2) to the middle length fiber group (G3) and then have an decreasing number of edges from the middle length fiber group (G3) to the longer fiber groups (G4 and G5). For instance, UHML was increased by 1.60 mm when *GFL325* gained four additional edges relative to the network of G1. When *GFL325* gained 58 additional edges in the G2 network, UHML was increased by 1.04 mm. However, when 106 edges were eliminated from *GFL325* in the G3 network, UHML was increased by

2.92 mm. Such tendencies were not only found for *GFL325*, but also observed for many of other gene nodes in the networks. Therefore, UHML could be improved by either gain or loss of nodes or edges from individual nodes in different controlling patterns, thus suggesting another aspect of the mechanism underlying UHML development.

#### 3.4.2.2 Shared nodes and edges among the *GFL* gene networks of fiber-length groups

To further scrutinize the impacts of the edge variation of the gene networks on UHML, we further dissected and compared the *GFL* gene networks of the five UHML RIL groups. From G1 to G5, a total of 2,242 edges (Fig. 24) were found to be shared among the *GFL* gene networks of the UHML groups. Further examination showed that these edges were connected by 211 nodes in the networks. The nodes and edges shared among the networks are listed in Table A-1. Of the shared nodes, *GFL339* interacted with the largest number of *GFL* genes (53 nodes) in the networks of all five fiber-length groups, from the shortest UHML G1 through the longest UHML G5, followed by *GFL340*, *GF0341*, *GFL342*, etc. This finding suggested that *GFL339* might play a leading role in the network of each fiber-length group. Of the 2,242 shared edges, 38 were found in the networks of all five fiber-length RIL groups.

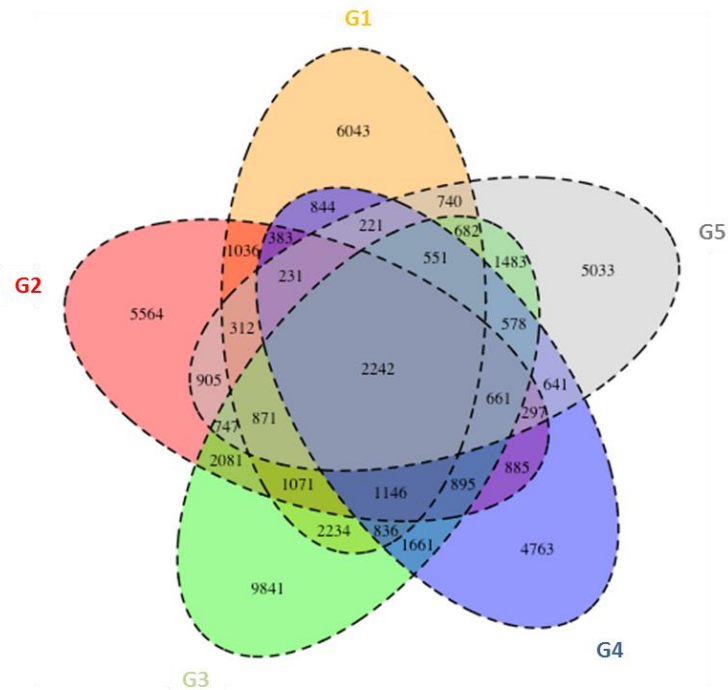


**Figure 24** Numbers of unique and shared edges among the *GFL* gene networks of different UHML RIL groups

### 3.4.2.3 Nodes and edges unique to the *GFL* network of each UHML RIL group

The above systems analysis suggested that the variation of number of edges in the *GFL* gene networks played an important role in UHML. Therefore, to investigate the dynamics of the networks in UHML development, the edges that were only observed in or unique to the network of each fiber-length group were studied (Table 16). There were 6,043 (31.08% of the total edges of the network) edges unique for G1, 5,564 (28.79%) for G2, 9,841 (35.68%) for G3, 4,763 (28.29%) for G4, and 5033 (31.08%) for G5 (Fig. 24). Some of the unique edges might be contributed by the genes that are playing critical roles in the networks, i.e., that have a large number of edges according to our results of

**Table 16** Summary of the edges of each gene unique to the *GFL* gene networks of each fiber-length group derived from 474 *GFL* genes, and their Pearson correlation coefficients with of UHML and corresponding number of unique edges of *GFL* genes

|                       | G1                     | G2    | G3    | G4    | G5    |          |
|-----------------------|------------------------|-------|-------|-------|-------|----------|
| UHM (mm)              | 26.16                  | 27.76 | 28.80 | 29.85 | 31.72 |          |
| No. of unique edges*  | 6043                   | 5564  | 9841  | 4763  | 5033  |          |
| % of unique edges (%) | 31.08                  | 28.79 | 35.68 | 28.29 | 31.08 |          |
| Gene ID               | Number of unique edges |       |       |       |       | <i>r</i> |
| <i>GFL001</i>         | 9                      | 11    | 12    | 1     | 10    | -0.200   |
| <i>GFL002</i>         | 11                     | 3     | 39    | 4     | 8     | -0.066   |
| <i>GFL003</i>         | 2                      | 1     | 0     | 1     | 1     | NA       |
| <i>GFL004</i>         | 13                     | 4     | 15    | 3     | 7     | -0.383   |
| <i>GFL005</i>         | 47                     | 7     | 8     | 40    | 8     | -0.436   |
| <i>GFL006</i>         | 12                     | 21    | 41    | 25    | 19    | 0.235    |
| <i>GFL007</i>         | 0                      | 0     | 0     | 0     | 0     | NA       |
| <i>GFL008</i>         | 7                      | 3     | 14    | 3     | 2     | -0.342   |
| <i>GFL009</i>         | 4                      | 12    | 22    | 8     | 14    | 0.400    |
| <i>GFL010</i>         | 19                     | 35    | 11    | 17    | 28    | 0.084    |
| <i>GFL011</i>         | 25                     | 11    | 15    | 19    | 21    | -0.032   |
| <i>GFL012</i>         | 56                     | 18    | 61    | 10    | 8     | -0.652   |
| <i>GFL013</i>         | 40                     | 24    | 21    | 19    | 11    | -0.951*  |
| <i>GFL014</i>         | 18                     | 14    | 21    | 6     | 32    | 0.405    |
| <i>GFL015</i>         | 51                     | 20    | 33    | 17    | 13    | -0.826   |
| <i>GFL016</i>         | 25                     | 37    | 11    | 14    | 25    | -0.267   |
| <i>GFL017</i>         | 11                     | 35    | 16    | 22    | 25    | 0.316    |
| <i>GFL018</i>         | 10                     | 7     | 13    | 2     | 4     | -0.588   |
| <i>GFL019</i>         | 13                     | 13    | 27    | 11    | 18    | 0.213    |
| <i>GFL020</i>         | 7                      | 20    | 21    | 16    | 4     | -0.228   |
| <i>GFL021</i>         | 0                      | 0     | 1     | 0     | 1     | NA       |
| <i>GFL022</i>         | 2                      | 18    | 21    | 3     | 5     | -0.120   |
| <i>GFL023</i>         | 3                      | 1     | 4     | 1     | 2     | -0.246   |
| <i>GFL024</i>         | 21                     | 16    | 37    | 4     | 14    | -0.317   |
| <i>GFL025</i>         | 14                     | 12    | 24    | 9     | 16    | 0.051    |
| <i>GFL026</i>         | 13                     | 15    | 30    | 20    | 9     | -0.113   |
| <i>GFL027</i>         | 37                     | 23    | 17    | 35    | 20    | -0.450   |
| <i>GFL028</i>         | 6                      | 11    | 14    | 8     | 11    | 0.400    |
| <i>GFL029</i>         | 18                     | 16    | 26    | 14    | 9     | -0.534   |
| <i>GFL030</i>         | 14                     | 11    | 27    | 14    | 13    | -0.006   |

**Table 16** Continued

|                       | G1                     | G2    | G3    | G4    | G5    |          |
|-----------------------|------------------------|-------|-------|-------|-------|----------|
| UHM (mm)              | 26.16                  | 27.76 | 28.80 | 29.85 | 31.72 |          |
| No. of unique edges*  | 6043                   | 5564  | 9841  | 4763  | 5033  |          |
| % of unique edges (%) | 31.08                  | 28.79 | 35.68 | 28.29 | 31.08 |          |
| Gene ID               | Number of unique edges |       |       |       |       | <i>r</i> |
| <i>GFL031</i>         | 18                     | 19    | 8     | 13    | 17    | -0.219   |
| <i>GFL032</i>         | 0                      | 4     | 6     | 2     | 2     | NA       |
| <i>GFL033</i>         | 10                     | 16    | 15    | 0     | 24    | NA       |
| <i>GFL034</i>         | 0                      | 0     | 0     | 0     | 0     | NA       |
| <i>GFL035</i>         | 4                      | 5     | 24    | 6     | 4     | -0.003   |
| <i>GFL036</i>         | 1                      | 0     | 1     | 2     | 0     | NA       |
| <i>GFL037</i>         | 18                     | 7     | 17    | 12    | 11    | -0.364   |
| <i>GFL038</i>         | 6                      | 4     | 10    | 5     | 2     | -0.420   |
| <i>GFL039</i>         | 15                     | 43    | 75    | 7     | 15    | -0.177   |
| <i>GFL040</i>         | 7                      | 8     | 4     | 7     | 17    | 0.669    |
| <i>GFL041</i>         | 12                     | 7     | 40    | 11    | 4     | -0.165   |
| <i>GFL042</i>         | 0                      | 0     | 0     | 0     | 0     | NA       |
| <i>GFL043</i>         | 11                     | 9     | 43    | 9     | 10    | -0.035   |
| <i>GFL044</i>         | 21                     | 24    | 6     | 19    | 17    | -0.275   |
| <i>GFL045</i>         | 4                      | 4     | 15    | 5     | 4     | 0.009    |
| <i>GFL046</i>         | 4                      | 9     | 29    | 14    | 20    | 0.597    |
| <i>GFL047</i>         | 7                      | 7     | 43    | 6     | 10    | 0.042    |
| <i>GFL048</i>         | 16                     | 11    | 19    | 20    | 15    | 0.214    |
| <i>GFL049</i>         | 16                     | 18    | 51    | 14    | 20    | 0.041    |
| <i>GFL050</i>         | 19                     | 21    | 14    | 21    | 21    | 0.227    |
| <i>GFL051</i>         | 13                     | 8     | 32    | 7     | 10    | -0.116   |
| <i>GFL052</i>         | 1                      | 2     | 9     | 2     | 2     | 0.084    |
| <i>GFL053</i>         | 15                     | 15    | 36    | 11    | 5     | -0.343   |
| <i>GFL054</i>         | 10                     | 8     | 7     | 14    | 3     | -0.405   |
| <i>GFL055</i>         | 7                      | 2     | 6     | 6     | 2     | -0.483   |
| <i>GFL056</i>         | 6                      | 4     | 15    | 2     | 6     | -0.054   |
| <i>GFL057</i>         | 8                      | 12    | 16    | 14    | 5     | -0.200   |
| <i>GFL058</i>         | 16                     | 23    | 16    | 12    | 14    | -0.498   |
| <i>GFL059</i>         | 25                     | 8     | 9     | 8     | 31    | 0.216    |
| <i>GFL060</i>         | 21                     | 14    | 36    | 16    | 19    | -0.052   |



**Table 16** Continued

|                       | G1                     | G2    | G3    | G4    | G5    |          |
|-----------------------|------------------------|-------|-------|-------|-------|----------|
| UHM (mm)              | 26.16                  | 27.76 | 28.80 | 29.85 | 31.72 |          |
| No. of unique edges*  | 6043                   | 5564  | 9841  | 4763  | 5033  |          |
| % of unique edges (%) | 31.08                  | 28.79 | 35.68 | 28.29 | 31.08 |          |
| Gene ID               | Number of unique edges |       |       |       |       | <i>r</i> |
| <i>GFL061</i>         | 35                     | 48    | 34    | 11    | 14    | -0.749   |
| <i>GFL062</i>         | 33                     | 24    | 16    | 21    | 19    | -0.752   |
| <i>GFL063</i>         | 3                      | 1     | 0     | 3     | 0     | NA       |
| <i>GFL064</i>         | 4                      | 2     | 1     | 1     | 0     | NA       |
| <i>GFL065</i>         | 3                      | 3     | 6     | 0     | 6     | NA       |
| <i>GFL066</i>         | 13                     | 7     | 23    | 7     | 9     | -0.201   |
| <i>GFL067</i>         | 12                     | 7     | 30    | 13    | 9     | -0.041   |
| <i>GFL068</i>         | 11                     | 9     | 13    | 4     | 6     | -0.624   |
| <i>GFL069</i>         | 49                     | 37    | 35    | 8     | 12    | -0.900*  |
| <i>GFL070</i>         | 10                     | 18    | 21    | 11    | 13    | 0.005    |
| <i>GFL071</i>         | 54                     | 42    | 31    | 11    | 16    | -0.912*  |
| <i>GFL072</i>         | 12                     | 3     | 36    | 7     | 6     | -0.121   |
| <i>GFL073</i>         | 3                      | 7     | 27    | 6     | 15    | 0.388    |
| <i>GFL074</i>         | 10                     | 5     | 6     | 2     | 10    | -0.075   |
| <i>GFL075</i>         | 13                     | 62    | 21    | 30    | 18    | -0.141   |
| <i>GFL076</i>         | 22                     | 27    | 55    | 21    | 17    | -0.176   |
| <i>GFL077</i>         | 2                      | 2     | 0     | 0     | 0     | NA       |
| <i>GFL078</i>         | 10                     | 11    | 48    | 11    | 9     | -0.036   |
| <i>GFL079</i>         | 13                     | 22    | 31    | 16    | 10    | -0.236   |
| <i>GFL080</i>         | 19                     | 20    | 41    | 9     | 6     | -0.428   |
| <i>GFL081</i>         | 10                     | 10    | 9     | 16    | 13    | 0.601    |
| <i>GFL082</i>         | 16                     | 13    | 16    | 7     | 13    | -0.459   |
| <i>GFL083</i>         | 25                     | 25    | 50    | 7     | 10    | -0.434   |
| <i>GFL084</i>         | 1                      | 1     | 1     | 2     | 0     | NA       |
| <i>GFL085</i>         | 28                     | 12    | 30    | 15    | 14    | -0.497   |
| <i>GFL086</i>         | 19                     | 22    | 29    | 47    | 18    | 0.207    |
| <i>GFL087</i>         | 16                     | 9     | 56    | 23    | 18    | 0.117    |
| <i>GFL088</i>         | 0                      | 3     | 7     | 1     | 0     | NA       |
| <i>GFL089</i>         | 16                     | 27    | 6     | 19    | 11    | -0.341   |
| <i>GFL090</i>         | 6                      | 8     | 4     | 5     | 10    | 0.415    |

**Table 16** Continued

|                       | G1                     | G2    | G3    | G4    | G5    |          |
|-----------------------|------------------------|-------|-------|-------|-------|----------|
| UHM (mm)              | 26.16                  | 27.76 | 28.80 | 29.85 | 31.72 |          |
| No. of unique edges*  | 6043                   | 5564  | 9841  | 4763  | 5033  |          |
| % of unique edges (%) | 31.08                  | 28.79 | 35.68 | 28.29 | 31.08 |          |
| Gene ID               | Number of unique edges |       |       |       |       | <i>r</i> |
| <i>GFL091</i>         | 28                     | 5     | 21    | 21    | 16    | -0.218   |
| <i>GFL092</i>         | 14                     | 20    | 33    | 28    | 11    | -0.031   |
| <i>GFL093</i>         | 0                      | 3     | 0     | 0     | 0     | NA       |
| <i>GFL094</i>         | 12                     | 16    | 42    | 23    | 16    | 0.161    |
| <i>GFL095</i>         | 5                      | 25    | 7     | 8     | 12    | 0.014    |
| <i>GFL096</i>         | 9                      | 3     | 11    | 16    | 7     | 0.189    |
| <i>GFL097</i>         | 11                     | 5     | 10    | 4     | 12    | 0.085    |
| <i>GFL098</i>         | 11                     | 8     | 9     | 3     | 4     | -0.861   |
| <i>GFL099</i>         | 22                     | 13    | 50    | 17    | 27    | 0.145    |
| <i>GFL100</i>         | 9                      | 17    | 20    | 6     | 5     | -0.421   |
| <i>GFL101</i>         | 3                      | 5     | 1     | 0     | 2     | NA       |
| <i>GFL102</i>         | 8                      | 24    | 4     | 8     | 8     | -0.264   |
| <i>GFL103</i>         | 11                     | 4     | 36    | 5     | 20    | 0.235    |
| <i>GFL104</i>         | 14                     | 16    | 14    | 11    | 14    | -0.343   |
| <i>GFL105</i>         | 4                      | 6     | 11    | 1     | 1     | -0.404   |
| <i>GFL106</i>         | 17                     | 15    | 20    | 11    | 13    | -0.523   |
| <i>GFL107</i>         | 38                     | 13    | 44    | 14    | 24    | -0.312   |
| <i>GFL108</i>         | 3                      | 6     | 13    | 2     | 11    | 0.444    |
| <i>GFL109</i>         | 10                     | 34    | 38    | 13    | 10    | -0.215   |
| <i>GFL110</i>         | 1                      | 7     | 2     | 1     | 2     | -0.179   |
| <i>GFL111</i>         | 12                     | 31    | 7     | 7     | 21    | 0.003    |
| <i>GFL112</i>         | 11                     | 7     | 25    | 3     | 9     | -0.142   |
| <i>GFL113</i>         | 3                      | 5     | 13    | 5     | 9     | 0.488    |
| <i>GFL114</i>         | 25                     | 16    | 53    | 20    | 6     | -0.344   |
| <i>GFL115</i>         | 1                      | 0     | 0     | 0     | 0     | NA       |
| <i>GFL116</i>         | 22                     | 31    | 24    | 9     | 26    | -0.164   |
| <i>GFL117</i>         | 10                     | 4     | 42    | 11    | 18    | 0.230    |
| <i>GFL118</i>         | 6                      | 7     | 4     | 2     | 3     | -0.776   |
| <i>GFL119</i>         | 14                     | 6     | 36    | 39    | 7     | 0.091    |
| <i>GFL120</i>         | 2                      | 4     | 1     | 0     | 2     | NA       |

**Table 16** Continued

|                       | G1                     | G2    | G3    | G4    | G5    |          |
|-----------------------|------------------------|-------|-------|-------|-------|----------|
| UHM (mm)              | 26.16                  | 27.76 | 28.80 | 29.85 | 31.72 |          |
| No. of unique edges*  | 6043                   | 5564  | 9841  | 4763  | 5033  |          |
| % of unique edges (%) | 31.08                  | 28.79 | 35.68 | 28.29 | 31.08 |          |
| Gene ID               | Number of unique edges |       |       |       |       | <i>r</i> |
| <i>GFLI21</i>         | 11                     | 8     | 37    | 9     | 7     | -0.108   |
| <i>GFLI22</i>         | 11                     | 23    | 18    | 11    | 11    | -0.294   |
| <i>GFLI23</i>         | 13                     | 11    | 24    | 12    | 6     | -0.350   |
| <i>GFLI24</i>         | 4                      | 4     | 2     | 1     | 1     | -0.897*  |
| <i>GFLI25</i>         | 19                     | 26    | 17    | 20    | 6     | -0.714   |
| <i>GFLI26</i>         | 8                      | 12    | 13    | 4     | 1     | -0.665   |
| <i>GFLI27</i>         | 18                     | 9     | 38    | 23    | 5     | -0.216   |
| <i>GFLI28</i>         | 2                      | 2     | 0     | 2     | 0     | NA       |
| <i>GFLI29</i>         | 10                     | 8     | 14    | 4     | 14    | 0.211    |
| <i>GFLI30</i>         | 11                     | 12    | 23    | 9     | 11    | -0.080   |
| <i>GFLI31</i>         | 8                      | 1     | 0     | 4     | 2     | NA       |
| <i>GFLI32</i>         | 3                      | 2     | 2     | 2     | 0     | NA       |
| <i>GFLI33</i>         | 9                      | 10    | 13    | 6     | 8     | -0.328   |
| <i>GFLI34</i>         | 4                      | 2     | 12    | 3     | 0     | NA       |
| <i>GFLI35</i>         | 23                     | 21    | 38    | 31    | 16    | -0.148   |
| <i>GFLI36</i>         | 28                     | 4     | 64    | 12    | 9     | -0.224   |
| <i>GFLI37</i>         | 38                     | 15    | 21    | 6     | 9     | -0.830   |
| <i>GFLI38</i>         | 10                     | 11    | 7     | 15    | 1     | -0.497   |
| <i>GFLI39</i>         | 3                      | 12    | 13    | 14    | 5     | 0.145    |
| <i>GFLI40</i>         | 8                      | 35    | 7     | 51    | 27    | 0.429    |
| <i>GFLI41</i>         | 22                     | 16    | 63    | 21    | 35    | 0.254    |
| <i>GFLI42</i>         | 3                      | 16    | 31    | 5     | 7     | -0.025   |
| <i>GFLI43</i>         | 23                     | 12    | 58    | 23    | 9     | -0.183   |
| <i>GFLI44</i>         | 51                     | 13    | 33    | 13    | 17    | -0.664   |
| <i>GFLI45</i>         | 24                     | 15    | 35    | 7     | 15    | -0.370   |
| <i>GFLI46</i>         | 36                     | 16    | 18    | 29    | 6     | -0.710   |
| <i>GFLI47</i>         | 7                      | 2     | 16    | 2     | 3     | -0.228   |
| <i>GFLI48</i>         | 2                      | 3     | 15    | 0     | 9     | NA       |
| <i>GFLI49</i>         | 22                     | 7     | 19    | 3     | 3     | -0.742   |
| <i>GFLI50</i>         | 5                      | 9     | 9     | 7     | 7     | 0.220    |

**Table 16** Continued

|                       | G1                     | G2    | G3    | G4    | G5    |          |
|-----------------------|------------------------|-------|-------|-------|-------|----------|
| UHM (mm)              | 26.16                  | 27.76 | 28.80 | 29.85 | 31.72 |          |
| No. of unique edges*  | 6043                   | 5564  | 9841  | 4763  | 5033  |          |
| % of unique edges (%) | 31.08                  | 28.79 | 35.68 | 28.29 | 31.08 |          |
| Gene ID               | Number of unique edges |       |       |       |       | <i>r</i> |
| <i>GFL151</i>         | 5                      | 4     | 6     | 2     | 6     | 0.068    |
| <i>GFL152</i>         | 9                      | 9     | 12    | 6     | 11    | 0.135    |
| <i>GFL153</i>         | 26                     | 16    | 44    | 13    | 15    | -0.318   |
| <i>GFL154</i>         | 26                     | 5     | 21    | 9     | 6     | -0.635   |
| <i>GFL155</i>         | 5                      | 4     | 7     | 4     | 6     | 0.261    |
| <i>GFL156</i>         | 23                     | 24    | 15    | 15    | 23    | -0.222   |
| <i>GFL157</i>         | 1                      | 5     | 4     | 3     | 2     | 0.021    |
| <i>GFL158</i>         | 19                     | 34    | 42    | 14    | 13    | -0.367   |
| <i>GFL159</i>         | 7                      | 14    | 19    | 15    | 16    | 0.679    |
| <i>GFL160</i>         | 12                     | 5     | 29    | 3     | 6     | -0.217   |
| <i>GFL161</i>         | 23                     | 25    | 49    | 13    | 25    | -0.070   |
| <i>GFL162</i>         | 19                     | 11    | 35    | 9     | 9     | -0.329   |
| <i>GFL163</i>         | 38                     | 23    | 27    | 11    | 7     | -0.936*  |
| <i>GFL164</i>         | 9                      | 2     | 9     | 2     | 2     | -0.598   |
| <i>GFL165</i>         | 13                     | 10    | 16    | 6     | 12    | -0.213   |
| <i>GFL166</i>         | 33                     | 17    | 36    | 15    | 12    | -0.651   |
| <i>GFL167</i>         | 10                     | 11    | 19    | 6     | 2     | -0.533   |
| <i>GFL168</i>         | 9                      | 12    | 44    | 12    | 11    | 0.028    |
| <i>GFL169</i>         | 4                      | 8     | 20    | 6     | 10    | 0.265    |
| <i>GFL170</i>         | 16                     | 15    | 36    | 16    | 14    | -0.073   |
| <i>GFL171</i>         | 9                      | 12    | 27    | 6     | 11    | -0.022   |
| <i>GFL172</i>         | 44                     | 9     | 19    | 19    | 24    | -0.387   |
| <i>GFL173</i>         | 14                     | 17    | 36    | 17    | 18    | 0.133    |
| <i>GFL174</i>         | 5                      | 15    | 40    | 16    | 16    | 0.271    |
| <i>GFL175</i>         | 1                      | 0     | 7     | 0     | 1     | NA       |
| <i>GFL176</i>         | 26                     | 23    | 14    | 8     | 7     | -0.941*  |
| <i>GFL177</i>         | 48                     | 13    | 11    | 8     | 17    | -0.640   |
| <i>GFL178</i>         | 2                      | 7     | 3     | 0     | 4     | NA       |
| <i>GFL179</i>         | 3                      | 8     | 16    | 7     | 10    | 0.444    |
| <i>GFL180</i>         | 2                      | 0     | 1     | 0     | 0     | NA       |

**Table 16** Continued

|                       | G1                     | G2    | G3    | G4    | G5    |          |
|-----------------------|------------------------|-------|-------|-------|-------|----------|
| UHM (mm)              | 26.16                  | 27.76 | 28.80 | 29.85 | 31.72 |          |
| No. of unique edges*  | 6043                   | 5564  | 9841  | 4763  | 5033  |          |
| % of unique edges (%) | 31.08                  | 28.79 | 35.68 | 28.29 | 31.08 |          |
| Gene ID               | Number of unique edges |       |       |       |       | <i>r</i> |
| <i>GFL181</i>         | 0                      | 0     | 0     | 0     | 0     | NA       |
| <i>GFL182</i>         | 11                     | 10    | 23    | 5     | 22    | 0.391    |
| <i>GFL183</i>         | 28                     | 14    | 9     | 29    | 21    | -0.036   |
| <i>GFL184</i>         | 4                      | 18    | 11    | 6     | 7     | -0.111   |
| <i>GFL185</i>         | 3                      | 1     | 5     | 3     | 1     | -0.259   |
| <i>GFL186</i>         | 5                      | 4     | 12    | 7     | 2     | -0.185   |
| <i>GFL187</i>         | 14                     | 15    | 24    | 26    | 18    | 0.480    |
| <i>GFL188</i>         | 21                     | 7     | 7     | 27    | 28    | 0.482    |
| <i>GFL189</i>         | 2                      | 4     | 7     | 4     | 3     | 0.150    |
| <i>GFL190</i>         | 32                     | 9     | 54    | 16    | 28    | -0.022   |
| <i>GFL191</i>         | 6                      | 12    | 9     | 18    | 11    | 0.520    |
| <i>GFL192</i>         | 18                     | 13    | 14    | 6     | 6     | -0.914*  |
| <i>GFL193</i>         | 1                      | 2     | 3     | 1     | 1     | -0.161   |
| <i>GFL194</i>         | 1                      | 3     | 12    | 9     | 5     | 0.440    |
| <i>GFL195</i>         | 8                      | 20    | 33    | 14    | 18    | 0.257    |
| <i>GFL196</i>         | 12                     | 21    | 27    | 12    | 15    | -0.039   |
| <i>GFL197</i>         | 27                     | 41    | 43    | 13    | 12    | -0.588   |
| <i>GFL198</i>         | 8                      | 4     | 8     | 4     | 1     | -0.778   |
| <i>GFL199</i>         | 13                     | 8     | 34    | 14    | 13    | 0.062    |
| <i>GFL200</i>         | 4                      | 4     | 9     | 3     | 4     | -0.063   |
| <i>GFL201</i>         | 4                      | 11    | 21    | 13    | 7     | 0.162    |
| <i>GFL202</i>         | 3                      | 1     | 6     | 2     | 5     | 0.388    |
| <i>GFL203</i>         | 8                      | 9     | 17    | 3     | 6     | -0.279   |
| <i>GFL204</i>         | 3                      | 11    | 28    | 6     | 8     | 0.086    |
| <i>GFL205</i>         | 7                      | 8     | 21    | 19    | 20    | 0.815    |
| <i>GFL206</i>         | 3                      | 0     | 3     | 1     | 3     | NA       |
| <i>GFL207</i>         | 1                      | 8     | 3     | 2     | 5     | 0.200    |
| <i>GFL208</i>         | 56                     | 39    | 16    | 17    | 12    | -0.905*  |
| <i>GFL209</i>         | 2                      | 4     | 5     | 3     | 5     | 0.659    |
| <i>GFL210</i>         | 11                     | 9     | 30    | 4     | 6     | -0.229   |

**Table 16** Continued

|                       | G1                     | G2    | G3    | G4    | G5    |          |
|-----------------------|------------------------|-------|-------|-------|-------|----------|
| UHM (mm)              | 26.16                  | 27.76 | 28.80 | 29.85 | 31.72 |          |
| No. of unique edges*  | 6043                   | 5564  | 9841  | 4763  | 5033  |          |
| % of unique edges (%) | 31.08                  | 28.79 | 35.68 | 28.29 | 31.08 |          |
| Gene ID               | Number of unique edges |       |       |       |       | <i>r</i> |
| <i>GFL211</i>         | 5                      | 1     | 1     | 1     | 3     | -0.336   |
| <i>GFL212</i>         | 20                     | 15    | 67    | 11    | 14    | -0.118   |
| <i>GFL213</i>         | 6                      | 1     | 1     | 2     | 4     | -0.214   |
| <i>GFL214</i>         | 6                      | 5     | 23    | 3     | 5     | -0.082   |
| <i>GFL215</i>         | 12                     | 22    | 60    | 8     | 17    | -0.019   |
| <i>GFL216</i>         | 8                      | 6     | 18    | 3     | 13    | 0.221    |
| <i>GFL217</i>         | 2                      | 2     | 14    | 3     | 3     | 0.073    |
| <i>GFL218</i>         | 13                     | 5     | 29    | 0     | 6     | NA       |
| <i>GFL219</i>         | 17                     | 13    | 50    | 27    | 19    | 0.146    |
| <i>GFL220</i>         | 10                     | 9     | 43    | 8     | 15    | 0.093    |
| <i>GFL221</i>         | 13                     | 28    | 19    | 20    | 34    | 0.727    |
| <i>GFL222</i>         | 9                      | 4     | 16    | 4     | 13    | 0.258    |
| <i>GFL223</i>         | 3                      | 3     | 5     | 8     | 6     | 0.752    |
| <i>GFL224</i>         | 13                     | 28    | 59    | 10    | 17    | -0.063   |
| <i>GFL225</i>         | 9                      | 12    | 35    | 8     | 6     | -0.143   |
| <i>GFL226</i>         | 9                      | 12    | 28    | 34    | 52    | 0.976**  |
| <i>GFL227</i>         | 2                      | 6     | 11    | 2     | 2     | -0.146   |
| <i>GFL228</i>         | 11                     | 28    | 10    | 45    | 13    | 0.163    |
| <i>GFL229</i>         | 21                     | 26    | 20    | 18    | 9     | -0.818   |
| <i>GFL230</i>         | 32                     | 6     | 45    | 12    | 13    | -0.338   |
| <i>GFL231</i>         | 6                      | 6     | 24    | 13    | 3     | -0.038   |
| <i>GFL232</i>         | 14                     | 21    | 46    | 12    | 15    | -0.073   |
| <i>GFL233</i>         | 13                     | 17    | 15    | 14    | 33    | 0.771    |
| <i>GFL234</i>         | 1                      | 2     | 0     | 1     | 1     | NA       |
| <i>GFL235</i>         | 5                      | 7     | 12    | 14    | 13    | 0.877    |
| <i>GFL236</i>         | 2                      | 0     | 0     | 0     | 1     | NA       |
| <i>GFL237</i>         | 14                     | 11    | 15    | 7     | 4     | -0.825   |
| <i>GFL238</i>         | 10                     | 7     | 45    | 2     | 3     | -0.176   |
| <i>GFL239</i>         | 21                     | 25    | 29    | 30    | 10    | -0.404   |
| <i>GFL240</i>         | 2                      | 6     | 2     | 0     | 0     | NA       |

**Table 16** Continued

|                       | G1                     | G2    | G3    | G4    | G5    |          |
|-----------------------|------------------------|-------|-------|-------|-------|----------|
| UHM (mm)              | 26.16                  | 27.76 | 28.80 | 29.85 | 31.72 |          |
| No. of unique edges*  | 6043                   | 5564  | 9841  | 4763  | 5033  |          |
| % of unique edges (%) | 31.08                  | 28.79 | 35.68 | 28.29 | 31.08 |          |
| Gene ID               | Number of unique edges |       |       |       |       | <i>r</i> |
| <i>GFL241</i>         | 19                     | 14    | 20    | 9     | 5     | -0.824   |
| <i>GFL242</i>         | 52                     | 14    | 36    | 17    | 14    | -0.709   |
| <i>GFL243</i>         | 6                      | 8     | 17    | 6     | 2     | -0.304   |
| <i>GFL244</i>         | 10                     | 12    | 16    | 13    | 65    | 0.801    |
| <i>GFL245</i>         | 4                      | 8     | 12    | 4     | 5     | -0.068   |
| <i>GFL246</i>         | 41                     | 38    | 13    | 18    | 10    | -0.876   |
| <i>GFL247</i>         | 19                     | 16    | 36    | 5     | 11    | -0.350   |
| <i>GFL248</i>         | 3                      | 6     | 10    | 7     | 5     | 0.275    |
| <i>GFL249</i>         | 6                      | 11    | 30    | 14    | 9     | 0.122    |
| <i>GFL250</i>         | 3                      | 1     | 0     | 1     | 0     | NA       |
| <i>GFL251</i>         | 4                      | 14    | 5     | 5     | 5     | -0.205   |
| <i>GFL252</i>         | 14                     | 17    | 29    | 30    | 16    | 0.270    |
| <i>GFL253</i>         | 11                     | 7     | 36    | 8     | 5     | -0.159   |
| <i>GFL254</i>         | 3                      | 3     | 18    | 1     | 7     | 0.150    |
| <i>GFL255</i>         | 41                     | 23    | 28    | 17    | 8     | -0.942*  |
| <i>GFL256</i>         | 15                     | 15    | 11    | 38    | 15    | 0.250    |
| <i>GFL257</i>         | 2                      | 3     | 7     | 5     | 2     | 0.087    |
| <i>GFL258</i>         | 25                     | 11    | 40    | 11    | 13    | -0.318   |
| <i>GFL259</i>         | 15                     | 31    | 4     | 8     | 8     | -0.488   |
| <i>GFL260</i>         | 5                      | 15    | 5     | 4     | 10    | 0.060    |
| <i>GFL261</i>         | 8                      | 12    | 23    | 9     | 18    | 0.456    |
| <i>GFL262</i>         | 19                     | 4     | 29    | 10    | 26    | 0.305    |
| <i>GFL263</i>         | 19                     | 12    | 8     | 9     | 9     | -0.798   |
| <i>GFL264</i>         | 13                     | 2     | 1     | 3     | 4     | -0.564   |
| <i>GFL265</i>         | 20                     | 9     | 36    | 6     | 13    | -0.226   |
| <i>GFL266</i>         | 13                     | 4     | 8     | 8     | 15    | 0.297    |
| <i>GFL267</i>         | 15                     | 20    | 81    | 15    | 10    | -0.094   |
| <i>GFL268</i>         | 12                     | 26    | 41    | 21    | 12    | -0.080   |
| <i>GFL269</i>         | 25                     | 8     | 61    | 7     | 15    | -0.159   |
| <i>GFL270</i>         | 15                     | 9     | 13    | 4     | 8     | -0.666   |

**Table 16** Continued

|                       | G1                     | G2    | G3    | G4    | G5    |          |
|-----------------------|------------------------|-------|-------|-------|-------|----------|
| UHM (mm)              | 26.16                  | 27.76 | 28.80 | 29.85 | 31.72 |          |
| No. of unique edges*  | 6043                   | 5564  | 9841  | 4763  | 5033  |          |
| % of unique edges (%) | 31.08                  | 28.79 | 35.68 | 28.29 | 31.08 |          |
| Gene ID               | Number of unique edges |       |       |       |       | <i>r</i> |
| <i>GFL271</i>         | 11                     | 14    | 22    | 11    | 5     | -0.406   |
| <i>GFL272</i>         | 2                      | 3     | 2     | 1     | 0     | NA       |
| <i>GFL273</i>         | 12                     | 15    | 68    | 13    | 20    | 0.087    |
| <i>GFL274</i>         | 15                     | 36    | 15    | 14    | 8     | -0.491   |
| <i>GFL275</i>         | 0                      | 6     | 1     | 3     | 2     | NA       |
| <i>GFL276</i>         | 2                      | 1     | 3     | 4     | 6     | 0.895*   |
| <i>GFL277</i>         | 21                     | 26    | 19    | 25    | 18    | -0.335   |
| <i>GFL278</i>         | 22                     | 18    | 30    | 15    | 8     | -0.627   |
| <i>GFL279</i>         | 4                      | 1     | 1     | 6     | 5     | 0.429    |
| <i>GFL280</i>         | 0                      | 1     | 2     | 1     | 0     | NA       |
| <i>GFL281</i>         | 4                      | 1     | 3     | 1     | 1     | -0.690   |
| <i>GFL282</i>         | 14                     | 9     | 46    | 16    | 10    | -0.045   |
| <i>GFL283</i>         | 9                      | 12    | 10    | 11    | 12    | 0.659    |
| <i>GFL284</i>         | 5                      | 6     | 15    | 14    | 8     | 0.408    |
| <i>GFL285</i>         | 26                     | 28    | 50    | 17    | 8     | -0.485   |
| <i>GFL286</i>         | 7                      | 2     | 9     | 2     | 0     | NA       |
| <i>GFL287</i>         | 24                     | 34    | 45    | 15    | 26    | -0.161   |
| <i>GFL288</i>         | 4                      | 3     | 13    | 9     | 14    | 0.808    |
| <i>GFL289</i>         | 6                      | 6     | 36    | 4     | 5     | -0.056   |
| <i>GFL290</i>         | 16                     | 11    | 8     | 11    | 16    | 0.034    |
| <i>GFL291</i>         | 13                     | 6     | 16    | 7     | 4     | -0.568   |
| <i>GFL292</i>         | 8                      | 3     | 9     | 3     | 10    | 0.221    |
| <i>GFL293</i>         | 2                      | 11    | 45    | 17    | 13    | 0.249    |
| <i>GFL294</i>         | 29                     | 6     | 24    | 6     | 26    | -0.061   |
| <i>GFL295</i>         | 14                     | 9     | 7     | 10    | 3     | -0.872   |
| <i>GFL296</i>         | 19                     | 14    | 14    | 17    | 14    | -0.544   |
| <i>GFL297</i>         | 28                     | 21    | 23    | 18    | 23    | -0.529   |
| <i>GFL298</i>         | 17                     | 8     | 56    | 9     | 19    | 0.033    |
| <i>GFL299</i>         | 26                     | 24    | 15    | 14    | 11    | -0.938*  |
| <i>GFL300</i>         | 22                     | 19    | 26    | 15    | 11    | -0.718   |



**Table 16** Continued

|                       | G1                     | G2    | G3    | G4    | G5    |          |
|-----------------------|------------------------|-------|-------|-------|-------|----------|
| UHM (mm)              | 26.16                  | 27.76 | 28.80 | 29.85 | 31.72 |          |
| No. of unique edges*  | 6043                   | 5564  | 9841  | 4763  | 5033  |          |
| % of unique edges (%) | 31.08                  | 28.79 | 35.68 | 28.29 | 31.08 |          |
| Gene ID               | Number of unique edges |       |       |       |       | <i>r</i> |
| <i>GFL301</i>         | 5                      | 19    | 11    | 6     | 3     | -0.379   |
| <i>GFL302</i>         | 9                      | 7     | 24    | 4     | 6     | -0.180   |
| <i>GFL303</i>         | 8                      | 2     | 4     | 2     | 1     | -0.816   |
| <i>GFL304</i>         | 41                     | 5     | 40    | 13    | 32    | -0.101   |
| <i>GFL305</i>         | 8                      | 14    | 37    | 13    | 11    | 0.054    |
| <i>GFL306</i>         | 0                      | 0     | 0     | 0     | 1     | NA       |
| <i>GFL307</i>         | 14                     | 8     | 12    | 9     | 9     | -0.595   |
| <i>GFL308</i>         | 26                     | 29    | 23    | 14    | 15    | -0.831   |
| <i>GFL309</i>         | 5                      | 2     | 5     | 2     | 1     | -0.707   |
| <i>GFL310</i>         | 1                      | 3     | 0     | 0     | 3     | NA       |
| <i>GFL311</i>         | 14                     | 22    | 54    | 17    | 10    | -0.131   |
| <i>GFL312</i>         | 10                     | 6     | 19    | 6     | 10    | -0.001   |
| <i>GFL313</i>         | 5                      | 4     | 18    | 4     | 2     | -0.169   |
| <i>GFL314</i>         | 21                     | 19    | 16    | 13    | 11    | -0.983** |
| <i>GFL315</i>         | 17                     | 11    | 51    | 14    | 29    | 0.263    |
| <i>GFL316</i>         | 13                     | 36    | 37    | 11    | 11    | -0.299   |
| <i>GFL317</i>         | 2                      | 1     | 2     | 2     | 0     | NA       |
| <i>GFL318</i>         | 24                     | 24    | 19    | 8     | 4     | -0.933*  |
| <i>GFL319</i>         | 11                     | 16    | 17    | 40    | 27    | 0.708    |
| <i>GFL320</i>         | 3                      | 0     | 13    | 3     | 4     | NA       |
| <i>GFL321</i>         | 3                      | 2     | 8     | 3     | 3     | 0.041    |
| <i>GFL322</i>         | 30                     | 29    | 30    | 13    | 16    | -0.791   |
| <i>GFL323</i>         | 17                     | 16    | 92    | 11    | 16    | -0.041   |
| <i>GFL324</i>         | 6                      | 6     | 13    | 17    | 10    | 0.552    |
| <i>GFL325</i>         | 24                     | 15    | 38    | 12    | 12    | -0.398   |
| <i>GFL326</i>         | 5                      | 11    | 16    | 3     | 9     | 0.053    |
| <i>GFL327</i>         | 3                      | 5     | 6     | 2     | 3     | -0.242   |
| <i>GFL328</i>         | 3                      | 5     | 4     | 3     | 6     | 0.579    |
| <i>GFL329</i>         | 12                     | 13    | 34    | 9     | 11    | -0.094   |
| <i>GFL330</i>         | 3                      | 5     | 4     | 3     | 0     | NA       |

**Table 16** Continued

|                       | G1                     | G2    | G3    | G4    | G5    |          |
|-----------------------|------------------------|-------|-------|-------|-------|----------|
| UHM (mm)              | 26.16                  | 27.76 | 28.80 | 29.85 | 31.72 |          |
| No. of unique edges*  | 6043                   | 5564  | 9841  | 4763  | 5033  |          |
| % of unique edges (%) | 31.08                  | 28.79 | 35.68 | 28.29 | 31.08 |          |
| Gene ID               | Number of unique edges |       |       |       |       | <i>r</i> |
| <i>GFL331</i>         | 0                      | 3     | 3     | 3     | 1     | NA       |
| <i>GFL332</i>         | 17                     | 6     | 43    | 8     | 13    | -0.077   |
| <i>GFL333</i>         | 10                     | 3     | 17    | 3     | 1     | -0.454   |
| <i>GFL334</i>         | 41                     | 13    | 54    | 33    | 12    | -0.400   |
| <i>GFL335</i>         | 9                      | 18    | 16    | 36    | 14    | 0.355    |
| <i>GFL336</i>         | 15                     | 16    | 15    | 27    | 11    | -0.014   |
| <i>GFL337</i>         | 11                     | 27    | 15    | 11    | 26    | 0.378    |
| <i>GFL338</i>         | 12                     | 7     | 40    | 15    | 13    | 0.089    |
| <i>GFL339</i>         | 22                     | 8     | 45    | 18    | 18    | -0.011   |
| <i>GFL340</i>         | 27                     | 29    | 5     | 16    | 22    | -0.321   |
| <i>GFL341</i>         | 9                      | 8     | 16    | 3     | 8     | -0.206   |
| <i>GFL342</i>         | 2                      | 4     | 17    | 7     | 1     | -0.018   |
| <i>GFL343</i>         | 11                     | 6     | 14    | 4     | 4     | -0.573   |
| <i>GFL344</i>         | 15                     | 33    | 16    | 13    | 23    | 0.017    |
| <i>GFL345</i>         | 3                      | 12    | 29    | 8     | 11    | 0.200    |
| <i>GFL346</i>         | 3                      | 4     | 20    | 12    | 7     | 0.312    |
| <i>GFL347</i>         | 18                     | 12    | 23    | 21    | 31    | 0.794    |
| <i>GFL348</i>         | 30                     | 17    | 16    | 58    | 8     | -0.123   |
| <i>GFL349</i>         | 7                      | 3     | 8     | 3     | 6     | -0.128   |
| <i>GFL350</i>         | 10                     | 7     | 21    | 9     | 13    | 0.223    |
| <i>GFL351</i>         | 1                      | 0     | 2     | 1     | 2     | NA       |
| <i>GFL352</i>         | 20                     | 5     | 18    | 18    | 13    | -0.107   |
| <i>GFL353</i>         | 26                     | 25    | 7     | 9     | 11    | -0.748   |
| <i>GFL354</i>         | 14                     | 14    | 13    | 17    | 28    | 0.825    |
| <i>GFL355</i>         | 8                      | 9     | 22    | 12    | 12    | 0.290    |
| <i>GFL356</i>         | 8                      | 12    | 39    | 5     | 9     | -0.053   |
| <i>GFL357</i>         | 57                     | 12    | 42    | 19    | 14    | -0.664   |
| <i>GFL358</i>         | 22                     | 9     | 91    | 16    | 11    | -0.093   |
| <i>GFL359</i>         | 4                      | 2     | 0     | 0     | 2     | NA       |
| <i>GFL360</i>         | 7                      | 2     | 34    | 6     | 4     | -0.050   |

**Table 16** Continued

|                       | G1                     | G2    | G3    | G4    | G5    |          |
|-----------------------|------------------------|-------|-------|-------|-------|----------|
| UHM (mm)              | 26.16                  | 27.76 | 28.80 | 29.85 | 31.72 |          |
| No. of unique edges*  | 6043                   | 5564  | 9841  | 4763  | 5033  |          |
| % of unique edges (%) | 31.08                  | 28.79 | 35.68 | 28.29 | 31.08 |          |
| Gene ID               | Number of unique edges |       |       |       |       | <i>r</i> |
| <i>GFL361</i>         | 22                     | 11    | 30    | 13    | 6     | -0.536   |
| <i>GFL362</i>         | 7                      | 4     | 29    | 2     | 7     | -0.031   |
| <i>GFL363</i>         | 3                      | 9     | 46    | 14    | 27    | 0.491    |
| <i>GFL364</i>         | 5                      | 31    | 11    | 6     | 5     | -0.298   |
| <i>GFL365</i>         | 6                      | 0     | 2     | 0     | 2     | NA       |
| <i>GFL366</i>         | 12                     | 14    | 38    | 20    | 22    | 0.381    |
| <i>GFL367</i>         | 3                      | 13    | 16    | 10    | 13    | 0.573    |
| <i>GFL368</i>         | 20                     | 13    | 5     | 6     | 4     | -0.894*  |
| <i>GFL369</i>         | 7                      | 10    | 32    | 10    | 4     | -0.110   |
| <i>GFL370</i>         | 7                      | 6     | 4     | 3     | 3     | -0.926*  |
| <i>GFL371</i>         | 10                     | 7     | 21    | 6     | 15    | 0.250    |
| <i>GFL372</i>         | 14                     | 20    | 32    | 11    | 5     | -0.421   |
| <i>GFL373</i>         | 19                     | 9     | 66    | 5     | 14    | -0.095   |
| <i>GFL374</i>         | 5                      | 14    | 13    | 13    | 14    | 0.724    |
| <i>GFL375</i>         | 18                     | 22    | 24    | 18    | 19    | -0.082   |
| <i>GFL376</i>         | 11                     | 9     | 21    | 4     | 16    | 0.165    |
| <i>GFL377</i>         | 1                      | 12    | 5     | 9     | 9     | 0.516    |
| <i>GFL378</i>         | 7                      | 17    | 6     | 3     | 2     | -0.583   |
| <i>GFL379</i>         | 8                      | 34    | 17    | 35    | 16    | 0.204    |
| <i>GFL380</i>         | 31                     | 42    | 18    | 20    | 21    | -0.601   |
| <i>GFL381</i>         | 2                      | 1     | 6     | 4     | 0     | NA       |
| <i>GFL382</i>         | 8                      | 10    | 12    | 17    | 16    | 0.908*   |
| <i>GFL383</i>         | 4                      | 2     | 1     | 0     | 1     | NA       |
| <i>GFL384</i>         | 5                      | 2     | 52    | 15    | 9     | 0.128    |
| <i>GFL385</i>         | 2                      | 6     | 9     | 6     | 5     | 0.368    |
| <i>GFL386</i>         | 1                      | 3     | 3     | 1     | 1     | -0.250   |
| <i>GFL387</i>         | 4                      | 2     | 3     | 2     | 1     | -0.868   |
| <i>GFL388</i>         | 21                     | 21    | 26    | 14    | 25    | 0.108    |
| <i>GFL389</i>         | 9                      | 9     | 38    | 7     | 8     | -0.058   |
| <i>GFL390</i>         | 0                      | 4     | 7     | 5     | 4     | NA       |

**Table 16** Continued

|                       | G1                     | G2    | G3    | G4    | G5    |          |
|-----------------------|------------------------|-------|-------|-------|-------|----------|
| UHM (mm)              | 26.16                  | 27.76 | 28.80 | 29.85 | 31.72 |          |
| No. of unique edges*  | 6043                   | 5564  | 9841  | 4763  | 5033  |          |
| % of unique edges (%) | 31.08                  | 28.79 | 35.68 | 28.29 | 31.08 |          |
| Gene ID               | Number of unique edges |       |       |       |       | <i>r</i> |
| <i>GFL391</i>         | 8                      | 11    | 8     | 6     | 13    | 0.389    |
| <i>GFL392</i>         | 14                     | 27    | 37    | 7     | 11    | -0.296   |
| <i>GFL393</i>         | 13                     | 11    | 24    | 35    | 12    | 0.234    |
| <i>GFL394</i>         | 7                      | 9     | 2     | 6     | 5     | -0.397   |
| <i>GFL395</i>         | 1                      | 4     | 7     | 0     | 1     | NA       |
| <i>GFL396</i>         | 4                      | 7     | 10    | 0     | 3     | NA       |
| <i>GFL397</i>         | 15                     | 8     | 13    | 13    | 9     | -0.456   |
| <i>GFL398</i>         | 18                     | 8     | 23    | 5     | 3     | -0.618   |
| <i>GFL399</i>         | 6                      | 16    | 27    | 29    | 10    | 0.257    |
| <i>GFL400</i>         | 10                     | 3     | 8     | 1     | 1     | -0.768   |
| <i>GFL401</i>         | 16                     | 13    | 37    | 12    | 10    | -0.205   |
| <i>GFL402</i>         | 14                     | 50    | 20    | 5     | 7     | -0.449   |
| <i>GFL403</i>         | 5                      | 2     | 5     | 3     | 3     | -0.391   |
| <i>GFL404</i>         | 26                     | 14    | 17    | 15    | 11    | -0.840   |
| <i>GFL405</i>         | 15                     | 12    | 39    | 6     | 3     | -0.345   |
| <i>GFL406</i>         | 16                     | 24    | 38    | 11    | 40    | 0.495    |
| <i>GFL407</i>         | 11                     | 19    | 16    | 7     | 7     | -0.540   |
| <i>GFL408</i>         | 13                     | 21    | 6     | 20    | 9     | -0.233   |
| <i>GFL409</i>         | 13                     | 31    | 33    | 14    | 24    | 0.149    |
| <i>GFL410</i>         | 14                     | 3     | 39    | 10    | 7     | -0.111   |
| <i>GFL411</i>         | 23                     | 17    | 8     | 11    | 9     | -0.839   |
| <i>GFL412</i>         | 5                      | 3     | 12    | 13    | 5     | 0.253    |
| <i>GFL413</i>         | 2                      | 2     | 4     | 5     | 4     | 0.760    |
| <i>GFL414</i>         | 15                     | 15    | 21    | 8     | 14    | -0.260   |
| <i>GFL415</i>         | 9                      | 9     | 9     | 29    | 7     | 0.181    |
| <i>GFL416</i>         | 7                      | 8     | 57    | 18    | 19    | 0.241    |
| <i>GFL417</i>         | 9                      | 6     | 31    | 11    | 7     | -0.019   |
| <i>GFL418</i>         | 16                     | 35    | 16    | 4     | 36    | 0.213    |
| <i>GFL419</i>         | 29                     | 11    | 58    | 12    | 19    | -0.167   |
| <i>GFL420</i>         | 10                     | 2     | 5     | 2     | 2     | -0.741   |

**Table 16** Continued

|                       | G1                     | G2    | G3    | G4    | G5    |          |
|-----------------------|------------------------|-------|-------|-------|-------|----------|
| UHM (mm)              | 26.16                  | 27.76 | 28.80 | 29.85 | 31.72 |          |
| No. of unique edges*  | 6043                   | 5564  | 9841  | 4763  | 5033  |          |
| % of unique edges (%) | 31.08                  | 28.79 | 35.68 | 28.29 | 31.08 |          |
| Gene ID               | Number of unique edges |       |       |       |       | <i>r</i> |
| <i>GFL421</i>         | 1                      | 4     | 5     | 7     | 11    | 0.994*** |
| <i>GFL422</i>         | 4                      | 10    | 13    | 4     | 15    | 0.573    |
| <i>GFL423</i>         | 4                      | 11    | 6     | 9     | 20    | 0.824    |
| <i>GFL424</i>         | 2                      | 2     | 3     | 1     | 1     | -0.555   |
| <i>GFL425</i>         | 7                      | 15    | 46    | 7     | 14    | 0.067    |
| <i>GFL426</i>         | 20                     | 8     | 18    | 6     | 18    | -0.115   |
| <i>GFL427</i>         | 2                      | 0     | 6     | 0     | 3     | NA       |
| <i>GFL428</i>         | 0                      | 0     | 0     | 0     | 0     | NA       |
| <i>GFL429</i>         | 9                      | 15    | 10    | 8     | 19    | 0.537    |
| <i>GFL430</i>         | 4                      | 6     | 2     | 6     | 25    | 0.767    |
| <i>GFL431</i>         | 3                      | 6     | 15    | 11    | 4     | 0.159    |
| <i>GFL432</i>         | 12                     | 9     | 35    | 7     | 7     | -0.172   |
| <i>GFL433</i>         | 17                     | 7     | 16    | 22    | 20    | 0.506    |
| <i>GFL434</i>         | 0                      | 1     | 0     | 2     | 2     | NA       |
| <i>GFL435</i>         | 11                     | 11    | 22    | 11    | 31    | 0.744    |
| <i>GFL436</i>         | 33                     | 50    | 20    | 7     | 20    | -0.591   |
| <i>GFL437</i>         | 6                      | 3     | 6     | 4     | 2     | -0.674   |
| <i>GFL438</i>         | 6                      | 2     | 4     | 2     | 6     | 0.033    |
| <i>GFL439</i>         | 31                     | 12    | 11    | 8     | 3     | -0.904*  |
| <i>GFL440</i>         | 13                     | 9     | 11    | 7     | 19    | 0.408    |
| <i>GFL441</i>         | 5                      | 2     | 21    | 3     | 4     | -0.037   |
| <i>GFL442</i>         | 41                     | 11    | 26    | 9     | 8     | -0.768   |
| <i>GFL443</i>         | 6                      | 16    | 54    | 7     | 6     | -0.073   |
| <i>GFL444</i>         | 8                      | 4     | 8     | 3     | 8     | -0.026   |
| <i>GFL445</i>         | 26                     | 20    | 35    | 13    | 20    | -0.346   |
| <i>GFL446</i>         | 22                     | 4     | 15    | 5     | 19    | -0.076   |
| <i>GFL447</i>         | 24                     | 25    | 11    | 21    | 15    | -0.576   |
| <i>GFL448</i>         | 17                     | 11    | 42    | 11    | 13    | -0.110   |
| <i>GFL449</i>         | 7                      | 5     | 28    | 4     | 6     | -0.056   |
| <i>GFL450</i>         | 0                      | 0     | 0     | 0     | 2     | NA       |

**Table 16** Continued

|                       | G1                     | G2    | G3    | G4    | G5    |          |
|-----------------------|------------------------|-------|-------|-------|-------|----------|
| UHM (mm)              | 26.16                  | 27.76 | 28.80 | 29.85 | 31.72 |          |
| No. of unique edges*  | 6043                   | 5564  | 9841  | 4763  | 5033  |          |
| % of unique edges (%) | 31.08                  | 28.79 | 35.68 | 28.29 | 31.08 |          |
| Gene ID               | Number of unique edges |       |       |       |       | <i>r</i> |
| <i>GFL451</i>         | 3                      | 8     | 7     | 4     | 5     | 0.058    |
| <i>GFL452</i>         | 12                     | 18    | 45    | 18    | 25    | 0.322    |
| <i>GFL453</i>         | 9                      | 9     | 17    | 5     | 13    | 0.184    |
| <i>GFL454</i>         | 26                     | 11    | 13    | 13    | 34    | 0.321    |
| <i>GFL455</i>         | 1                      | 3     | 1     | 3     | 2     | 0.314    |
| <i>GFL456</i>         | 1                      | 2     | 18    | 23    | 9     | 0.521    |
| <i>GFL457</i>         | 1                      | 0     | 3     | 2     | 0     | NA       |
| <i>GFL458</i>         | 17                     | 23    | 16    | 13    | 16    | -0.432   |
| <i>GFL459</i>         | 14                     | 6     | 4     | 9     | 9     | -0.312   |
| <i>GFL460</i>         | 0                      | 2     | 2     | 2     | 2     | NA       |
| <i>GFL461</i>         | 3                      | 9     | 36    | 9     | 7     | 0.081    |
| <i>GFL462</i>         | 22                     | 4     | 6     | 9     | 19    | -0.011   |
| <i>GFL463</i>         | 13                     | 7     | 8     | 5     | 34    | 0.592    |
| <i>GFL464</i>         | 15                     | 22    | 10    | 27    | 38    | 0.769    |
| <i>GFL465</i>         | 8                      | 13    | 60    | 9     | 12    | 0.022    |
| <i>GFL466</i>         | 30                     | 9     | 62    | 11    | 15    | -0.218   |
| <i>GFL467</i>         | 17                     | 25    | 52    | 7     | 17    | -0.143   |
| <i>GFL468</i>         | 24                     | 3     | 7     | 5     | 13    | -0.369   |
| <i>GFL469</i>         | 55                     | 13    | 44    | 14    | 10    | -0.702   |
| <i>GFL470</i>         | 0                      | 0     | 1     | 2     | 0     | NA       |
| <i>GFL471</i>         | 2                      | 19    | 2     | 10    | 7     | 0.060    |
| <i>GFL472</i>         | 8                      | 4     | 8     | 6     | 7     | -0.032   |
| <i>GFL473</i>         | 2                      | 5     | 3     | 4     | 10    | 0.823    |
| <i>GFL474</i>         | 17                     | 11    | 11    | 11    | 15    | -0.199   |

(\*) significant at  $P \leq 0.05$ ; (\*\*) significant at  $P \leq 0.01$ ; (\*\*\*) significant at  $P \leq 0.001$

above analysis. For instance, 16 unique edges for the G3 network were contributed by *GFL165* (Table 16) that had 383 edges in the *GFL* network of the entire RIL population (Table 12).

Two network-specific nodes were found, one (*GFL450*) specific for the network of G5 and the other (*GFL093*) for that of G2 (Table 16). Unique edges connected from *GFL450* were only observed in G5, and those connected from *GFL093* were only in G2. As shown in Table 8, *GFL093* had a negative effect on UHML whereas *GFL450* had positive effect on UHML when they had increased expressions. The uniqueness of the *GFL* genes for the networks may play a critical role in the UHMLs of the RIL groups, though additional studies will be needed to test the hypothesis.

### **3.5 *GFL* genes of diploid cottons and molecular mechanisms of fiber length evolution in the process of cotton polyploidization**

Cultivated tetraploid cottons originated through a process of hybridization and polyploidization between an A-genome diploid species and a D-genome diploid species (Zhang et al. 2014). It has been documented that fiber (seed trichomes) lengths vary dramatically from diploids to tetraploid cottons. Therefore, it was hypothesized that the *GFL* genes isolated from the tetraploid cottons must have different networks from those of diploid cottons and these differences may contribute to the observed UHML variation between diploid and tetraploid cottons. To test this hypothesis, 10-dpa fibers (for A-genome diploid species) or seed coats (for the D-genome diploid species) were collected from two A-genome diploid species and five D-genome diploid species. The genes

expressed in the tissues were sequenced and profiled in expression. The orthologous of all 474 *GFL* genes of the tetraploid cottons were identified from the genes expressed in 10-dpa fibers or seed coats of the diploids, suggesting the conservation of the *GFL* genes during the process of polyploidization from diploids to tetraploids.

Gene networks were constructed from the *GFL* orthologous genes of the A- and D-genome diploids, respectively. As a result, 428 of the 474 A-genome diploid *GFL* orthologous genes were constructed into a single network, with a total of 5,775 edges (Fig. 25) and 436 of the 474 D-genome diploid *GFL* orthologous genes were constructed into a single network, with a total of 5,395 edges (Fig. 26), under a significance level of  $P \leq 0.05$  (Table 17). The number of nodes for the A-genome diploid network was 46 fewer than the number of nodes of the tetraploids, and the number of nodes for the D-genome diploid network was 38 less than that of tetraploids. The number of nodes of the *GFL* gene network increased by 10.75% and 8.72% during the process of polyploidization from diploid cottons, A-genome and D-genome, to tetraploid cottons. Furthermore, the number of edges varied dramatically from diploids to tetraploids. Of all possible interactions (edges), 46.38% were found in the network of tetraploid cottons, whereas only 5.69 and 6.32% were observed in the networks of A- and D-genome diploids, respectively. The process of polyploidization from diploids to tetraploids thus led to an increase of edges by nearly 10-fold (Fig. 27). In comparison among the D-, A- and AD-genome species that have a fiber length from short to longer fibers, the numbers of nodes varied by 1.87% between D- and A-genome species and 10.75% or 8.72% between A- or D-genome species and AD-genome species whereas the numbers of edges



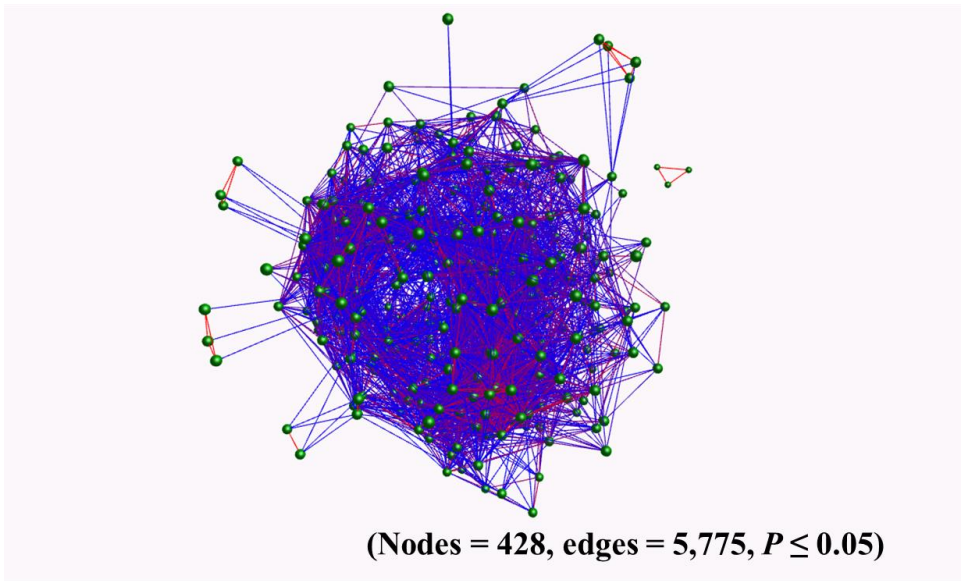


**Figure 25** The network of the *GFL* orthologous genes in the A-genome diploids

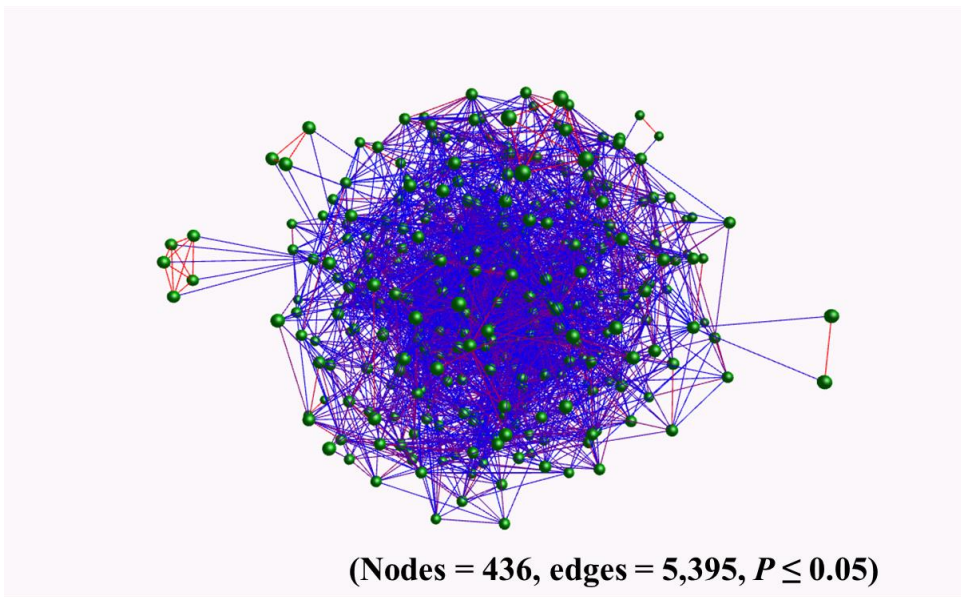


**Figure 26** The network of the *GFL* orthologous genes in the D-genome diploids

**Table 17** Comparison of the networks of the *GFL* genes among A- and D-genome diploid species and AD-genome tetraploid cottons

| <b>subject</b>                     | <b>tetraploid (AADD)</b> | <b>diploid (AA)</b> | <b>diploid (DD)</b> |
|------------------------------------|--------------------------|---------------------|---------------------|
| No. of RILs, accessions or species | 200                      | 8                   | 9                   |
| # of <i>GFL</i> genes identified   | 474                      | 474                 | 474                 |
| # of edges in network              | 51,993                   | 5,775               | 5,395               |
| # of nodes in network              | 474                      | 428                 | 436                 |
| # of all possible edges            | 112101                   | 91378               | 94830               |
| % of edges in network              | 46.38                    | 6.32                | 5.69                |
| Markov clusters                    | 3                        | 29                  | 31                  |

varied by 7.04% between D- and A-genome species and by over 8-fold between A- or D-genome species and AD-genome species. This result further suggested the importance of the edge number variation of the networks in UHML performance.

Careful examination of the network edges revealed that 238 edges were shared among the networks of the A-genome diploids, D-genome diploids, and AD-genome tetraploid cottons (Fig. 28; Tables 18 and 19). The shared edges were contributed by 176 *GFL* genes, with an average of 2.7 edges per gene and a range from 1 to 12 edges (Table 19). There were 384 (238 + 146) edges shared between the networks of A- and D-genome species, whereas there were 3,262 edges common between the networks of A- and AD-genome species, and 3,006 edges common between the networks of D- and AD-genome species (Fig. 28). The network of AD-genome cotton shared more edges with that of A-genome species than D-genome species by 8.52%. In comparison, the network of AD-genome species have also many more network-specific edges (45,963) than that of either A (2,368)- or D (2,514)-genome species. These changes may have contributed to the difference of UHML among the A-, D- and AD-genome species.

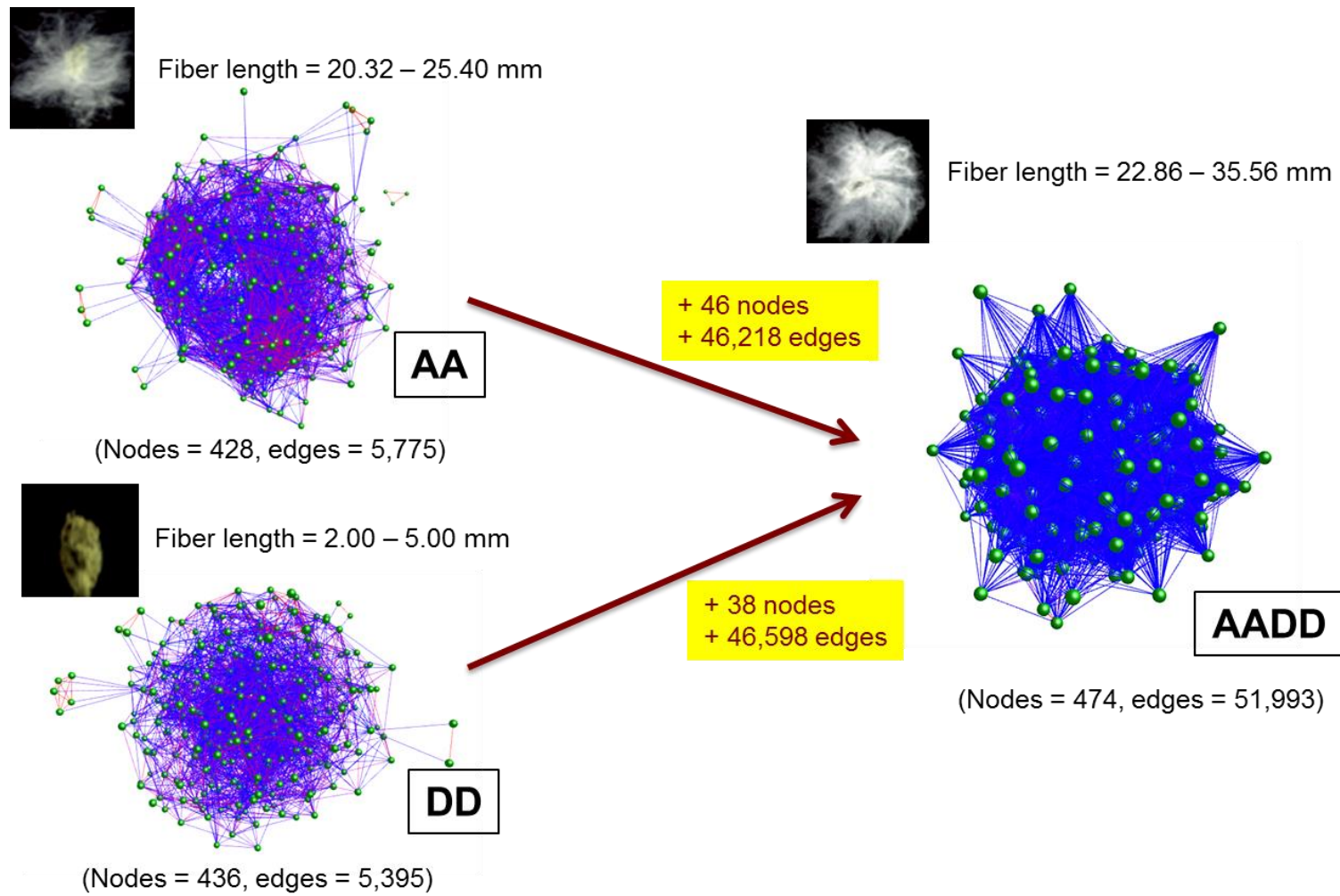


**Figure 27** Node and edge number variations of the *GFL* gene network from diploids (AA and DD) to tetraploid cottons (AADD). Fiber pictures were from Paterson et al. (2012).

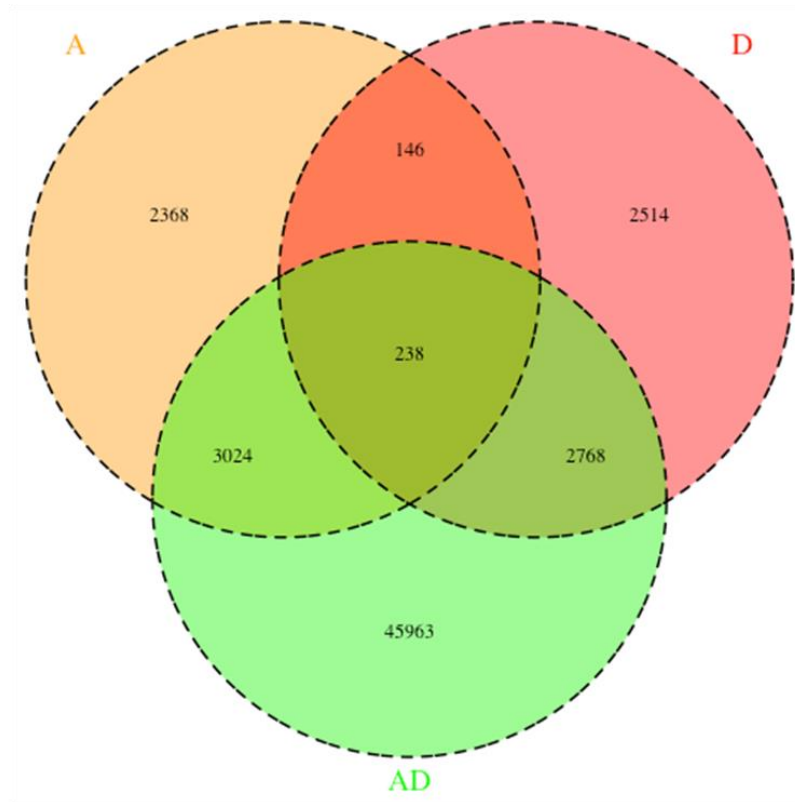


**Figure 28** Variation of numbers of edges among the *GFL* networks of A-, D- and AD-genome species

**Table 18** Correlation coefficients ( $P \leq 0.05$ ) of edges shared among the *GFL* networks of tetraploid (AADD), A-genome diploid (AA) and D-genome diploid (DD) species

| Gene ID <sup>a</sup> | Gene ID <sup>a</sup> | AA    | DD    | AADD  |
|----------------------|----------------------|-------|-------|-------|
| <i>GFL409</i>        | <i>GFL123</i>        | 0.762 | 0.700 | 0.321 |
| <i>GFL242</i>        | <i>GFL370</i>        | 0.810 | 0.762 | 0.307 |
| <i>GFL322</i>        | <i>GFL274</i>        | 0.786 | 0.783 | 0.336 |
| <i>GFL322</i>        | <i>GFL207</i>        | 0.738 | 0.850 | 0.212 |
| <i>GFL339</i>        | <i>GFL256</i>        | 0.791 | 0.879 | 0.289 |
| <i>GFL269</i>        | <i>GFL309</i>        | 0.810 | 0.728 | 0.548 |
| <i>GFL061</i>        | <i>GFL220</i>        | 0.755 | 0.703 | 0.324 |
| <i>GFL285</i>        | <i>GFL232</i>        | 0.833 | 0.733 | 0.304 |
| <i>GFL285</i>        | <i>GFL301</i>        | 0.905 | 0.767 | 0.287 |
| <i>GFL158</i>        | <i>GFL157</i>        | 0.826 | 0.700 | 0.439 |
| <i>GFL087</i>        | <i>GFL163</i>        | 0.755 | 0.895 | 0.202 |
| <i>GFL087</i>        | <i>GFL026</i>        | 0.874 | 0.762 | 0.150 |
| <i>GFL143</i>        | <i>GFL319</i>        | 0.850 | 0.854 | 0.256 |
| <i>GFL143</i>        | <i>GFL230</i>        | 0.810 | 0.932 | 0.206 |
| <i>GFL143</i>        | <i>GFL371</i>        | 0.738 | 0.895 | 0.159 |
| <i>GFL143</i>        | <i>GFL220</i>        | 0.738 | 0.733 | 0.225 |
| <i>GFL143</i>        | <i>GFL095</i>        | 0.857 | 0.714 | 0.235 |
| <i>GFL143</i>        | <i>GFL098</i>        | 0.762 | 0.850 | 0.258 |
| <i>GFL143</i>        | <i>GFL331</i>        | 0.762 | 0.733 | 0.306 |
| <i>GFL143</i>        | <i>GFL128</i>        | 0.790 | 0.711 | 0.222 |
| <i>GFL143</i>        | <i>GFL115</i>        | 0.905 | 0.800 | 0.412 |
| <i>GFL452</i>        | <i>GFL055</i>        | 0.762 | 0.700 | 0.155 |
| <i>GFL049</i>        | <i>GFL190</i>        | 0.934 | 0.776 | 0.310 |
| <i>GFL049</i>        | <i>GFL180</i>        | 0.755 | 0.733 | 0.427 |
| <i>GFL049</i>        | <i>GFL034</i>        | 0.896 | 0.731 | 0.279 |
| <i>GFL366</i>        | <i>GFL173</i>        | 0.762 | 0.750 | 0.514 |
| <i>GFL366</i>        | <i>GFL190</i>        | 0.743 | 0.819 | 0.275 |
| <i>GFL366</i>        | <i>GFL127</i>        | 0.786 | 0.800 | 0.348 |
| <i>GFL366</i>        | <i>GFL237</i>        | 0.857 | 0.700 | 0.452 |
| <i>GFL366</i>        | <i>GFL394</i>        | 0.762 | 0.733 | 0.270 |
| <i>GFL308</i>        | <i>GFL295</i>        | 0.762 | 0.767 | 0.318 |
| <i>GFL069</i>        | <i>GFL246</i>        | 0.850 | 0.748 | 0.386 |
| <i>GFL069</i>        | <i>GFL127</i>        | 0.786 | 0.929 | 0.190 |

**Table 18** Continued

| Gene ID <sup>a</sup> | Gene ID <sup>a</sup> | AA    | DD    | AADD  |
|----------------------|----------------------|-------|-------|-------|
| <i>GFL069</i>        | <i>GFL159</i>        | 0.762 | 0.874 | 0.196 |
| <i>GFL069</i>        | <i>GFL120</i>        | 0.738 | 0.753 | 0.301 |
| <i>GFL323</i>        | <i>GFL129</i>        | 0.755 | 0.717 | 0.264 |
| <i>GFL012</i>        | <i>GFL202</i>        | 0.811 | 0.717 | 0.238 |
| <i>GFL012</i>        | <i>GFL084</i>        | 0.779 | 0.883 | 0.179 |
| <i>GFL334</i>        | <i>GFL244</i>        | 0.811 | 0.790 | 0.176 |
| <i>GFL334</i>        | <i>GFL060</i>        | 0.756 | 0.717 | 0.165 |
| <i>GFL334</i>        | <i>GFL223</i>        | 0.756 | 0.800 | 0.179 |
| <i>GFL268</i>        | <i>GFL065</i>        | 0.766 | 0.837 | 0.458 |
| <i>GFL233</i>        | <i>GFL325</i>        | 0.881 | 0.800 | 0.322 |
| <i>GFL233</i>        | <i>GFL244</i>        | 0.792 | 0.849 | 0.142 |
| <i>GFL233</i>        | <i>GFL223</i>        | 0.738 | 0.767 | 0.607 |
| <i>GFL135</i>        | <i>GFL079</i>        | 0.786 | 0.703 | 0.492 |
| <i>GFL135</i>        | <i>GFL190</i>        | 0.826 | 0.826 | 0.246 |
| <i>GFL135</i>        | <i>GFL026</i>        | 0.905 | 0.753 | 0.191 |
| <i>GFL135</i>        | <i>GFL030</i>        | 0.762 | 0.787 | 0.373 |
| <i>GFL135</i>        | <i>GFL130</i>        | 0.905 | 0.728 | 0.277 |
| <i>GFL135</i>        | <i>GFL225</i>        | 0.857 | 0.837 | 0.316 |
| <i>GFL135</i>        | <i>GFL343</i>        | 0.810 | 0.845 | 0.333 |
| <i>GFL135</i>        | <i>GFL207</i>        | 0.810 | 0.703 | 0.372 |
| <i>GFL135</i>        | <i>GFL198</i>        | 0.976 | 0.812 | 0.244 |
| <i>GFL135</i>        | <i>GFL236</i>        | 0.762 | 0.778 | 0.325 |
| <i>GFL135</i>        | <i>GFL007</i>        | 0.905 | 0.728 | 0.168 |
| <i>GFL013</i>        | <i>GFL081</i>        | 0.756 | 0.874 | 0.204 |
| <i>GFL325</i>        | <i>GFL244</i>        | 0.856 | 0.832 | 0.164 |
| <i>GFL325</i>        | <i>GFL163</i>        | 0.833 | 0.750 | 0.571 |
| <i>GFL325</i>        | <i>GFL060</i>        | 0.810 | 0.817 | 0.340 |
| <i>GFL325</i>        | <i>GFL046</i>        | 0.738 | 0.833 | 0.383 |
| <i>GFL197</i>        | <i>GFL080</i>        | 0.786 | 0.727 | 0.317 |
| <i>GFL232</i>        | <i>GFL329</i>        | 0.738 | 0.767 | 0.273 |
| <i>GFL319</i>        | <i>GFL103</i>        | 0.934 | 0.770 | 0.348 |
| <i>GFL079</i>        | <i>GFL293</i>        | 0.905 | 0.700 | 0.386 |
| <i>GFL079</i>        | <i>GFL052</i>        | 0.833 | 0.717 | 0.288 |
| <i>GFL048</i>        | <i>GFL349</i>        | 0.764 | 0.785 | 0.275 |

**Table 18** Continued

| Gene ID <sup>a</sup> | Gene ID <sup>a</sup> | AA    | DD    | AADD  |
|----------------------|----------------------|-------|-------|-------|
| <i>GFL219</i>        | <i>GFL329</i>        | 0.786 | 0.700 | 0.339 |
| <i>GFL219</i>        | <i>GFL230</i>        | 0.738 | 0.763 | 0.226 |
| <i>GFL244</i>        | <i>GFL060</i>        | 0.792 | 0.916 | 0.188 |
| <i>GFL246</i>        | <i>GFL120</i>        | 0.778 | 0.904 | 0.273 |
| <i>GFL304</i>        | <i>GFL448</i>        | 0.939 | 0.902 | 0.153 |
| <i>GFL304</i>        | <i>GFL016</i>        | 0.810 | 0.854 | 0.208 |
| <i>GFL163</i>        | <i>GFL389</i>        | 0.905 | 0.800 | 0.253 |
| <i>GFL163</i>        | <i>GFL038</i>        | 0.786 | 0.865 | 0.321 |
| <i>GFL163</i>        | <i>GFL330</i>        | 0.952 | 0.729 | 0.511 |
| <i>GFL173</i>        | <i>GFL190</i>        | 0.778 | 0.937 | 0.288 |
| <i>GFL085</i>        | <i>GFL162</i>        | 0.791 | 0.700 | 0.186 |
| <i>GFL392</i>        | <i>GFL321</i>        | 0.854 | 0.817 | 0.221 |
| <i>GFL267</i>        | <i>GFL190</i>        | 0.862 | 0.836 | 0.309 |
| <i>GFL267</i>        | <i>GFL026</i>        | 0.810 | 0.750 | 0.312 |
| <i>GFL267</i>        | <i>GFL225</i>        | 0.857 | 0.733 | 0.335 |
| <i>GFL267</i>        | <i>GFL343</i>        | 0.786 | 0.850 | 0.809 |
| <i>GFL267</i>        | <i>GFL198</i>        | 0.905 | 0.733 | 0.248 |
| <i>GFL267</i>        | <i>GFL180</i>        | 0.946 | 0.733 | 0.266 |
| <i>GFL373</i>        | <i>GFL400</i>        | 0.851 | 0.797 | 0.256 |
| <i>GFL336</i>        | <i>GFL377</i>        | 0.862 | 0.800 | 0.332 |
| <i>GFL170</i>        | <i>GFL188</i>        | 0.762 | 0.833 | 0.159 |
| <i>GFL329</i>        | <i>GFL230</i>        | 0.738 | 0.831 | 0.310 |
| <i>GFL329</i>        | <i>GFL121</i>        | 0.810 | 0.733 | 0.212 |
| <i>GFL329</i>        | <i>GFL168</i>        | 0.857 | 0.700 | 0.318 |
| <i>GFL329</i>        | <i>GFL220</i>        | 0.762 | 0.800 | 0.515 |
| <i>GFL329</i>        | <i>GFL095</i>        | 0.857 | 0.798 | 0.305 |
| <i>GFL329</i>        | <i>GFL081</i>        | 0.756 | 0.717 | 0.279 |
| <i>GFL329</i>        | <i>GFL152</i>        | 0.881 | 0.733 | 0.143 |
| <i>GFL329</i>        | <i>GFL098</i>        | 0.738 | 0.750 | 0.406 |
| <i>GFL329</i>        | <i>GFL309</i>        | 0.810 | 0.800 | 0.388 |
| <i>GFL329</i>        | <i>GFL115</i>        | 0.786 | 0.900 | 0.614 |
| <i>GFL190</i>        | <i>GFL026</i>        | 0.850 | 0.836 | 0.146 |
| <i>GFL190</i>        | <i>GFL030</i>        | 0.743 | 0.852 | 0.280 |
| <i>GFL190</i>        | <i>GFL225</i>        | 0.970 | 0.903 | 0.180 |
| <i>GFL190</i>        | <i>GFL237</i>        | 0.778 | 0.751 | 0.262 |

**Table 18** Continued

| Gene ID <sup>a</sup> | Gene ID <sup>a</sup> | AA    | DD    | AADD  |
|----------------------|----------------------|-------|-------|-------|
| <i>GFL190</i>        | <i>GFL343</i>        | 0.743 | 0.836 | 0.267 |
| <i>GFL190</i>        | <i>GFL198</i>        | 0.755 | 0.785 | 0.260 |
| <i>GFL190</i>        | <i>GFL180</i>        | 0.873 | 0.743 | 0.255 |
| <i>GFL060</i>        | <i>GFL230</i>        | 0.786 | 0.848 | 0.409 |
| <i>GFL060</i>        | <i>GFL363</i>        | 0.756 | 0.785 | 0.142 |
| <i>GFL060</i>        | <i>GFL220</i>        | 0.810 | 0.700 | 0.386 |
| <i>GFL060</i>        | <i>GFL073</i>        | 0.786 | 0.800 | 0.369 |
| <i>GFL050</i>        | <i>GFL124</i>        | 0.790 | 0.870 | 0.211 |
| <i>GFL464</i>        | <i>GFL147</i>        | 0.894 | 0.811 | 0.171 |
| <i>GFL092</i>        | <i>GFL203</i>        | 0.862 | 0.718 | 0.282 |
| <i>GFL029</i>        | <i>GFL424</i>        | 0.764 | 0.756 | 0.141 |
| <i>GFL103</i>        | <i>GFL051</i>        | 0.881 | 0.783 | 0.720 |
| <i>GFL103</i>        | <i>GFL456</i>        | 0.833 | 0.767 | 0.285 |
| <i>GFL188</i>        | <i>GFL044</i>        | 0.773 | 0.725 | 0.195 |
| <i>GFL188</i>        | <i>GFL377</i>        | 0.738 | 0.883 | 0.502 |
| <i>GFL247</i>        | <i>GFL398</i>        | 0.810 | 0.800 | 0.296 |
| <i>GFL247</i>        | <i>GFL331</i>        | 0.738 | 0.733 | 0.383 |
| <i>GFL230</i>        | <i>GFL220</i>        | 0.833 | 0.831 | 0.439 |
| <i>GFL230</i>        | <i>GFL095</i>        | 0.905 | 0.735 | 0.322 |
| <i>GFL230</i>        | <i>GFL081</i>        | 0.781 | 0.763 | 0.186 |
| <i>GFL230</i>        | <i>GFL115</i>        | 0.881 | 0.729 | 0.518 |
| <i>GFL026</i>        | <i>GFL394</i>        | 0.810 | 0.833 | 0.334 |
| <i>GFL026</i>        | <i>GFL343</i>        | 0.762 | 0.733 | 0.283 |
| <i>GFL026</i>        | <i>GFL124</i>        | 0.738 | 0.733 | 0.486 |
| <i>GFL026</i>        | <i>GFL185</i>        | 0.762 | 0.717 | 0.386 |
| <i>GFL026</i>        | <i>GFL236</i>        | 0.762 | 0.717 | 0.538 |
| <i>GFL404</i>        | <i>GFL171</i>        | 0.833 | 0.767 | 0.171 |
| <i>GFL404</i>        | <i>GFL052</i>        | 0.881 | 0.800 | 0.141 |
| <i>GFL114</i>        | <i>GFL363</i>        | 0.805 | 0.712 | 0.166 |
| <i>GFL114</i>        | <i>GFL318</i>        | 0.762 | 0.867 | 0.375 |
| <i>GFL078</i>        | <i>GFL043</i>        | 0.857 | 0.800 | 0.178 |
| <i>GFL078</i>        | <i>GFL220</i>        | 0.738 | 0.700 | 0.455 |
| <i>GFL121</i>        | <i>GFL327</i>        | 0.786 | 0.711 | 0.241 |
| <i>GFL121</i>        | <i>GFL227</i>        | 0.761 | 0.783 | 0.219 |
| <i>GFL121</i>        | <i>GFL211</i>        | 0.833 | 0.800 | 0.195 |



**Table 18** Continued

| Gene ID <sup>a</sup> | Gene ID <sup>a</sup> | AA    | DD    | AADD  |
|----------------------|----------------------|-------|-------|-------|
| <i>GFL121</i>        | <i>GFL193</i>        | 0.810 | 0.883 | 0.424 |
| <i>GFL311</i>        | <i>GFL175</i>        | 0.810 | 0.739 | 0.331 |
| <i>GFL016</i>        | <i>GFL275</i>        | 0.738 | 0.800 | 0.435 |
| <i>GFL171</i>        | <i>GFL020</i>        | 0.847 | 0.745 | 0.498 |
| <i>GFL171</i>        | <i>GFL253</i>        | 0.762 | 0.733 | 0.278 |
| <i>GFL171</i>        | <i>GFL377</i>        | 0.810 | 0.717 | 0.381 |
| <i>GFL171</i>        | <i>GFL045</i>        | 0.762 | 0.800 | 0.295 |
| <i>GFL171</i>        | <i>GFL052</i>        | 0.857 | 0.750 | 0.298 |
| <i>GFL127</i>        | <i>GFL020</i>        | 0.798 | 0.762 | 0.170 |
| <i>GFL127</i>        | <i>GFL280</i>        | 0.819 | 0.717 | 0.271 |
| <i>GFL020</i>        | <i>GFLA01</i>        | 0.822 | 0.778 | 0.325 |
| <i>GFL020</i>        | <i>GFL130</i>        | 0.749 | 0.728 | 0.304 |
| <i>GFL020</i>        | <i>GFL192</i>        | 0.798 | 0.738 | 0.453 |
| <i>GFL020</i>        | <i>GFL198</i>        | 0.872 | 0.745 | 0.251 |
| <i>GFL020</i>        | <i>GFL178</i>        | 0.847 | 0.843 | 0.246 |
| <i>GFL020</i>        | <i>GFL185</i>        | 0.872 | 0.762 | 0.208 |
| <i>GFL338</i>        | <i>GFL073</i>        | 0.786 | 0.750 | 0.218 |
| <i>GFL046</i>        | <i>GFL256</i>        | 0.741 | 0.854 | 0.236 |
| <i>GFL030</i>        | <i>GFL343</i>        | 0.905 | 0.733 | 0.344 |
| <i>GFL354</i>        | <i>GFL371</i>        | 0.786 | 0.778 | 0.332 |
| <i>GFL354</i>        | <i>GFL211</i>        | 0.762 | 0.800 | 0.453 |
| <i>GFL354</i>        | <i>GFL236</i>        | 0.833 | 0.767 | 0.183 |
| <i>GFL205</i>        | <i>GFL105</i>        | 0.738 | 0.703 | 0.374 |
| <i>GFL159</i>        | <i>GFL185</i>        | 0.952 | 0.778 | 0.301 |
| <i>GFL159</i>        | <i>GFL063</i>        | 0.905 | 0.787 | 0.158 |
| <i>GFL371</i>        | <i>GFL306</i>        | 0.738 | 0.762 | 0.157 |
| <i>GFL014</i>        | <i>GFL385</i>        | 0.762 | 0.717 | 0.139 |
| <i>GFL053</i>        | <i>GFL214</i>        | 0.778 | 0.728 | 0.337 |
| <i>GFL168</i>        | <i>GFL327</i>        | 0.905 | 0.820 | 0.412 |
| <i>GFL168</i>        | <i>GFL115</i>        | 0.905 | 0.750 | 0.546 |
| <i>GFL130</i>        | <i>GFL198</i>        | 0.810 | 0.800 | 0.378 |
| <i>GFL130</i>        | <i>GFL240</i>        | 0.810 | 0.733 | 0.415 |
| <i>GFL130</i>        | <i>GFL120</i>        | 0.905 | 0.733 | 0.383 |
| <i>GFL182</i>        | <i>GFL389</i>        | 0.738 | 0.733 | 0.145 |

**Table 18** Continued

| Gene ID <sup>a</sup> | Gene ID <sup>a</sup> | AA    | DD    | AADD  |
|----------------------|----------------------|-------|-------|-------|
| <i>GFL182</i>        | <i>GFL275</i>        | 0.738 | 0.833 | 0.321 |
| <i>GFL225</i>        | <i>GFL343</i>        | 0.738 | 0.850 | 0.371 |
| <i>GFL367</i>        | <i>GFL120</i>        | 0.952 | 0.817 | 0.656 |
| <i>GFL417</i>        | <i>GFL398</i>        | 0.790 | 0.728 | 0.243 |
| <i>GFL220</i>        | <i>GFL073</i>        | 0.738 | 0.767 | 0.414 |
| <i>GFL220</i>        | <i>GFL095</i>        | 0.952 | 0.849 | 0.357 |
| <i>GFL220</i>        | <i>GFL309</i>        | 0.810 | 0.717 | 0.463 |
| <i>GFL220</i>        | <i>GFL115</i>        | 0.929 | 0.750 | 0.561 |
| <i>GFL106</i>        | <i>GFL180</i>        | 0.771 | 0.717 | 0.438 |
| <i>GFL407</i>        | <i>GFL152</i>        | 0.738 | 0.767 | 0.170 |
| <i>GFL165</i>        | <i>GFL038</i>        | 0.905 | 0.898 | 0.393 |
| <i>GFL453</i>        | <i>GFL066</i>        | 0.810 | 0.723 | 0.140 |
| <i>GFL324</i>        | <i>GFL198</i>        | 0.762 | 0.817 | 0.305 |
| <i>GFL095</i>        | <i>GFL098</i>        | 0.738 | 0.723 | 0.279 |
| <i>GFL095</i>        | <i>GFL327</i>        | 0.976 | 0.705 | 0.253 |
| <i>GFL095</i>        | <i>GFL309</i>        | 0.857 | 0.748 | 0.139 |
| <i>GFL095</i>        | <i>GFL115</i>        | 0.976 | 0.874 | 0.372 |
| <i>GFL123</i>        | <i>GFL134</i>        | 0.790 | 0.709 | 0.222 |
| <i>GFL123</i>        | <i>GFL124</i>        | 0.833 | 0.867 | 0.500 |
| <i>GFL123</i>        | <i>GFL387</i>        | 0.778 | 0.800 | 0.395 |
| <i>GFL237</i>        | <i>GFL394</i>        | 0.857 | 0.867 | 0.325 |
| <i>GFL237</i>        | <i>GFL343</i>        | 0.810 | 0.750 | 0.330 |
| <i>GFL410</i>        | <i>GFL194</i>        | 0.857 | 0.833 | 0.277 |
| <i>GFL389</i>        | <i>GFL084</i>        | 0.810 | 0.817 | 0.160 |
| <i>GFL150</i>        | <i>GFL377</i>        | 0.738 | 0.845 | 0.384 |
| <i>GFL150</i>        | <i>GFL052</i>        | 0.881 | 0.812 | 0.346 |
| <i>GFL459</i>        | <i>GFL471</i>        | 0.833 | 0.729 | 0.423 |
| <i>GFL459</i>        | <i>GFL427</i>        | 0.755 | 0.809 | 0.221 |
| <i>GFL398</i>        | <i>GFL098</i>        | 0.976 | 0.700 | 0.195 |
| <i>GFL398</i>        | <i>GFL065</i>        | 0.826 | 0.762 | 0.314 |
| <i>GFL022</i>        | <i>GFL055</i>        | 0.766 | 0.833 | 0.176 |
| <i>GFL169</i>        | <i>GFL424</i>        | 0.909 | 0.781 | 0.158 |
| <i>GFL301</i>        | <i>GFL211</i>        | 0.810 | 0.867 | 0.195 |
| <i>GFL301</i>        | <i>GFL034</i>        | 0.822 | 0.782 | 0.270 |

**Table 18** Continued

| Gene ID <sup>a</sup> | Gene ID <sup>a</sup> | AA    | DD    | AADD  |
|----------------------|----------------------|-------|-------|-------|
| <i>GFL108</i>        | <i>GFL055</i>        | 0.738 | 0.983 | 0.204 |
| <i>GFL108</i>        | <i>GFL042</i>        | 0.784 | 0.762 | 0.159 |
| <i>GFL377</i>        | <i>GFL045</i>        | 0.952 | 0.767 | 0.322 |
| <i>GFL377</i>        | <i>GFL052</i>        | 0.762 | 0.867 | 0.228 |
| <i>GFL394</i>        | <i>GFL198</i>        | 0.810 | 0.800 | 0.210 |
| <i>GFL138</i>        | <i>GFL034</i>        | 0.970 | 0.714 | 0.225 |
| <i>GFL471</i>        | <i>GFL331</i>        | 0.762 | 0.700 | 0.171 |
| <i>GFL251</i>        | <i>GFL331</i>        | 0.781 | 0.733 | 0.384 |
| <i>GFL343</i>        | <i>GFL198</i>        | 0.857 | 0.833 | 0.310 |
| <i>GFL343</i>        | <i>GFL185</i>        | 0.881 | 0.750 | 0.220 |
| <i>GFL038</i>        | <i>GFL330</i>        | 0.905 | 0.759 | 0.367 |
| <i>GFL038</i>        | <i>GFL387</i>        | 0.898 | 0.729 | 0.263 |
| <i>GFL327</i>        | <i>GFL309</i>        | 0.833 | 0.736 | 0.543 |
| <i>GFL327</i>        | <i>GFL115</i>        | 0.929 | 0.745 | 0.548 |
| <i>GFL148</i>        | <i>GFL164</i>        | 0.786 | 0.700 | 0.285 |
| <i>GFL045</i>        | <i>GFL052</i>        | 0.762 | 0.817 | 0.218 |
| <i>GFL045</i>        | <i>GFL331</i>        | 0.762 | 0.883 | 0.277 |
| <i>GFL164</i>        | <i>GFL387</i>        | 0.826 | 0.733 | 0.361 |
| <i>GFL164</i>        | <i>GFL383</i>        | 0.738 | 0.822 | 0.156 |
| <i>GFL055</i>        | <i>GFL032</i>        | 0.881 | 0.733 | 0.177 |
| <i>GFL211</i>        | <i>GFL331</i>        | 0.857 | 0.900 | 0.390 |
| <i>GFL211</i>        | <i>GFL120</i>        | 0.738 | 0.750 | 0.491 |
| <i>GFL309</i>        | <i>GFL128</i>        | 0.743 | 0.929 | 0.409 |
| <i>GFL309</i>        | <i>GFL115</i>        | 0.833 | 0.767 | 0.454 |
| <i>GFL105</i>        | <i>GFL202</i>        | 0.756 | 0.843 | 0.242 |
| <i>GFL105</i>        | <i>GFL084</i>        | 0.810 | 0.782 | 0.254 |
| <i>GFL198</i>        | <i>GFL185</i>        | 0.833 | 0.833 | 0.250 |
| <i>GFL198</i>        | <i>GFL180</i>        | 0.755 | 0.717 | 0.345 |
| <i>GFL052</i>        | <i>GFL331</i>        | 0.738 | 0.783 | 0.394 |
| <i>GFL330</i>        | <i>GFL250</i>        | 0.881 | 0.746 | 0.442 |
| <i>GFL202</i>        | <i>GFL084</i>        | 0.805 | 0.700 | 0.325 |
| <i>GFL185</i>        | <i>GFL034</i>        | 0.786 | 0.748 | 0.226 |
| <i>GFL180</i>        | <i>GFL034</i>        | 0.827 | 0.782 | 0.161 |

a: the gene nodes forming the shared edges.

**Table 19** List of nodes (*GFL* genes) that have edges common among the networks of the A-, D- and AD-genome species

| GeneID        | # of edges | % of shared edges |
|---------------|------------|-------------------|
| <i>GFL256</i> | 2          | 0.84              |
| <i>GFL257</i> | 2          | 0.84              |
| <i>GFL258</i> | 1          | 0.42              |
| <i>GFL259</i> | 1          | 0.42              |
| <i>GFL260</i> | 1          | 0.42              |
| <i>GFL261</i> | 5          | 2.10              |
| <i>GFL262</i> | 1          | 0.42              |
| <i>GFL263</i> | 1          | 0.42              |
| <i>GFL264</i> | 1          | 0.42              |
| <i>GFL265</i> | 2          | 0.84              |
| <i>GFL266</i> | 9          | 3.78              |
| <i>GFL267</i> | 6          | 2.52              |
| <i>GFL268</i> | 1          | 0.42              |
| <i>GFL269</i> | 1          | 0.42              |
| <i>GFL270</i> | 3          | 1.26              |
| <i>GFL271</i> | 12         | 5.04              |
| <i>GFL272</i> | 2          | 0.84              |
| <i>GFL273</i> | 8          | 3.36              |
| <i>GFL274</i> | 5          | 2.10              |
| <i>GFL275</i> | 6          | 2.52              |
| <i>GFL276</i> | 1          | 0.42              |
| <i>GFL277</i> | 2          | 0.84              |
| <i>GFL278</i> | 1          | 0.42              |
| <i>GFL279</i> | 3          | 1.26              |
| <i>GFL280</i> | 4          | 1.68              |
| <i>GFL281</i> | 1          | 0.42              |
| <i>GFL282</i> | 1          | 0.42              |
| <i>GFL283</i> | 10         | 4.20              |
| <i>GFL284</i> | 1          | 0.42              |
| <i>GFL285</i> | 8          | 3.36              |
| <i>GFL286</i> | 2          | 0.84              |
| <i>GFL287</i> | 1          | 0.42              |
| <i>GFL288</i> | 4          | 1.68              |

**Table 19** Continued

| GeneID        | # of edges | % of shared edges |
|---------------|------------|-------------------|
| <i>GFL289</i> | 3          | 1.26              |
| <i>GFL290</i> | 2          | 0.84              |
| <i>GFL291</i> | 2          | 0.84              |
| <i>GFL292</i> | 1          | 0.42              |
| <i>GFL293</i> | 5          | 2.10              |
| <i>GFL294</i> | 5          | 2.10              |
| <i>GFL295</i> | 1          | 0.42              |
| <i>GFL296</i> | 1          | 0.42              |
| <i>GFL297</i> | 1          | 0.42              |
| <i>GFL298</i> | 1          | 0.42              |
| <i>GFL299</i> | 1          | 0.42              |
| <i>GFL300</i> | 1          | 0.42              |
| <i>GFL301</i> | 4          | 1.68              |
| <i>GFL302</i> | 4          | 1.68              |
| <i>GFL303</i> | 1          | 0.42              |
| <i>GFL304</i> | 6          | 2.52              |
| <i>GFL305</i> | 4          | 1.68              |
| <i>GFL306</i> | 3          | 1.26              |
| <i>GFL307</i> | 2          | 0.84              |
| <i>GFL308</i> | 2          | 0.84              |
| <i>GFL309</i> | 1          | 0.42              |
| <i>GFL310</i> | 6          | 2.52              |
| <i>GFL311</i> | 8          | 3.36              |
| <i>GFL312</i> | 1          | 0.42              |
| <i>GFL313</i> | 2          | 0.84              |
| <i>GFL314</i> | 3          | 1.26              |
| <i>GFL315</i> | 1          | 0.42              |
| <i>GFL316</i> | 2          | 0.84              |
| <i>GFL317</i> | 2          | 0.84              |
| <i>GFL318</i> | 3          | 1.26              |
| <i>GFL319</i> | 1          | 0.42              |
| <i>GFL320</i> | 11         | 4.62              |
| <i>GFL321</i> | 2          | 0.84              |
| <i>GFL322</i> | 1          | 0.42              |

**Table 19** Continued

| GeneID        | # of edges | % of shared edges |
|---------------|------------|-------------------|
| <i>GFL323</i> | 1          | 0.42              |
| <i>GFL324</i> | 5          | 2.10              |
| <i>GFL325</i> | 3          | 1.26              |
| <i>GFL326</i> | 3          | 1.26              |
| <i>GFL327</i> | 4          | 1.68              |
| <i>GFL328</i> | 1          | 0.42              |
| <i>GFL329</i> | 2          | 0.84              |
| <i>GFL330</i> | 1          | 0.42              |
| <i>GFL331</i> | 1          | 0.42              |
| <i>GFL332</i> | 2          | 0.84              |
| <i>GFL333</i> | 2          | 0.84              |
| <i>GFL334</i> | 2          | 0.84              |
| <i>GFL335</i> | 3          | 1.26              |
| <i>GFL336</i> | 4          | 1.68              |
| <i>GFL337</i> | 7          | 2.94              |
| <i>GFL338</i> | 1          | 0.42              |
| <i>GFL339</i> | 2          | 0.84              |
| <i>GFL340</i> | 1          | 0.42              |
| <i>GFL341</i> | 1          | 0.42              |
| <i>GFL342</i> | 1          | 0.42              |
| <i>GFL343</i> | 2          | 0.84              |
| <i>GFL344</i> | 1          | 0.42              |
| <i>GFL345</i> | 3          | 1.26              |
| <i>GFL346</i> | 1          | 0.42              |
| <i>GFL347</i> | 2          | 0.84              |
| <i>GFL348</i> | 2          | 0.84              |
| <i>GFL349</i> | 4          | 1.68              |
| <i>GFL350</i> | 9          | 3.78              |
| <i>GFL351</i> | 1          | 0.42              |
| <i>GFL352</i> | 3          | 1.26              |
| <i>GFL353</i> | 7          | 2.94              |
| <i>GFL354</i> | 1          | 0.42              |
| <i>GFL355</i> | 1          | 0.42              |
| <i>GFL356</i> | 1          | 0.42              |

**Table 19** Continued

| GeneID        | # of edges | % of shared edges |
|---------------|------------|-------------------|
| <i>GFL357</i> | 1          | 0.42              |
| <i>GFL358</i> | 1          | 0.42              |
| <i>GFL359</i> | 3          | 1.26              |
| <i>GFL360</i> | 3          | 1.26              |
| <i>GFL361</i> | 1          | 0.42              |
| <i>GFL362</i> | 1          | 0.42              |
| <i>GFL363</i> | 1          | 0.42              |
| <i>GFL364</i> | 1          | 0.42              |
| <i>GFL365</i> | 1          | 0.42              |
| <i>GFL366</i> | 1          | 0.42              |
| <i>GFL367</i> | 1          | 0.42              |
| <i>GFL368</i> | 1          | 0.42              |
| <i>GFL369</i> | 2          | 0.84              |
| <i>GFL370</i> | 3          | 1.26              |
| <i>GFL371</i> | 1          | 0.42              |
| <i>GFL372</i> | 5          | 2.10              |
| <i>GFL373</i> | 5          | 2.10              |
| <i>GFL374</i> | 10         | 4.20              |
| <i>GFL375</i> | 4          | 1.68              |
| <i>GFL376</i> | 1          | 0.42              |
| <i>GFL377</i> | 1          | 0.42              |
| <i>GFL378</i> | 1          | 0.42              |
| <i>GFL379</i> | 3          | 1.26              |
| <i>GFL380</i> | 9          | 3.78              |
| <i>GFL381</i> | 8          | 3.36              |
| <i>GFL382</i> | 5          | 2.10              |
| <i>GFL383</i> | 1          | 0.42              |
| <i>GFL384</i> | 1          | 0.42              |
| <i>GFL385</i> | 1          | 0.42              |
| <i>GFL386</i> | 2          | 0.84              |
| <i>GFL387</i> | 2          | 0.84              |
| <i>GFL388</i> | 1          | 0.42              |
| <i>GFL389</i> | 1          | 0.42              |
| <i>GFL390</i> | 3          | 1.26              |

**Table 19** Continued

| GeneID        | # of edges | % of shared edges |
|---------------|------------|-------------------|
| <i>GFL391</i> | 1          | 0.42              |
| <i>GFL392</i> | 4          | 1.68              |
| <i>GFL393</i> | 1          | 0.42              |
| <i>GFL394</i> | 1          | 0.42              |
| <i>GFL395</i> | 1          | 0.42              |
| <i>GFL396</i> | 1          | 0.42              |
| <i>GFL397</i> | 3          | 1.26              |
| <i>GFL398</i> | 1          | 0.42              |
| <i>GFL399</i> | 1          | 0.42              |
| <i>GFL400</i> | 5          | 2.10              |
| <i>GFL401</i> | 2          | 0.84              |
| <i>GFL402</i> | 3          | 1.26              |
| <i>GFL403</i> | 1          | 0.42              |
| <i>GFL404</i> | 1          | 0.42              |
| <i>GFL405</i> | 1          | 0.42              |
| <i>GFL406</i> | 7          | 2.94              |
| <i>GFL407</i> | 1          | 0.42              |
| <i>GFL408</i> | 12         | 5.04              |
| <i>GFL409</i> | 1          | 0.42              |
| <i>GFL410</i> | 3          | 1.26              |
| <i>GFL411</i> | 1          | 0.42              |
| <i>GFL412</i> | 1          | 0.42              |
| <i>GFL413</i> | 1          | 0.42              |
| <i>GFL414</i> | 7          | 2.94              |
| <i>GFL415</i> | 3          | 1.26              |
| <i>GFL416</i> | 2          | 0.84              |
| <i>GFL417</i> | 6          | 2.52              |
| <i>GFL418</i> | 2          | 0.84              |
| <i>GFL419</i> | 4          | 1.68              |
| <i>GFL420</i> | 1          | 0.42              |
| <i>GFL421</i> | 1          | 0.42              |
| <i>GFL422</i> | 2          | 0.84              |
| <i>GFL423</i> | 1          | 0.42              |
| <i>GFL424</i> | 3          | 1.26              |



**Table 19** Continued

| GeneID        | # of edges | % of shared edges |
|---------------|------------|-------------------|
| <i>GFL425</i> | 2          | 0.84              |
| <i>GFL426</i> | 4          | 1.68              |
| <i>GFL427</i> | 3          | 1.26              |
| <i>GFL428</i> | 1          | 0.42              |
| <i>GFL429</i> | 4          | 1.68              |
| <i>GFL430</i> | 1          | 0.42              |
| <i>GFL431</i> | 1          | 0.42              |

#### 4. DISCUSSION AND CONCLUSION

UHML has long been assumed to be one of the most important fiber traits for cotton commerce. However, it is unknown how many genes control UHML in the cotton genome. Although a number of genes differentially expressed in developing fibers have been identified and studied extensively (Ji et al. 2003; Arpat et al. 2004; Chaudhary et al. 2008; Hovav et al. 2008; Yang et al. 2008; Rapp et al. 2010; Lacape et al. 2012; Li et al. 2013; Yoo and Wendel 2014), most of them focused on comparative studies of genes differentially expressed between different fiber developmental stages, different tissues, and/or between cultivated and wild type species. So far, a total of 21 genes that control UHML or trichome development have been cloned in cotton and other plant species. However, the underlying molecular mechanisms of UHML development in cultivated cotton species are still to be answered.

We, in this study, used a new high-throughput gene/QTL cloning system recently developed in Dr. Hongbin Zhang's Laboratory to isolate the genes controlling UHML from cultivated tetraploid cottons. A total of 474 *GFL* genes controlling UHML were isolated and characterized. This number of genes is 20-fold more than the total number of fiber-length genes that have been reported worldwide in the past 20 years. Each of the 474 *GFL* genes has relatively small effects on UHML, ranging from 2.64% to 7.92%. Of the 474 *GFL* genes, 88.6% have negative effects on UHML, and 11.4% have positive effects.

Over 70% of the 474 *GFL* genes were annotated using the available gene description with an E-value  $\leq 1.0E-06$ . The *GFL* genes encode a diversity of proteins or enzymes. The GO analysis has revealed that 61.18% of the *GFL* genes are assigned to the Biological Process category, 62.87% to the Molecular Function category and 66.67% to the Cellular Component category. Among the GO terms assigned, the cellular process and metabolism of the Biological Process category, and the binding and catalytic of the Molecular Function category are the most important biological processes in which the *GFL* genes are involved. The enzymes or proteins encoded by the 474 *GFL* genes are mapped to 60 KEGG metabolic pathways (Table 11). “Starch and sucrose metabolism” and “Purine metabolism” are the two pathways in which most of the *GFL* genes are involved. Therefore, fiber cell extension is likely determined by a number of biological processes and metabolic pathways in which the 474 *GFL* genes are involved.

Study of the molecular mechanisms underlying fiber UHML reveals that the 474 *GFL* genes interact, forming a single interaction network, in which each *GFL* gene interacts with at least one other *GFL* gene. Within the network, the number of interaction edges of a *GFL* gene (node) varies from 20 to 383. The number of its edges or interactions with other genes in the network is significantly correlated with the effect of a *GFL* gene on fiber UHML phenotype, suggesting the roles of the gene x gene interactions in fiber UHML development. Therefore, the molecular mechanisms of controlling fiber UHML phenotype involve not only *GFL* genes *per se*, but also the degree, number and directions of their interactions.

Furthermore, this study shows that the *GFL* gene network varies among cotton RILs with different fiber UHML. Although the variations in the number of nodes (genes) are limited between cotton RILs with different UHMLs, the variations in the number of edges (interactions) are dramatic. For example, the numbers of nodes in the *GFL* gene networks remained constant across the fiber-length RIL groups G1, G2 and G3, even though their node compositions were slightly different. But, the numbers of edges across these groups differed by 42% between G1 and G3 and by 43% between G2 and G3. Variation in the number of nodes was found between the *GFL* gene networks of G4 and G5; however, the maximum of their node variations was only 11 genes, only accounting for 2% of the 474 *GFL* genes, which is much smaller than the variation of their interaction edges between the networks. Therefore, we assume that gene x gene interaction, or epistasis within the *GFL* gene network play important roles in the cotton fiber UHML development.

For most of the 474 *GFL* genes, the gain or loss of edges from the gene-gene interaction networks among different fiber-length RIL groups was not significantly correlated with the variation of UHML; however, 20 (4.22%) of them did significantly correlate, negatively or positively, with the variation of UHML ( $P \leq 0.05$ ). These results suggest that the variation of interactions among the *GFL* genes contribute to the fiber UHML, at least for some of the genes. Therefore, we hypothesize that the unique gene-gene interactions of the *GFL* gene network may be major players in the regulation of UHML. The discovery of the large number of unique gene-gene interactions for each fiber-length RIL group, especially for the longest and shortest fiber length groups, might

be an indication of their roles in UHML development. However, further studies are needed to address how these unique interaction edges regulate fiber UHML and what molecular mechanisms trigger the variation of the unique gene x gene interactions.

One of the major economical traits that have evolved dramatically from diploid to tetraploid cotton is fiber length. This study shows that the fiber length change from diploid cottons to tetraploid cottons, as those of fiber UHMLs among different fiber-length groups, has also resulted from the variation of the numbers of *GFL* genes and their interactions. In this study, a total of 428 *GFL* orthologous genes were identified in the 10-dpa developing fibers of the A-genome diploid species, forming a total of 5,775 interaction edges, and a total of 436 *GFL* orthologous genes were identified in the 10-dpa developing fibers of the D-genome diploid species, forming a total of 5,395 interaction edges. While 8 – 10% of the number of nodes in the *GFL* gene networks has increased from A- or D- genome diploid species to tetraploid cottons, an increase of 8-fold of gene-gene interactions were observed from the diploid cottons to tetraploid cottons. This result implies that process of polyploidization might facilitate the interactions of the *GFL* genes, even though the numbers of genes controlling the trait are relatively consistent. This change might have contributed to the increased fiber UHML in the modern cultivated tetraploid cottons.

Cotton fiber UHML is a typical quantitative trait, as indicated by its continuous phenotypic variation (Fig. 4). The results of this study have provided a first line of evidence for the hypothesis that quantitative traits are controlled by numerous genes each of which has small effects. Moreover, this study has added several new findings to

the molecular basis of quantitative genetics. First, the genes controlling a quantitative trait contribute to the trait not only positively, but also negatively; the trait performance is the result of balance between the genes having positive and negative effects. Second, the genes controlling a quantitative trait encode a variety of proteins or enzymes that are involved in multiple biological processes and metabolic pathways. Third, the genes controlling a quantitative trait interact, forming an interaction network; therefore, the performance of a quantitative trait is the consequence of interactions among the genes controlling the traits. Within the gene networks, although the number of genes and functions of genes may vary among different genotypes, the gene x gene interactions play important roles in the performance of a quantitative trait. Finally, the genes involved in the gene network controlling a quantitative trait are different in number of gene x gene interactions, thus playing different roles in the trait development.

The 474 cloned *GFL* genes and findings resulted from this study have, for the first time worldwide, provided new concepts, new knowledge and new tools for development of new methods enabling enhanced cotton breeding, such as gene-based breeding. It is based on not only the genotypes or alleles of the target genes to be selected for, like marker- or genomics-assisted breeding, but also the action, action direction (positive or negative), gene x gene interaction, gene x nongene element interaction (e.g. miRNA) and G x E interactions of the genes controlling the target trait. In addition, since the markers used for gene-based breeding are derived from the cloned genes controlling the trait, the risk of genetic recombination between the markers and target genes is minimized. Therefore, gene-based breeding is far more powerful and

efficient than the currently-used marker- or genomics-assisted breeding for enhanced plant breeding.

## REFERENCES

- Appelquist WL, Cronn R and Wendel JF. 2001. Comparative development of fiber in wild and cultivated cotton. *Evolution & Development* **3**(1): 3-17.
- Argiriou A, Kalivas A, Michailidis G and Tsaftaris A. 2012. Characterization of PROFILIN genes from allotetraploid (*Gossypium hirsutum*) cotton and its diploid progenitors and expression analysis in cotton genotypes differing in fiber characteristics. *Molecular Biology Reports* **39**(4): 3523-3532.
- Arpat AB, Waugh M, Sullivan JP, Gonzales M, Frisch D, Main D, Wood T, Leslie A, Wing RA and Wilkins TA. 2004. Functional genomics of cell elongation in developing cotton fibers. *Plant Molecular Biology* **54**(6): 911-929.
- Avci U, Pattathil S, Singh B, Brown VL, Hahn MG and Haigler CH. 2013. Cotton fiber cell walls of *Gossypium hirsutum* and *Gossypium barbadense* have differences related to loosely-bound xyloglucan. *PloS One* **8**(2): e56315.
- Basra AS and Malik CP. 1984. Development of the cotton fiber. *International Review of Cytology* **89**: 66-113.
- Braden CA and Smith CW. 2004. Fiber length development in near-long staple upland cotton. *Crop Science* **44**(5): 1553 -1559
- Chaudhary B, Hovav R, Rapp R, Verma N, Udall JA and Wendel JF. 2008. Global analysis of gene expression in cotton fibers from wild and domesticated *Gossypium barbadense*. *Evolution & Development* **10**(5): 567-582.
- Chen X, Guo W, Liu B, Zhang Y, Song X, Cheng Y, Zhang L and Zhang T. 2012. Molecular mechanisms of fiber differential development between *G. barbadense* and *G. hirsutum* revealed by genetical genomics. *PloS One* **7**(1): e30056.
- Conesa A, Gotz S, Garcia-Gomez JM, Terol J, Talon M and Robles M. 2005. Blast2GO: a universal tool for annotation, visualization and analysis in functional genomics research. *Bioinformatics* **21**(18): 3674-3676.
- Conesa A and Gotz S. 2008. Blast2GO: A comprehensive suite for functional analysis in plant genomics. *International Journal of Plant Genomics* **2008**: 1-13.
- Dhindsa RS, Beasley CA and Ting IP. 1975. Osmoregulation in cotton fiber: accumulation of potassium and malate during growth. *Plant Physiology* **56**(3): 394-398.



- Gotz S, Garcia-Gomez JM, Terol J, Williams TD, Nagaraj SH, Nueda MJ, Robles M, Talon M, Dopazo J and Conesa A. 2008. High-throughput functional annotation and data mining with the Blast2GO suite. *Nucleic Acids Research* **36**(10): 3420-3435.
- Gotz S, Arnold R, Sebastian-Leon P, Martin-Rodriguez S, Tischler P, Jehl MA, Dopazo J, Rattei T and Conesa A. 2011. B2G-FAR, a species-centered GO annotation repository. *Bioinformatics* **27**(7): 919-924.
- Grabherr MG, Haas BJ, Yassour M, Levin JZ, Thompson DA, Amit I, Adiconis X, Fan L, Raychowdhury R, Zeng Q, Chen Z, Mauceli E, Hacohen N, Gnirke A, Rhind N, di Palma F, Birren BW, Nusbaum C, Lindblad-Toh K, Friedman N and Regev A. 2011. Full-length transcriptome assembly from RNA-Seq data without a reference genome. *Nature Biotechnology* **29**(7): 644-652.
- Guan XY, Li QJ, Shan CM, Wang S, Mao YB, Wang LJ and Chen XY. 2008. The HD-Zip IV gene GaHOX1 from cotton is a functional homologue of the *Arabidopsis* GLABRA2. *Physiologia Plantarum* **134**(1): 174-182.
- Haas BJ, Papanicolaou A, Yassour M, Grabherr M, Blood PD, Bowden J, Couger MB, Eccles D, Li B, Lieber M, Macmanes MD, Ott M, Orvis J, Pochet N, Strozzi F, Weeks N, Westerman R, William T, Dewey CN, Henschel R, Leduc RD, Friedman N and Regev A. 2013. *De novo* transcript sequence reconstruction from RNA-seq using the Trinity platform for reference generation and analysis. *Nature Protocols* **8**(8): 1494-1512.
- Hao J, Tu L, Hu H, Tan J, Deng F, Tang W, Nie Y and Zhang X. 2012. GbTCP, a cotton TCP transcription factor, confers fibre elongation and root hair development by a complex regulating system. *Journal of Experimental Botany* **63**(17): 6267-6281.
- Hovav R, Udall JA, Hovav E, Rapp R, Fligel L and Wendel JF. 2008. A majority of cotton genes are expressed in single-celled fiber. *Planta* **227**(2): 319-329.
- Huang GQ, Gong SY, Xu WL, Li W, Li P, Zhang CJ, Li DD, Zheng Y, Li FG and Li XB. 2013. A fasciclin-like arabinogalactan protein, GhFLA1, is involved in fiber initiation and elongation of cotton. *Plant Physiology* **161**(3): 1278-1290.
- Humphries JA, Walker AR, Timmis JN and Orford SJ. 2005. Two WD-repeat genes from cotton are functional homologues of the *Arabidopsis thaliana* TRANSPARENT TESTA GLABRA1 (TTG1) gene. *Plant Molecular Biology* **57**(1): 67-81.
- Ji SJ, Lu YC, Feng JX, Wei G, Li J, Shi YH, Fu Q, Liu D, Luo JC and Zhu YX. 2003. Isolation and analyses of genes preferentially expressed during early cotton fiber

- development by subtractive PCR and cDNA array. *Nucleic Acids Research* **31**(10): 2534-2543.
- Jiang C, Wright RJ, El-Zik KM and Paterson AH. 1998. Polyploid formation created unique avenues for response to selection in *Gossypium* (cotton). *Proceedings of the National Academy of Sciences of the United States of America* **95**(8): 4419-4424.
- Kanehisa M and Goto S. 2000. KEGG: kyoto encyclopedia of genes and genomes. *Nucleic Acids Research* **28**:27-30.
- Kanehisa M, Goto S, Sato Y, Kawashima M, Furumichi M and Tanabe M. 2014. Data, information, knowledge and principle: back to metabolism in KEGG. *Nucleic Acids Research* **42**: D199-D205.
- Karademir E, Karademir C, Ekininci R and Gencer O. 2010. Relationship between yield, fiber length and other fiber-related traits in advanced cotton strains. *Notulae Botanicae Horti Agrobotanici Cluj-Napoca* **38**(3): 111-116.
- Kim HJ, Triplett BA, Zhang HB, Lee MK, Hinchliffe DJ, Li P and Fang DD. 2012. Cloning and characterization of homeologous cellulose synthase catalytic subunit 2 genes from allotetraploid cotton (*Gossypium hirsutum* L.). *Gene* **494**(2): 181-189.
- Lacape JM, Claverie M, Vidal RO, Carazzolle MF, Guimaraes Pereira GA, Ruiz M, Pre M, Llewellyn D, Al-Ghazi Y, Jacobs J, Dereeper A, Huguet S, Giband M and Lanaud C. 2012. Deep sequencing reveals differences in the transcriptional landscapes of fibers from two cultivated species of cotton. *PloS One* **7**(11): e48855.
- Lee J, Burns TH, Light G, Sun Y, Fokar M, Kasukabe Y, Fujisawa K, Maekawa Y and Allen RD. 2010. Xyloglucan endotransglycosylase/hydrolase genes in cotton and their role in fiber elongation. *Planta* **232**(5): 1191-1205.
- Li B and Dewey CN. 2011. RSEM: accurate transcript quantification from RNA-Seq data with or without a reference genome. *BMC Bioinformatics* **12**: 323.
- Li X, Yuan D, Zhang J, Lin Z and Zhang X. 2013. Genetic mapping and characteristics of genes specifically or preferentially expressed during fiber development in cotton. *PloS One* **8**(1): e54444.
- Li XB, Fan XP, Wang XL, Cai L and Yang WC. 2005. The cotton ACTIN1 gene is functionally expressed in fibers and participates in fiber elongation. *The Plant Cell* **17**(3): 859-875.

- Liu Q, Talbot M and Llewellyn DJ. 2013. Pectin methylesterase and pectin remodelling differ in the fibre walls of two *Gossypium* species with very different fibre properties. *PLoS One* **8**(6): e65131.
- Luo M, Xiao Y, Li X, Lu X, Deng W, Li D, Hou L, Hu M, Li Y and Pei Y. 2007. GhDET2, a steroid 5alpha-reductase, plays an important role in cotton fiber cell initiation and elongation. *The Plant Journal* **51**(3): 419-430.
- Machado A, Wu Y, Yang Y, Llewellyn DJ and Dennis ES. 2009. The MYB transcription factor GhMYB25 regulates early fibre and trichome development. *The Plant Journal* **59**(1): 52-62.
- Meinert MC and Delmer DP. 1977. Changes in biochemical composition of the cell wall of the cotton fiber during development. *Plant Physiology* **59**(6): 1088-1097.
- Meredith WR and Bridge RR. 1972. Heterosis and gene action in cotton, *Gossypium hirsutum* L.. *Crop Science* **12**(3): 304-310.
- Michailidis G, Argiriou A, Darzentas N and Tsaftaris A. 2009. Analysis of xyloglucan endotransglycosylase/hydrolase (XTH) genes from allotetraploid (*Gossypium hirsutum*) cotton and its diploid progenitors expressed during fiber elongation. *Journal of Plant Physiology* **166**(4): 403-416.
- NCC. 2012. National Cotton Council of America: United States cotton production. Available at <http://www.cotton.org/econ/world/detail.cfm> (verified 22 Feb. 2014).
- Padmalatha KV, Patil DP, Kumar K, Dhandapani G, Kanakachari M, Phanindra ML, Kumar S, Mohan TC, Jain N, Prakash AH, Vamadevaiah H, Katageri IS, Leelavathi S, Reddy MK, Kumar PA and Reddy VS. 2012. Functional genomics of fuzzless-lintless mutant of *Gossypium hirsutum* L. cv. MCU5 reveal key genes and pathways involved in cotton fibre initiation and elongation. *BMC Genomics* **13**: 624.
- Pang CY, Wang H, Pang Y, Xu C, Jiao Y, Qin YM, Western TL, Yu SX and Zhu YX. 2010. Comparative proteomics indicates that biosynthesis of pectic precursors is important for cotton fiber and *Arabidopsis* root hair elongation. *Molecular & Cellular Proteomics* **9**(9): 2019-2033.
- Paterson AH, Wendel JF, Gundlach H, Guo H, Jenkins J, Jin D, Llewellyn D, Showmaker KC, Shu S, Udall J, Yoo MJ, Byers R, Chen W, Doron-Faigenboim A, Duke MV, Gong L, Grimwood J, Grover C, Grupp K, Hu G, Lee TH, Li J, Lin L, Liu T, Marler BS, Page JT, Roberts AW, Romanel E, Sanders WS,

- Szadkowski E, Tan X, Tang H, Xu C, Wang J, Wang Z, Zhang D, Zhang L, Ashrafi H, Bedon F, Bowers JE, Brubaker CL, Chee PW, Das S, Gingle AR, Haigler CH, Harker D, Hoffmann LV, Hovav R, Jones DC, Lemke C, Mansoor S, ur Rahman M, Rainville LN, Rambani A, Reddy UK, Rong JK, Saranga Y, Scheffler BE, Scheffler JA, Stelly DM, Triplett BA, Van Deynze A, Vaslin MF, Waghmare VN, Walford SA, Wright RJ, Zaki EA, Zhang T, Dennis ES, Mayer KF, Peterson DG, Rokhsar DS, Wang X and Schmutz J. 2012. Repeated polyploidization of *Gossypium* genomes and the evolution of spinnable cotton fibres. *Nature* **492**(7429): 423-427.
- Pu L, Li Q, Fan X, Yang W and Xue Y. 2008. The R2R3 MYB transcription factor GhMYB109 is required for cotton fiber development. *Genetics* **180**(2): 811-820.
- Qu J, Ye J, Geng YF, Sun YW, Gao SQ, Zhang BP, Chen W and Chua NH. 2012. Dissecting functions of KATANIN and WRINKLED1 in cotton fiber development by virus-induced gene silencing. *Plant Physiology* **160**(2): 738-748.
- Rapp RA, Haigler CH, Flagel L, Hovav RH, Udall JA and Wendel JF. 2010. Gene expression in developing fibres of Upland cotton (*Gossypium hirsutum* L.) was massively altered by domestication. *BMC Biology* **8**: 139.
- Reiter WD. 2002. Biosynthesis and properties of the plant cell wall. *Current Opinion in Plant Biology* **5**(6): 536-542.
- Ruan YL, Llewellyn DJ and Furbank RT. 2001. The control of single-celled cotton fiber elongation by developmentally reversible gating of plasmodesmata and coordinated expression of sucrose and K<sup>+</sup> transporters and expansin. *The Plant Cell* **13**(1): 47-60.
- Shi YH, Zhu SW, Mao XZ, Feng JX, Qin YM, Zhang L, Cheng J, Wei LP, Wang ZY and Zhu YX. 2006. Transcriptome profiling, molecular biological, and physiological studies reveal a major role for ethylene in cotton fiber cell elongation. *The Plant Cell* **18**(3): 651-664.
- Smart LB, Vojdani F, Maeshima M and Wilkins TA. 1998. Genes involved in osmoregulation during turgor-driven cell expansion of developing cotton fibers are differentially regulated. *Plant Physiology* **116**(4): 1539-1549.
- Smith CW and Cothren JT. 1999. Cotton : origin, history, technology, and production (ed. CW Smith, JT Cothren), pp. xiii, 850 p., [858] p. of plates : ill. (some col.) ; 826 cm. Wiley, New York.

- Sun Y, Veerabomma S, Abdel-Mageed HA, Fokar M, Asami T, Yoshida S and Allen RD. 2005. Brassinosteroid regulates fiber development on cultured cotton ovules. *Plant & Cell Physiology* **46**(8): 1384-1391.
- Tan J, Tu L, Deng F, Hu H, Nie Y and Zhang X. 2013. A genetic and metabolic analysis revealed that cotton fiber cell development was retarded by flavonoid naringenin. *Plant Physiology* **162**(1): 86-95.
- Theocharidis A, van Dongen S, Enright AJ and Freeman TC. 2009. Network visualization and analysis of gene expression data using BioLayout Express(3D). *Nature Protocols* **4**(10): 1535-1550.
- Ulloa M and Meredith WR, Jr. 2000. Genetic linkage map and QTL analysis of agronomic and fiber quality traits in an intraspecific population. *The Journal of Cotton Science* **4**(3): 161-170.
- USDA. 2014. Cotton and wool outlook No. CWS-14C. Washington, D.C.
- Wang H, Guo Y, Lv F, Zhu H, Wu S, Jiang Y, Li F, Zhou B, Guo W and Zhang T. 2010a. The essential role of GhPEL gene, encoding a pectate lyase, in cell wall loosening by depolymerization of the de-esterified pectin during fiber elongation in cotton. *Plant Molecular Biology* **72**(4-5): 397-406.
- Wang HY, Wang J, Gao P, Jiao GL, Zhao PM, Li Y, Wang GL and Xia GX. 2009. Down-regulation of GhADF1 gene expression affects cotton fibre properties. *Plant Biotechnology Journal* **7**(1): 13-23.
- Wang J, Wang HY, Zhao PM, Han LB, Jiao GL, Zheng YY, Huang SJ and Xia GX. 2010b. Overexpression of a profilin (GhPFN2) promotes the progression of developmental phases in cotton fibers. *Plant & Cell Physiology* **51**(8): 1276-1290.
- Wang K, Wang Z, Li F, Ye W, Wang J, Song G, Yue Z, Cong L, Shang H, Zhu S, Zou C, Li Q, Yuan Y, Lu C, Wei H, Gou C, Zheng Z, Yin Y, Zhang X, Liu K, Wang B, Song C, Shi N, Kohel RJ, Percy RG, Yu JZ, Zhu YX, Wang J and Yu S. 2012. The draft genome of a diploid cotton *Gossypium raimondii*. *Nature Genetics* **44**(10): 1098-1103.
- Wang L, Li XR, Lian H, Ni DA, He YK, Chen XY and Ruan YL. 2010c. Evidence that high activity of vacuolar invertase is required for cotton fiber and Arabidopsis root elongation through osmotic dependent and independent pathways, respectively. *Plant Physiology* **154**(2): 744-756.

- Wang L and Ruan YL. 2010. Unraveling mechanisms of cell expansion linking solute transport, metabolism, plasmodesmal gating and cell wall dynamics. *Plant Signaling & Behavior* **5**(12): 1561-1564.
- Wang S, Wang JW, Yu N, Li CH, Luo B, Gou JY, Wang LJ and Chen XY. 2004. Control of plant trichome development by a cotton fiber MYB gene. *The Plant Cell* **16**(9): 2323-2334.
- Wendel JF. 1989. New World tetraploid cottons contain Old World cytoplasm. *Proceedings of the National Academy of Sciences of the United States of America* **86**(11): 4132-4136.
- Wendel JF, Olson PD and Stewart JM. 1989. Genetic diversity, introgression, and independent domestication of Old World cultivated cottons. *American Journal of Botany* **76**(12): 1795-1806.
- Wendel JF and Cronn RC. 2003. Polyploidy and the evolutionary history of cotton. *Advances in Agronomy* **78**: 139-186.
- Xiao YH, Li DM, Yin MH, Li XB, Zhang M, Wang YJ, Dong J, Zhao J, Luo M, Luo XY, Hou L, Hu L and Pei Y. 2010. Gibberellin 20-oxidase promotes initiation and elongation of cotton fibers by regulating gibberellin synthesis. *Journal of Plant Physiology* **167**(10): 829-837.
- Xu SM, Brill E, Llewellyn DJ, Furbank RT and Ruan YL. 2012. Overexpression of a potato sucrose synthase gene in cotton accelerates leaf expansion, reduces seed abortion, and enhances fiber production. *Molecular Plant* **5**(2): 430-441.
- Yang YW, Bian SM, Yao Y and Liu JY. 2008. Comparative proteomic analysis provides new insights into the fiber elongating process in cotton. *Journal of Proteome Research* **7**(11): 4623-4637.
- Yoo MJ and Wendel JF. 2014. Comparative evolutionary and developmental dynamics of the cotton (*Gossypium hirsutum*) fiber transcriptome. *PLoS Genetics* **10**(1): e1004073.

## APPENDIX A

**Table A-1** Nodes and numbers of edges shared among the *GFL* gene networks of different fiber-length groups

| geneID        | No. of edges | geneID        | No. of edges | geneID        | No. of edges | geneID        | No. of edges | geneID        | No. of edges |
|---------------|--------------|---------------|--------------|---------------|--------------|---------------|--------------|---------------|--------------|
| <i>GFL339</i> | 53           | <i>GFL049</i> | 18           | <i>GFL417</i> | 8            | <i>GFL201</i> | 4            | <i>GFL057</i> | 2            |
| <i>GFL340</i> | 47           | <i>GFL159</i> | 18           | <i>GFL097</i> | 8            | <i>GFL120</i> | 4            | <i>GFL193</i> | 1            |
| <i>GFL341</i> | 47           | <i>GFL060</i> | 18           | <i>GFL355</i> | 8            | <i>GFL401</i> | 4            | <i>GFL323</i> | 1            |
| <i>GFL342</i> | 44           | <i>GFL350</i> | 18           | <i>GFL277</i> | 7            | <i>GFL082</i> | 4            | <i>GFL190</i> | 1            |
| <i>GFL343</i> | 43           | <i>GFL210</i> | 18           | <i>GFL106</i> | 7            | <i>GFL240</i> | 4            | <i>GFL316</i> | 1            |
| <i>GFL344</i> | 41           | <i>GFL222</i> | 17           | <i>GFL381</i> | 7            | <i>GFL065</i> | 4            | <i>GFL018</i> | 1            |
| <i>GFL345</i> | 39           | <i>GFL171</i> | 16           | <i>GFL188</i> | 7            | <i>GFL056</i> | 3            | <i>GFL076</i> | 1            |
| <i>GFL346</i> | 37           | <i>GFL170</i> | 16           | <i>GFL068</i> | 7            | <i>GFL151</i> | 3            | <i>GFL100</i> | 1            |
| <i>GFL347</i> | 37           | <i>GFL237</i> | 15           | <i>GFL284</i> | 7            | <i>GFL267</i> | 3            | <i>GFL092</i> | 1            |
| <i>GFL348</i> | 37           | <i>GFL048</i> | 14           | <i>GFL370</i> | 7            | <i>GFL195</i> | 3            | <i>GFL430</i> | 1            |
| <i>GFL349</i> | 36           | <i>GFL147</i> | 14           | <i>GFL196</i> | 7            | <i>GFL224</i> | 3            | <i>GFL221</i> | 1            |
| <i>GFL350</i> | 36           | <i>GFL053</i> | 14           | <i>GFL242</i> | 7            | <i>GFL105</i> | 3            | <i>GFL459</i> | 1            |
| <i>GFL351</i> | 35           | <i>GFL089</i> | 13           | <i>GFL205</i> | 7            | <i>GFL253</i> | 3            | <i>GFL177</i> | 1            |
| <i>GFL352</i> | 35           | <i>GFL139</i> | 13           | <i>GFL392</i> | 7            | <i>GFL133</i> | 3            | <i>GFL180</i> | 1            |
| <i>GFL353</i> | 34           | <i>GFL292</i> | 13           | <i>GFL217</i> | 6            | <i>GFL138</i> | 3            | <i>GFL062</i> | 1            |
| <i>GFL354</i> | 33           | <i>GFL130</i> | 13           | <i>GFL124</i> | 6            | <i>GFL396</i> | 3            | <i>GFL098</i> | 1            |
| <i>GFL355</i> | 33           | <i>GFL354</i> | 13           | <i>GFL225</i> | 6            | <i>GFL211</i> | 3            | <i>GFL136</i> | 1            |
| <i>GFL356</i> | 33           | <i>GFL258</i> | 13           | <i>GFL016</i> | 6            | <i>GFL275</i> | 3            | <i>GFL249</i> | 1            |
| <i>GFL357</i> | 32           | <i>GFL375</i> | 12           | <i>GFL108</i> | 6            | <i>GFL331</i> | 3            | <i>GFL052</i> | 1            |
| <i>GFL358</i> | 31           | <i>GFL297</i> | 11           | <i>GFL050</i> | 6            | <i>GFL008</i> | 3            | <i>GFL250</i> | 1            |
| <i>GFL359</i> | 31           | <i>GFL020</i> | 11           | <i>GFL148</i> | 6            | <i>GFL317</i> | 3            | <i>GFL238</i> | 1            |
| <i>GFL360</i> | 30           | <i>GFL285</i> | 11           | <i>GFL414</i> | 6            | <i>GFL183</i> | 3            | <i>GFL341</i> | 1            |
| <i>GFL361</i> | 30           | <i>GFL293</i> | 11           | <i>GFL309</i> | 6            | <i>GFL110</i> | 3            | <i>GFL302</i> | 1            |
| <i>GFL362</i> | 29           | <i>GFL371</i> | 11           | <i>GFL215</i> | 6            | <i>GFL328</i> | 3            | <i>GFL126</i> | 1            |
| <i>GFL363</i> | 28           | <i>GFL080</i> | 11           | <i>GFL123</i> | 6            | <i>GFL312</i> | 3            | <i>GFL303</i> | 1            |
| <i>GFL129</i> | 27           | <i>GFL319</i> | 10           | <i>GFL047</i> | 5            | <i>GFL212</i> | 2            | <i>GFL204</i> | 1            |
| <i>GFL019</i> | 26           | <i>GFL388</i> | 10           | <i>GFL114</i> | 5            | <i>GFL472</i> | 2            | <i>GFL162</i> | 1            |
| <i>GFL078</i> | 26           | <i>GFL289</i> | 10           | <i>GFL087</i> | 5            | <i>GFL141</i> | 2            | <i>GFL156</i> | 1            |
| <i>GFL338</i> | 24           | <i>GFL061</i> | 10           | <i>GFL330</i> | 5            | <i>GFL038</i> | 2            | <i>GFL219</i> | 1            |
| <i>GFL269</i> | 24           | <i>GFL336</i> | 10           | <i>GFL127</i> | 5            | <i>GFL207</i> | 2            | <i>GFL167</i> | 1            |
| <i>GFL165</i> | 24           | <i>GFL073</i> | 10           | <i>GFL283</i> | 5            | <i>GFL407</i> | 2            | <i>GFL432</i> | 1            |
| <i>GFL367</i> | 24           | <i>GFL261</i> | 10           | <i>GFL229</i> | 5            | <i>GFL467</i> | 2            | <i>GFL301</i> | 1            |
| <i>GFL274</i> | 23           | <i>GFL239</i> | 10           | <i>GFL230</i> | 5            | <i>GFL232</i> | 2            | <i>GFL144</i> | 1            |
| <i>GFL324</i> | 22           | <i>GFL327</i> | 10           | <i>GFL203</i> | 5            | <i>GFL295</i> | 2            | <i>GFL389</i> | 1            |
| <i>GFL026</i> | 22           | <i>GFL220</i> | 10           | <i>GFL169</i> | 5            | <i>GFL155</i> | 2            | <i>GFL473</i> | 1            |
| <i>GFL046</i> | 21           | <i>GFL287</i> | 9            | <i>GFL377</i> | 4            | <i>GFL382</i> | 2            | <i>GFL431</i> | 1            |
| <i>GFL335</i> | 21           | <i>GFL135</i> | 9            | <i>GFL096</i> | 4            | <i>GFL385</i> | 2            | <i>GFL463</i> | 1            |
| <i>GFL030</i> | 20           | <i>GFL252</i> | 9            | <i>GFL192</i> | 4            | <i>GFL032</i> | 2            | <i>GFL265</i> | 1            |
| <i>GFL117</i> | 20           | <i>GFL168</i> | 9            | <i>GFL157</i> | 4            | <i>GFL322</i> | 2            | <i>GFL209</i> | 1            |
| <i>GFL409</i> | 20           | <i>GFL025</i> | 9            | <i>GFL246</i> | 4            | <i>GFL318</i> | 2            |               |              |
| <i>GFL329</i> | 20           | <i>GFL027</i> | 9            | <i>GFL216</i> | 4            | <i>GFL182</i> | 2            |               |              |
| <i>GFL173</i> | 20           | <i>GFL121</i> | 8            | <i>GFL445</i> | 4            | <i>GFL189</i> | 2            |               |              |
| <i>GFL282</i> | 19           | <i>GFL150</i> | 8            | <i>GFL314</i> | 4            | <i>GFL194</i> | 2            |               |              |